SERPENTINIZED ULTRAMAFIC ROCKS OF THE MANITOBA NICKEL BELT

by

COLIN J. A. COATS

A thesis presented in partial
fulfillment of the requirements
for the degree of Doctor of Philosophy

to

The Department of Geology
UNIVERSITY OF MANITOBA
WINNIPEG, MANITOBA, CANADA.

1966

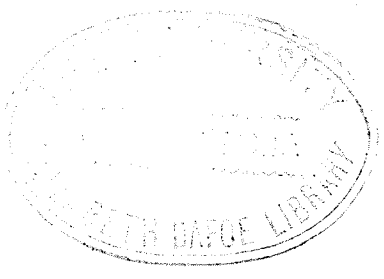

ABSTRACT

Serpentinized ultramafic rocks of Churchill age occur along a northeasterly trending zone of complexly faulted gneissic rocks in the Setting Lake-Moak Lake region of central Manitoba.

The ultramafic rocks are classified as serpentinites, tremolite serpentinites, tremolite phlogopite serpentinites, phlogopite serpentinites, serpentinized peridotites, tremolite olivine orthopyroxenites and amphibole orthopyroxenites. They originated from dunites, peridotites and orthopyroxenites.

The predominant serpentine is a fibrous variety resembling chrysotile, which can only be satisfactorily indexed on the basis of a 3-layer structure. The derived 3-layer ortho-hexagonal cell has dimensions of a_o = 5.346Å, b_o = 9.205Å and c_o = 21.93Å. Minor occurrences of antigorite and lizardite are identified by optical, X-ray diffraction and differential thermal analysis methods.

Alteration of serpentinite adjacent to siliceous country rocks results in the formation of chlorite, anthophyllite and tremolite zones with gain of Si, Al, Ca and Mn and loss of Mg, Fe, OH, Cr and Ni. Intrusion of serpentinite by pegmatite results in formation of phlogopite, chlorite, tremolite, anthophyllite and talc-carbonate zones. SiO_2, Al_2O_3, K_2O and CO_2 are acquired by the ultramafic rock, while MgO, FeO and H_2O are removed. Ni is relatively immobile during this type of alteration.

The average composition of nickel belt serpentinites is typical of alpine-type peridotites. They contain higher MgO and lower SiO_2 and CaO than rocks believed representative of the upper mantle. MnO and TiO_2 show an inverse relationship to the MgO/FeO ratios.

The intrusion of ultrabasic magma as a crystal mush up faults from a source in the mantle, quick marginal cooling and subsequent serpentinization are considered the most likely mode of origin for the ultramafic rocks.

TABLE OF CONTENTS

LIST OF TABLES

TABLE PAGE

LIST OF FIGURES

LIST OF PLATES

PLATE PAGE

PLATE PAGE

SERPENTINIZED ULTRAMAFIC ROCKS OF THE MANITOBA NICKEL BELT

CHAPTER 1

INTRODUCTION

The boundary zone between the Churchill and Superior structural provinces of the Precambrian Shield in north-central Manitoba is defined, in an approximate manner, by a linear belt of serpentinized ultramafic intrusive rocks with associated occurrences of nickel sulphide ore. This structural and geologically important zone has been designated the Manitoba nickel belt. The ultramafic intrusive rocks, about which this work is wholly concerned, occur within the north-easterly trending zone, over a known distance of 125 miles and a maximum width of 8 miles.

Geophysical evidence indicates the structural aspects of the belt extend to the southwest and northeast for considerable distances, in part concealed by overlying Paleozoic formations. The present study concerns that section of the zone between latitudes 54° 30', to 56° 00'N., and longitudes 97° 30' to 99° 00'W. (Figure 1). It is within this Precambrian area that most of the ultramafic intrusive rocks have been found.

The discovery of high grade nickel ore at Thompson in February 1956 by the International Nickel Company of Canada Limited, engendered a great deal of interest in the regional structure of the Manitoba nickel belt. Despite the lack of outcrop in many areas and a covering of glacial drift, which in places

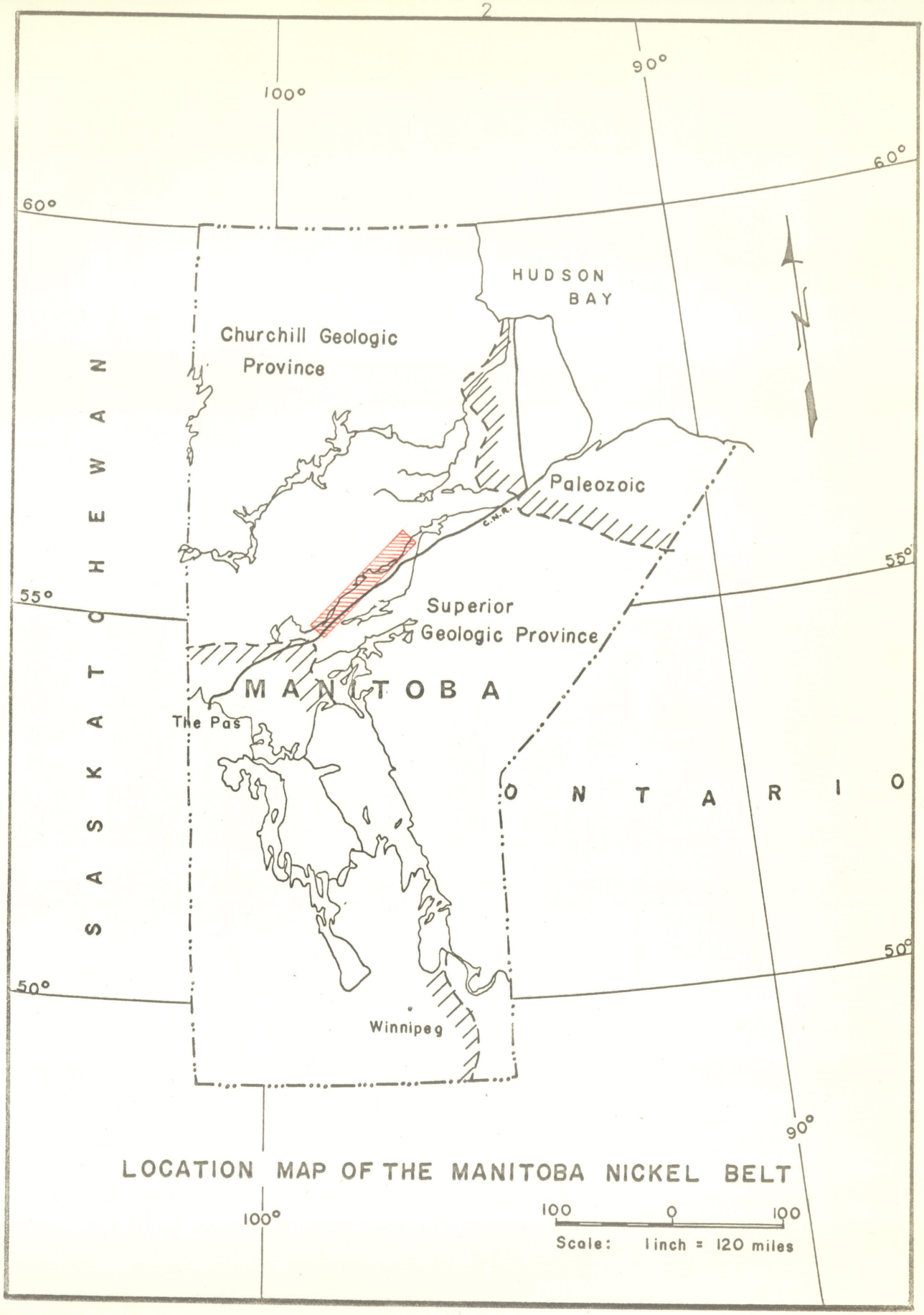

LOCATION MAP OF THE MANITOBA NICKEL BELT

FIG. 1

reaches a thickness of over 200 feet, the nickel belt was soon recognized as being a major tectonic feature of the Canadian Shield.

Coupled with the increasing activities of mining and exploration companies in the region, the Geological Survey of Canada and the Manitoba Mines Branch have augmented their programs of surface geological mapping along the belt. Regional seismic and gravity studies have been conducted by Staff members of the Department of Geology, University of Manitoba and by the Dominion Observatory in Ottawa. This work has all helped to produce a basic understanding of the nature of the Churchill-Superior boundary and the geological structure of the nickel belt.

STATEMENT OF PROBLEM

The decision to undertake a program of research on the ultramafic intrusive rocks of the Manitoba nickel belt, rested on two factors. Firstly, the linear belts of serpentinites and serpentinized peridotites accompanied by regional gravity anomalies, which are found in island arc and alpine type mountain chains, have always been of great interest to geologists and geophysicists alike. They represent major structure features of the earth's crust, have been considered in theories on the origin of continents and permit close examination of the earth's mantle material. As such, the study would be a contribution to the Upper Mantle Project.

Secondly, the association of nickel sulphides with the

serpentinites, introduces an economic aspect to the study. The origin of nickel sulphide ores in many ore bodies is still an enigma, although it is generally conceded that the nickel is derived from an ultramafic rock source at some stage in their history. It is hoped that this research project will contribute in some way, no matter how minor, to our knowledge of these most interesting rocks.

MAP OF THE ULTRAMAFIC INTRUSIVE ROCKS AND LOCATION OF SAMPLE MATERIAL

Figure 2 is a plan of the ultramafic intrusive rocks which are presently known to occur along the belt. The greater proportion of the locations and form of individual bodies has been taken from published data by Zurbrigg (1963). The location of all ultramafic bodies occurring in the Halfway Lake, central Setting Lake, Wabowden and Clarke Lake areas has been compiled from the records of Falconbridge Nickel Mines Limited.

Samples used in this study are located on Figure 2 by a black dot and number. The greatest number of samples have been obtained from diamond drill core and most of the remainder from surface exposures. Two samples have been used from the Thompson mine and a small number selected from the dump material at the Pipe Mine.

METHODS OF STUDY

Over 250 samples of serpentinite and serpentinized perido-

ULTRAMAFIC INTRUSIONS OF THE MANITOBA NICKEL BELT

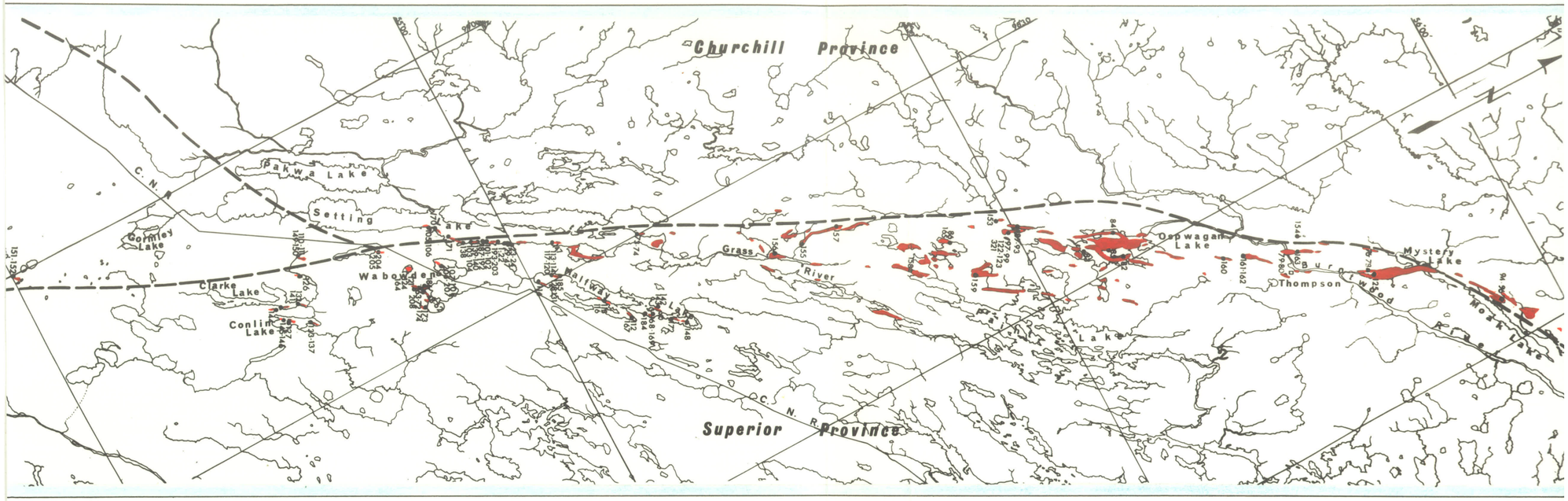

LEGEND

- Ultramafic intrusion
- 133-137 Sample number
- Axis of gravity low

FIGURE 2

tite have been examined in thin section with particular attention being paid to the morphology of the serpentine minerals. Identification of the serpentine group minerals has been made by means of X-ray diffraction and differential thermal analysis methods. The IBM. 1620 digital computer was programed to index a new structural variety of serpentine in the orthochrysotile group. Complete rock analyses of 200 specimens of ultramafic rock were prepared using the X-Ray Fluorescence Spectrometer (ARL. Vacuum X-Ray Quantometer). Of these new analyses, 135 are included in this report.

ACKNOWLEDGEMENTS

Throughout this investigation the assistance and guidance given by Dr. H. D. B. Wilson and Dr. R. B. Ferguson has been greatly appreciated. My thanks also go to other members of the Faculty in the Department of Geology, who gave freely of their time and knowledge on many occasions.

Sample material was supplied by Falconbridge Nickel Mines Limited and International Nickel Company with the permission of Mr. G. P. Mitchell and Mr. J. Keith Diebel, which is greatly appreciated. Particular thanks go to Dr. J. J. Brummer and Dr. A. R. Graham of Falconbridge who gave material and moral assistance to the project on innumerable occasions. Specimens numbered with an M-prefix were obtained from properties optioned by Falconbridge from Consolidated Marbenor Mines Limited, National

Malartic Gold Mines Limited and Rio Tinto Canadian Exploration Limited.

Olivine compositions were determined by Mr. R. N. Delabio of the Geological Survey of Canada. Work on the sulphide mineralogy was done by Dr. Y. Ogura as part of a more comprehensive study of sulphide-silicate relationships in ultrabasic rocks. With Dr. Ogura's permission, a brief description of the Manitoba occurrences is included as Chapter V in this report. My thanks go to Mr. K. Ramlal for his willing tuition and assistance on the X-ray analytical procedures. Mr. R. Pryhitko did all the photographic work and Miss Kay Thompson assisted in drafting work.

The author gratefully acknowledges the financial assistance of the Falconbridge Scholarship for the years 1963-64 and 1964-65.

Lastly, I wish to thank my wife Doreen, who typed this manuscript, and whose continued encouragement made it possible.

CHAPTER 11

GEOLOGY OF THE MANITOBA NICKEL BELT

AGE RELATIONSHIP OF THE CHURCHILL-SUPERIOR PRECAMBRIAN BLOCKS

The subdivision of the Precambrian rocks of the Canadian Shield into well defined structural provinces was first based on the dominant structural trends prevailing in those regions. (Gill, 1952). Subsequently, an ever increasing number of age determinations enabled more precise boundaries to be given to the structural provinces. It is now well established that a vast interval of time elapsed between the final movements of the Kenoran orogeny within the Superior province, to the Hudsonian revolution affecting principally the rocks of the Churchill province.

Stockwell (1964) has recorded 131 age determinations on orogenic micas from the Superior block, showing a range of 2,230-2, 730 million years with an M (mean) value of 2,490 and an MM. (mean minus standard deviation) of 2,390 million years. For the Churchill province, 141 determinations show a range of 1,450-2,010 million years, an M. value of 1,735 and an MM. value of 1,640 million years. The Churchill-Superior contact zone thus represents a major time interval as well as structural boundary.

ASPECTS OF REGIONAL STRUCTURE

The serpentinized ultramafic rocks occur along an intensely deformed and complexly faulted zone over a known distance of 125 miles and a width of up to 8 miles. This zone approximates the location of the axis of a regional gravity low anomaly (Figure 2), as indicated by Wilson and Brisbin (1961). The intensely faulted zone forms the northwest edge of a 50 mile wide gneissic belt which trends northeast across the exposed Precambrian area of central Manitoba. A pronounced Bouguer anomaly high, running parallel to the low some 35 miles to the southeast and named the Nelson River "high" by Innes (1960), approximately coincides with the centre of the gneissic belt.

In a statistical study of structural trends in the Churchill-Superior contact zone, Wilson and Brisbin (1962) identified and listed the four principal geological units which make up the boundary zone and adjacent areas. The four units are; (1) the Superior block with its predominant east-west structural trends, (2) the Churchill block lying to the northwest of the gravity low, (3) the faulted zone coinciding with the gravity low and (4) the Nelson River gneissic belt lying between the fault zone and the western limit of greenstone belts in the Superior block. Frequency diagrams of trend lines and statistical plots of attitudes on equal area nets, point up distinct features in each of the four units. The Superior block shows predominant east-west strikes and dips either vertical, or steep to the north or south. The gneissic belt shows identical patterns to those of the Superior block

and it can safely be assumed to constitute a part of that province. Evidence from Churchill data illustrates the great difference in the nature and regularity of the folding as compared with the Superior. The Churchill block shows a much wider variation in strike plots with no consistent predominant direction and a broad circle of points on the equal area net projection. The latter could be produced by a series of folds overturned towards the southeast and tilted so that the axes now plunge northeast. An additional valid interpretation would be a series of folds, overturned to the south and cross folded. In the area immediately to the west of the faulted zone, structural trends are generally northeast-southwest.

In contrast to structural patterns of both the Superior and Churchill blocks as derived by Wilson and Brisbin (1962), the fault zone plots show essentially vertical dips and northeast-southwest strikes.

REGIONAL GRAVITY AND SEISMIC INTERPRETATIONS

Some evidence on the structural nature of the contact has been obtained by regional gravity and seismic studies. The gravity pattern has been discussed at some length by Wilson and Brisbin (1960). As previously mentioned, a strong continuous low Bouguer gravity anomaly closely follows the zone of intense faulting. Within the area of Fig. 2, the gravity low trends northeast-southwest with a distinct, but slight

change in direction at a point close to Mystery Lake. A subsidiary branch of the anomaly leaves the main anomaly on the northwest side, near Wabowden. Beyond the area of Fig. 2, to the northeast and southwest the gravity low anomaly remains strong and is still distinct as it is traced beneath the overlying Paleozoic sedimentary rocks. It branches into two at both ends, close to the Pas in the southwest and in the Lowlands of Hudson Bay to the northeast.

The Nelson River gravity high anomaly runs parallel to the gravity low in a great arc for more than 500 miles, from a point near Gillam on the CNR. to the north end of Lake Winnepegosis and across to the Saskatchewan border. From here it swings to the south through southeast Saskatchewan, practically to the International Boundary. A less well defined gravity high parallels the low on its northwest side.

An interpretation of the gravity pattern has been made by Wilson and Brisbin (1962) using single and two-layered crustal models. Best agreement occurs between observed gravity values and those computed for a two-layered crust, having a thickness of 35±5 km., a top layer density of 2.7 gm/cc., a lower layer density of 3.0 gm/cc., and underlain by mantle material with a density of 3.3 gm/cc. The layered crustal model assumes regional warping or folding of both the intermediate density boundary and the Mohorovicic discontinuity. In comparing features of the Manitoba belt with island arc structures in other parts of the world (eg. Vening Meinesz, 1954), it is possible that the crustal downwarp also forms the locus of major crustal

faulting, with the surface expression of the faulting coinciding with the axis of the gravity low.

In a study of the crustal structure from a seismic profile between the North Star Mine near Flin Flon, Manitoba and the village of Mafeking, Hall and Brisbin (1965) obtained depth values for the Conrad and Mohorovicic discontinuities using converted head waves. The seismic line crosses the inferred Superior-Churchill boundary zone close to The Pas, where the Precambrian basement is covered by a veneer of Paleozoic sedimentary rocks having a maximum thickness of 500 feet.

The seismic crustal model derived from the study shows a decrease in the depth to the Conrad discontinuity from approximately 15 km. beneath the Churchill province to about 12 km. immediately south of the boundary line with the Superior province. The Mohorovicic discontinuity shows a similar reduction in depth from 35 km. to 32 km. on crossing the boundary zone.

Considerable discrepancy is evident between the observed values for the Bouguer anomaly along the profile and those computed for the crustal model. The only similarity between the observed and theoretical curves lies in the general increase in gravity values towards the south end of the profile. High density near surface greenstone belts in the Precambrian north of the boundary, are considered to account for most of the disagreement. Immediately south of the boundary line, the observed gravity low suggests the presence of a near surface, low density mass. This can be correlated with the gravity low, which closely follows the fault zone to the northeast. IN add-

ition, Hall and Brisbin (1965) state,

"The coincidence in the location of the regional gravity high and the structural high on the C discontinuity of this feature if eventually confirmed, would lend support to the interpretation of Wilson and Brisbin (1960), that the gneissic zone associated with the Churchill-Superior boundary marks the position of a major crustal upwarp".

GENERAL GEOLOGY

The geology of various areas which comprise or include parts of the Manitoba nickel belt has been described by Dawson (1941, 1952), Gill (1951), Quinn (1954), Patterson (1963), Zurbrigg (1963), Davies (1960, 1962, 1964) and Bell (1965). A preliminary geological map of the Hambone Lake area by Godard (1965) is also available. Incomplete mapping coverage and a general low percentage of rock exposures however, precludes the possibility of giving a complete geological picture of this complex zone. In the following section, a compilation and summary of the known geology, taken from these authors, is given to provide an understanding of the geological and structural setting of the ultramafic rocks.

The dominant rock type along the belt is a sedimentary series of foliated and commonly banded gneissic rocks. These include areas of partially granitized sedimentary gneiss and granite gneiss containing inclusions of sedimentary gneiss. They are composed of quartz and feldspar with lesser quantities of biotite, hornblende and pyroxene. Some of the gneisses contain considerable garnet, while others are abundant in magnetite and cordierite. Pegmatite or granitic material may be present

in irregular sill-like intrusions of narrow width. Dark green to black, hornblende-plagioclase gneiss or amphibolite forms distinct bands within the light coloured felsic gneisses, from a few feet to several hundred feet across. Commonly, the narrower amphibolite bands are disjointed and broken, indicating their inability to fold in conformity with the enclosing gneisses.

Recognizable linear bands of metasedimentary and metavolcanic rocks have been mapped within the generally gneissic terrain of the belt. Volcanic rocks, which form a minor part of the formations along the belt, consist of fine to medium grained andesite and basalt. Highly distorted pillow structures have been noted in a volcanic band on an island in Setting Lake near the south end of the zone and also at Ospwagan and Upper Ospwagan Lakes in the central area of the belt.

The metasedimentary rocks probably represent the least altered series of rocks in the region. The principal lithologic units are greywacke, micaceous quartzite, biotite schist, quartz-biotite-sillimanite gneiss, argillite, iron formation, minor conglomerate and calcareous sediments. Minerals commonly present within the quartz and biotite-rich sedimentary rocks include sillimanite, plagioclase, microcline, muscovite, garnet, epidote and hornblende.

These rocks, together with the associated volcanic bands, are identical in lithology to the Assean Lake series, named by Dawson (1941) from the Assean-Split Lakes area on the northeast extension of the belt, about 40 miles northeast of Moak Lake. They occur interbedded with the more prevalent granitic

gneisses, against which they may show sharp or gradational contacts. The easily recognized lithology of the sedimentary bands and their associated volcanic rocks, gives them the status of marker horizons in the gneisses of predominant granitic texture and composition. They outline the nature of the folding to which the region has been subjected. Zurbrigg (1962) has noted a recurring spacial relationship between the ultramafic intrusive rocks of the belt and the linear sedimentary and volcanic bands.

Large bodies of rather massive to slightly foliated grey and pink granites and granodiorites are present at intervals within the gneisses along the belt. Many are elongated masses, which in part are conformable and may be regarded as syntectonic. Some extensive areas of granitic rocks, occasionally gneissic in texture are hybrid mixtures of sedimentary gneiss and granite.

Serpentinites and serpentinized ultramafic rocks are found as generally conformable, elongate and sinuous bodies confined to the faulted zone. (Fig. 2 and 3).

STRUCTURE OF THE NICKEL BELT

A major zone of extreme deformation and faulting, followed consistently by the axis of the regional gravity low anomaly, extends from an area south of Clarke Lake northwards through Setting, Halfway, Phillips, Paint, Ospwagan, Mystery and Moak Lakes and the Odei River to Assean Lake. The section between Clarke and Moak Lakes along which the vast majority of ultramafic intrusions have so far been found, is outlined on Fig. 3.

The ultramafic intrusive rocks, together with known major faults are located to show their proximity to the regional gravity low axis. It is evident that all three are related and have formed as a direct result of a major geological event. Without doubt the faults shown on Fig. 3 represent a small percentage of those actually present. The prevalent cover of glacial deposits and the absence of published data from exploratory drilling, leaves large gaps in our knowledge of the faulted zone.

All of the known faults trend northeasterly, parallel to the structural trends of the affected rocks. The surface expression of the faults has a well defined topographic effect with many of them occurring along the beds of lakes and rivers and in drift-filled depressions. A large number of the ultramafic intrusive bodies shown on Fig. 3 lie on or close to an established fault line. As many of the others show evidence of marginal shearing, it can be presumed that all of the ultramafic intrusions have a spacial relationship to the fault system.

Despite the scant information available, it is apparent that the whole system is a complex zone of anastomozing faults forming a crude braided pattern. This pattern is equally evident on a smaller scale if a single fault such as the major dislocation extending the length of Setting Lake along its eastern margin is considered. Compilation of drill hole geology in this location shows that separate individual faults and shears form an intricate anastomozing pattern through the rocks on both sides of a zone of mylonite. The latter presumably marks the locus of the most intense shearing.

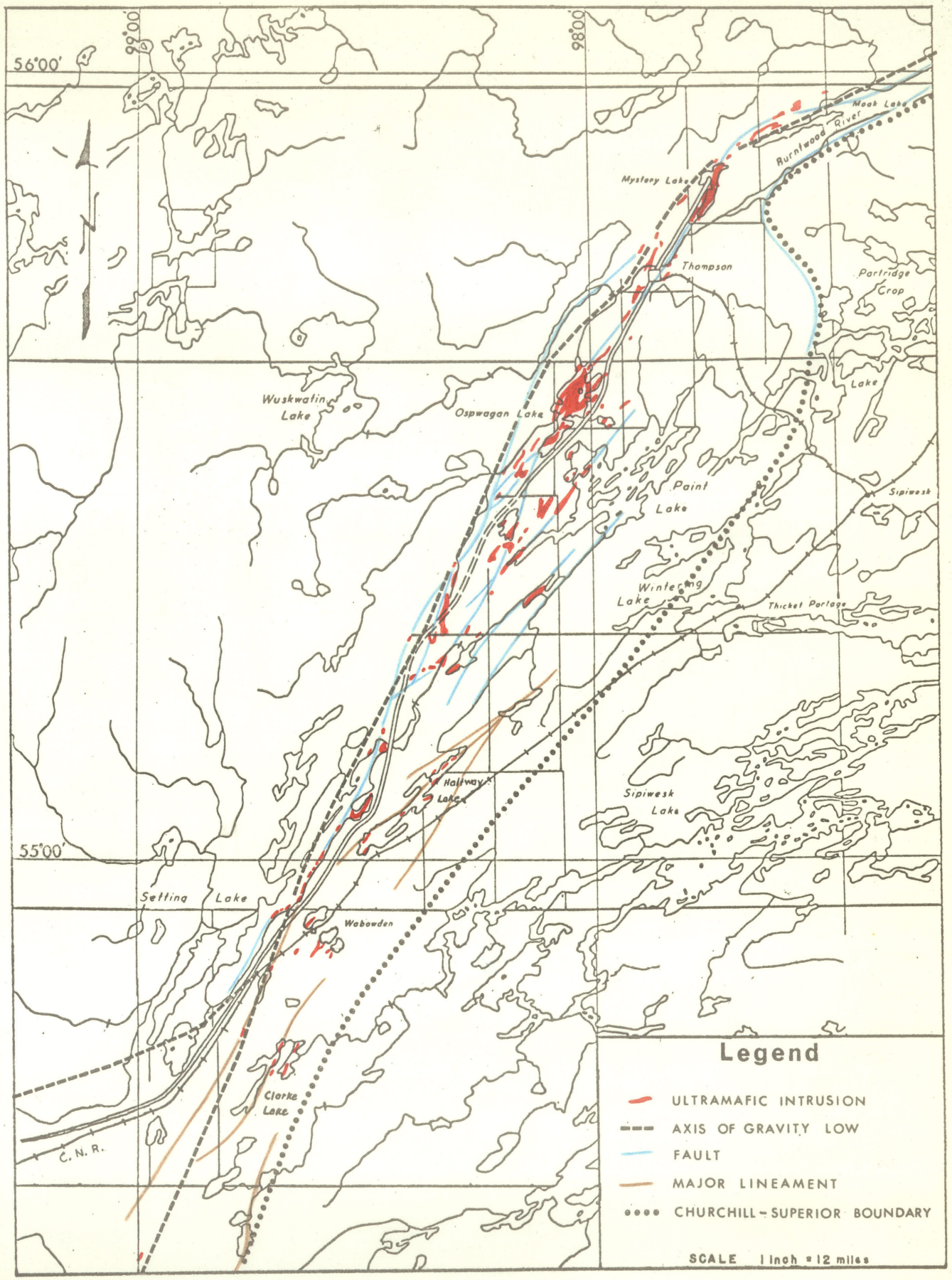

FIG. 3 : Relation of ultramafic rocks to structural elements, Manitoba nickel belt.

Patterson (1963) has recorded the effects of faulting through Ospwagan Lake, Mystery Lake and along Odei River northeast of Moak Lake. At these localities intense shearing and contortions of the rocks point to the through-going fault system. As a general observation from mapping and diamond drill holes, Zurbrigg (1962) has noted that faults, crush and shear zones of unknown displacement are frequently encountered and that the acid gneisses exhibit post-crystalline crushing and micro-shearing over large areas.

Little evidence is available on the attitude and direction of movement of individual faults. Wilson and Brisbin (1960) have suggested the arcuate faulting to be essentially thrusting, using the analogy of island arc and alpine-type structures. The regional local braided fault pattern previously mentioned, suggests major wrench fault movements. From a study of probable fault-produced drag folds along the Ospwagan-Mystery-Moak fault line, Patterson (1963) has suggested the movement was essentially right-handed.

At present, little information is available on the complex folding which has affected the faulted zone and adjacent blocks along the belt. Apparently the entire series of gneisses and sedimentary rocks has been deformed to near vertical series of isoclinal folds. Plunges of drag folds and linear features change from northeast to southwest in several places along the belt (Davies, 1962).

METAMORPHISM AND THE NATURE OF THE CHURCHILL-SUPERIOR BOUNDARY

A systematic study of metamorphic grade along the entire nickel belt has not yet been made, but certain general aspects are known. In his study of the Thompson-Moak Lakes area, Patterson (1963) considered the fault-bounded area of pyroxene-bearing granitic rocks lying south of the Burntwood River and having a westerly margin approximately 13 miles east of Thompson, to be part of the Superior block and hence Archean (Fig. 3). This series of rocks has the east-west structural trends of the Superior and a metamorphic grade in the pyroxene granulite facies. The closest available age date determination is 2400 million years for a pyroxene granite on Dafoe Lake, about 55 miles east of Thompson (Lowdon, 1961).

A metamorphic grade of middle to upper amphibolite facies characterizes the rocks of Patterson's (1963) Proterozoic or West block. A major zone of faulting separates the Proterozoic rocks from the Archean in this area. At the Thompson mine, well within the boundary of this Proterozoic area, mineral assemblages indicate stability within the amphibolite facies (Zurbrigg, 1962). The presence of sillimanite and garnet suggests a relatively high grade of regional metamorphism, probably within the sillimanite-almandine sub-facies.

The Assean Lake-type rocks, as mapped in the vicinity of Mystery Lake, range from the upper greenschist to the upper amphibolite facies. The lower grade may represent retrograde effect due to shearing (Patterson 1963). Further south, along the zone of faulting from Ospwagan Lake to the north end of

Setting Lake, the grade of metamorphism appears to fall between the lower granulite and the upper amphibolite facies (Godard, J. 1965).*

Along the length of Setting Lake, west of the principal fault, quartz and biotite-rich garnet gneisses of the Assean Lake type contain sillimanite as they do at Thompson. To the east of Setting Lake and up to approximately 6 miles east of the CN. railway line, a retrograde amphibolite facies has been imposed on the granulite facies of the Superior terrain (Rance, H. 1965).*

It thus seems established that the metamorphic grade of the 8-10 mile wide strip of rocks which constitute the faulted zone, belongs principally to the amphibolite facies, in part retrogressive from the lower pyroxene granulite facies. Occasional visible retrograde effects on the amphibolite facies are associated with shearing.

In the most recent time-stratigraphic classification of the divisions of the Canadian Shield, Stockwell (1964) has used an MM. age of 2390 million years to represent the end of the Kenoran orogeny and the dividing point between the Archean and Proterozoic eons. Similarly an MM. age of 1640 million years represents the end of the Hudsonian orogeny and the unit of time between those values has been termed the Aphebian. It is not possible to measure the time from the beginning to the end of deposition of sedimentary rocks in the Precambrian. The

---

* Personal communication.

age of deposition of the Churchill rocks is therefore not known. It is possible they were derived by erosion of the ancient Superior cratonic block and hence deposited during the Proterozoic to be later folded during the Hudsonian. Should this have been the case, it would be unreasonable to assume the lithologic and metamorphic boundaries to be one and the same. An overprint of the Hudsonian on the Superior Archean rocks expressed in metamorphism and igneous intrusions would be expected. Some isolated areas of the Superior province have indeed been variously affected during the Hudsonian (Stockwell, 1964).

The visual boundary line between the Churchill and the Superior, would therefore represent the eastern limit of the Hudsonian metamorphic overprint on the Kenoran orogen. It may or may not also represent the line of division between the Archean and Proterozoic on the time-stratigraphic scale. The boundary line between the provinces can thus be given a tentative location based on the following points.

1. It must fall between the general limits established by scattered K-Ar age dates on orogenic biotites.
2. It should separate the predominant east-west structural trends of the Superior from the northeast trends and lineaments of the nickel belt.
3. It should form the eastern margin of recognizable mineralogical changes due to metamorphism of the Hudsonian orogeny on the rocks of the Superior province.

Using these criteria and the geological data from the sources quoted previously, the Churchill-Superior boundary line

has been tentatively established (Fig. 3). It follows the Burntwood River to Apussigmasi Lake, where it swings south and then southeast to Bryce Bay of Partridge Crop Lake. From this point it again turns southwest, passing through Wintering Lake and approximately midway between the southwest extremity of Sipiwesk Lake and Halfway Lake and southwest a few miles east of Clarke Lake.

Undoubtedly, additional and more detailed mapping combined with many more age date determinations will adjust the location of the boundary accordingly.

AGE OF THE ULTRAMAFIC ROCKS

The serpentinized ultramafic intrusive rocks of the Manitoba nickel belt show a striking parallelism afforded by their location along zones of strong dislocation. It has been shown that the faulted zone of the belt, for at least the length under consideration (Fig. 3), lies entirely within the Churchill province. The faults, acid igneous intrusive rocks and metamorphism of the belt, originated as a result of the Hudsonian orogeny which came to an end approximately 1640 million years ago.

Some of the ultramafic rocks show mineralogical changes due to metamorphism and metasomatism and some may have been involved in the folding of the region. The latter point however, cannot be substantiated at the present time. The abundance of pegmatite dykes cutting through many of the ultramafic bodies indicates they predate the main period of granitization and pegmatite intrusion which conceivably represents the culmination

or perhaps later phase of the orogeny. Many of the ultramafic intrusive bodies show the effects of post-serpentinite movements indicating continued fault activity subsequent to their emplacement.

The string of ultramafic intrusions, intense deformation and the presence of a gravity low anomaly are characteristic features of present day island arcs, alpine mountain systems or the eroded roots of former mountain systems (Hess, 1937, 1955). The analogy of the Manitoba belt to the island arc-alpine mountain type of structure has previously been made by Wilson and Brisbin (1961). Hess (1955) considers alpine type serpentinites were emplaced during the first great deformation of a mountain system and hence date the birth of the orogeny concerned. They also locate the alpine mountain trend when present in Precambrian Shield areas.

In view of these factors therefore, it seems probable that the nickel belt serpentinized ultramafic rocks were emplaced at some early or possibly middle stage during the Hudsonian orogeny.

CHAPTER 111

PETROLOGY AND MINERALOGY OF THE ULTRAMAFIC ROCKS

INTRODUCTION

Reference has already been made to structural environment and geological setting of the ultramafic rocks along the nickel belt. Known occurrences of these rocks, largely determined by geophysical surveys, diamond drilling and subsurface work are shown on Fig. 2.

The ultramafic intrusions range in size from elongate lensoidal bodies less than 1000 feet in length and 150 feet in width, to larger masses with maximum dimensions of $5\frac{1}{2}$ miles by 1 mile. The longer bodies are generally more irregular in shape, while retaining a basic lensoid form. The dominant strike of the intrusions is northeast, generally parallel to the structural elements of the host rocks. The linear distribution of the intrusions along major fractures, referred to in the previous section, suggests that the movement to their present positions was essentially vertical and that their present attitudes are generally vertical or steeply dipping.

The ultramafic rocks have been subjected to metamorphism and metasomatism in varying degrees, evidence for which is seen in their mineralogical make-up and chemical composition. Although sample material was not available for every individual intrusion along the belt, the petrologic descriptions and general conclusions based on the samples used are considered

to be reasonably representative of the belt as a whole.

This chapter presents a petrographic classification of the ultramafic rock types sampled, and descriptions of their constituent minerals. In view of their interest and importance, the mineralogy of the serpentine group minerals is presented later, as a separate chapter.

ULTRAMAFIC ROCK TYPES

GENERAL TYPES

The ultramafic rocks show considerable variation in colour, texture and mineral content, as observable in hand specimen. Most samples examined were specimens of fresh drill core where such features are often displayed to their best advantage. The easily recognized serpentinites, composed almost entirely of serpentine group minerals, range in colour from bright apple-green through dark olive-green to a dark greenish-black or black. Occasionally, some may be dark red due to the presence throughout of fine hematite. In general the serpentinites are massive, extremely fine-grained, brittle, and have a splintery or conchoidal fracture. Magnetite is a ubiquitous associate of the serpentine-rich rocks. Magnetite may occur as fine disseminations, as large irregular shaped dendritic aggregates, as subparallel streaky bands, or a branching network of fracture-filling veinlets. The textural pattern of magnetite is not consistent over any great distance in a single serpentinite

body. A coarse granular texture is observable in some specimens where individual serpentine pseudomorphs are outlined by fine magnetite.

Colours and textures of the ultramafic rock vary widely with the presence of other minerals in addition to serpentine. The predominant colour is greyish green to greenish-black. These rocks are massive or schistose and are rougher to the touch in contrast to the "soapiness" of the serpentinites. Shiny cleavage surfaces of pyroxene, flakes of chlorite and phlogopite and acicular bundles of fibrous amphibole are easily recognizable in hand specimen. Highly schistose rocks are not abundant but do occur as a result of marginal shearing of the ultramafic bodies.

PETROGRAPHIC CLASSIFICATION

In this study, 250 thin sections were prepared and of these, approximately 200 were selected for more detailed study. The classification of the ultramafic rocks as presented here is based on their present mineralogy. The original nature of the intrusion has been taken into consideration in establishing the group name, only in the case of the less altered varieties. Estimated modal compositions determined visually from thin sections are considered to have an accuracy for each constituent, of approximately 5-10%. Modal compositions of all specimens used in the classification are listed by groups in Appendix V111. Specimens 1-72 inclusive are listed separately in this Appendix because they represent consecutive samples in a detailed study

of two single ultramafic bodies.

Eight groups have been recognized and Table 1 lists the range of modal composition present within each group. The grouping is illustrated on a four-component triangular diagram in Fig. 4. The ultramafic rock groups are as follows:

A. SERPENTINITE is typically a completely serpentinized rock containing variable quantities of secondary magnetite. Small amounts of brucite, phlogopite, spinel, carbonate, talc, chlorite, and sulphide minerals may also be present.

B. TREMOLITE SERPENTINITE constitutes the next most abundant ultramafic rock type, and is characterized by the presence of considerable secondary tremolite. Phlogopite content is less than 5%. Occasional remnant olivines and pyroxenes indicate the original peridotite composition of the rock. Magnetite and spinel are common accessories and as with the serpentinites, secondary brucite, carbonate, talc, chlorite and sulphide minerals may also be present.

C. TREMOLITE-PHLOGOPITE SERPENTINITE is a variant of the tremolite serpentinite having a phlogopite content greater than 5%. As with other subdivisions, this is an arbitrary boundary designed to describe the rock more accurately. Minor olivine and orthopyroxene occur as remnant constituents in the predominant serpentine (20-54%) and tremolite (10-55%) mixture.

D. PHLOGOPITE SERPENTINITE describes the rather minor group of serpentinite rocks containing greater than 10% phlogopite but completely lacking in tremolite. Chlorite, magnetite, spinel, carbonate and talc are occasionally present.

TABLE 1

RANGE OF ESTIMATED MODAL COMPOSITIONS IN ULTRAMAFIC ROCK TYPES OF THE MANITOBA NICKEL BELT

GROUP	ROCK NAME	SERPENTINE	OLIVINE	ORTHO-PYROXENE	TREMOLITE	ANTHOPYLLITE	BRUCITE	PHLOGOPITE	MAGNETITE	CHROME SPINEL	CARBONATE	TALC	CHLORITE	CLINO-PYROXENE	SULPHIDE	VERMICULITE
A	SERPENTINITE	63-98	-	-	<1	-	1	3	25	5	7	10	5	-	25	-
B	TREMOLITE-SERPENTINITE	10-85	10	10	6-89	-	<1	2	9	3	8	15	12	-	15	-
C	TREMOLITE-PHLOGOPITE SERPENTINITE	20-54	10	15	10-55	-	Tr	5-35	5	Tr	5	10	10	-	3	-
D	PHLOGOPITE-SERPENTINITE	65-88	-	-	-	-	-	10-16	15	1	1	<1	5	-	-	-
E	SERPENTINIZED PERIDOTITE	28-45	10-40	35	25	-	1	1	1-10	5	3	-	15	-	15	-
F	TREMOLITE-OLIVINE ORTHOPYROXENITE	45	20	20-60	45	-	-	20	5	1	9	2	4	20	8	-
G	AMPHIBOLE ORTHOPYROXENITE	5	2	22-60	70	20	-	3-35	3	<1	<1	2	-	-	5	-
H	MISCELLANEOUS ALTERED TYPES	75	20	-	48	30	1	25	10	15	35	48	35	-	15	40

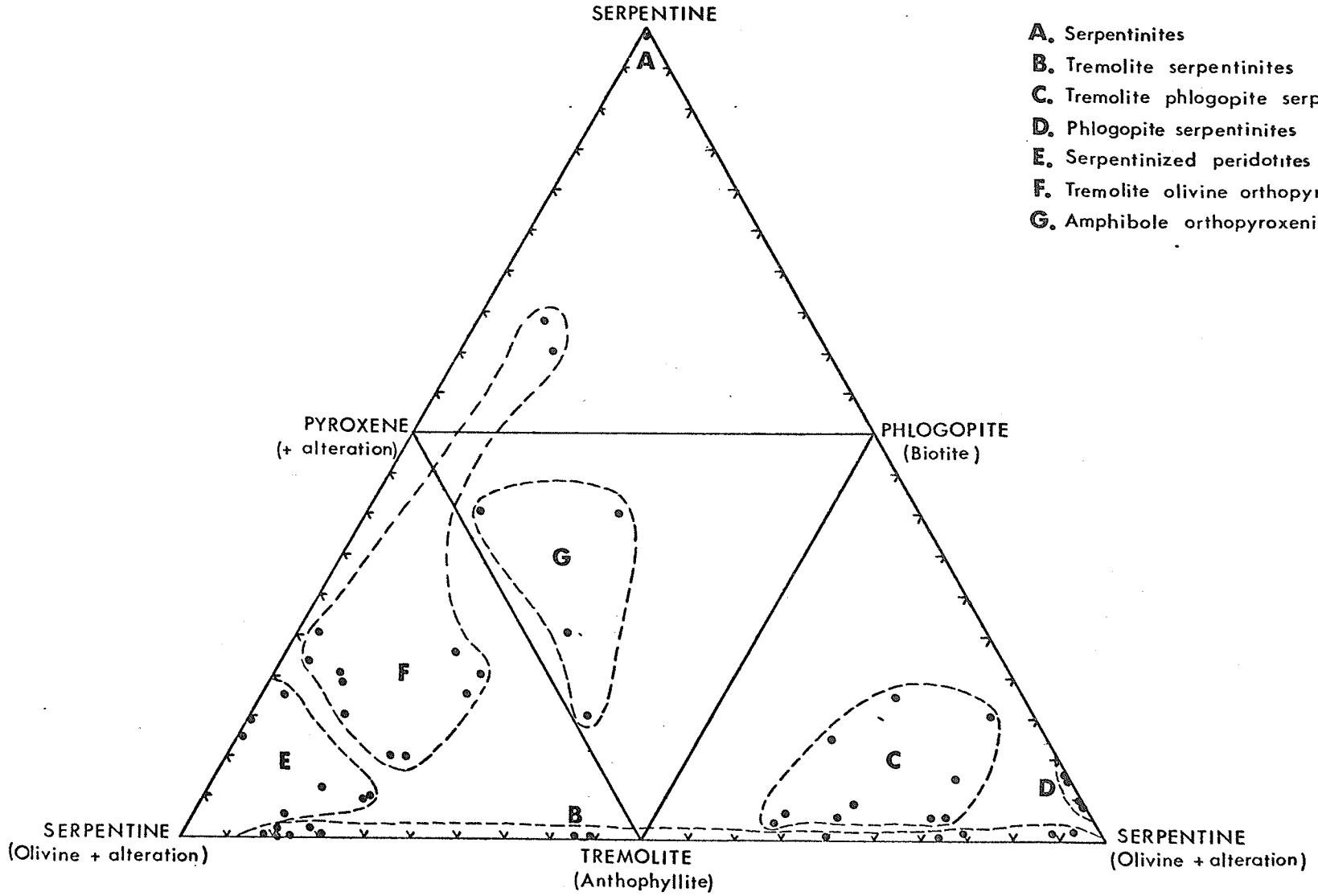

FIG. 4 : Four component triangular plot of modal compositions of the ultramafic rock groups. Miscellaneous types (group H) have been omitted. Compiled from data in Appendix V111.

E. SERPENTINIZED PERIDOTITE contains sufficient unaltered olivine and pyroxene to determine with reasonable certainty the percentage of original constituents. Olivine plus serpentine comprise more than 50% of the rock with orthopyroxene and tremolite combining to form at least 10%. These rocks have an average content of 35% serpentine. Magnetite and spinel are the principal accessories.

F. TREMOLITE-OLIVINE ORTHOPYROXENITE describes a group of rocks similar to (E.) above, which have at least 50% orthopyroxene and tremolite. Olivine and serpentine are present together or singly and constitute less than 50% of the total. Clinopyroxene is rare except for one specimen (#127) in which it occurs as a principle constituent along with serpentine, olivine and tremolite. Magnetite and chrome spinels are generally present in small amounts in most samples. Phlogopite, when present, may be a major constituent as in #147A, where it forms 20% of the rock and is associated with olivine and orthopyroxene.

G. AMPHIBOLE ORTHOPYROXENITE is a small group of rocks differing from the tremolite-olivine orthopyroxenite group in having an almost total lack of olivine and serpentine. Orthopyroxene (22-60%) and either tremolite (0-70%) or anthophyllite (0-20%) constitute the bulk of the minerals present. Biotite and phlogopite are also conspicuous.

H. MISCELLANEOUS ALTERED TYPES. Into this group are placed those rocks whose modal compositions preclude a place in the previous groups. They are essentially anthophyllite, vermiculite, talc, carbonate or chlorite-rich serpentinites. A few are

completely lacking in serpentine but contain considerable amphibole, talc and phlogopite.

It should be emphasized at this point, that the groups outlined above do not indicate the mineralogy of any one or more individual ultramafic intrusions, but reflect only the mineralogy as it pertains to single specimens. As will be shown later in the study of a single body, the mineralogy changes abrupty in many places, reflecting differences in composition and their reactions to metamorphic and metasomatic processes.

PETROGRAPHY OF THE ULTRAMAFIC ROCKS

OLIVINE

Olivine is a rare constituent of the highly serpentinized and tremolitized ultramafic rocks of the nickel belt and can rarely be recognized in hand specimen. More commonly, rounded serpentine pseudomorphs and a granular texture are the obvious features indicative of original olivine-rich rocks. Thin section study however, has shown the presence of olivine in widely scattered locations as illustrated in Fig. 5. Olivine apparently occurs more frequently towards the southwest end of the belt, but this is probably due to the larger number of samples examined in that area. Olivine is most abundant in groups E and F of the mineralogical classification, with occasional appearances in rocks of groups B, C, G and H.

Parially serpentinized olivine grains have a wide range in size and shape in different specimens. Commonly they are

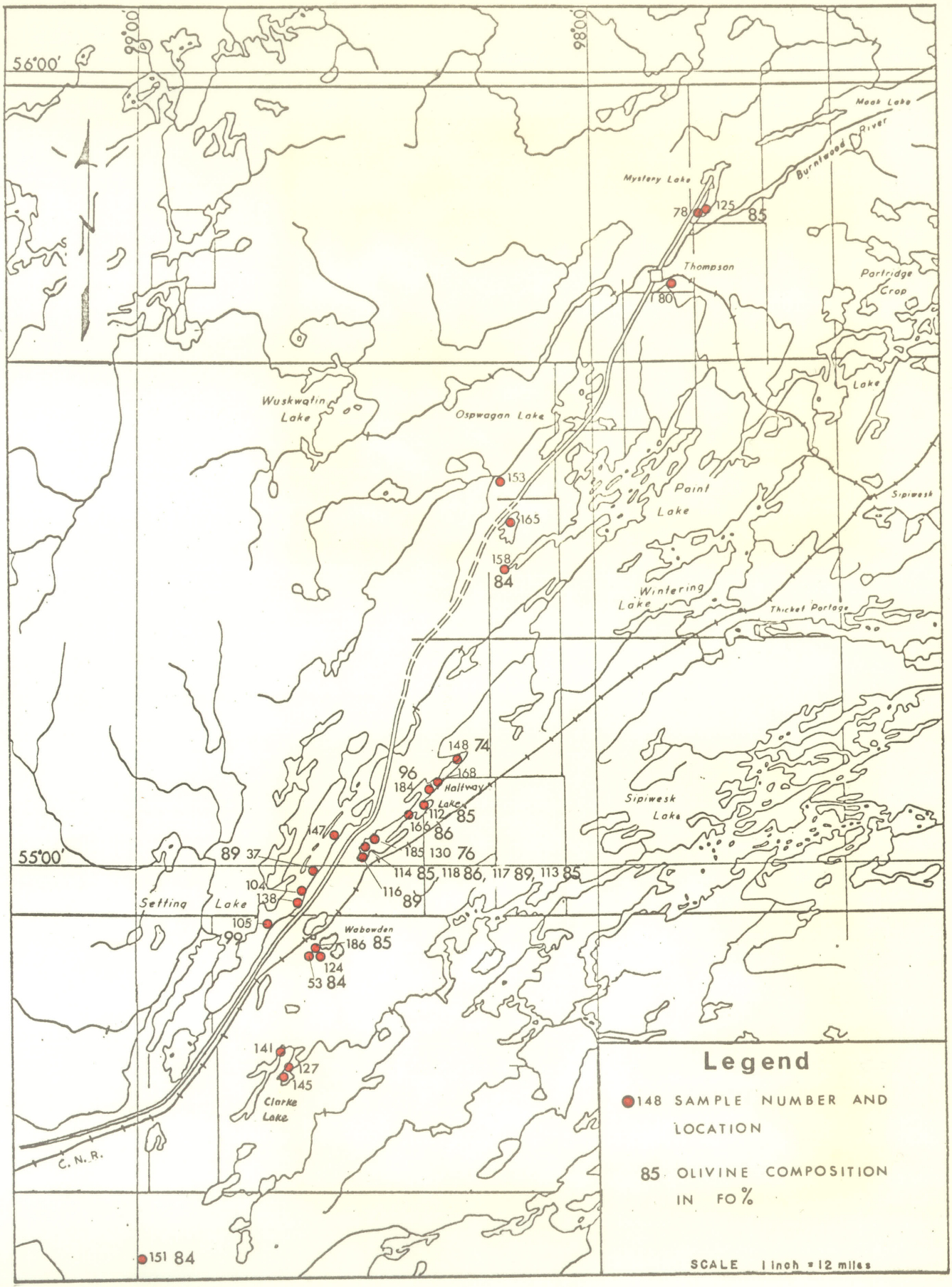

FIG. 5 : Geographical distribution of olivine in ultramafic rocks and some olivine compositions.

subrounded to elongate-oval shaped with maximum dimensions of 6x4 mm. and averaging 2x1.5 mm. In a few places they exhibit a highly irregular form. Unaltered olivine generally occurs as subangular to subrounded remnant fragments more or less evenly distributed throughout partially serpentinized grains (Plate 1). The unaltered particles are seldom larger than .2x .15 mm. and generally much less. The remnant fragments of each olivine grain retain optical continuity as illustrated in Plate 2.

The degree of serpentinization of most olivine occurrences is greater than 60% but in some specimens is much less. Boundary outlines of the original olivine crystals can usually be identified by a change in the orientation of a group of unserpentinized remnants or by a distinct zone of secondary magnetite, which in some grains completely encircles the pseudomorph (Plate 3). Magnetite-rich pseudomorphs after olivine of this type give the rock a mottled appearance when viewed in hand specimen.

Olivine, poikilitically enclosed in broad plates of orthopyroxene occurs in some of the less serpentinized and more pyroxene-rich ultramafic rocks. This texture is well developed in sample #186 and is illustrated in Plate 4. Serpentine is partly or completely pseudomorphic after olivine leaving the pyroxene relatively unaltered. Irregular fractures in the olivine extend out through the surrounding pyroxene.

OLIVINE COMPOSITION

Olivine composition determinations were made on 19 samples

PHOTOMICROGRAPHS * OLIVINE

PLATE 1: Angular remnant olivine fragments in serpentine composed of cross-fibre veinlets and a fine grained felted mass. Secondary magnetite and subhedral spinels are also present. #158 (x54).

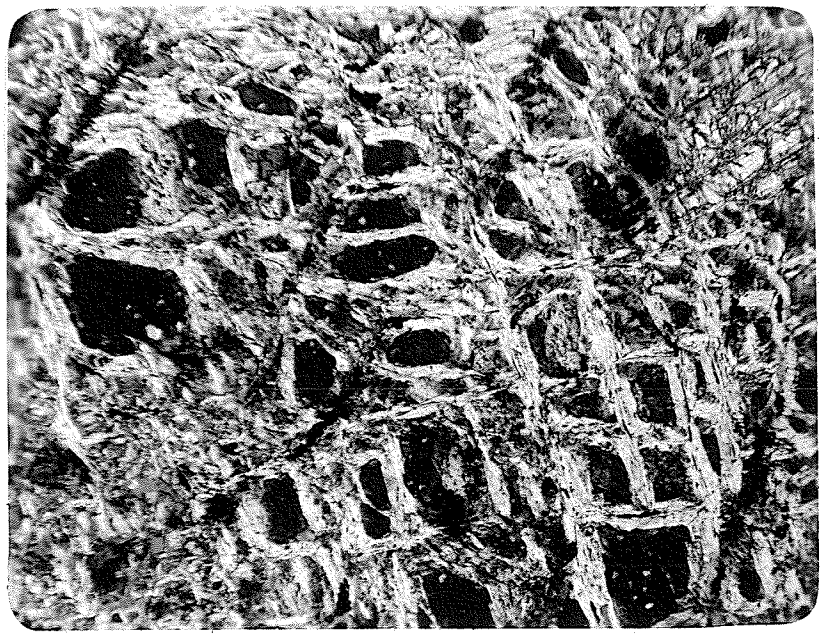

PLATE 2: Olivine grain subdivided into roughly quadrilateral areas by mesh serpentine. Fragments at extinction, show optical continuity. #185 (x78).

PHOTOMICROGRAPHS * OLIVINE

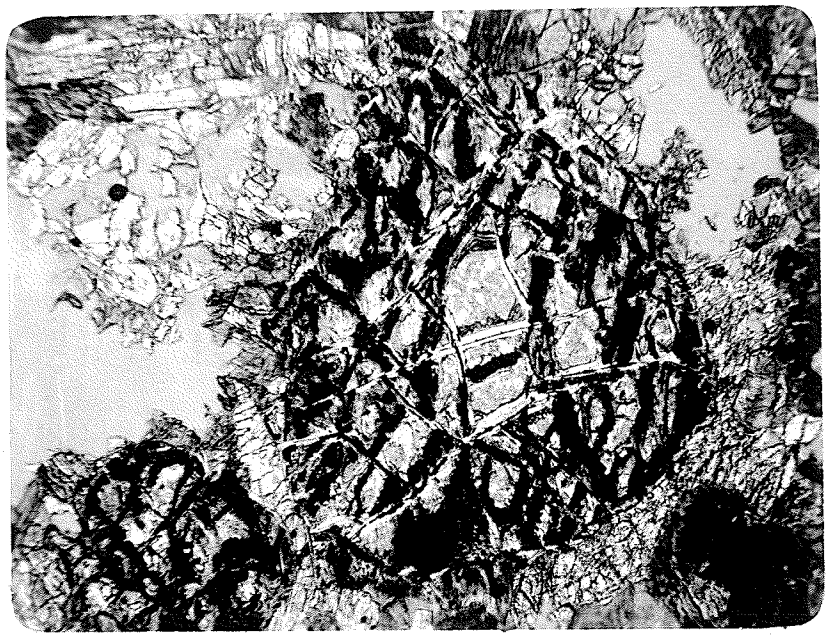

PLATE 3: Serpentinized olivines containing abundant secondary magnetite. The surrounding material is predominantly secondary tremolite. #51.(x50).

PLATE 4: Partially serpentinized, rounded olivine crystals enclosed poikilitically in brown orthopyroxene. Radiating fractures from olivine extend out through the pyroxene #186 (x115).

TABLE 2

COMPOSITION VARIATION IN OLIVINE IN ORDER OF INCREASING FORSTERITE CONTENT

Sample	Field No.	% Fo *
148	M17A-426	73.9
130	W62B-595	76.1
53	M11A22-39A	83.9
151	H140B-390	83.9
158	Paint South	84.2
113	W62K-492	84.7
114	W62K-540	84.9
112	M20A-463	85.0
186	M11A39-252	85.4
118	W62L-885	85.6
125	Mys. Isl.	85.7
166	W62xB-62	86.6
75	ASS.1-4	87.0
185	W62D-475	88.1
117	W62L-734	89.1
37	M14C-368	89.5
116	W62N-526	89.7
184	M19B-104	96.4
105	M8AE-253	99.6

* Olivine Compositions by R. N. Delabio, G. S. C. 1965.

from the nickel belt by Mr. R. N. Delabio of the Geological Survey using the X-ray methods outlined by Jambor and Smith (1964). Table 2 lists the olivine compositions in order of increasing forsterite content. Because of the small quantity available, no attempt was made to make determinations on the additional occurrences of olivine shown on Fig. 5.

Table 2 shows a considerable range in composition of olivine from scattered localities along the nickel belt. The overall range is Fo 74-99, but 15 of the samples have compositions in the range Fo84-90 with a mean of Fo 86.2. This correlates reasonably well with the data compiled by Smith (1961) for olivine compositions in ultramafic rocks of the Precambrian Shield. Three composition determinations in Table 2 appear to be anomalous. Samples #148 and #130 from Halfway Lake intrusions contain unusually low magnesium contents, 74 and 76 percent forsterite respectively, whereas sample #105 from Setting Lake is essentially pure forsterite (Fo 99.6). The magnesium-rich olivine #184, with a forsterite content of 96.4 percent was contained in a band of carbonate rock adjacent to an ultramafic intrusion. The rock constitutes a forsterite marble of probable sedimentary origin.

The Halfway Lake olivines are prominant constituents in rocks classified as tremolite-olivine orthopyroxenites and differ in their mode of occurrence from the general description of olivines given above. The orthopyroxenites are composed of large plates of orthopyroxene in an advanced stage of replacement by tremolite (Plate 8), in a matrix of lath shaped and stubby crystals of tremolite. Highly irregular olivine patches

enclosing stubby tremolite and clinochlore crystals are scattered through the matrix. Abundant magnetite in the olivine occurs as diffuse, branching, irregular masses and aggregations, which separate areas of unaltered olivine into irregularly shaped but optically continuous fragments (Plate 5). Serpentine is absent in most grains, but when it does occur, is a yellowish brown, almost isotropic variety confined to the outer margins of the olivine-magnetite areas, and accompanied in some cases by small green spinels. The appearance and textural relationships of this olivine suggest it may be of secondary origin.

Olivine #105 with its high forsterite content ($Fo_{99.6}$) occurs in a coarse grained orthopyroxenite in Setting Lake. Associated minerals are anthophyllite and phlogopite, with minor quantities sulphide, magnetite, serpentine and red spinel. The olivine is partially altered to serpentine and talc but is free of secondary magnetite. Such an unusually rich forsterite might suggest a secondary origin by regeneration from serpentine, but whether this is actually the case is uncertain.

An additional occurrence of olivine in Setting Lake merits mention in that it has developed by recrystallization due to intense shearing. Sample #104 is a tremolite-bearing olivine orthopyroxenite, on which shearing has superimposed a pseudo-banded texture. Highly fractured and irregularly shaped crystals of orthopyroxene, extensively replaced by fine shreds of chlorite and tremolite needles, occur as narrow bands separating poorly defined zones of serpentine containing lenses and

PHOTOMICROGRAPHS * OLIVINE

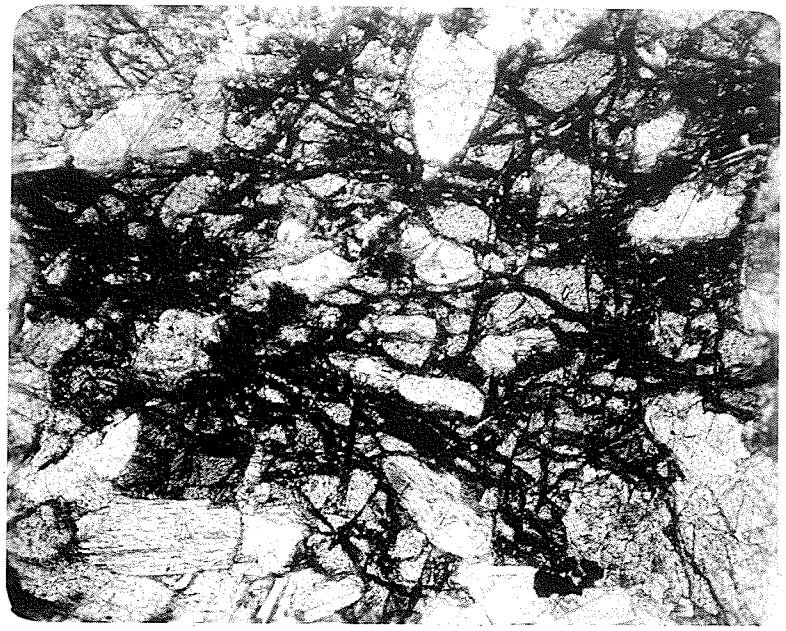

PLATE 5: Olivine (grey), perhaps of secondary origin, poikilitically enclosing tremolite laths (white). Fine granular magnetite abundant but no serpentine is present. #148. (x50).

PLATE 6: Regenerated string-like olivine grains (high relief) in serpentine (S). Fine flaky chlorite (C) forms central band. Sulphides (black). #104. (x100).

individual flakes of chlorite, laths of tremolite and small, often elongated, string-like grains of olivine (Plate 6). The exact composition of this olivine was not obtainable. Although its optic sign was indeterminate, its high 2V indicates a magnesium-rich forsterite. It is difficult to imagine igneous olivine surviving the serpentinization, recrystallization and shearing to which this rock has been subjected.

The regeneration of olivine by metamorphism of serpentine has been described by a number of writers, principally Hess (1960) and Durrell (1940). The latter writer has described the formation of granoblastic olivine and associated clinochlore at a serpentine contact with quartz monzonite. The iron released as magnetite by the serpentinization of igneous olivine was not reincorporated during transformation of the serpentine, resulting in a more magnesium-rich olivine.

The investigation of the system MgO-SiO_2-H_2O by Bowen and Tuttle (1949) clearly demonstrated that olivine is regenerated from serpentine in the presence of water vapour above approximately 500°C. In the absence of water, the recrystallization takes place at a higher temperature, starting at about 600°C. (Brindley and Zussman 1957). Exact optical criteria for the identification of regenerated olivine in serpentinites and serpentinized ultramafic rocks however, has yet to be formulated.

PYROXENE

Both orthopyroxene and clinopyroxene are found in the less serpentinized ultramafic intrusions of the nickel belt, with

the former occurring in by far the greater frequency. Orthopyroxene is present as an important constituent in groups E, F and G of the mineralogical classification outlined in Table 1. It is also found in minor quantities in some of the rocks of groups B and C. Except for varying textural relationships, there is little difference in either composition or alteration of orthopyroxene in the tremolite-olivine orthopyroxenites, amphibole orthopyroxenites or serpentinized peridotites.

As seen in thin section, orthopyroxene occurs as broad, ragged, plate-like crystals ranging up to a maximum size of 9x5 mm. On an average, the pyroxene forms anhedral, equidimentional grains with dimensions of 2.5x2.5 mm. It ranges from colourless to the pale pink pleochroic colours of hypersthene, has a large 2V, negative optic sign, and characteristic straight extinction. As determined by its optics, the orthopyroxene ranges in composition between En77-85, with a mean of En 82.

Commonly, orthopyroxene plates enclose rounded olivines or serpentine pseudomorphs after olivine, and occasionally small spinels in a poikilitic relationship. Of much rarer occurrence, but considerable interest in the orthopyroxenes of the belt, are exceedingly fine lamellae of exsolved calciferous monoclinic pyroxene, oriented parallel to (100) (Plate 7). This feature, which was noted in only 4 samples of orthopyroxene, has been described in detail by Poldervaart and Hess (1951).

Alteration of orthopyroxene takes place to tremolite, anthophyllite, talc, chlorite or serpentine. A brown, dusty, opaque alteration of unknown composition is present in a few

PHOTOMICROGRAPHS * ORTHOPYROXENE

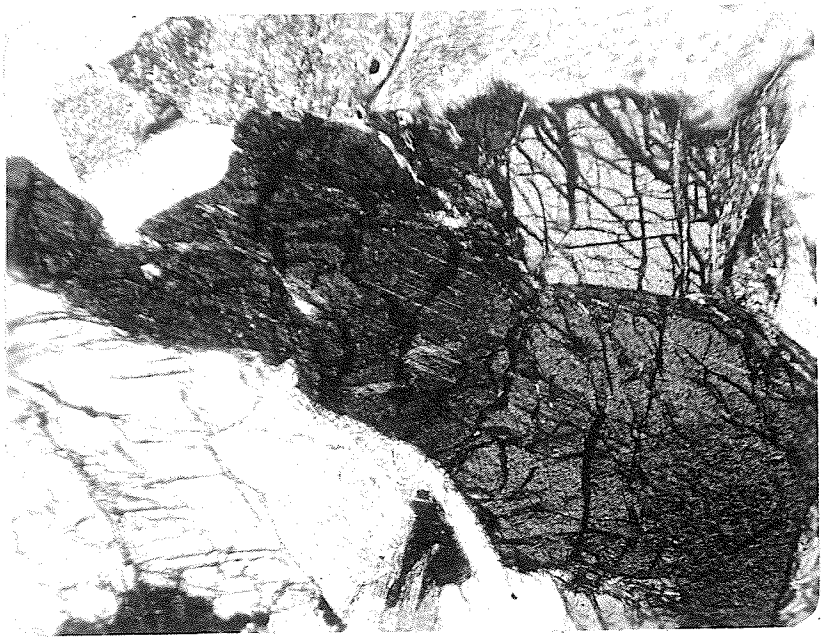

PLATE 7: Fine exsolution lamellae of calciferous monoclinic pyroxene parallel to (100) of orthopyroxene. The host mineral is at extinction. #166 (x54).

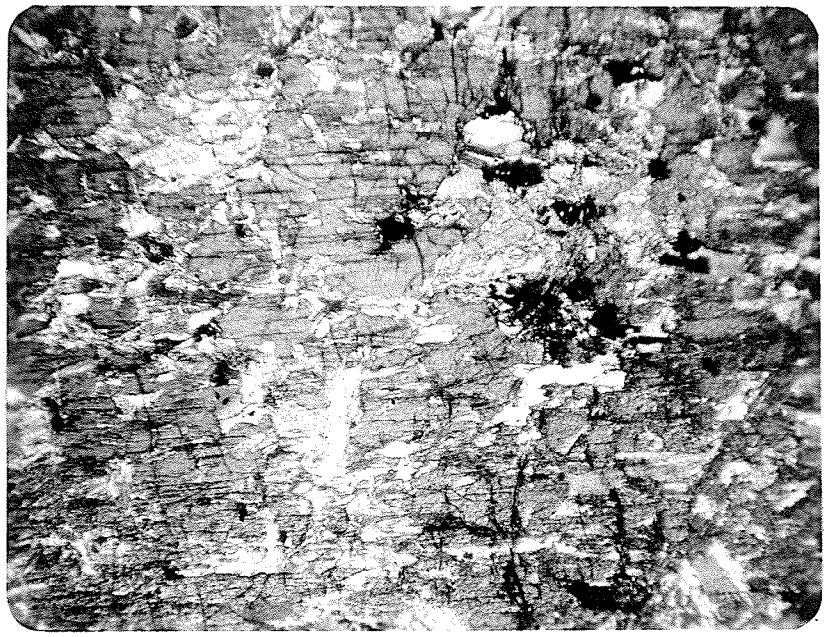

PLATE 8: Orthopyroxene (grey) being replaced by wispy laths of tremolite (white). The replacement is guided, but not completely controlled by the pyroxene cleavage #130. (x34).

samples. In the tremolitized rocks, orthopyroxene is readily replaced by colourless tremolite (Plate 8). The process can be seen at all stages of development. Wispy laths to needle shaped crystals of tremolite, aligned parallel to and cross cutting the pyroxene cleavage, increase in abundance until only scattered, highly corroded vestiges of the original pyroxene remain. In the final stage, textural relationships in the tremolite are the only clue to the former presence of the pyroxene (Plate 13).

Where tremolitization has not been a dominant factor in the alteration of the ultramafic rocks, the resistance of orthopyroxene compared with olivine, to the process of serpentinization is readily apparent. Serpentine first attacks the pyroxene along cleavages (Plate 9), progressively increasing in extent until only ghost-like remnants are preserved. (Plate 10). The process is completed with the formation of a "bastite" pseudomorph, the textural pattern of which occasionally indicates the nature of its parent mineral. Features of this type will be considered further in the section on serpentine minerals.

Monoclinic pyroxene-bearing ultramafic rocks are extremely rare. Only three of the samples examined in thin section contained clinopyroxene (#29, 30, 127). Two of these, #29 and 30 are adjacent samples from an intrusion in Setting Lake, which has been classified as a tremolitized clinopyroxenite. Both contain approximately equal amounts of tremolite and clinopyroxene with minor chlorite, magnetite and associated sulphides. The clinopyroxene occurs as evenly scattered, corroded remnants

PHOTOMICROGRAPHS * ORTHOPYROXENE

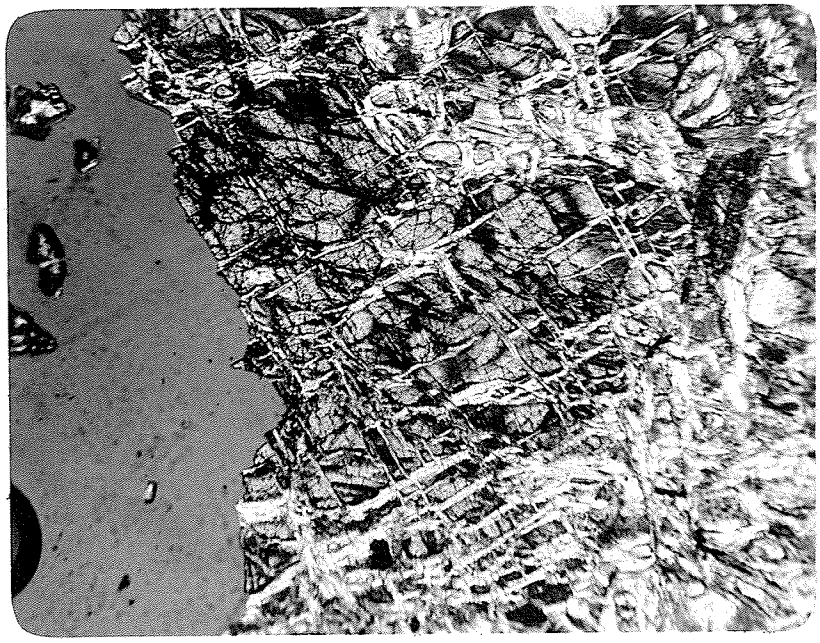

PLATE 9: Serpentine (cross-fibre chrysotile) veinlets preferentially replacing orthopyroxene along cleavages, as seen in basal section. #185 (x78).

PLATE 10: Highly serpentinized orthopyroxene (white) enclosing serpentine pseudomorph after olivine and a few red spinels. #125. (x115).

surrounded and extensively replaced by colourless anhedral tremolite. The optical properties of the colourless pyroxene, $2V=(+)40°-45°$, $Z \wedge C=41°$, suggests it is an augite.

CHROME SPINELS

Minerals of the spinel group, referred to here as the chrome spinels, are common accessories in the ultramafic rocks. They occur as disseminated grains seldom making up more than 1% by volume, as estimated from thin sections. Grain size of the spinels ranges up to 1.4 mm. across, but generally they are much smaller, with an average size of .3x.3 mm. Larger grains are anhedral and highly fractured. The smaller crystals tend to be more euhedral but perfect form is generally not attained.

Textural relationships of the spinels with sourrounding minerals are variable. Small spinels are enclosed within partially serpentinized olivine and orthopyroxene crystals (Plates 1, 10), in serpentine, anthophyllite, tremolite, magnetite and sulphides. At Mystery Lake, spinel occurs preferentially with sulphides, which form a network surrounding rounded granules of serpentine. Smaller crystals are occasionally seen within those granules, which undoubtedly represent original grains of olivine. Two distinct ages of spinel are also indicated in a peridotite from Halfway Lake (#117). Small reddish-brown grains are enclosed in olivines and these in turn have highly irregular grains of a light brown spinel molded around the margins. A second generation of spinel is evident in some

highly altered rocks, such as the ultramafic body invaded by pegmatite, immediately south of Wabowden. Clouds of minute euhedral to subhedral spinels are present in tremolite and have evidently been derived during alteration, from orthopyroxene.

Fractures in spinels may occasionally be filled with sulphide as at Mystery Lake (#125) or with magnetite and serpentine (#118).

A considerable range in composition of the chrome spinels is indicated by variation of unit cell edge dimensions. Cell edge determinations on twelve chrome spinel concentrates were made in the X-Ray Crystallography laboratory, University of Manitoba, using the method outlined in Appendix 111. Accuracy of the determinations is considered to be generally about .002Å, with variations from this value in some samples. Concentrates could only be prepared from material having a higher than average content of spinel minerals and an effort was made to include as large a variety of colours as possible. Table 3 lists the cell edge dimensions, accuracies of the values and the colour of spinels as seen in thin section.

The colour variation in the chrome spinels is one of their most striking features. A selection of nearly all coloured varieties is illustrated in Plates 11 and 12. From a total of fifty-seven occurrences, as observed in thin section, the principal colours and their frequency are as follows:

1) Reddish-brown	54%
2) Brown	14%

TABLE 3

CELL EDGE DIMENSIONS OF SOME CHROME SPINELS

SAMPLE	LOCALITY	COLOUR	CELL EDGE (Å)	ACCURACY (Å)
128A	Halfway Lake	Pale green	8.112	±.001
117	Halfway Lake	Reddish-brown	8.115	.002
132A	Clarke Lake	Yellow	8.122	.002
118	Halfway Lake	Yellow-brown	8.124	.002
185	Halfway Lake	Reddish-brown (zoned)	8.134	.002
128B	Halfway Lake	Brown	8.141	.001
112	Halfway Lake	Pale yellow-brown	8.146	.002
125	Mystery Lake-Is	Dark red-brown	8.256	.002
82	Ospwagan Lake	Opaque	8.256	.003
76	Mystery Lake	Dark red-brown	8.259	.002
31	Setting Lake	Opaque	8.295	.005
126	Clarke Lake	Opaque	8.32	.01

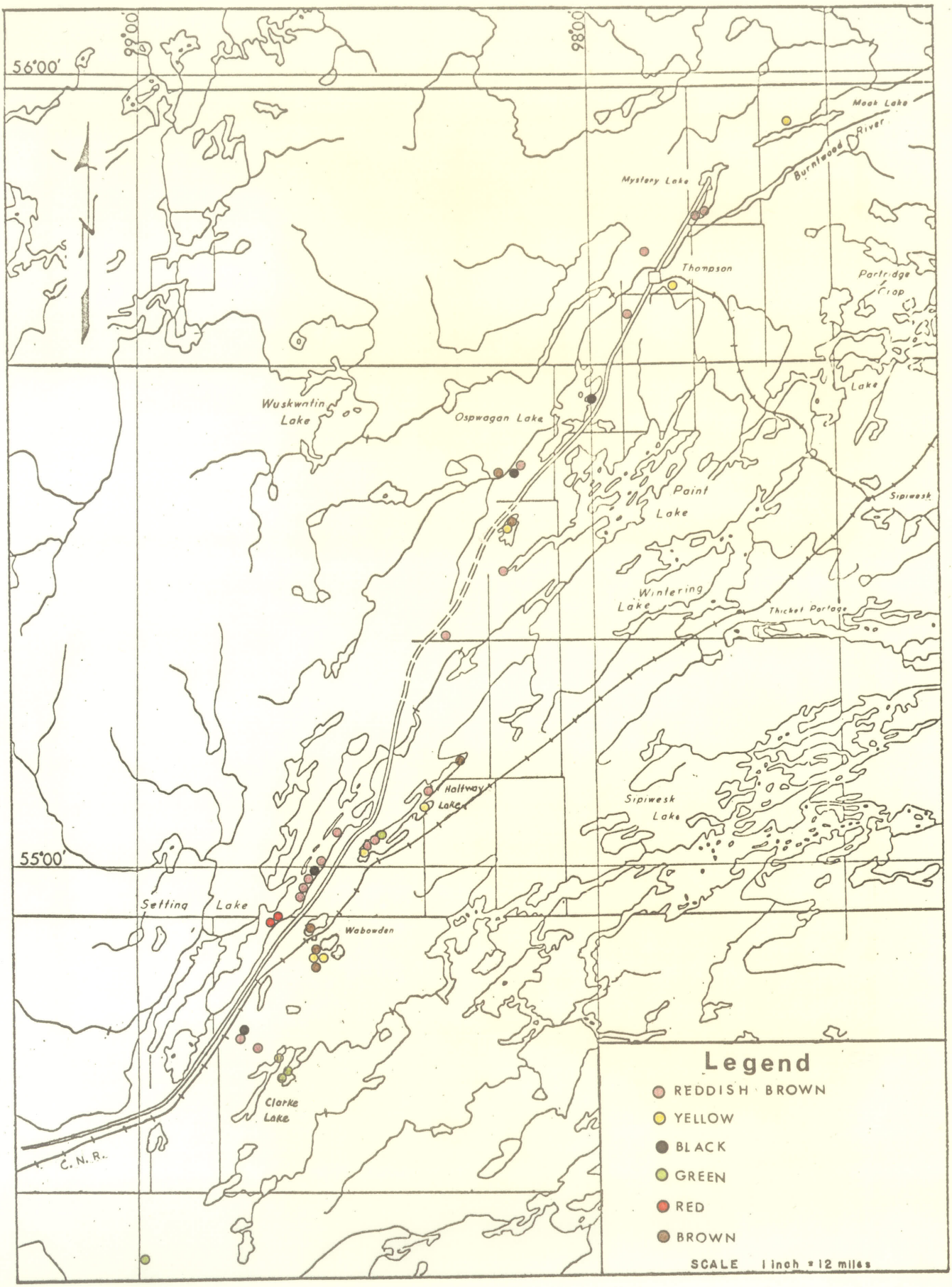

FIG. 6 : Geographical distribution of coloured chrome spinels in the nickel belt ultramafic rocks.

3) Yellow-brown, yellow 12%

4) Green, brownish-green 9%

5) Black 7%

6) Red 4%

Figure 6 shows the geographical distribution of the principal coloured spinels in the ultramafic rocks along the Manitoba nickel belt. Where thin section examination indicated the presence of more than one colour variety within an individual ultramafic body, the colour plotted is that with the greater abundance and frequency. No particular colour variety of spinel shows any preferred geographical location, indicating that their compositional differences are not due entirely to environmental conditions, which undoubtedly varied from place to place.

From Figure 6 and the list of colour frequencies, it can be seen that the reddish-brown spinel is by far the most abundant (Plate 11A). This group includes those reddish-brown spinels which are distinctly colour zoned (Plate 11D). The central area is nearly opaque, grading outwards through a reddish-brown zone to a yellow-brown marginal zone. Narrow opaque rims are evident in the yellow-brown spinel of Plate 11B. The opaque material has resulted from incipient alteration. MacGregor and Smith (1963) describe alteration of this type in the chrome spinels of the Mount Albert ultramafic intrusion. Narrow opaque rims of a second spinel phase, first develop around parts of the grain, gradually increasing in thickness and extent until the entire grain is completely altered spinel. A similar alteration of chromite from the Webster-Addie ultra-

PHOTOMICROGRAPHS * CHROME SPINELS

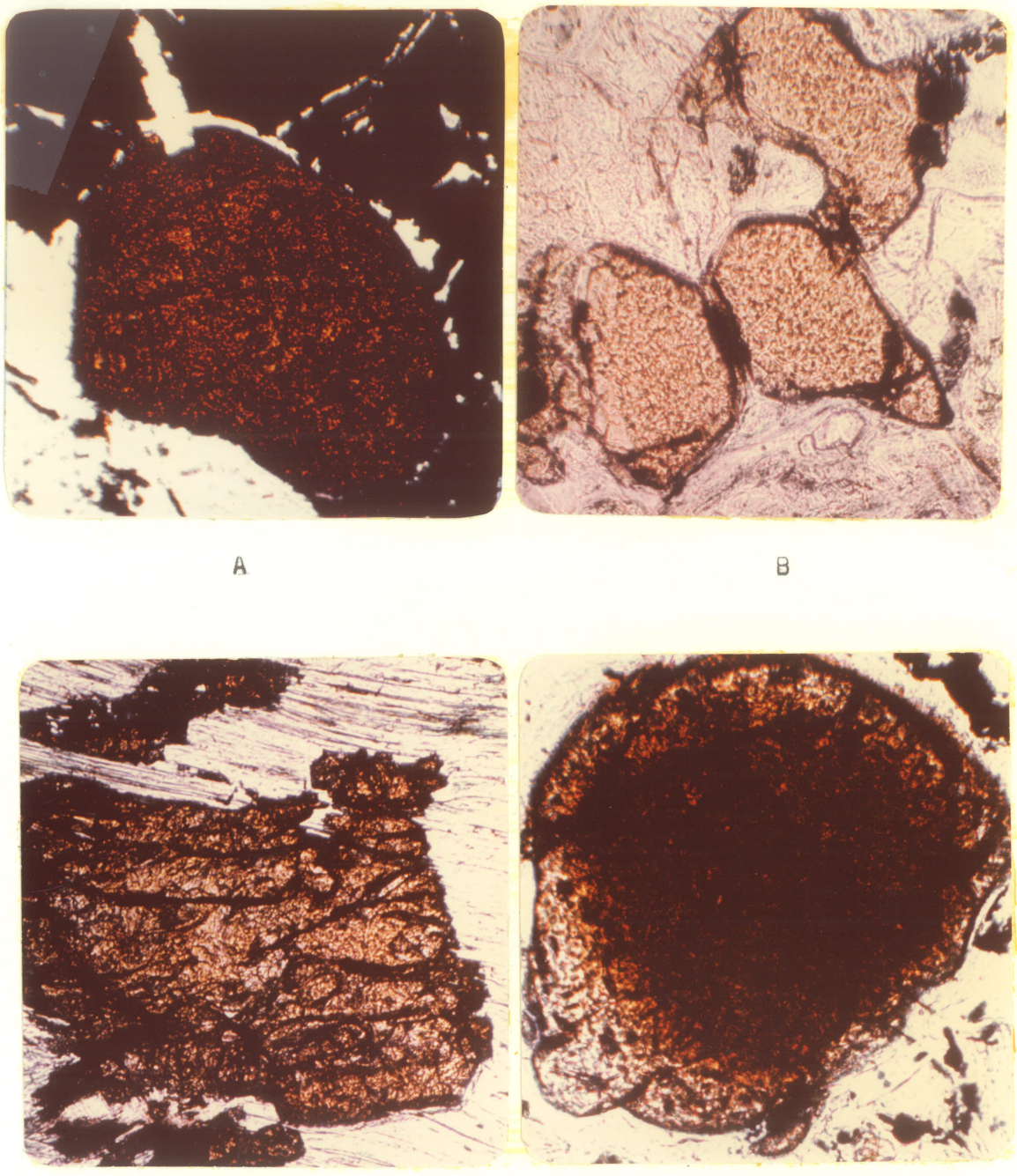

A B C D

PLATE 11:

A. Reddish-brown spinel with associated sulphides. Mystery Lake #125. (x115).
B. Yellow-brown spinel with opaque rims. Halfway Lake #112. (x34).
C. Brown spinel in phlogopite. South end Halfway L. #128. (x63).
D. Zoned reddish-brown spinel. Top group, NW. of Thompson #154. (x176).

PHOTOMICROGRAPHS * CHROME SPINELS

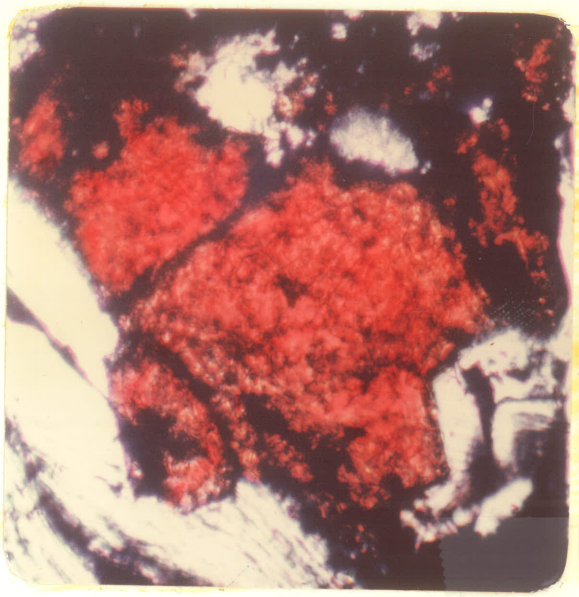

A

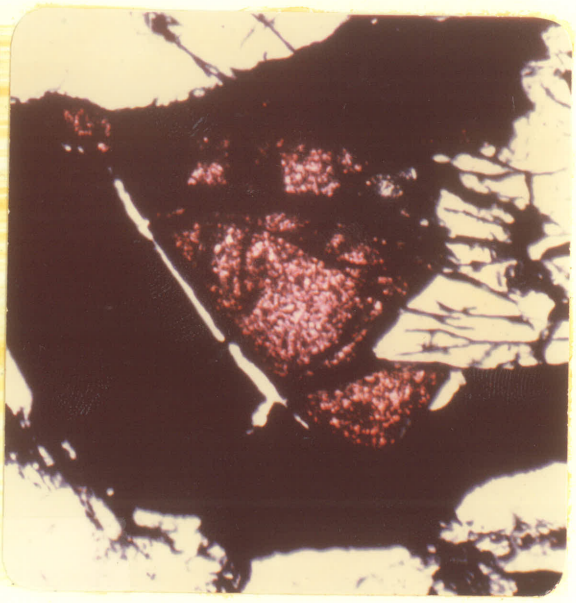

B

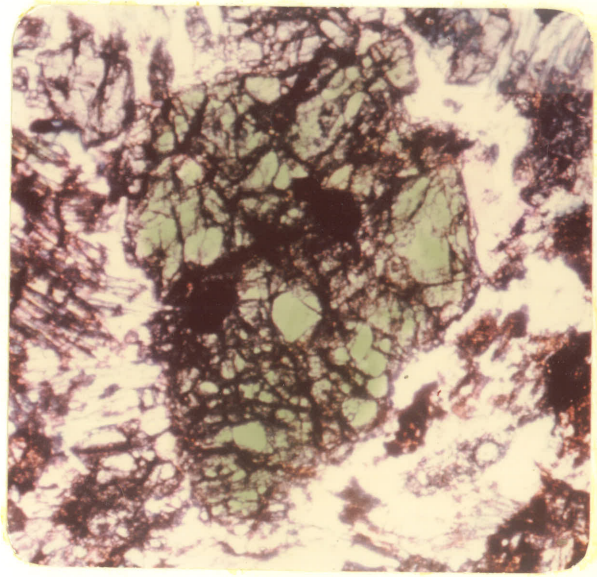

C

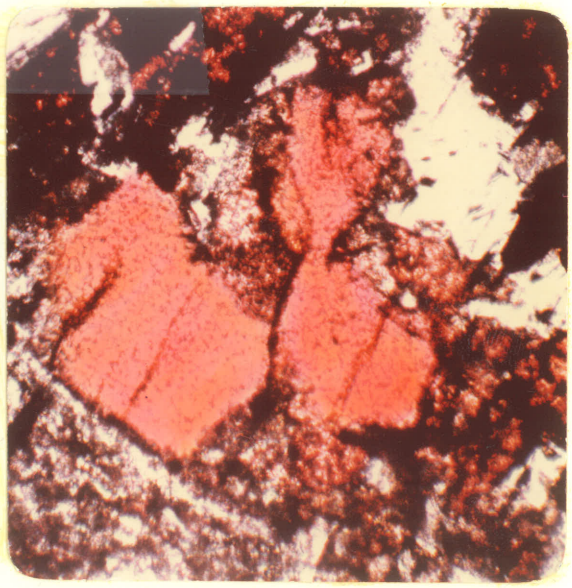

D

PLATE 12:

A. Red spinel. Setting Lake #170A. (x224).
B. Plum-coloured spinel with associated sulphides. Setting Lake #170. (x113).
C. Pale green spinel. Halfway Lake #128A. (x48).
D. Red spinel. Setting Lake, #105. (x25).

mafic ring, has been described by Miller (1953). It is common also in chromite from the Shetland Islands, as described by Phillips (1927). Advanced alteration of this type however, has not been encountered in the chrome spinels from the nickel belt.

Of much rarer occurrence are the red and green spinels illustrated in Plate 12. The plum-coloured variety (12B) has been included with the red spinels in calculating frequency.

Unit cell determinations of selected spinels (Table 3) show a wide range of values, from 8.112Å-8.32Å. Even from such a small number of determinations, it is evident that an approximate correlation exists between the spinel colour, which is reflective of composition and the unit cell dimension. The paler coloured varieties have the smallest unit cells, while the dark reddish-brown and black spinels have in general, much larger cell dimensions. However, some digression from this relationship is evident from Table 3. Reddish-brown to dark red brown spinels show a considerable range of cell size (8.115-8.259Å), while varying little in colour.

MacGregor and Smith (1963) have formulated determinative curves for the chrome spinels, plotting unit cell values against content of Al_2O_3, Cr_2O_3, $Cr_2O_3+Fe_2O_3$, MgO and FeO. Increasing cell size results from an increasing content of chromium and ferric iron at the expense of aluminum in the trivalent or octahedral sites of the crystal structure. Similarly, an increase also takes place when ferrous iron substitutes for magnesium in the divalent or tetrahedral sites. The difference in the ionic radii of the substituting cations in both sites accounts for the variation in the unit cell dimension, which

hence constitutes a parameter for estimating chemical composition.

A high chromium and low iron content is responsible for the bright red spinels shown in Plates 12A and 12D. With increasing ferrous iron and a high chromium content, the spinel colours trend toward reddish-browns and opaque grains with a reddish tinge. (Plates 11A and 11D). Completely opaque and black spinels have cell dimensions towards the high end of the scale and probably approach true chromites in composition. The yellow and yellow-brown to brown varieties have a high alumina content. (Plates 11B, 11C). Ferric iron is considered to produce the brown colour (Deer, Howie and Zussman, vol. 5, 1962). The green spinel (Plate 12C), with an extremely small unit cell is undoubtedly a magnesium and aluminum-rich variety, somewhere close to pleonaste in composition.

Chemical analyses of the chrome spinels are not available. It is uncertain therefore, whether a chemical correlation exists between the different spinel types and the composition of the host ultramafic rocks. A correlation between the composition of chromites and host rocks has been established for a number of areas in the Western Hemisphere by Thayer (1946).

AMPHIBOLES

Tremolite

The extensive development of clearly secondary amphiboles in many of the ultramafic rocks, testifies to the considerable metamorphism and metasomatism which they have undergone since consolidation and serpentinization. Tremolite is abundant in rocks of groups B, C, E, F and G and is only absent in the

pure serpentinites. Anthophyllite occurs in a number of bodies where marginal alteration is extensive.

Tremolite varies from colourless to pale green and faintly pleochroic. Crystal habit is variable from anhedral grains forming an equidimentional mosaic to acicular, spear-shaped grains up to 2 mm. long. Grain size in a single specimen is often variable. Lensoid aggregates of tremolite in serpentine give a rude foliation to a specimen from the Joey Lake body. In general however, tremolite occurs as lath-shaped crystals with stubby cross sections. Optical examination of a large number of specimens has shown the mineral to be optically negative, $2V=70-80°$ (est.) and $Z \wedge C$ varying between 17°-23°.

In many cases, tremolite can be directly observed replacing primary pyroxene. Where replacement has gone to completion, the occasional aligned schiller inclusions or poikilitic texture with serpentinized pseudomorphs after olivine, testify to the original presence of pyroxene. The latter feature is illustrated in Plate 13, where oriented, anhedral tremolite crystals have completely replaced poikilitic pyroxene. Although not seen in the photograph, remnant pyroxene is visible in other parts of the section. Such a specimen is classified as a tremolite serpentinite. Where the tremolite content is high compared to serpentine, it is often impossible to decipher the primary mineralogy. Small areas of serpentine in which minute tremolite laths appear to be growing, are surrounded by compact tremolite of varying grain size.

Occasionally tremolite shows some serpentinization (Plates

PHOTOMICROGRAPHS * TREMOLITE

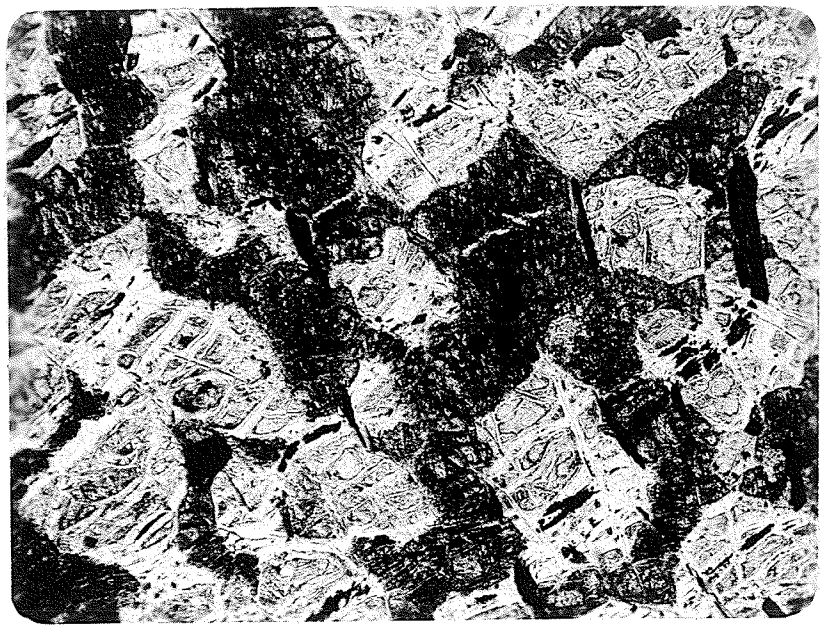

PLATE 13: Poikilitic plate of tremolite (at extinction) pseudomorphic after pyroxene and enclosing serpentine pseudomorphs after olivine. #164. (x42).

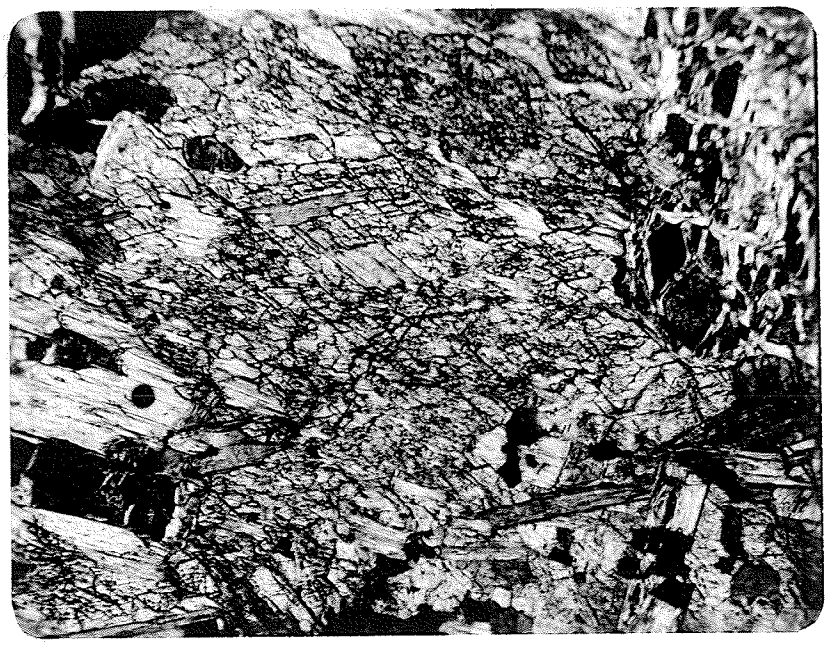

PLATE 14: Basal section of tremolite being replaced by phlogopite flakes, which are aligned parallel to cleavages. #59. (x69).

15, 16). Narrow veinlets of a late generation of serpentine, which is usually yellowish-brown and distinctly pleochroic, cut across tremolite crystals and occupy cleavages. Complete disintegration however, is rare. The alteration of tremolite to phlogopite is a common hydrothermal effect, prevalent in the Wabowden ultramafic body, which has been intersected and altered by innumerable narrow pegmatites. (Plate 14). The alteration of tremolite to carbonate and talc is occasionally seen in the specimens examined.

Anthophyllite

Rhombic amphibole is a relatively rare mineral in the ultramafic rocks compared to the more general occurrence of tremolite. It occurs as fibres and needles in bundles arranged in radiating groups, which may reach up to 6 mm. across. When abundant in hand specimen, it is greyish-green to white, brittle, and arranged as parallel fibres or small easily identifiable rosettes. Some anthophyllite occurs as coarse blade-like crystals up to 3 mm. long, showing excellent prismatic cleavage and cross fractures. With this form, it closely resembles monoclinic amphibole in general appearance. Optically, the mineral shows parallel extinction, positive elongation, a large optic angle and positive sign. A further check on its identification was made from massive material by X-ray diffraction. (Diffractogram #63).

Anthophyllite occurs as narrow, but near-massive zones adjacent to pegmatite dykes in the M11A Wabowden body. The brittle fibres are occasionally arranged in parallel bundles

PHOTOMICROGRAPHS * TREMOLITE

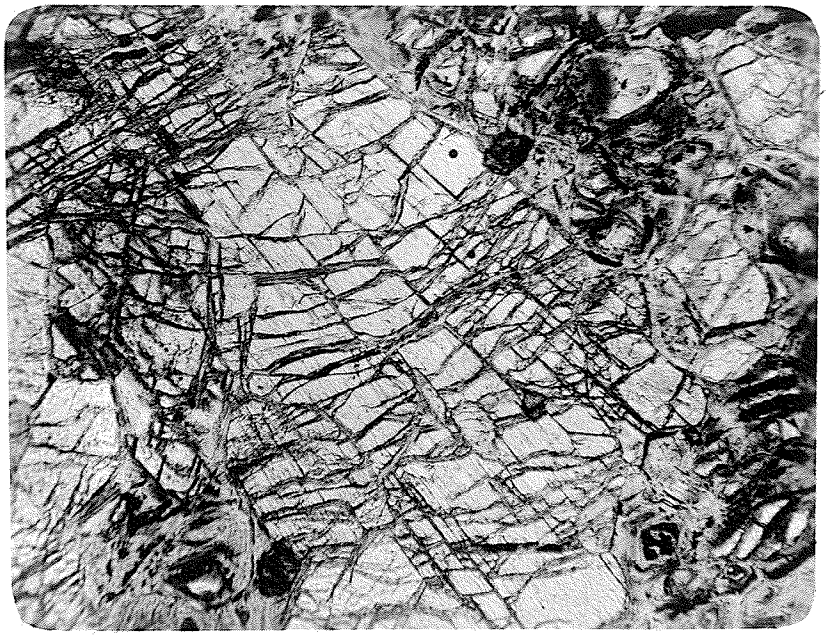

PLATE 15: Tremolite crystal finely veined by a brownish-green pleochroic serpentine. Three grains of spinel are visible, one of which is enclosed within the tremolite. #112. (x72).

PLATE 16: Twinned tremolite crystal veined by cross-fibre serpentine. Clinochlore (white, at top) is unaffected by the serpentine. #113. (x113).

at right angles to the contact and may reach 1½ inches long. Massive anthophyllite in the marginal zone of a body in Setting Lake (#15, 19, 20) shows a well developed rosette pattern (Plate 17). Fine radiating needles of anthophyllite pierce through partially serpentinized olivine grains in the amphibolitized ultramafic rocks which outcrop at the southwest end of Assean Lake (#75). The needles also penetrate chlorite, but show some evidence of replacement by carbonate and talc. (Plate 18). A similar texture is preserved in the highly altered specimen from Manasan (#162) which is essentially a talc-carbonate-chlorite anthophyllite rock.

PHLOGOPITE

Phlogopitic mica is a relatively common secondary mineral in the ultramafic rocks, although usually present in minor quantities. It becomes a major constituent in some of the hydrothermally altered ultramafic rocks adjacent to pegmatites in the Wabowden body (sample nos. 48-72 incl.). Chemical and mineralogical details of this alteration will be presented in a later section. Phlogopite is important in the altered zones of other bodies, which it is presumed, have been affected by nearby granitic intrusions. Tremolite-phlogopite serpentinites (group C), phlogopite serpentinites (group D) and the amphibole orthopyroxenites (group G) all have significant contents of phlogopite.

Crystals of phlogopite occur in thin section as broad, lath-shaped prismatic section, in places with ragged termin-

PHOTOMICROGRAPHS * ANTHOPHYLLITE

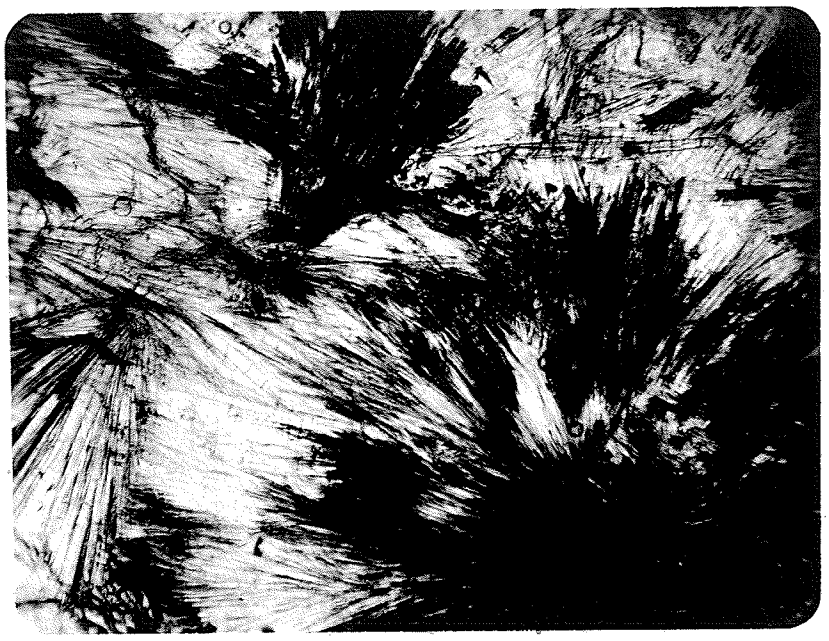

PLATE 17: Fibrous rosette pattern of anthophyllite as developed in a massive specimen from Setting Lake. Fine grained magnetite is also present. #15. (x22).

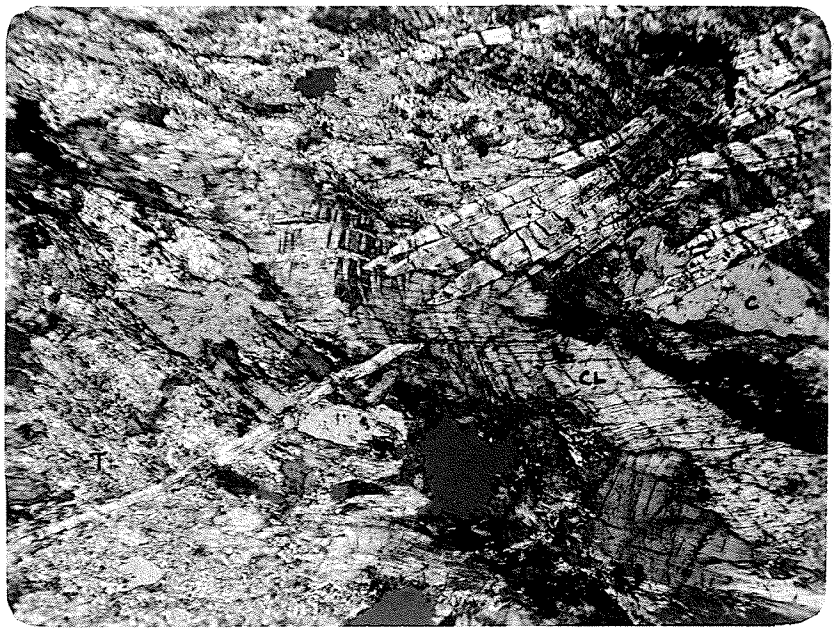

PLATE 18: Acicular anthophyllite crystals penetrating chlorite flakes (CL) but being partially replaced by talc (T) and carbonate (C). #75. (x78).

ations, anhedral basal sections, or as near-equidimensional flakes. They are often deformed and exhibit bent cleavage traces. In occasional specimens of phlogopite serpentinite, the phlogopite may occur as isolated flakes or grouped into clusters in the serpentine, producing a glomeroporphyritic texture. The larger crystals range in size from 6x1.5 mm. to 1.5x1 mm., but the smaller and more irregular flakes average 1x.8 mm. No indication of preferred orientation of phlogopite is visible in any of the samples examined.

Characteristically, the phlogopite is faintly pleochroic from colourless to pale golden yellow. Estimated 2V ranges from 0-5° and the optic sign is negative. A bluish-green pleochroic material forms narrow rims around individual crystals, extends in fine wisps along cleavages and radiates out short distances from cross fractures. It is pleochroic with X= colourless, Y=bluish-green and Z=bluish-green and has an adsorption formula similar to the phlogopite, (X <Y=Z). On basal sections the bluish-green material forms diffuse patches. These patches and rims have their cleavage traces and extinction positions parallel to those of the phlogopite host. The birefringence of the phlogopite is much higher than the rims. The green material is evidently an incipient chloritic alteration of the phlogopite.

The relationship of phlogopite to surrounding minerals is variable. Elongate flakes and equidimentional plates occur in partially serpentinized olivine and to a lesser extent in orthopyroxene (#165). Phlogopite commonly replaces tremolite

(#58), a process which can be seen in all scales of magnitude. Minute phlogopite flakes develop parallel to the tremolite cleavage and eventually join up to form large irregularly terminated crystals. The reverse relationship is not uncommon, where acicular tremolite crystals spear through anhedral plates of phlogopite (#60). Large anhedral plates are often poikilitic with inclusions of magnetite, anhedral tremolites, anthophyllite needles, spinels, and grains of sulphide (#147A, 116). Occasionally, fine lenses and ribbons of a black opaque mineral with brown translucent margins occupy the phlogopite cleavages. Phlogopite is often replaced by a colourless to extremely pale green pleochroic chlorite identified by X-ray diffraction as being clinochlore, near leuchtenbergite in composition (Plate 19). The alteration progresses until a complete transformation to clinochlore has been attained (Plate 20).

CHLORITE

This mineral is common in the serpentinites and derives largely from the period of later metamorphism. Its mode of occurrence and composition are variable. In many places the presence of colourless chlorite in the serpentinites was only recognized during a study of the serpentine group minerals by X-ray diffraction.

The predominant chlorite is a colourless, magnesium-rich clinochlore (leuchtenbergite), which occurs as isolated flakes, narrow lenses of fine grained material or as highly irregular

PHOTOMICROGRAPHS * PHLOGOPITE, CLINOCHLORE

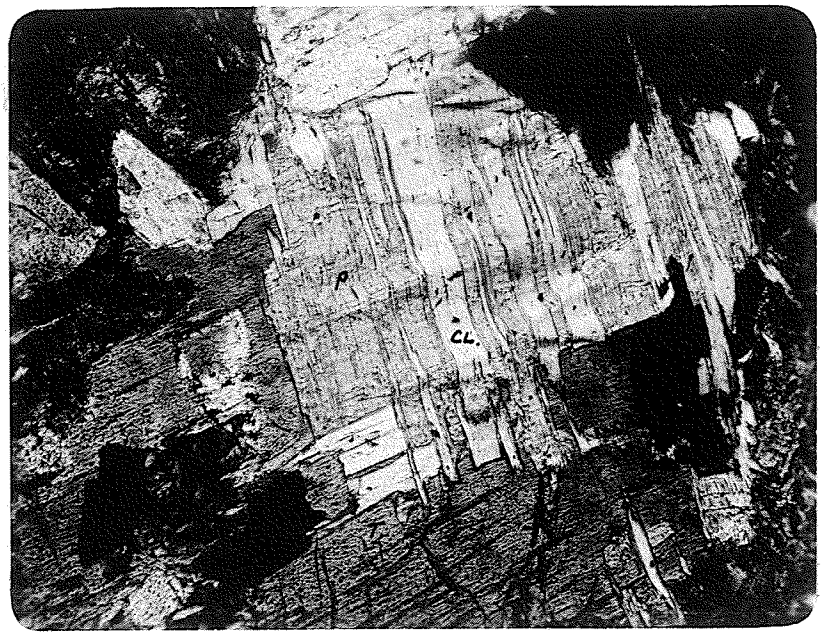

PLATE 19: Alteration of phlogopite (P) to colourless clinochlore (CL) in bands parallel to cleavages. The chlorite is also partially replacing the surrounding tremolite (T). #145. (x75).

PLATE 20: Clinochlore crystals (CL) surrounding remnant tremolite fragments (T). Narrow lenses carbonate and an opaque oxide occupy the chlorite cleavages. #136. (x40).

shaped poikilitic plates. The latter may reach 4x6 mm. in size, enclosing rounded areas of serpentinized olivine, residual orthopyroxene and grains of tremolite (Plate 21). By comparison to the partial chlorite alteration of phlogopite, illustrated in Plate 19, it is inferred that this mode of occurrence represents a clinochlore pseudomorph after phlogopite. Occasional fine tapered lenses of carbonate occupy cleavages of the clinochlore (#55, 201). This feature reaches its best development in an apple-green serpentinite from Setting Lake (#201), which is spotted with the pale brown and white composite crystals. The carbonate from this occurrence is dolomite, as identified by X-ray powder photograph (#A1220). Schwartz (1958) discusses the tendency for carbonate aggregates to occur as lenses on parallel bands in unaltered biotite, chlorite and muscovite phenocrysts, during hydrothermal alteration. They have resulted from growth by crystallization, in some cases by complete replacement and in others, by forcible partition of the cleavages. A ubiquitous associate of the large clinochlore plates is fine lenses and ribbons of a black mineral, occupying the cleavages in a similar manner to the dolomite described above. On basal sections the mineral is seen to form irregular plates of varying size (Plate 22). Some of the thinner plates and margins of the larger ones are translucent and have a deep reddish-brown colour. Its nature and composition is not known.

Clinochlore occasionally forms fine grained lense-like pods in sheared serpentinite (#84, 100, 104). Individual flakes show parallel orientation (Plate 6) and are elongated

PHOTOMICROGRAPHS * CLINOCHLORE

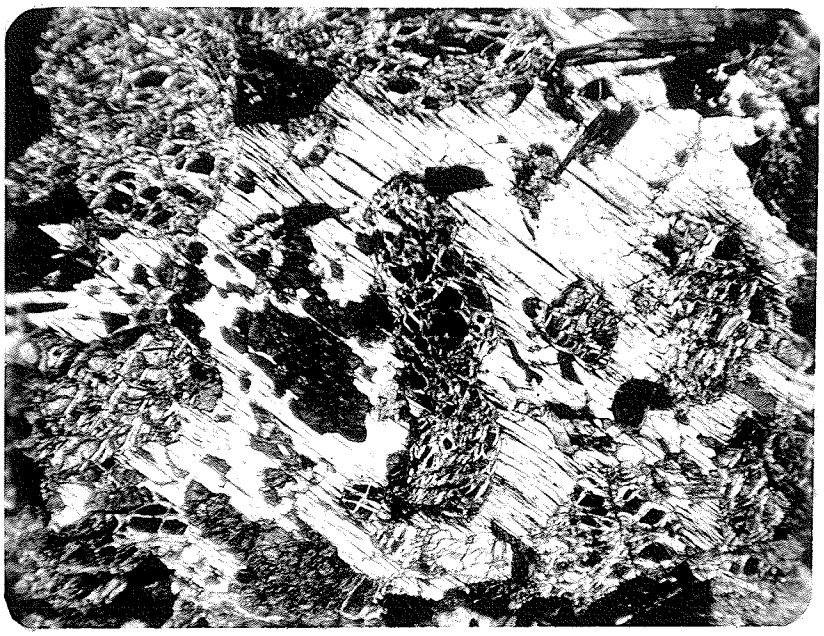

PLATE 21: Poikilitic clinochlore enclosing partially serpentinized olivine, hypersthene and tremolite. #52. (x30).

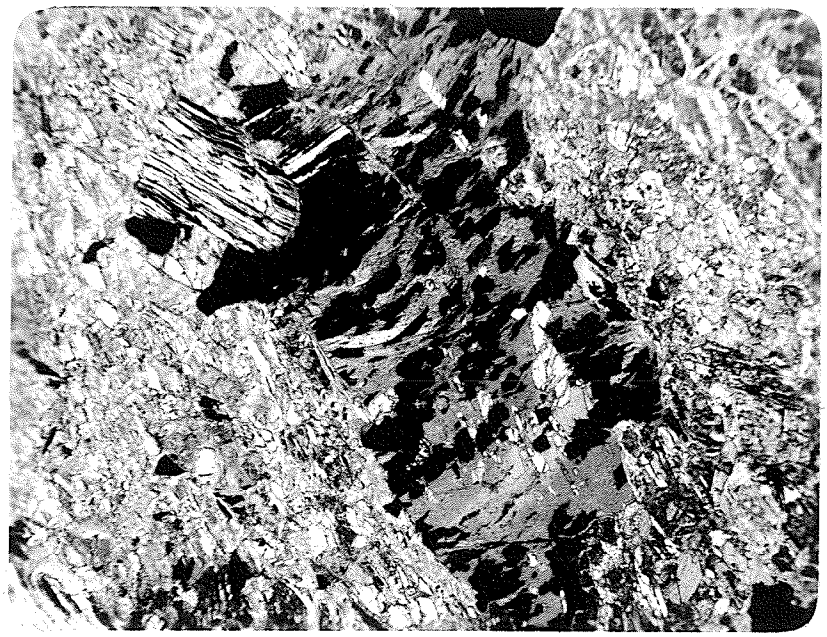

PLATE 22: Basal (001) section of clinochlore showing black plate-like flakes with brown translucent margins, lying parallel to the cleavage. Inclusions are tremolite (white). #17. (x54).

parallel to the general foliation. Colourless chlorite may also occupy irregular to triangular-shaped areas between serpentine pseudomorphs forming a matte of unoriented flakes. Adjacent areas commonly amalgamate to form a crude network. Optically, the colourless clinochlore has greyish-brown birefringence colours, negative elongation and generally straight extinction. The mineral is optically positive with an extremely small optic angle (<5°).

Two occurrences of a rather unusual chlorite in serpentinite (#99, 189) have been identified as leuchtenbergite (X-ray diffractogram #99). Both are nearly colourless, showing a pale greenish tinge on careful examination, but are strikingly pleochroic from pale green to black, with greatest absorption parallel to the cleavage. Birefringence is anomalous brown, with some parts of the larger and greener flakes showing a bluish tinge. Extinction is straight, but rather uneven and sweeping. Elongation is negative and the mineral is optically positive with a small 2V. In specimen #99, from one of the Pipe Lake serpentinites, the pleochroic chlorite occurs as minute wisps and flakes dispersed throughout the serpentine, but more commonly is confined to innumerable oriented lenses with the chlorite itself oriented normal to the lense walls (Plate 23). It is not known at present, why these chlorites, although structurally identical to the colourless clinochlores, should have such anomalous pleochroism.

A green pleochroic chlorite, associated with tremolite occurs along a marginal zone in the M14 serpentinite in Setting

PHOTOMICROGRAPHS * CHLORITE, VERMICULITE

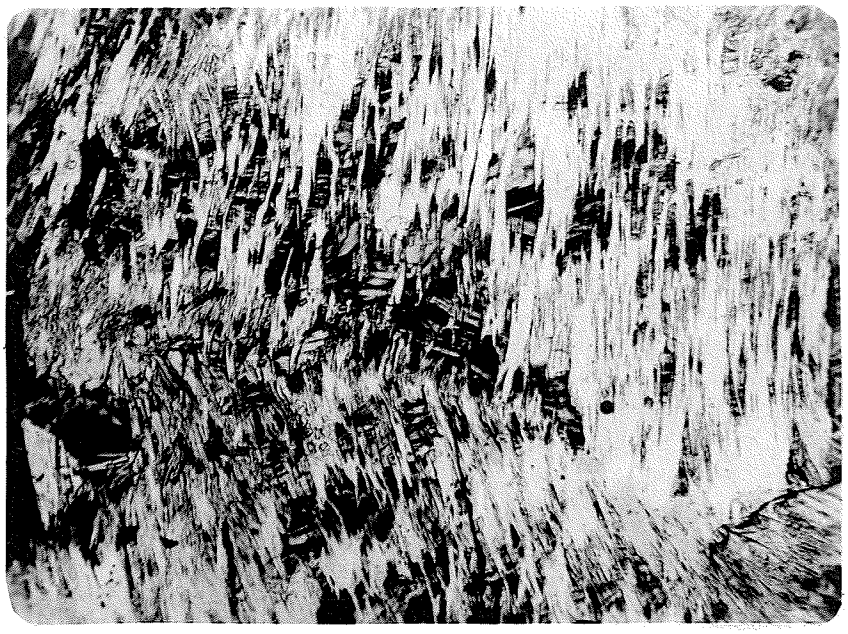

PLATE 23: Oriented lenses of leuchtenbergite in serpentine. The hightly pleochroic flakes are aligned approximately normal to the lens walls. #99 (XN, x50).

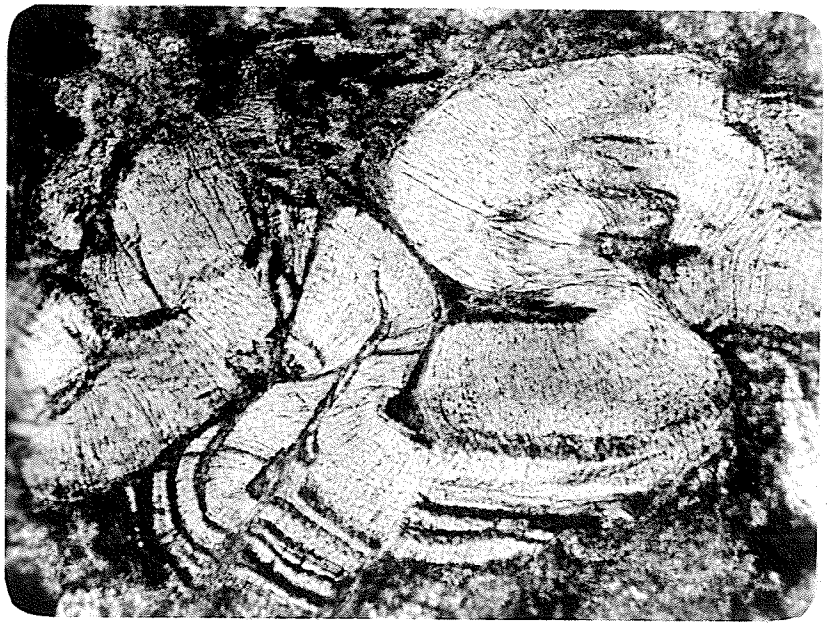

PLATE 24: Vermiculite, showing highly contorted and convoluted structure. Surrounding material principally carbonate and talc. #133. (x107).

Lake. (#21). Almost 4 inches of pure chlorite rock occur adjacent to the biotite-quartz-feldspar gneissic country rock. The chlorite is pleochroic as follows, X=pale yellow brown, Y=blue green, Z=deep blue-green; the optic sign is negative and 2V=5°. Identification by X-ray diffraction (Diffractogram #21) indicates the chlorite is chromium-bearing kotschubeite.

VERMICULITE

Minor occurrences of vermiculite are present in highly altered ultramafic bodies from Halfway Lake (128A, 129) and Conlin Lake (#133, 134, 136). Vermiculite constitutes 40% of one specimen examined and is associated with carbonate and serpentine. Minerals present with vermiculite in other samples include anthophyllite, talc, phlogopite, chlorite, carbonate, serpentine and oxide minerals. The vermiculite presents a prominant micaceous and "vermicular" habit as curved and twisted flakes up to 1.5 mm. across (Plate 24), or in close packed clumps of smaller crystals. The mineral exfoliates upon heating due to the release of water. This characteristic was observed on flakes scraped from sample #129. Optically the vermiculite is pleochroic, with X=pale golden brown, Y=pale green and Z=pale green. Some specimens are faintly pleochroic in light brown and do not show the green colour. Birefringence ranges up to red-blue of the first order. It is biaxial negative with an extremely small axial angle (0-5°). Narrow interlayered bands of pale brown phlogopite are often present

in the curved vermiculite. The phlogopite shows the typical green marginal alteration described above, and its mode of occurrence suggest that it represents the host mineral from which the vermiculite has been derived.

BRUCITE

Brucite is a minor constituent of the ultramafic rocks of the nickel belt, but has a fairly wide distribution, occurring in all rock groups except the amphibole orthopyroxenites. The mineral is restricted to serpentine, from which it apparently has derived by metamorphic processes. Brucite occurs as generally small, lath-like to more equant grains with perfect basal cleavage. Birefringence colours are greyish yellows of the first order. Near-basal sections are close to isotropic and show that the mineral is uniaxial positive. Extinction is parallel but may be highly irregular with an intricate pattern developed. In many instances, colourless clinochlore presents similar optical properties to brucite. Although the chlorite is biaxial, only perfect interference figures enable the observer to estimate the low axial angle. In general however, birefringence colours of brucite are slightly higher than those of clinochlore.

TALC

Talc is a relatively rare mineral in the ultramafic rocks

but does become a major constituent in the marginal alteration of some bodies. Specimens from the Manasan body, 4 miles southwest of Thompson (#161, 162) are white to pale greyish-green massive rocks composed of talc, dolomite, anthophyllite, chlorite, together with minor magnetite and serpentine. Talc forms a fine grained felt-like matte associated with granular dolomite enclosing and partially replacing local areas of coarse chlorite. Talc is abundant in a marginal altered ultramafic from Halfway Lake (#128B). Here, talc appears to have completely replaced original orthopyroxene and is now associated with phlogopite, anthophyllite, chlorite and vermiculite.

In the majority of occurrences however, talc is present in minor amounts and its development appears to have been at a late stage in the metamorphic history. It may occasionally be found replacing secondary tremolite along cleavages and narrow fracture zones (#74, 152), and rarely forms an incipient alteration along cleavage planes of phlogopite (#142). Talc is also found in unmodified serpentinite. It replaces the central areas of mesh serpentine or combined with carbonate, forms irregular diffuse blebs replacing larger and less select areas of the serpentinite (#142). Late fractures filled with talc or a combination of talc, carbonate and opaque oxides, are of rare occurrence. In a specimen from Bowden Lake (#107), talc flakes, up to .6 mm. long are oriented normal to the direction of a veinlet, which crosses and follows boundaries of serpentine pseudomorphs in a serpentinite.

CARBONATES

The carbonate content of the ultramafic rocks is generally low but has a wide distribution, being present in minor amounts in more than half the specimens examined. Calcite and dolomite are both present, with the latter probably in greater frequency. Many samples reacted vigourously in dilute hydrochloric acid during analysis for carbon dioxide, while others, although containing carbonate, showed no effervescence. The presence of small amounts of dolomite can be detected on the diffraction patterns of many otherwise pure serpentinites.

Carbonate is often intimately associated with talc in the replacement of tremolite. It forms lenses and narrow bands in the cleavages of phlogopite (#126). A similar association of dolomite and chlorite has already been described (#119, 201). Carbonate alone or in association with fine granular magnetite may occupy serpentine mesh centres (#207) or occur as cross-cutting late stringers in serpentinite.

MAGNETITE

Magnetite is present in varying quantities in all the ultramafic rock types. Primary subhedral grains are often recognizable but in the serpentinites, magnetite of secondary origin is the prevalent type. The release of iron from primary iron-bearing silicate minerals during serpentinization is a well documented phenomena. Reference has been made previously to the occurrence of magnetite in serpentinized or partially

serpentinized olivine and orthopyroxene crystals. In completely serpentinized rocks, which form the bulk of the ultramafic suite along the nickel belt, the mode of occurrence of magnetite occasionally enables an estimate to be made of the primary mineralogy. Original olivine and pyroxene, altered pseudomorphically to serpentine, release iron which crystallizes as magnetite in situ and thus preserves recognizable "ghost" textures (Plate 33).

Commonly however, secondary magnetite does not show any particular control as regards amount at any one place or in locus of deposition. It may be present as clouds of minute particles in serpentine, as irregular shaped larger grains with a more even pattern of distribution, or as dendritic irregularly-branching aggregates which range up $\frac{1}{2}$ inch across. These concentrations normally include innumerable fragments of serpentine which appear to have become trapped within the aggregating magnetite. Narrow veins and subparallel stringers of magnetite are also common, occurring alone or accompanying one or more of the other forms.

The aggregate and vein-filling magnetite textures can clearly be seen in Plate 25. This shows a specimen of serpentinite core (Plate 25B) and its thin section (Plate 25A) from the M14 body in Setting Lake. An analogy is made between the M14 specimen and a sample of magnetite in apple-green serpentinite from the Fox River Sill (Plate 25C). The Fox River Sill is a layered and differentiated ultramafic body at least 5000 feet thick, which outcrops on the Fox River about 140 miles

PLATE 25

A. Magnetite aggregates in serpentine. M 14 Q ultramafic body, Setting Lake (X 50)

B. Specimen of serpentinite drill core showing magnetite aggregates and veinlets. M 14 Q ultramafic body, Setting Lake. (1½ times natural size.)

C. Serpentinite showing magnetite aggregates and veinlets. Fox River Sill, Man. (1½ times natural size).

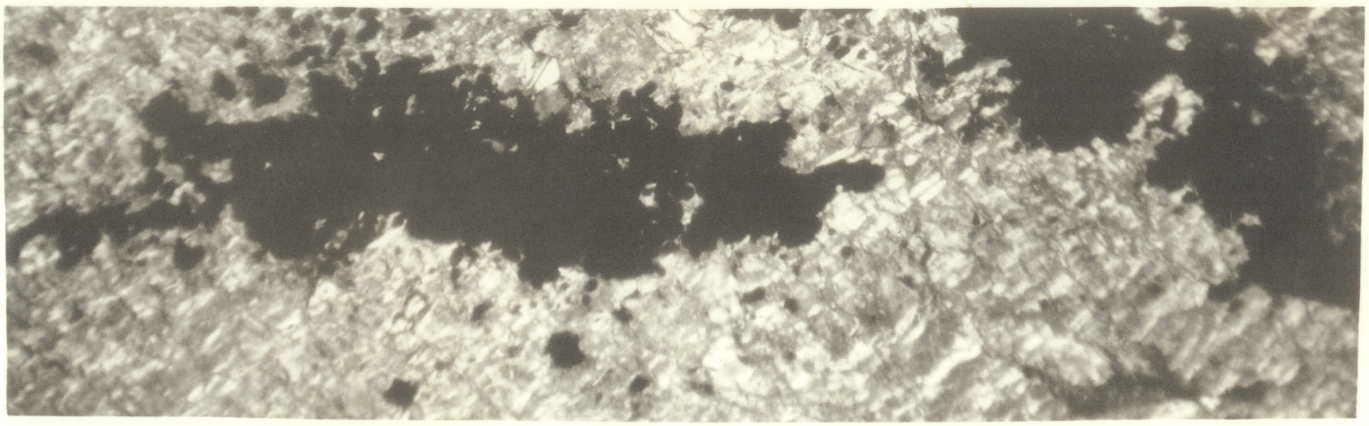

A.

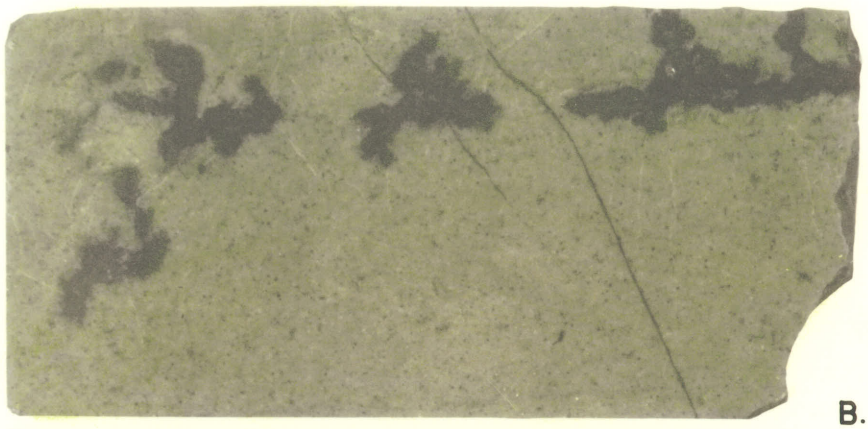

B.

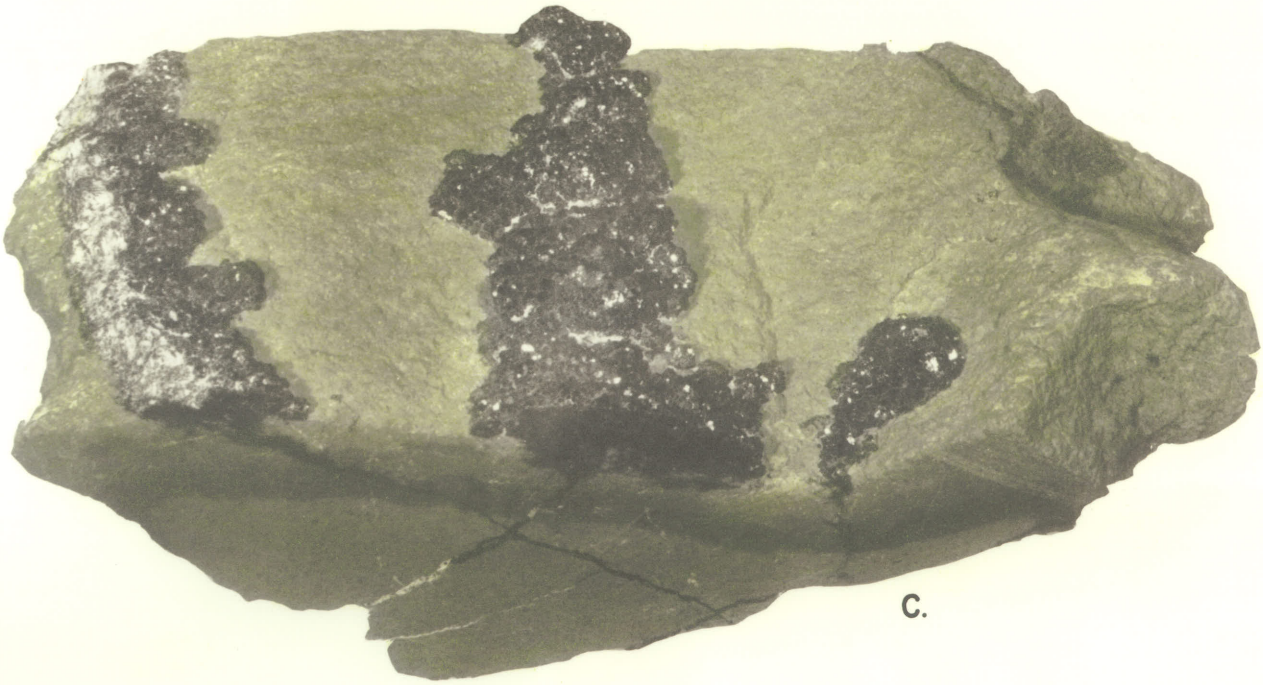

C.

Plate 25.

east of Thompson. The specimen is interesting in that it shows linear but highly irregular masses of magnetite displaying well developed cube and octahedral faces, connected by narrow veinlets of magnetite. Only small amounts of finely disseminated magnetite remain in the surrounding serpentine. This mode of occurrence suggests the accumulation of iron during serpentinization, its movement as a solution along fractures and subsequent deposition as an aggregate at some suitable location. The similarity of texture between the Fox River specimen and the short length of core (Plate 25B) from the nickel belt is striking, and it is suggested that both have had a similar mode or origin.

In a discussion on the origin of intrusive magnetite, Shand (1947) has suggested that residual solutions from a gabroic magma would contain ferrous iron in the form of a ferrous hydroxide hydrosol. This may adequately explain the movement of considerable iron during the process of serpentinization. On the breakdown of primary silicates and their replacement by serpentine, the major portion of the iron released would be in the form of Fe^{++} ions. With the large quantities of water necessary for serpentinization, being readily available, the Fe^{++} ions would form a ferrous hydroxide hydrosol or colloidal solution. In this form, transportation of the iron and accumulation at suitable loci could be attained. Such locations might well be areas of reduced water content or higher oxygen fugacity. At any rate, loss of water from the hydroxide brings about oxidation to magnetite according to the equation

$$3Fe(OH)_2 = Fe_3O_4 + 2H_2O + H_2$$

It is suggested that a process of this type brought about the aggregation of secondary magnetite in many of the serpentinites.

CHAPTER 1V

MORPHOLOGY AND MINERALOGY OF THE SERPENTINES

INTRODUCTION

By reason of the fact serpentine is the predominant mineral in the ultramafic bodies along Manitoba's nickel belt, it was believed desirable to investigate its morphology and mineralogy in some detail. In this chapter, the descriptive petrography of the serpentines as gathered from a large number of thin sections, is correlated with X-ray powder diffraction patterns and differential thermal analysis curves from some of the purer samples of serpentinite, in an effort to elucidate the nature of the serpentine minerals present. Comparison of X-ray and differential thermal data of the nickel belt serpentines is made with other occurrences of serpentine from Manitoba, and with recorded information on serpentines from other parts of the world.

PETROLOGY AND MORPHOLOGY OF THE SERPENTINES

No information on the texture of possible type of serpentine can be gained from hand specimen examination. All serpentines, free from the contaminating minerals described in the previous chapter, are massive, fine grained rocks with a brittle or splintery fracture. Occasionally, specimens of

smooth drill core will show a coarse granular texture in which the attitude of minute fibrous serpentine veinlets may be observed, but this is of rare occurrence. The massive, structurless serpentinites vary in colour from dark greyish-green and greenish-black depending mainly on the magnetite content, to bright apple-green varieties in which a few magnetite or sulphide grains break the complete uniformity of colour and texture. Serpentine also is the predominant silicate mineral in many of the highly altered types previously described. The term serpentine, in some instances modified by dominant morphology, will be used in this section where positive identification by X-ray diffraction has not been attempted or is still doubtful.

Optically, the serpentines can in general be identified as belonging to chrysotile, antigorite or lizardite groups. Optical data of the three groups, taken from the literature is included as Table 4. Although the work of some of the earlier writers mentioned in the Table, is not based on the strict classification of serpentines as presently used, the information they record is of value. Easily recognizable characteristics in each group can be summarized from Table 4 as follows: Serpentines of the chrysotile group are fibrous and may have negative or positive elongation. Except in the case of chrysotile asbestos, occurring as veins of silky fibres, which are flexible and separable, the fibrous nature of chrysotile is not generally recognizable in hand specimen. Antigorite has a variable platy habit with perfect basal cleavage. Elongation is always positive, the optic sign negative with a generally

TABLE 4

SUMMARY REVIEW OF RECORDED OPTICAL DATA ON SERPENTINES

a) CHRYSOTILE

MORPHOLOGY	ELONG.	2V SIGN	α γ	$\gamma - \alpha$	REFERENCE
Fibrous aggregates	α (-) γ (+)	(-)	1.538 1.570	.007-.008	SELFRIDGE (1936)
Fibers	(+)	0-50 (+)	1.493-1.557	.011-.014	ROGERS, KERR (1942)
Fibrous (Z11 c)	(+)	30-35 (+)	1.558		WINCHELL (1951)
Fibrous	α (-) γ (+)				FRANCIS (1956)
Fibers (11 x)	(+)	(-)	1.532-1.556		DEER, HOWIE, ZUSSMAN (1962)

(Table 4 - continued)

TABLE 4 (cont'd)

b) ANTIGORITE

Morphology	Elong.	2V SIGN	α γ	$\gamma - \alpha$	REFERENCE
Laminated		0-36 (-)			PHILLIPS (1927)
Fine cleavage units	(+)	(-)	1.555-1.580	.004-.006	SELFRIDGE (1936)
fibrous aspect Plates, replace crysotile	(+)	30-60 (-)	1.562-1.568	.006-.008	DURRELL (1940)
Anhedral to fibrolamellar aggregates	(+)	20-90 (-)	1.555-1.573	.007-.009	ROGERS, KERR (1942)
Lamellar, plates	(+)	Mod. (-)	Ny 1.55	.007	WINCHELL (1951)
Bladed aggregates, elong. parallel a		$47\frac{1}{2}$ (-)	1.561-1.567	.005	HESS, DENGO, SMITH (1952)
Flaky, prismatic					WILKINSON (1953)
Rectangular plates	(+)	59-61	1.564-1.573		FRANCIS (1956)
Platelike 11 001		37-61 (-)			DEER, HOWIE, ZUSSMAN (1962)
Platelets		35-42 (-)	1.529-1.549	.013-.018	GRUBB (1962)

c) LIZARDITE

Small flakes, basal cl.		0 (-)	1.545-1.555		MIDGELY (1951)
Fine, fibrous	(-),(+)	Near isotropic			GRUBB (1962)

moderate 2V. Lizardite descriptions are rare in the literature, but the species has been recognized from a number of localities by its X-ray diffraction pattern. Extremely fine grain size and platy habit appear to be the most important characteristics.

CHRYSOTILE

The predominant serpentine mineral of the nickel belt's ultramafic rocks belongs to the chrysotile group. Detailed examination of this mineral by X-ray diffraction will be discussed later. The fine texture and structure of fibrous chrysotile veinlets are often seen to their best advantage when serpentinization of the ultramafic is incomplete or has been arrested at an early stage. Where remnant olivine is present, colourless veins of chrysotile with varying widths, form an irregular cross-hatched pattern, isolating much rounded olivine fragments. It is not difficult to envisage the origin of such a texture. The irregular fractures of olivine are the locus of initial serpentinization. With subsequent widening of the veinlets, small sections between them remain as unaltered host mineral or are replaced by a variety of other minerals. Commonly a pleochroic yellowish-green to greenish-brown serpentine, possibly an iron-rich variety, partially or completely replaces the remaining areas (Plate 27). In a specimen from Bowden Lake, a carbonate mineral, darkened by a dusty brown material, occupies the areas between the chrysotile veinlets (Plate 26). The expulsion of secondary magnetite to form an encircling rim around the pseudomorph is clearly visible as are additional

PHOTOMICROGRAPHS * CHRYSOTILE

PLATE 26: Rounded serpentine pseudomorph after olivine outlined by magnetite rim. Areas between fibrous chrysotile veinlets occupied by carbonate and dusty brown material. A sulphide grain at left centre and finely dispersed magnetite present. #108. (x38).

PLATE 27: Fibrous chrysotile veinlets completely surrounding remnant olivine grains which are being further replaced by a greenish-brown serpentine or chlorite. Opaque minerals magnetite. #109. (x107).

areas of finely dispersed granular magnetite.

Textural patterns of the massive serpentinites are varied in detail but may be broadly subdivided into three groups.

a. Mesh serpentine, with more or less regularly disposed phases of alpha and gamma serpentine. (See below).

b. Close packed cross-fiber chrysotile veinlets showing pronounced parallelism within the confines of each pseudomorph.

c. Highly irregular system of cross-fiber veinlets and inter-vein serpentine.

Mesh texture serpentine is invariably fine grained, and composed of a pseudo-rectangular arrangement of bipartite chrysotile veinlets. Considerable variation is evident in the arrangement of the cross hatching and in separate specimens the veinlets outline areas of matrix which are rectangular, equidimensional, lensoid or highly asymmetrical (Plates 28, 29). It is occasionally possible to recognize the boundaries of pseudomorphs in mesh serpentine, by fine threads of secondary magnetite combined with slight changes in orientation of the mesh. The veinlets themselves are rarely greater than .1 mm. in width, with the fibers arranged normal to the vein margins. Bipartite and tripartite veinlets are the rule, with the two or three sets of parallel fibers abutting near the centre line, which is generally marked by a thin film of magnetite dust. Under high magnification, it is common to find dusty magnetite dispersed through the fibers as well. The veinlets have grey to greyish-yellow birefringence, negative elongation and

MICROPHOTOGRAPHS *CHRYSOTILE

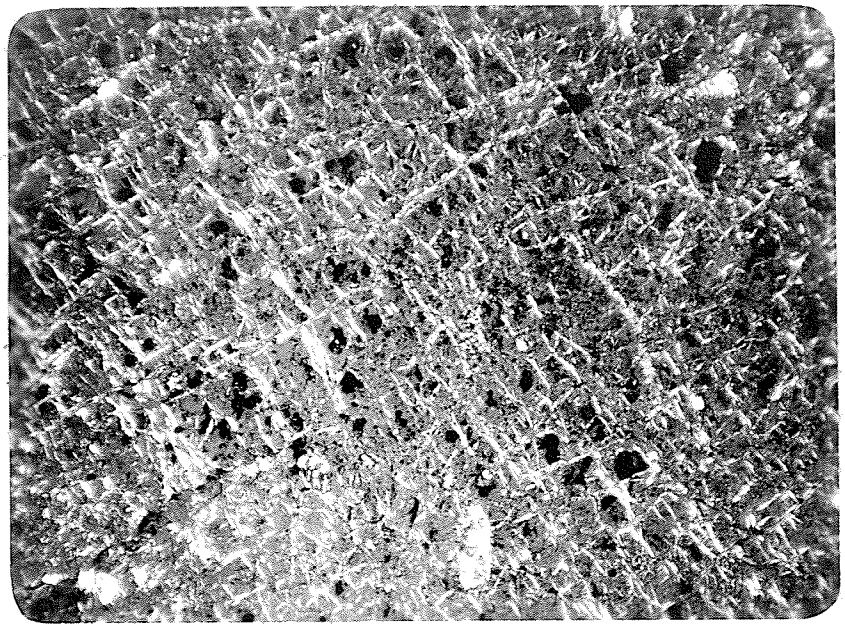

PLATE 28: Sub-rectangular mesh texture serpentine with evenly disseminated anhedral magnetite grains. Margins of fibrous alpha chrysotile (white) enclose pale yellowish isotropic material. #12. (x37).

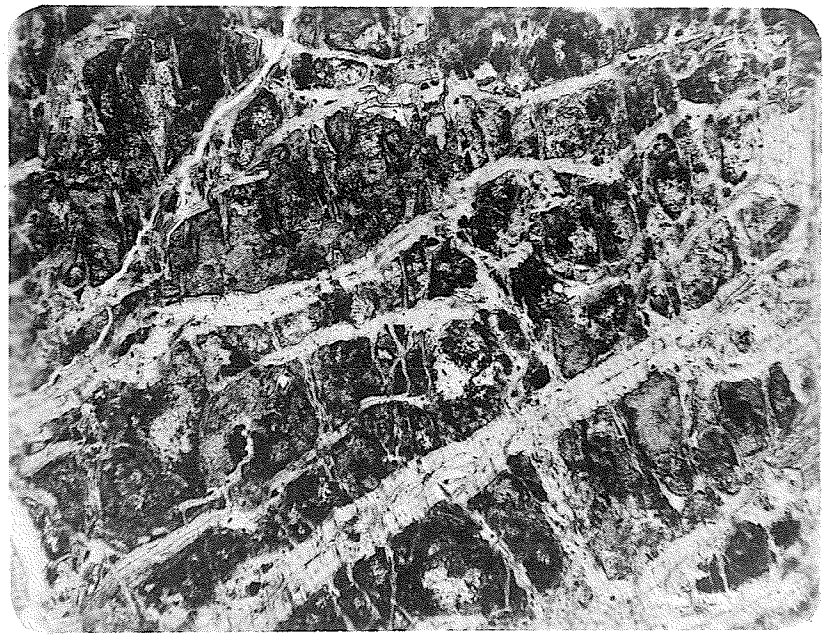

PLATE 29: Asymmetric mesh texture of alpha serpentine (light grey) with carbonate and dusty magnetite completely replacing the matrix. #59. (x69).

parallel extinction. Their optic orientation identifies them as alpha serpentine (Selfridge, 1936).

Matrix material is used as a general term here for the variable constituents occupying the centres of the alpha serpentine mesh. The matrix is occasionally isotropic and may be amorphous in some cases, but this has yet to be proven. Material of this type has previously been called serpophite. However fibrous structure is evident in most specimens, but there is always a distinct lower birefringence than the alpha serpentine of the meshes. Mesh centres are colourless to pale shades of yellowish-green and brown. Under high magnification, the fibration of mesh centres is seen to be due to numerous interwoven fibrolamellar platelets each with individual extinction, or to a continuous smooth surfaced area with a diffuse wavy extinction pattern. Elongation is generally positive and fibrous material of this type has been referred to as gamma serpentine. Discussion of some mesh textures and the optical orientation of fibrous material will be given below.

Mesh centres are commonly the preferred sites for alteration to take place, leaving the alpha serpentine rims unaltered. Carbonate or carbonate with dusty magnetite inclusions is occasionally present (Plates 29, 31). Hematite may occur with anhedral carbonate grains or alone as a fine grained infilling of the meshes.

The second general texture of the serpentinites is that of more or less distinct pseudomorphs, which are composed of closely packed parallel chrysotile veinlets. This feature can

PHOTOMICROGRAPHS * CHRYSOTILE

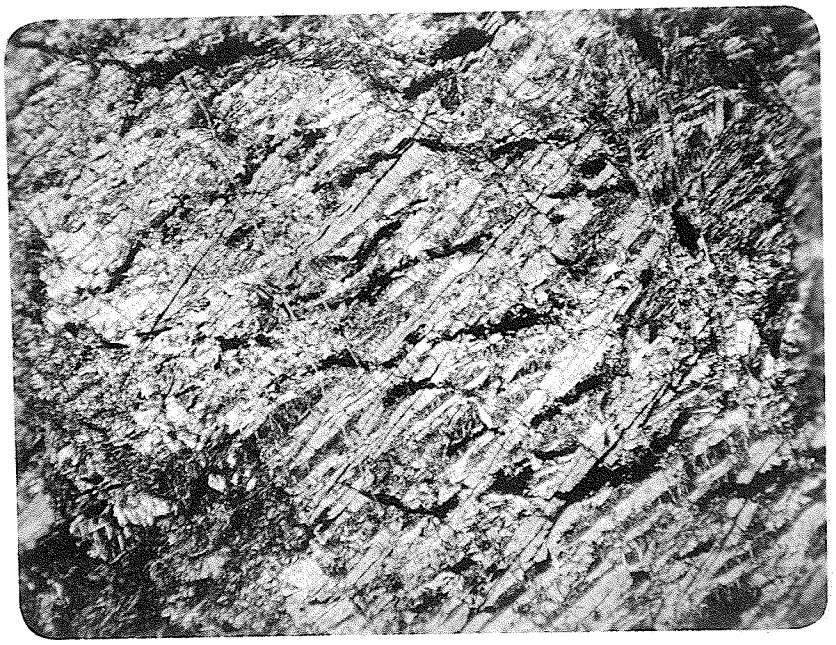

PLATE 30: Closely spaced sub-parallel fibrous veinlets of chrysotile outlining a single pseudomorph. Secondary magnetite has aggregated into stringy lenses. #37. (x34).

PLATE 31: Anastomozing veinlets of alpha serpentine bounded by thin magnetite films. Central areas of gamma serpentine with sweeping extinction (white), are partially replaced by carbonate. #107. (x95).

occasionally be seen in hand specimen. A gradation exists between the symmetrical mesh texture, to specimens where one set of veinlets are better developed leaving little matrix material (Plate 30). Parallelism of veinlets making up one pseudomorph may conform to adjacent pseudomorphs (#107, 189) in a specimen, suggesting a preferred orientation of the original olivine, before serpentinization. Distinctly different orientations of adjacent pseudomorphs have also been noted (#206). As with the alpha serpentine of the mesh texture, the fibers of the close packed veinlets have negative elongation. Vein centres are commonly a thin seam or train of magnetite granules. Variation of birefringence along fibre length at intervals gives the effect of zoning to some veins and the pattern may be repeated in adjacent veins (Plate 32).

The third division of serpentinite textures is a minor one, and includes specimens with highly irregular cross fibered alpha serpentine showing no particular pattern. Occasional poorly developed mesh textures containing gamma serpentine or finely divided near-isotropic material are present.

OPTICAL ORIENTATION OF FIBROUS CHRYSOTILE

When examined in detail, many features of the mesh texture and parallel vein serpentinites described above show interesting differences of structure and optical orientation. Fig. 7 illustrates a number of mesh textures and vein structures of chrysotile selected from samples in these groups. Two fiber types are recognized in the optical studies namely, alpha (α) -

PHOTOMICROGRAPHS * CHRYSOTILE

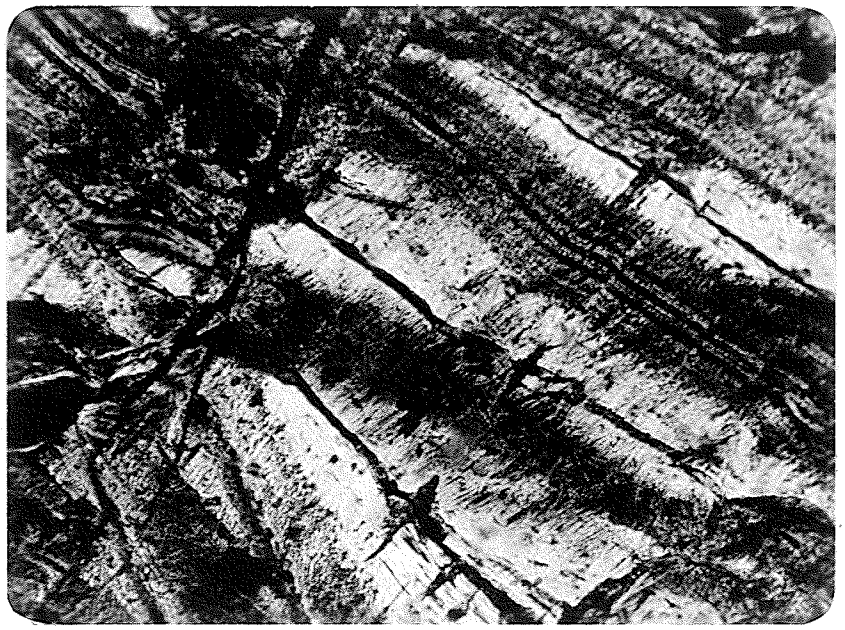

PLATE 32: Cross fiber veinlets of chrysotile (α-serpentine) showing zoning texture. Birefringence changes from dark grey near centre to yellow at edges. Opaque seams separate veins. #155 (x107).

PLATE 33: Leaf-shaped arrangement of fibrous chrysotile. All fibers have negative elongation. Fine magnetite grains are concentrated in the partings. #86. (x272).

serpentine, which is length-fast and hence has negative elongation, and gamma (γ) - serpentine, which is length-slow and considered to have positive elongation. In the mesh textures, alpha serpentine forms the rims and gamma serpentine the cores (Fig. 7 D, F, G) or the reverse arrangement may be the case as in (Fig 71), where gamma serpentine forms the rims and alpha serpentine the cores. Typical "hour-glass" texture is well developed in Fig. 7D and 7F. The optical orientation of the fibers in chrysotile veinlets is shown in Fig. 7C, E, H and J. In 7C (#90), narrow, finely fibrous median stems of gamma serpentine with feathery margins of alpha serpentine constitute a veinlet, which is separated from adjacent veinlets by trains of magnetite granules. The vein system in Fig. 7E (#88) consists of a branching series of cross-fiber alpha serpentines with fibrous, but nearly isotropic serpentine of the same orientation occupying the surrounding areas. The thin median strip of the veinlets has high birefringence and may be clear or contain a row of magnetite grains. Broad marginal bands with sweeping extinction characterize the veinlet in Fig. 7H (#92). The central bipartite zone is alpha serpentine and is bounded by low birefringent zones and the wide margin zones of fibers all with positive elongation.

The additional structures illustrated in Fig. 7A, B, J and K are textural patterns with distinctly different forms to those previously described, but which undoubtedly have a similar origin. Fig. 7A is the diagrammatic representation of the texture in Plate 33. The mutually interfering fiber systems

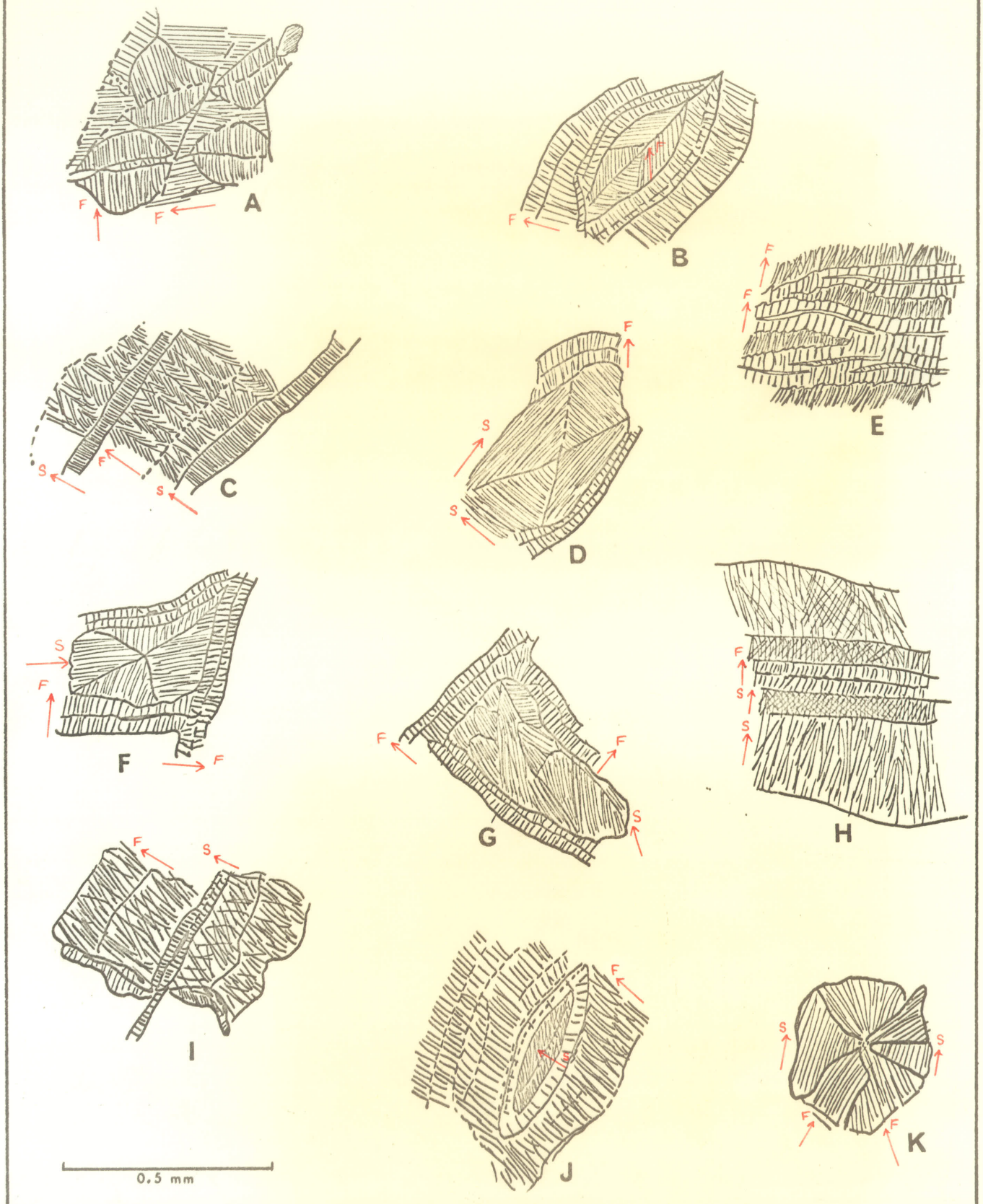

Textural patterns of some fibrous Manitoba serpentines

FIG. 7

adjoin at magnetite-filled partings, and all fibers have negative elongation. Samples shown as Fig. 7B (#142) and 7J (#65) are similar except that the fibrous material of the lensoid areas, enclosed by veinlets of alpha serpentine, has opposite orientation. In Fig. 7B, alpha-serpentine with opposing herring-bone textures forms the central area, whereas in Fig. 7J the central area is composed of gamma serpentine. Plate 34 illustrates the latter texture. A star-shaped pattern of fibers with flamboyant extinction is illustrated in Plate 35 and diagrammatically presented in Fig. 7K. The serpentine platelet is segmented into six areas, two of which contain gamma serpentine and the remaining four alpha serpentine. The latter radiate out from a central point, while the fibers of the former lie parallel to one another.

The variable optical orientation of fibrous chrysotile has been discussed by Francis (1956). It has been established (see mineralogy section below in this chapter), that chrysotile fibers have layered structure parallel to 001 and are identical to platy antigorite, except that they are rolled into tubes or hollow cylinders with the fiber axis corresponding to the "a" crystallographic direction, which is parallel to the Y optical direction. In measuring the fiber elongation, Y is compared with a mean of X and Z. If the fiber type is optically negative, with X as the acute bisectrix, the vibration speed along Y will be less than the mean and the fiber will have positive elongation. This would explain the optical orientation of gamma serpentine. Similarly, the negative elongation of alpha serpentine

PHOTOMICROGRAPHS * CHRYSOTILE

PLATE 34: Structure of central lensoid area between cross-fiber chrysotile veinlets. Black spots are magnetite grains. #65. (x208).

PLATE 35: Segmented arrangement of fibrous chrysotile showing flamboyant extinction. Two of the segments (upper right and lower left) are of γ-serpentine with different attitude to remaining α-serpentine. #73. (x160).

can be explained by a change from 2V(-) to 2V(+). In this case the vibration of Y parallel to the fiber axis would be faster than the mean of X and Z and the fiber would have negative elongation. It can be seen that a change of 2V and optic sign can account for the variable birefringence exhibited by many fibrous serpentines. From 2Vz acute in alpha serpentine to 2Vx acute in gamma serpentine, requires a change through 2V = 90°. The commonly seen, near isotropic fibrous material probably has this optical arrangement.

BASTITE

Bastite is defined as serpentine, pseudomorphic after pyroxene. Although fresh and parially serpentinized pyroxene is present in the ultramafics at a number of localities, recognizable bastite pseudomorphs are rare in the completely serpentinized rocks. This may not be due entirely to a paucity of pyroxene in the primary intrusives, for as Cooke (1937) has recognized in the serpentinites of the Thetford area, bastites tend to lose their identity and disappear into featureless serpentine. The reasons why this may occur are not known. The few bastite pseudomorphs recognizable in the nickel belt serpentinites, vary from prismatic sections containing magnetite granules and seams outlining original pyroxene cleavage, to diffuse areas of serpentine composed of elongate feathery crystals of fibrolamellar material. These have a preferred alignment and stand out from the surrounding serpentine. Some of the bastites contain small rounded areas of mesh serpentine

and magnetite which represents olivine in an original poikilitic pyroxene. Bastite material has consistent positive elongation. X-ray diffraction patterns of bastite by Francis (1956) and Whittaker and Zussman (1956) have identified it with chrysotile and lizardite patterns. The fibrolamellar platy habit and positive elongation of this mineral however, give it a close ressemblance to antigorite.

ANTIGORITE

Antigorite serpentinite has been identified from only one locality along the nickel belt. It forms an outcrop about 300 feet wide on a peninsula jutting out from the east shore of Ospwagan Lake. The outcrop constitutes part of the east appendage of a highly irregular shaped ultramafic body which underlies the greater part of the lake. In hand specimen the rock is dark green, fine grained and massive.

The antigorite occurs as elongated subrectangular flakes with a maximum length of 1.6 mm. Most exhibit rather ragged and feathery terminations. Poikilitic pseudomorphs after pyroxene and olivine are preserved in well developed textural patterns. These consist of areas, about 6x4 mm. in size, composed of rounded to oval shaped granules of fine antigorite set in a matrix of antigorite and closely spaced rows of granular magnetite. (Plate 36). Within some of the granules, which are pseudomorphic after olivine, the antigorite flakes have an interwoven radial arrangement. Much of the remainder of the rock is composed of a tightly compacted matte of elongate,

PHOTOMICROGRAPHS * ANTIGORITE

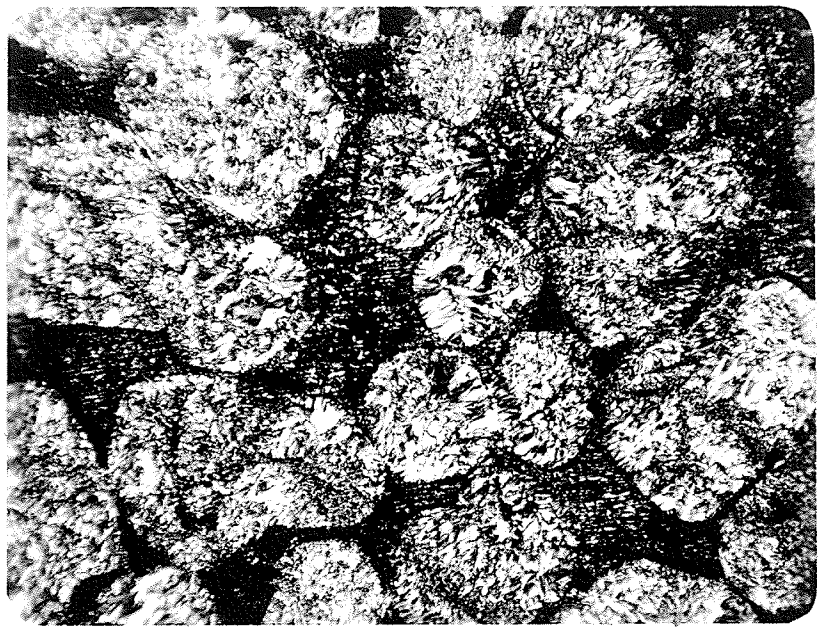

PLATE 36: Antigorite pseudomorphs after olivine in poikilitic pyroxene. Parallel lines of fine granular magnetite identify original pyroxene cleavage. #82. (x35).

PLATE 37: Fibrolamellar, feathery flakes of antigorite in antigorite serpentinite. Preferred orientation indicates probable pyroxene pseudomorph. #82A. (x88).

fibrolamellar flakes of antigorite. Some small areas show a preferred alignment of flakes associated with partings of fine magnetite grains (Plate 37). These probably represent original pyroxenes and so should correctly be termed bastites. As mentioned above, most bastites occurring in chrysotile-mesh serpentinites have a chrysotile structure. In this case, we have textures indicative of a pyroxene and olivine rich ultramafic rock which is now entirely composed of antigorite.

Optically the antigorite has a fibrolamellar, platy form with crystals being generally elongated parallel to the trace of the 001 cleavage. Most have ragged, feathery terminations. Extinction is straight, (-) $2V = 45°$ (approx.), and elongation is positive. Identification has been made by X-ray diffraction pattern, following the method of Whittaker and Zussman (1956), and by differential thermal analysis.

Although antigorite is not common in the nickel belt serpentinites, it is the principal serpentine mineral in a number of other serpentinized ultramafic rocks in Manitoba. Three samples from widely scattered localities were selected for comparison with the nickel belt antigorite and chrysotile. A specimen of serpentinite from Knee Lake (GSC. map 21-1961) contains a mixture of fine grained platy antigorite interspersed with areas of seemingly fibrous material. The latter are not veins as are described for chrysotile, but appear rather as short plates arranged side by side in a row and may be joined by a colourless fine grained isotropic strip to an adjacent row. When these are close packed in an area of the section,

PHOTOMICROGRAPHS * ANTIGORITE

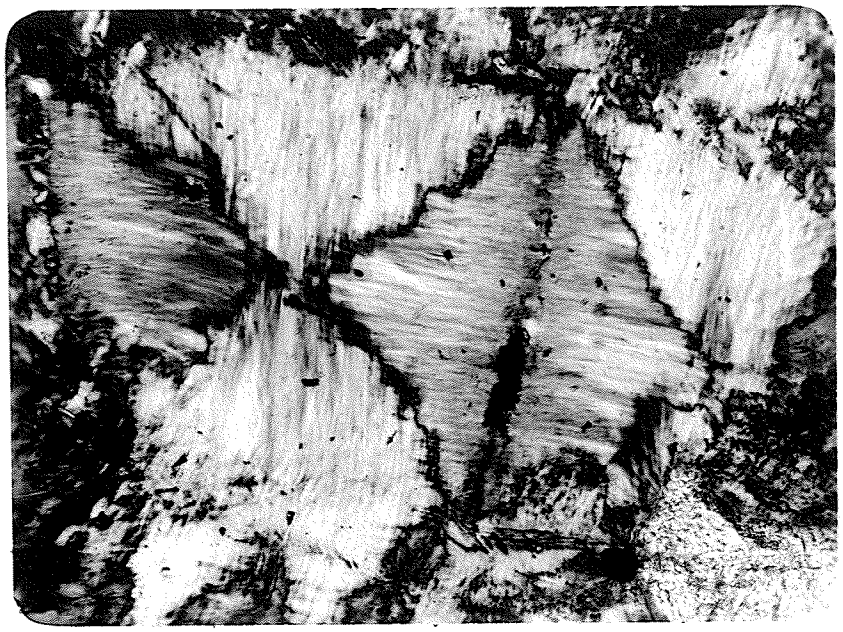

PLATE 38: "Hourglass" texture in antigorite. Fibrolamellar plates arranged in the manner common to gamma serpentine. Magnetite is present in median (right centre) but not in black cross. Carbonate (lower right) #305, Knee Lake, Manitoba (x240).

PLATE 39: Broad fibrolamellar plates of antigorite surrounding fine grained platy antigorite. The latter show preferred orientation in some areas. #310, Carrot River, Manitoba. (x44).

they have the appearance of interfering cross-fiber veinlets and in one case formed an "hour glass" texture (Plate 38). The fibration direction has positive elongation as does the finer grained material in the rock. Although the texture shown in Plate 38 has the form and optical elongation of gamma serpentine as described above in mesh textures, there is no equivalent rim material with opposite elongation. Identification by X-ray diffraction pattern (#305) shows this material to be entirely antigorite.

Plate 39 illustrates the texture of an antigorite serpentinite from the Carrot River (Man. Mines Branch Dept. Map 59-2). The rock is similar to the Knee Lake serpentinite in showing a highly variable grain size and in the arrangement of elongated antigorite flakes to form short vein-like sections of aggregates. A good example of this can be seen in Plate 39 at the top centre. Elongation is positive.

A third and somewhat unusual serpentinite is found east of Linklater Island in Island Lake (GSC. Map 26-1960). Talc and carbonate form the matrix to pale green, faintly pleochroic pieces of serpentine. These fragments are greatly varied in size and shape. Their most interesting aspect is in the nature of their fibration. In equidimensional plates, a knife-edge seam, equal in length to about one quarter the width of the plate, is present at the centre. From this seam, fibres radiate out in all directions in a gentle s-shaped pattern (Plate 40A). Extinction sweeps around the plate as a vague cross. In the elongated fragments (Plate 40A, lower right) the central seam

PHOTOMICROGRAPHS * CHRYSOTILE AND ANTIGORITE

PLATE 40: A. Rounded to elongated plates of fibrous chrysotile. Fibers radiate out in gentle curves from a short central seam. Matrix is talc, carbonate and magnetite. #311, Island Lake, Manitoba (x50).
B. Antigorite flakes replacing cross-fiber chrysotile (grey), Magnetite and carbonate (dark grey) #312, Island Lake, Manitoba (x100).

PLATE 41: Flame-like growths of antigorite replacing mesh serpentine. #5. (x25).

is longer and the pattern approaches that of bipartite cross-fiber chrysotile veins. Thin concentric banding is occasionally present towards the outer margin of the plates, and these show a slightly higher birefringence. The fibrous material has negative elongation. Minute opaque grains of probable magnetite are disseminated throughout. Commonly the radial fibrous plates are separated or partially encircled by narrow cross-fiber veinlets also having negative elongation and which are usually clouded with aggregates of magnetite. Talc and carbonate appear to have replaced the greater proportion of these in preference to the radial plates. It seems that the fibrous plates and veins composed a form of mesh serpentine.

Excellent evidence of the replacement of chrysotile serpentine by antigorite is shown by a specimen close to that described above (#312). Alteration is restricted to spotted anhedral masses of carbonate. Approximately 40-50% of the rock is antigorite occurring as groups of pointed laths and spear shaped crystals cutting through mesh serpentine and the carbonate aggregates which replace it. (Plate 40B). Antigorite also cuts through narrow veinlets of cross-fiber chrysotile asbestos. Magnetite is abundant throughout the mesh serpentine and carbonate but is surprisingly deficient in areas of new antigorite growth. Optically the antigorite is negative, 2V = 35°-45° (estimated), has positive elongation and straight extinction. The DTA. curve of this rock confirms the presence of both antigorite and chrysotile.

Returning to the serpentinites of the nickel belt, it

can be stated fairly safely that massive antigorite serpentinites are exceedingly rare. The Ospwagan Lake occurrence (#82) is the only one identified as such, at the present time. Late antigorite flakes replacing chrysotile mesh serpentine have been identified at two additional localities (#160, 5). Plate 41 illustrates the flame-like growth of antigorite spearing through fine mesh serpentine. In both samples however, the minor quantity of antigorite present negated the possibility of its being identified on the X-ray diffraction or DTA. curves.

The origin and mode of occurrence of antigorite has been widely discussed in the literature, with a general agreement that it usually replaces mesh serpentine. Its formation has been ascribed to conditions of high pressure (Benson, 1918), and to shearing stress accompanying metamorphism above the chlorite-biotite subfacies of the greenschist facies but equal to or slightly less than the albite-epidote amphibole facies (Hess, Smith and Dengo, 1952). Origin of antigorite by pure thermal metamorphism is considered probable by Wilkinson (1953) and Durrell (1940). Little can be added to this from the present study. The Ospwagan Lake antigorite (#82) shows relict textures of a primary peridotite (Plate 36), in no way deformed or altered by shearing. On the other hand, a body of intrusive granite occurs at the north end of the lake, within one-half mile of the sample location (Zurbrigg, 1963). It is of interest that specimens from the west side of the Ospwagan ultramafic body (#83, 84) are composed entirely of chrysotile serpentine with no evidence of antigorite. Thus, if the antigorite serpentinite

has developed from an original chrysotile serpentinite, textural features have been preserved and no remnant chrysotile remains. Thermal metamorphism for this process is considered the most likely.

LIZARDITE

Two probable occurrences of lizardite have been recognized in the nickel belt serpentinites. In a specimen from the mine dump at Pipe Lake (#122), two serpentine polymorphs are recognizable in thin section and in X-ray diffraction pattern (diffractogram #122). Sub-parallel cross fibre veinlets of clinochrysotile are separated by narrow lensoid areas of lizardite (Plate 42). The latter form a felt-like dense mass of interwoven fibrolamellar platelets which constitute about 20% of the rock. Elongation of the plates appears to be positive. The chrysotile veinlets are .3 mm. in width and have highly serrated margins. Each veinlet has a clear and colourless central spine which may contain oriented magnetite grains. Elongation of the fibers is positive, which makes them optically comparable to fibers of gamma serpentine.

The second occurrence of lizardite is by no means certain. A specimen from Setting Lake (#189) is composed of oval to slightly irregular shaped pseudomorphs made up of parallel, close packed chrysotile veinlets. A fine grained matte of ragged, interwoven platelets occupies veins and fills interstices between some of the pseudomorphs. (Plate 43). The platelets have straight extinction, positive elongation and slightly bluish-

PHOTOMICROGRAPHS * LIZARDITE

PLATE 42: Fine lizardite between cross-fiber veinlets of clinochrysotile. #122. (x192).

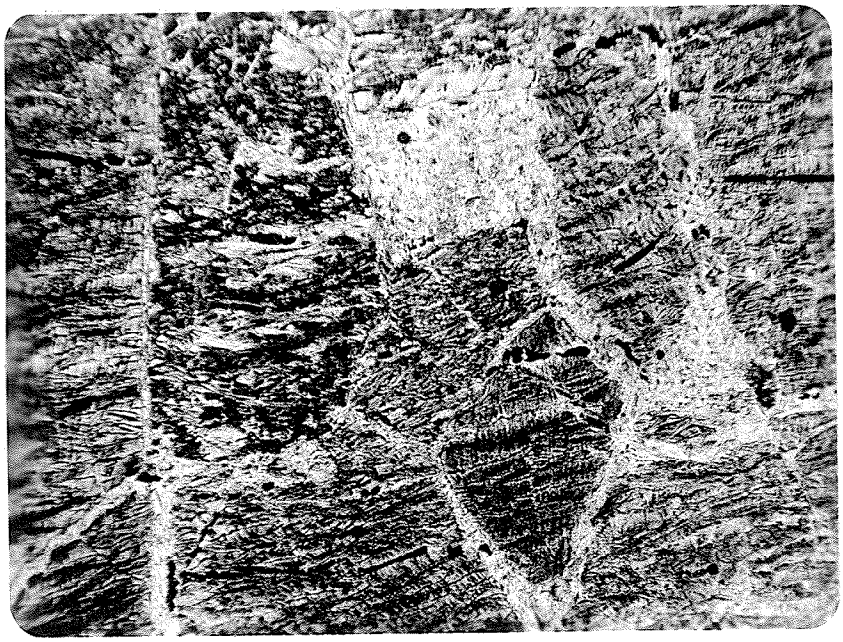

PLATE 43: Possible lizardite veining and filling interstices around pseudomorphs of close packed chrysotile veinlets. #190. (x25).

grey interference colours. Considerable chlorite is also present. The diffraction pattern did not clearly indicate the presence of a second serpentine mineral, but the optical properties indicate that it may be antigorite or lizardite and the morphology is suggestive of the latter type.

MINERALOGY OF THE SERPENTINE MINERALS

STRUCTURE OF THE SERPENTINES

The minerals of the serpentine group are phyllosilicates having layered structures similar to the kaolinite group. The basic unit of layering is a pseudo-hexagonal network of linked SiO_4 tetrahedra all pointing in one direction. Joined to it is a brucite layer, of which on one side only, two out of every three hydroxyls are replaced by apical oxygens. The perpendicular distance between composite sheets of this type is approximately 7.3Å, which determines the c parameter. The dimensional mismatching of the octahedral and tetrahedral layers and the different ways in which the two layers nevertheless accommodate one another, together with ordered and disordered stacking arrangements account for the various serpentine polymorphs. As listed by Deer, Howie and Zussman (1962), three ways in which the accommodation is brought about are, a) substitution of larger ions, such as Al and Fe^{+++} for Si in the tetrahedral layer and smaller ions such as Fe^{+++} and Al for Mg in the octahedral layer, b) by distortion of the ideal octahedral and or tetrahedral networks, and c) by curvature of the composite sheet

with its tetrahedral component on the inside of the curve.

Chrysotile serpentines are curved about the crystallographic x axis forming concentric cylinders elongated parallel to x. They are fibrous on a large scale and show tubular morphology when seen in the electron microscope (Bates, Sand and Mink, 1950; Nagy, 1953; Nagy and Faust, 1956: Kalousek and Mattart, 1957; Zussman, Brindley and Comer, 1957). The chrysotile cell is two-layered and two alternative stacking methods occur, with $\beta = 93°$ or $\beta = 90°$ for clino and ortho-chrysotile respectively. (Whittaker and Zussman 1956). A third chrysotile variety, where the axis of curvature is the crystallographic y axis instead of x, has been called parachrysotile.

Six-layer ortho-chrysotile structures are also known. A serpentine from Unst, Shetland Islands was first studied by Brindley and von Knorring (1954), who considered it to be an ortho-antigorite. Re-examination by Zussman and Brindley (1957) showed that the long spacing was parallel to c and that the mineral should be termed a 6-layer ortho-serpentine. The authors compare the X-ray powder data of this material with that from a synthetic Mg-Ge serpentine having a well-defined 6-layer structure and platy morphology.

The synthetic production of Mg-Al serpentines by Gillery (1959) shows that composition is the predominant factor in determining the polytype produced. Two types of 6-layer structure synthesized by Gillery have been referred to as the 6(3) and 6(2) layer structures. The first approximates to a 3-layer cell having hkl with $l = 2n$ usually more intense than $l = 2n \pm 1$,

and the other to a 2-layer cell having hkl with 1 = 3n, usually more intense than 1 = $3n \pm 1$. Gillery considers the 6-layer orthoserpentine of Zussman and Brindley (1957) as an example of the 6(2) layer type of structure.

Antigorite is a serpentine with platy morphology which shows markedly different structural characteristics. Aruja (1945) first showed that antigorite has a one layered cell with a "b" parameter similar to chrysotile and lizardite, but that the "a" dimension is about eight times greater than those of other serpentines. An explanation of the large "a" parameter has been sought in terms of "wave forms" with corrugations of the structure parallel to "b". Repeat distance of the waves would give the large "a" dimension. Studies on the structure of antigorite have been done by Zussman (1954) and Kunze (1956). Picrolite is a fibrous serpentine with the antigorite structure in which y is the fiber axis in contrast to chrysotile where the fiber axis is always in the x direction.

The serpentine variety lizardite, with a single layered, orthohexagonal cell was named by Whittaker and Zussman (1956), and its fine grained platy morphology was first described by Midgely (1951).

The cell parameters of serpentine minerals as compiled from sources quoted above by Deer, Howie and Zussman (1962), combined with the morphology of each group in the classification of Zussman, Brindley and Comer (1957) are listed in Table 5.

TABLE 5

CELL PARAMETERS AND MORPHOLOGY OF SERPENTINES

	CHRYSOTILE			LIZARDITE	6-LAYER ORTHO.	ANTIGORITE
	Clino	Ortho	Para			
a, Å	5.34	5.34	5.3	5.31	5.322	43.3
b, Å	9.25	9.2	9.24	9.20	9.219	9.23
c, Å	14.65	14.63	14.7	7.31	43.49	7.27
β	93°16'	90°	90°	90°	90°	91.6°
Layers/cell	2	2	2	1	6	1
Fibre axis	x	x	y			
Morphology (hand spec.)	Fibrous; occasionally massive.			Massive, platy.	Massive, fibrous	Massive, platy, fibrous
Morphology (elect. mic.)	Tubes, laths			Plates	Laths	Plates, laths.

CLASSIFICATION OF SERPENTINE MINERALS

X-ray and optical examination of a large number of serpentines by Selfridge (1936) showed that all specimens could be referred to one of two main divisions, each of which showed slight modification in the intensities of certain X-ray powder lines. One group gave a powder pattern similar to that of chrysotile asbestos and was termed serpentine. The name chrysotile was reserved for serpentine occurring as flexible fibres in veins. The second division contained varieties known as antigorite with powder patterns similar to that of antigorite from the Antigorio

valley, Piedmont, Italy. Similar conclusions were reached by Gruner (1937) who compared X-ray diffraction patterns of chrysotile with antigorite from the type locality and with both massive and fibrous serpentine varieties having an antigorite pattern.

Nagy and Faust (1956) conducted chemical, physical and mineralogical investigations and showed that serpentines are either chrysotile or antigorite or natural mixtures of these two minerals. The intensity of the 001 reflections of material treated with 1N HCl at 100°C, a process which destroys the diffracting power of chrysotile, compared to that of the untreated material provides a semi-quantitative method for the estimation of chrysotile content. The structure of lizardite is not affected by the above treatment and its presence would presumably affect the accuracy of the method.

The classification and nomenclature of the serpentine minerals have been discussed by Whittaker and Zussman (1956) and by Zussman, Brindley and Comer (1957) in relation to the available structure information. This classification, which is listed in Table 5, will be followed in this report. X-ray diffraction patterns of Manitoba serpentines were obtained in the manner described in Appendix 1V, and identification made by comparsion with the ASTM Powder Data File and other published information.

IDENTIFICATION BY X-RAY DIFFRACTION POWDER PATTERNS

Distinguishing between the X-ray diffraction powder patterns

of various serpentine polytypes is not an entirely straightforward process. Except for strong basal reflections, most peaks are broad and poorly defined. When minor differences in d spacings are considered together with the presence or absence of small peaks and the patterns viewed as a whole, the various types can be identified.

The distinction between clinochrysotile and orthochrysotile has been illustrated by Whittaker and Zussman (1956), using theoretical microdemsitometer curves for powder photos of mixtures taken with Cuk_{α} radiation. In the patterns for both of these minerals, there is a characteristic sharp rise at reflection 130 (d = 2.66Å) from which point a long "tail" gradually slopes. A number of important peaks are superimposed on the "tail". Clinochrysotile reflections $20\bar{2}$ (d = 2.549Å) and 202 (d = 2.45Å) are gradually replaced with increasing orthochrysotile content by an emergent peak at 2.500Å. On the back slope of the "tail" at higher angles of 2θ, the small 204 (d= 2.149Å) reflection of orthochrysotile is superseded by the 204 (d = 2.096Å) peak of clinochrysotile. The 205 (1.97Å) reflection of orthochrysotile, which is lacking in the monoclinic variety, forms the end of the "tail". Other differences include the 206 (d = 1.746Å) reflection of clinochrysotile and the 207 (d = 1.639Å) of orthochrysotile which is not present in pure clinochrysotile.

Krstanovic and Pavlovic (1964) have described an additional form of clinochrysotile, called by them the "Povlen-type". It is characterized by sharp reflections on powder diffraction

patterns, a 131 reflection of medium intensity and good resolution in the region of 2.5Å. The serpentine has lath-like morphology under the electron microscope and is considered to have a greater degree of order and much less curvature to the layers than normal clinochrysotile.

Antigorite patterns are in general, better resolved than those for the other serpentines. The strong peak at 2.53Å can be distinguished from the similar peak in lizardite, which has never been observed greater than 2.50Å. In addition, the distinctive pair of peaks at 1.56Å and 1.54Å are of lower intensity and not strictly equivalent to the strong pair at 1.535Å and 1.501Å for lizardite and 6-layered orthochrysotile. Many extra lines are present in the antigorite pattern which also assist in its recognition.

SERPENTINES OF THE MANITOBA NICKEL BELT

X-RAY DIFFRACTION

The X-ray powder diffraction patterns of most of the nickel belt's fibrous serpentines resemble in some ways the pattern of 6-layered orthochrysotile as recorded by Zussman and Brindley (1957). However the consistent absence of the high intensity relections, 209(d = 2.335Å), 2.0.15(d = 1.963Å) and 2.0.21(d = 1.636Å) and a number of weaker reflections, indicated that the mineral could not be correlated with any previously recorded form. Comparison of the d spacings with those of the 6-layer type reveáled that the principal difference lay in the almost total absence of hkl's with 1 odd. This suggested that the

pattern could be reindexed on the basis of a 3-layer cell.

Using selected reflections from the diffraction pattern of specimen #88 together with the appropriate indices from the 6-layer type of Zussman and Brindley (1957), the cell dimensions used for reindexing were derived as follows:

001	d(001)Å	d(001)Å		
006	7.37	44.22		
0.0.12	3.66	43.92		c_o = 43.86Å (average)
0.0.24	1.824	43.78	(For new cell)	c_o = 21.930Å
0.0.30	1.463	43.89		
0k0	d(0k0)Å	d(010)Å		
020	4.60	9.20		
060	1.535	9.21		b_o = 9.205Å (average)
h01	d(h01)Å			
206	2.498			a_o = 5.346Å

The new c parameter for the 3-layer structure is 21.930Å, which is slightly greater than half the value (43.59Å) used by Zussman and Brindley. Indexing of all reflections was done by IBM. 1620 computer using a Fortran program devised for the purpose. The program is included as Appendix V and can be used for indexing any orthorhombic powder pattern. All possible hkl's are derived for d(calc.) values, which lie within narrow limits of variation from the d(obs.) spacings. The limits of variation are as follows: for d >3.0Å, ± 0.15Å, for d=2.0-3.0Å, ± 0.05Å and for d <2.0Å, ± 0.02Å. Output data from the computer are

printed in the form d(calc), d(obs), h, k, 1.

Indexing was carried out on the combined reflections obtained from 15 specimens of pure serpentinite, whose diffraction patterns indicated essentially identical structures. Diffraction patterns from 4 of these samples #'s 5, 88, 155, 189) are reproduced at approximately half scale size in Fig. 8. Diffraction patterns of an additional 10 nickel belt serpentinites were similar, but contained extra peaks which could by attributed to the presence of such minerals as tremolite, chlorite and dolomite. These patterns are not included in the present work. All reflections from the 15 pure samples, the number of any particular d spacing obtained, together with I(meas.), dÅ(calc.) and hkl's are listed with the data from the 6-layer ortho-type, in Appendix V1. The results contained in this Appendix are condensed and presented in Table 6, again using the recorded data on the 6-layer ortho-type for comparison. In Table 6, the d(obs.) spacings listed are the predominant reflections in any single group, which normally show variations over a narrow range. These variations, in what are considered to be equivalent d spacings, are probably due to slight differences in the serpentine compositions combined with the minor errors involved in measuring the maxima of poorly defined peaks. Where more than one hkl is listed for a particular d(calc.) value the first one corresponds to that value and the additional ones, either to that value also or to d(calc.) values extremely close to values of d(obs.). Appendix V1 contains the complete range of d(calc.) and hkl's.

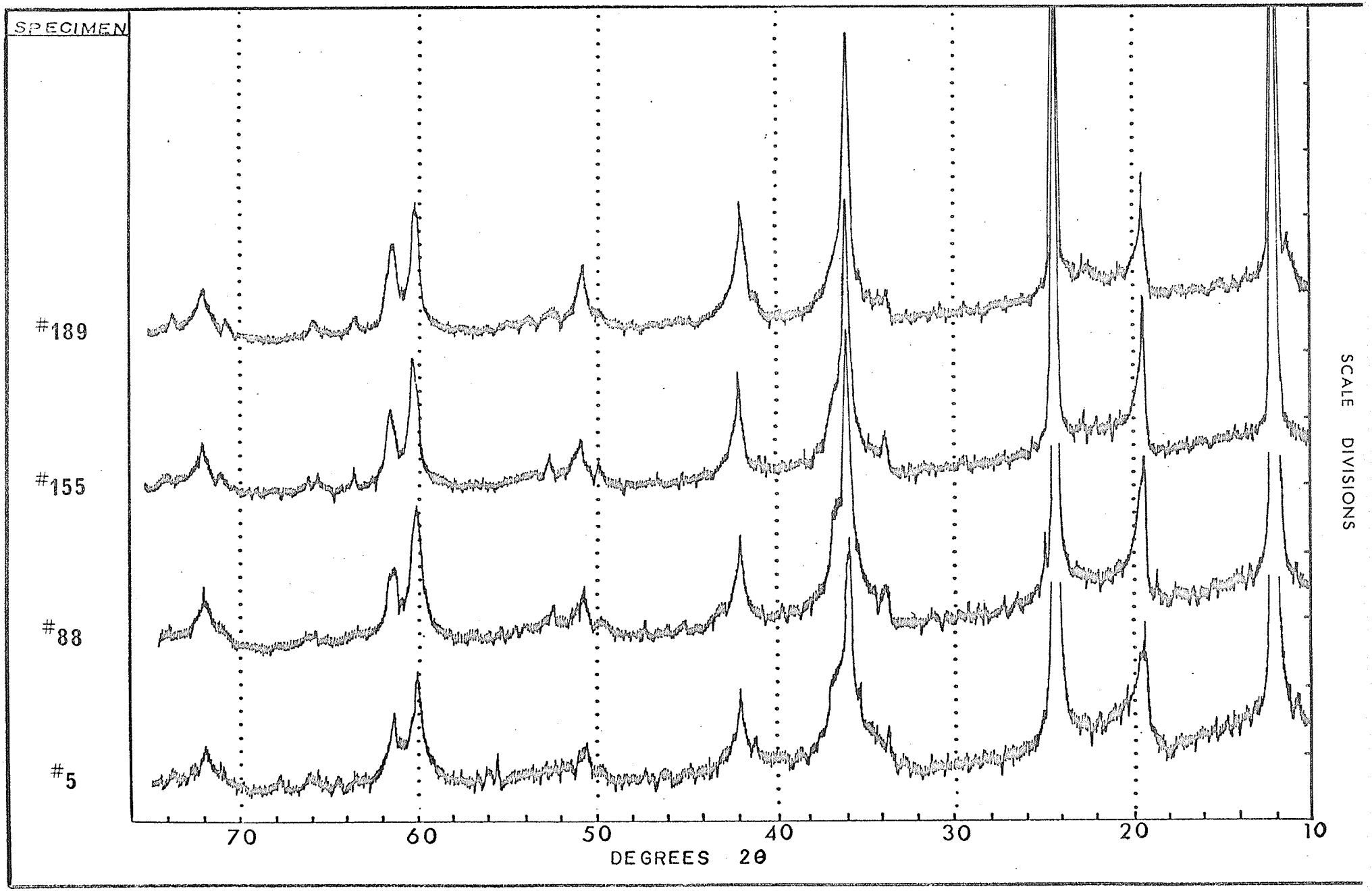

FIG. 8 : X-ray powder diffraction patterns of 3-layer serpentines. Cuk$_\alpha$ radiation.

Prominent differences between the 6-layer ortho-type of Zussman and Brindley (1957) and the 3-layer ortho-type in the Manitoba serpentinites are readily observable from Table 6. With certain exceptions the hkl's with 1 odd in the 6-layer cell are missing in the 3-layer type. Exceptions to this are the 203 reflection (d = 2.623Å), which may not be strictly equivalent to the 2.652Å reflection of the 3-layer type, the 0.2.15 reflection (d = 2.450) and the 409 reflection (d = 1.283Å). The low intensity 0.2.10 reflection (d = 3.17Å) of the 6-layer cell has no recognizable equivalent in the 3-layer pattern. Diffractogram records were not obtained beyond the angle 2θ=75° so that the smallest d spacing recorded for the 3-layer type is 1.281Å. It can be seen that the derived 3-layer ortho-hexagonal cell with a_o = 5.346Å, b_o = 9.205Å, c_o = 21.93Å (3x7.31Å), gives good agreement between observed and calculated d values for a wide range of reflections.

As previously mentioned, the only known occurrence of antigorite serpentine along the nickel belt is found at Ospwagan Lake. The X-ray diffraction pattern of a specimen from this occurrence (#82A) is reproduced in Fig. 9, along with patterns from Island Lake (sample #310) and from specimen 481-7 (Museum No. - Dept. of Geology) labelled as "williamsite", Lancaster Co. Pa. Details of the diffraction patterns are listed in Table 7, together with the data of the Caracas antigorite, described by Hess, Smith and Dengo (1952) and listed in the ASTM. file card 7-417. Specimen 481-7 (williamsite) from the Mineral Museum of the Department of Geology, University of

TABLE 6

COMPARISON OF X-RAY POWDER DIFFRACTION DATA OF 6-LAYER AND 3-LAYER ORTHOCHRYSOTILES

6-LAYER ORTHO-TYPE +			3-LAYER ORTHO-TYPE *			
dÅ	I	hkl	dÅ(obs)	I c/s	dÅ(calc)	hkl
7.33	100	006	7.40	400	7.310	003
4.60	60	020	4.60	76	4.602	020
4.40	10	023				
4.25	10	024	4.28	20	4.243	022,112
4.09	10	025				
3.90	5	026	3.90	36	3.894	023,113
3.66	100	0.0.12	3.66	225	3.655	006
3.53	5	028	3.52	16	3.525	024,114
3.35	5	029				
3.17	5	0.2.10				
3.02	5	0.2.11				
2.865	5	0.2.12	2.867	9	2.867	026,116
2.720	5	0.2.13				
2.623	30	203	2.652	20	2.653	201,018
2.502	100	206	2.502	141	2.500	133,212
2.450	10	0.2.15	2.442	47	2.439	108
2.335	70	209				
2.149	60	2.0.12	2.151	45	2.151	136
1.963	70	2.0.15				
1.815	5	0.0.24	1.824	12	1.827	0.0.12,052
1.791	10	2.0.18	1.791	26	1.792	0.1.12,139
1.739	10	310	1.740	16	1.740	150,241
1.636	40	2.0.21				
1.535	80	060	1.537	73	1.537	331,060
1.501	70	2.0.24	1.505	46	1.506	1.3.12,0.4.11
1.452	2	0.0.30	1.463	10	1.461	0.0.15,254,162
1.415	20	0.6.12	1.415	9	1.416	159,066
1.379	20	2.0.27				
1.327	10	403				
1.309	50	406	1.309	28	1.309	263
1.296	2	0.6.18				
1.283	5	409	1.281	12	1.281	421,1.3.15
1.276	5	2.0.30				
1.210	10	0.0.36				
1.182	2	2.0.33				
1.168	5	4.0.18				
1.121	5	4.0.21				

+Data from ASTM. 9-444 (Rf. Zussman and Brindley, 1957).
*Phillips diffractometer using CuK_{α} radiation, Ni filter. d (obs) are significant reflections from 15 pure samples. I c/s-Intensity measured as counts/seconds on 4×10^2 scale. d(calc) and hkl derived from assumed cell dimensions of a_o 5.346Å b_o =9.205Å c_o =21.930Å.

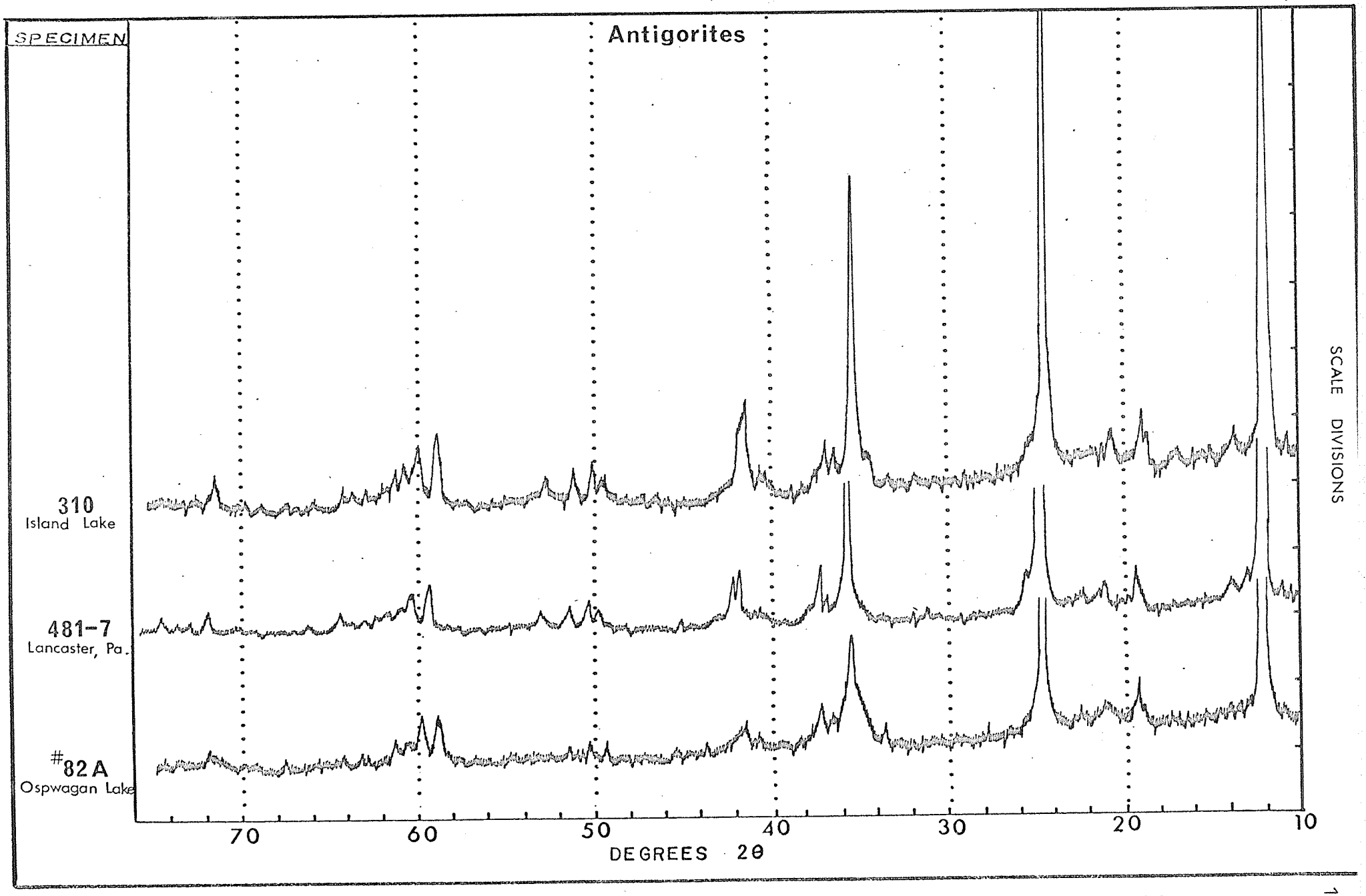

FIG. 9 : X-ray powder diffraction patterns of antigorites. Cuk$_\alpha$ radiation.

TABLE 7

X-RAY POWDER DIFFRACTION DATA OF ANTIGORITES *

ASTM. 7-417			82A		481-7		310	
dÅ	I	hkl	dÅ	I	dÅ	I	dÅ	I
8.05	10				7.9	25	8.14	18
7.30	400	001	7.31	400	7.20	1000	7.31	400
6.95	24	$20\bar{1}$			6.78	48	6.84	17
6.51	16	$30\bar{1}$			6.32	36	6.39	22
6.10	6	-						
5.78	8	401			5.72	13	5.83	9
							5.18	7
4.67	6	810					4.66	33
4.62	7	020	4.62	26	4.57	62		
4.27	4	910	4.21	12	4.19	42	4.27	20
4.01	6	$8\bar{1}\bar{1}$	3.95	10	3.97	35		
3.63	300	102	3.63	256	3.59	1000	3.64	400
3.51	24	302	3.51	11	3.48	70	3.51	18
2.88	2	$14.0.\bar{1}$			2.87	28		
			2.66	12				
2.59	4	930						
2.57	8	17.00			2.57	32	2.59	22
2.52	70	16.0.1	2.53	76	2.51	320	2.53	188
2.46	9	$93\bar{1}$	2.46	22	2.44	40	2.46	28
2.42	38	003	2.42	28	2.41	85	2.42	32
2.39	9	17.0.1	2.38	17	2.37	35	2.39	14
2.35	5	403					2.35	6
2.237	6	15.02			2.238	20	2.238	11
2.208	7	$16.0.\bar{2}$	2.21	11	2.201	20	2.222	18
2.167	22	$83\bar{2}$	2.161	20	2.161	80	2.176	58
2.150	20	16.0.2	2.141	11	2.144	78	2.166	48
2.126	4	$93\bar{2}$						
					2.10	20		
2.035	4	$11.3.\bar{2}$			2.011	13		
1.886	3	$15.0.\bar{3}$						
1.830	12	15.0.3	1.845	10	1.831	28	1.838	18
1.815	23	004	1.811	12	1.810	45	1.817	24
1.781	14	$93\bar{3}$			1.778	35	1.779	22
1.755	4	$10.3.\bar{3}$						
1.736	10	17.0.3			1.728	28	1.738	16
1.688	2	21.3.1						
1.640	2	22.3.1						
1.584	3	$17.0.\bar{4}$						
1.560	12	24.3.0	1.565	28	1.556	75	1.569	44
1.540	9	060	1.542	32	1.537	60	1.542	36
1.535	9	$24.3.\bar{1}$			1.532	60	1.533	26
1.524	13	15.04	1.528	14	1.521	40	1.523	22
1.509	8	061	1.509	12	1.503	30	1.512	21
1.497	10	$17.0.\bar{4}$	1.497	6	1.493	26	1.496	15
1.479	7	934	1.471	8	1.475	17	1.477	8
1.466	6	$18.0.\bar{4}$						
1.462	6	10.3.4						
1.451	10	$20\bar{5}$	1.453	6	1.459	21	1.461	10

TABLE 7 (cont'd)

ASTM. 7-417			82A		481-7		310	
dÅ	I	hkl	dÅ	I	dÅ	I	dÅ	I
1.448	9	205			1.446	32	1.449	12
1.443	5	-						
1.438	3	-					1.419	6
1.328	3	-					1.326	23
			1.313	10	1.313	32		
					1.297	16		
					1.275	24		

* Specimens: ASTM. 7-417 (Ref. Hess, Smith and Dengo, 1952)
82A - Ospwagan Lake, Man.
481-7 - Lancaster Co., Pa.
310 - Island Lake, Man.

Manitoba, is a bluish green, translucent serpentine with a massive texture and splintery fracture. A similar specimen (#F-1) has been investigated by Faust and Fahey (1962) and classified by them as antigorite. The nickel belt antigorite in hand specimen is dark greyish-green and massive and the Island Lake sample, dark green, fine grained and massive. Thus although these three specimens differ considerably in physical appearance, their X-ray diffraction patterns (Fig. 9) indicate they possess identical structures.

The X-ray diffractograms of a number of additional serpentinous minerals are reproduced in Fig. 10. They include clinochrysotile of the Pipe Lake serpentinite (#122) which also contains considerable lizardite, and asbestos fibers from the Cassiar Mine, B. C. The latter sample was ground for 10 hours in an automatic mullite mortar, dried and then

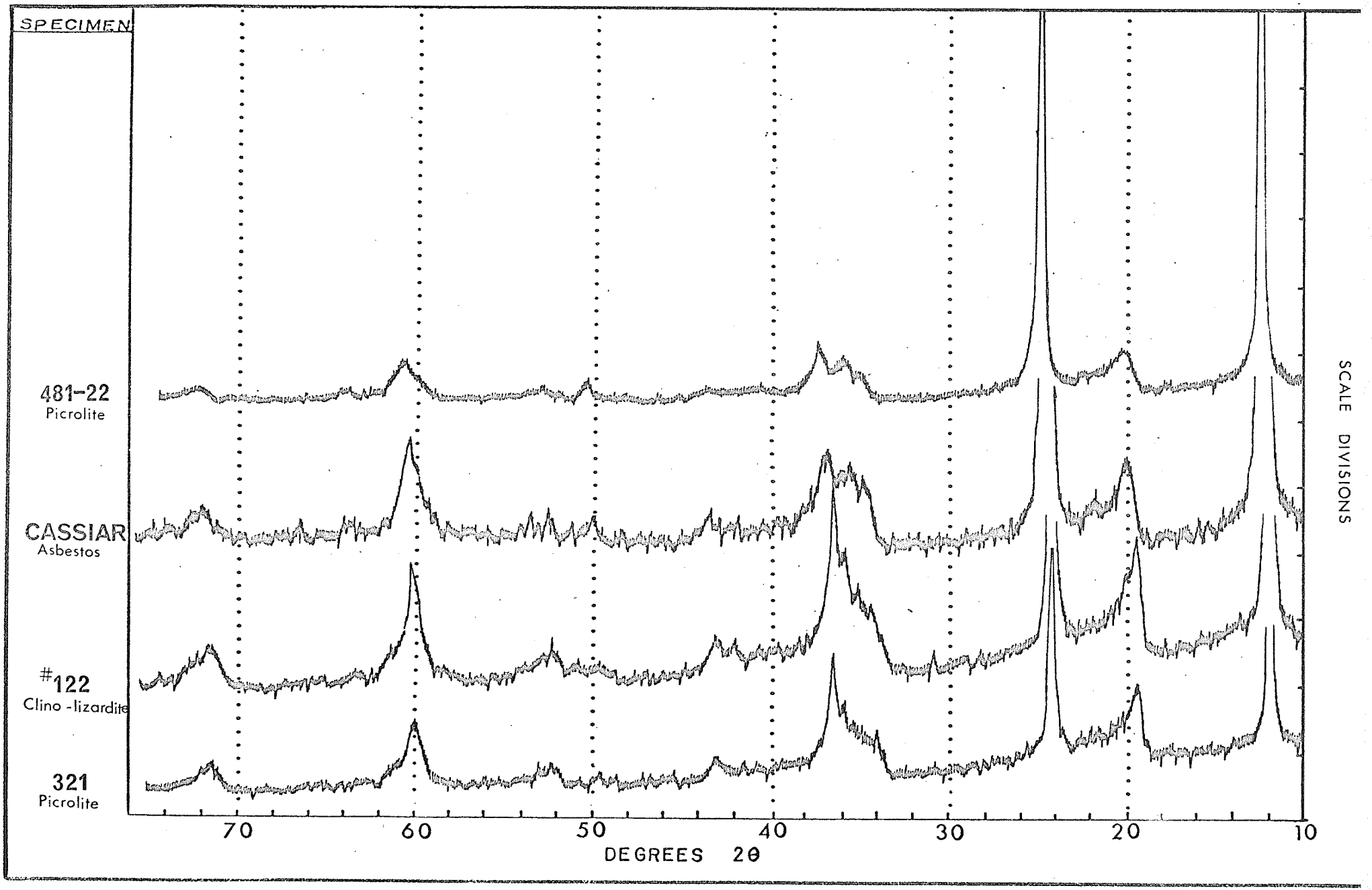

FIG. 10 : X-ray powder diffraction patterns of selected serpentines. Cuk$_\alpha$ radiation.

mixed with collodion for mounting in the specimen holder. Two varieties of picrolite (#481-22 Harford, Maryland, 321-Pipe Lake) gave clinochrysotile patterns and are also recorded on Fig. 10.

Picrolite veins are commonly encountered intersecting the nickel belt serpentinites. They are normally less than one inch in width, pale greyish green to dark apple green in colour, have a waxy lustre and a compact, brittle form. Most are quite hard, but those occurring as matrix material to pegmatite breccia fragments adjacent to serpentinite in the Wabowden body, are surprisingly soft. Although the picrolite veins are compact and massive, in thin section they are seen to be distinctly fibrous. The fibers have high birefringence and positive elongation, and lie essentially normal to the vein walls. A specimen of picrolite from Harford, Maryland (#481-22, Mineral Museum, Dept. of Geology) has a pronounced fibrous habit, but is brittle and splintery. This material breaks down on grinding to a white fluffy powder, which gives a diffraction pattern similar to that of chrysotile asbestos (Fig. 10).

Selfridge (1936) and Gruner (1937) have classified picrolite as antigorite. The present study shows that picrolite has a structure similar to chrysotile. Differential thermal analyses, as is shown in the next section, corroborate the X-ray diffraction evidence. X-ray powder photographs of picrolite vein material from Thetford, Quebec are closely similar to those of asbestos (Riordan, 1955), and cross-fibrous picrolite veins from Matheson, Ontario have been shown to be mainly composed of lizardite and clinochrysotile (Grubb, 1962).

DIFFERENTIAL THERMAL ANALYSIS

Investigation of the serpentinites by means of differential thermal analysis (DTA.) has been made using the equipment and method described in Appendix V11. Differential thermal curves assist in the identification of fine grained hydrous silicates and are especially useful in the study of serpentine minerals. Distinction can be made between the chrysotile and antigorite groups or the presence of a mixture of these two minerals. It is not possible however, to determine by DTA. the various polymorphs within the chrysotile group. A comprehensive study of serpentine group minerals by DTA. has been made by Faust and Fahey (1962).

A selection of typical and representative DTA. curves for nickel belt chrysotile specimens are presented in Fig. 11. The curves have been reduced in size from the originals by approximately one third. The major thermal effect evident in the DTA. curves of chrysotile begins at approximately 600°C., where the loss of constitutional water initiates the break-down of the chrysotile structure. The resultant endothermic trough reaches a minimum at a temperature between 660°-675° for the samples examined. The trough is thus a record of the heat absorption accompanying the destruction of the serpentine, a process which is normally complete by 700°C. A prominent exothermic peak occurs on the records between 803-815°C., related to the formation of forsterite. The height or intensity of this peak is very variable (Figs. 11E and 11F), and does not appear to be related to the intensity or temperature of

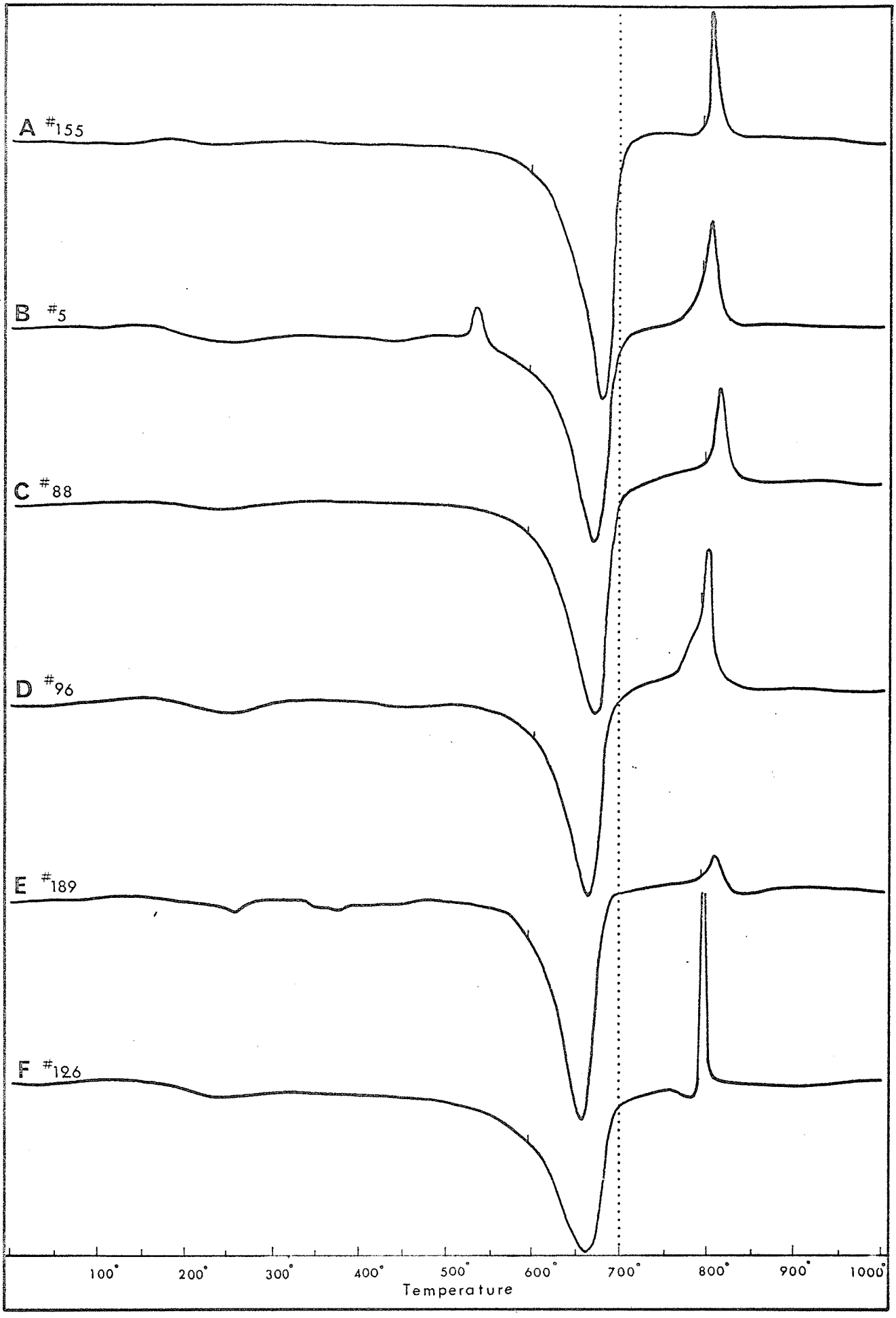

FIG. 11 : DTA. curves of 3-layer serpentines.

formation of the endothermic trough. It possibly bears a relationship to the composition of the olivine generated, but this remains to be determined. Faust and Fahey (1962) found no simple relationship of area and height of peak to the amount of sample used in the experiment. Small irregularities in the pattern of curves 11B and 11E are apparently due to the presence of minor quantities of contaminating minerals.

DTA. curves for specimens of antigorite are shown in Fig. 12. Two curves, 12A and 12B, for sample #82A from Ospwagan Lake are compared with those for three additional antigorite specimens from Manitoba, and to the specimen of "williamsite" (curve 12F), described in the previous section. The decomposition of antigorite takes place on heating in the 700-800°C. range. Antigorite can thus be easily distinguished from the chrysotile and lizardite minerals. In the samples examined, the minima of the endothermic trough varied between 755°-775°C. For specimen 82A, a minimum at 750°C. was obtained when heated in a nitrogen atmosphere compared with a temperature of 775°C. when heated in air. Apart from 12B, the curves were all obtained without the use of an artificial atmosphere. Immediately following the major endotherm a small exotherm is usually present between 810-815°C., no doubt related to the crystallization of olivine as a new phase. A small bow-shaped endotherm is generally present in the 870-875°C. range. This has generally been attributed to a possible phase transformation (Faust and Fahey, 1962). A slight inflection on the low temperature side of the major endothermic trough has been noted by a number

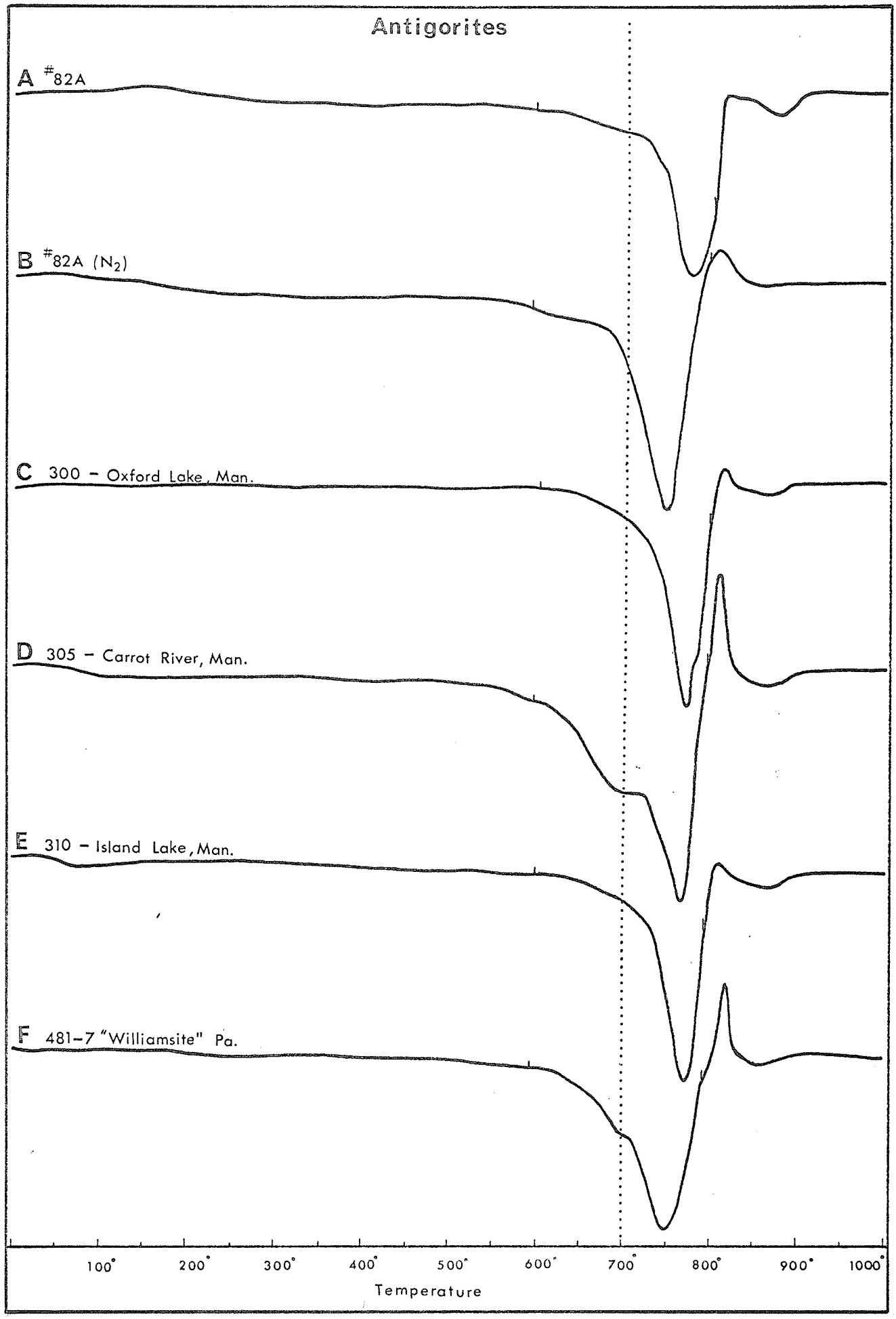

FIG. 12 : DTA. curves of antigorites.

of writers, and is a prominent feature of curves 12D and 12F. Faust and Fahey attribute the inflection to 1) the presence of chrysotile in the sample, 2) heterogeneity within the sample itself or 3) nonequilibrium factors. It is interesting to note that curve C-124 (p. 73) of those writers is not directly comparable to curve 12F above, and yet both are specimens of pure antigorite ("williamsite") from the same locality. Factors 2 and 3 therefore, may be important in producing certain features in DTA curves.

Below 600°C. and above 900°C., the antigorite curves are essentially straight lines. The complete absence or the very reduced size of the exothermic peak in antigorites as compared to that in chrysotiles has been discussed by Caillère and Hénin (1957). This feature depends on the temperature interval between dehydroxylation and recrystallization. In the chrysotiles, the interval is large, represented on the thermal curves by a nearly straight line. Sample material examined from this range is amorphous. Specimens of antigorite which have next to no exothermic peak, have been found to contain forsterite at a temperature slightly before the end of the endothermic peak.

Fig. 13 illustrates DTA. curves for a variety of serpentinous minerals. The clinochrysotile plus lizardite mixture in specimen #122 from Pipe Lake (curve 13A) shows a typical chrysotile pattern although the endothermic trough occurring at 680° C. is slightly higher than those of Fig. 11. The chrysotile and antigorite mixture previously described in specimen #312

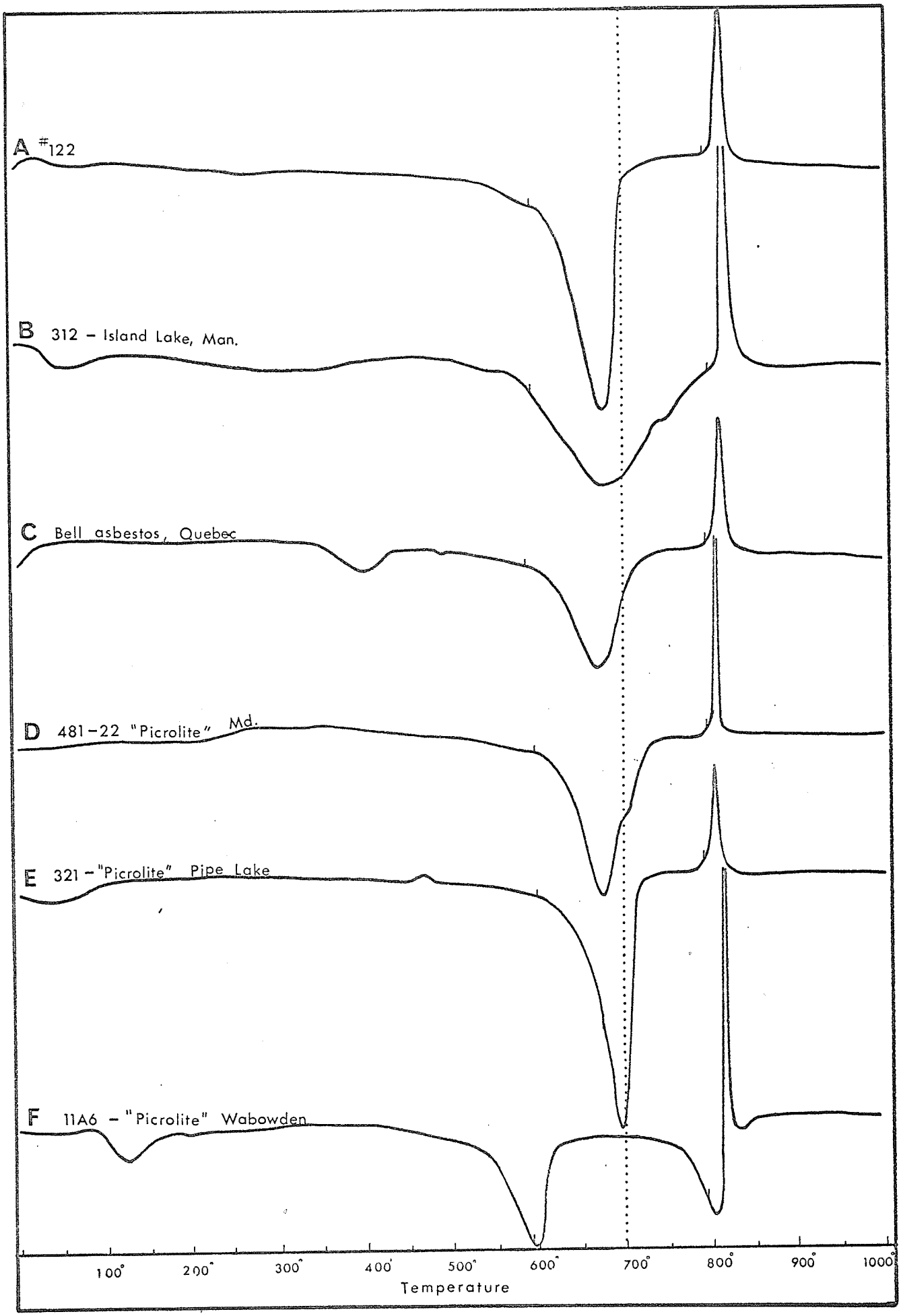

FIG. 13 : DTA. curves of selected serpentines.

from Island Lake shows up clearly in curve 13B. Endothermic troughs due to both minerals overlap one another, but the minima are recognizable. The chrysotile endotherm occurs at 680° and the antigorite at 750°. Asbestos fibers from the Bell Mine, Quebec give a typical chrysotile curve (13C), but both the endotherm and exotherm are reduced in intensity. This may be accounted for by the difficulty of packing the flexible fibers in the sample holder.

Differential thermal curves of picrolite are shown in Fig. 13D, E and F. The fibrous picrolite from Maryland (13D) has a chrysotile pattern with an intense exothermic peak at 810°. This curve differs considerably from the curves given by waxy picrolites obtained from the nickel belt. A deep steep-walled endothermic trough at 695° is a feature of the Pipe Lake specimen (curve 13E). Riordan (1955) records a similar temperature for the endotherm of picrolite from Thetford, Quebec, but the trough is wide and relatively shallow. No explanation can be given for the rather unusual curve (13F) for picrolite from the Wabowden serpentinite. Its features are well defined endotherms at 605° and 810°. An X-ray diffractogram of this mineral showed it to be poorly crystalline.

SUMMARY AND CONCLUSIONS

The optical investigation of Manitoba's nickel belt serpentinites shows them to be composed of cross-fiber chrysotile with two optical orientations, alpha serpentine and gamma ser-

pentine. The predominant fiber type is alpha serpentine with negative elongation. Fibrous material has three textural arrangements. (1) mesh texture serpentine with a more or less regular disposition of mutually interfering cross-fiber veinlets; (2) close-packed parallel veinlets and (3) a highly irregular branching network of veinlets with variable interstitial material. Pseudomorph boundaries in all three types are occasionally discernible. Antigorite has been identified in a small number of chrysotile serpentinites. It is of later replacement origin. One known occurrence at Ospwagan Lake is entirely composed of antigorite and it is believed to have originated by thermal metamorphism of chrysotile. From a variety of textural features, the rocks are considered to have originally been d unites and olivine-rich peridotites.

More detailed examination of fibrous serpentine composing the majority of the serpentinites, by X-ray diffraction procedures on powdered samples, has shown it to be a type not previously described. X-ray powder patterns of this serpentine can be satisfactorily indexed on the basis of a 3-layer cell with dimensions of a_o =5.346Å, b_o =9.205Å, c_o =21.930Å. The c parameter is approximately one half the value of that used by Zussman and Brindley (1957) in indexing a 6-layer serpentine from Unst. On the basis of X-ray and optical work, the Manitoba 3-layer serpentine is regarded as belonging to the orthochrysotile group. However until more detailed X-ray and electron diffraction studies prove the presence of a cylindrical structure, this conclusion must be considered tentative. The diffraction

studies have also indicated a mixture of clinochrysotile and lizardite in a specimen from Pipe Lake, and verified the occurrence of antigorite at Ospwagan Lake. Comparison has been made between the diffraction powder patterns of these minerals and with antigorite serpentinites from Island Lake, Oxford Lake and the Carrot River in Manitoba and with the well-known occurrence of antigorite ("williamsite") from Lancaster Co., Pennsylvania.

Differential thermal analysis of the serpentinites show that distinctions can be made between the chrysotile and the antigorite groups. DTA curves presented for the different serpentine minerals indicate that the different polymorphs of chrysotile cannot be distinguished from one another, nor from lizardite. For this, reliance must be made on X-ray diffraction methods. Thermal curves for picrolites, which generally give poorly resolved powder diffraction patterns, indicate they have the chrysotile structure.

CHAPTER V

MINERALOGRAPHY AND ORIGIN OF THE DISSEMINATED SULPHIDE MINERALS

INTRODUCTION

The occurrence of economic nickel sulphide deposits in association with the serpentinized ultramafic rocks of central Manitoba is the reason for the designation of this region as the Manitoba nickel belt. Nickel sulphides have two principal modes of occurrence. Massive, nickeliferous sulphides occur as irregular linear sheets, principally within sedimentary gneissic rocks at a number of localities, the most important being those at Thompson. Lower grade deposits of disseminated nickel-bearing sulphides occur in some of the serpentinized ultramafic rocks, the best known being those at Mystery and Moak Lakes. A large number of the serpentinite intrusive bodies emplaced along the belt contain disseminated sulphide minerals, which, although not present in sufficient quantity to constitute ore-grade material, are important in the consideration of ore genesis and the geochemistry of nickel. A description of the massive ore mineralogy is beyond the scope of this paper. For a detailed account of the Thompson mine geology and ore mineralogy, the reader is referred to the paper of Zurbrigg (1963). In the following section, a short description will be given of the sulphide mineralogy, as it pertains to dissemin-

ated occurrences in a number of serpentinite bodies. This will be followed by a discussion on the possible origins of such occurrences, and a brief reference to the distribution of nickel within them.

MINERALOGRAPHY OF THE SULPHIDE MINERALS

Disseminated sulphide minerals occurring within the serpentinized ultramafic rocks are pyrrhotite and pentlandite, with chalcopyrite, pyrite, marcasite and violarite also present in small amounts. Sulphide content of most specimens examined is less than 10% by volume, but some do contain much larger amounts, up to a maximum of 25%. In general the sulphide minerals occur as such finely divided particles or as fine intergranular net-textures intimately associated with the silicate minerals, that mechanical separation of pure sulphide material from all but the finest sized fractions would be unsatisfactory.

Pyrrhotite

Pyrrhotite is the dominant sulphide mineral in the ultramafic rocks, occurring in variable sized particles which are normally highly irregular in shape. Pentlandite is commonly present within the pyrrhotite and its modes of occurrence will be described below. In studying pyrrhotite and its textural relationship to the surrounding silicate minerals, it becomes obvious that the mineral has a basically interstitial occurrence in the form of ramifying net-textures, which differ only slightly

from specimen to specimen. Variation in the net-texture are illustrated in Plates 44 and 45.

A well developed pyrrhotite net-texture is seen in the mineralized serpentinite outcropping at the southwest end of Mystery Lake. In hand specimen, small rounded black serpentine pseudomorphs are clearly outlined by a network of pyrrhotite. Plate 44A illustrates this texture in polished section. Unlike most other localities, where net-texture pyrrhotite forms branching diffuse areas containing abundant silicate particles (Plates 44B, 45A, 45B), the Mystery occurrence is clearly defined, with smooth boundaries between the pseudomorphs and the enveloping pyrrhotite. It is common to find reddish-brown chrome spinels immersed in the sulphide.

Pentlandite

This mineral is present in only small amounts in the disseminated sulphide mineralization of the ultramafic rocks, but has a wide distribution. It always occurs in association with pyrrhotite and is present in a number of typical forms. One type of pentlandite takes the form of narrow, branching vein-like masses separating individual pyrrhotite grains (Plate 46). Such an occurrence, usually described as cell texture, is prominent in the nickel ores of the Sudbury region, (Hawley, 1962). Cross cutting relations between this type of pentlandite and the host pyrrhotite are absent, and it has been suggested in many descriptions of such material, that the pentlandite represents an accumulation of exsolved material at the pyrrhotite

PHOTOMICROGRAPHS * PYRRHOTITE TEXTURES

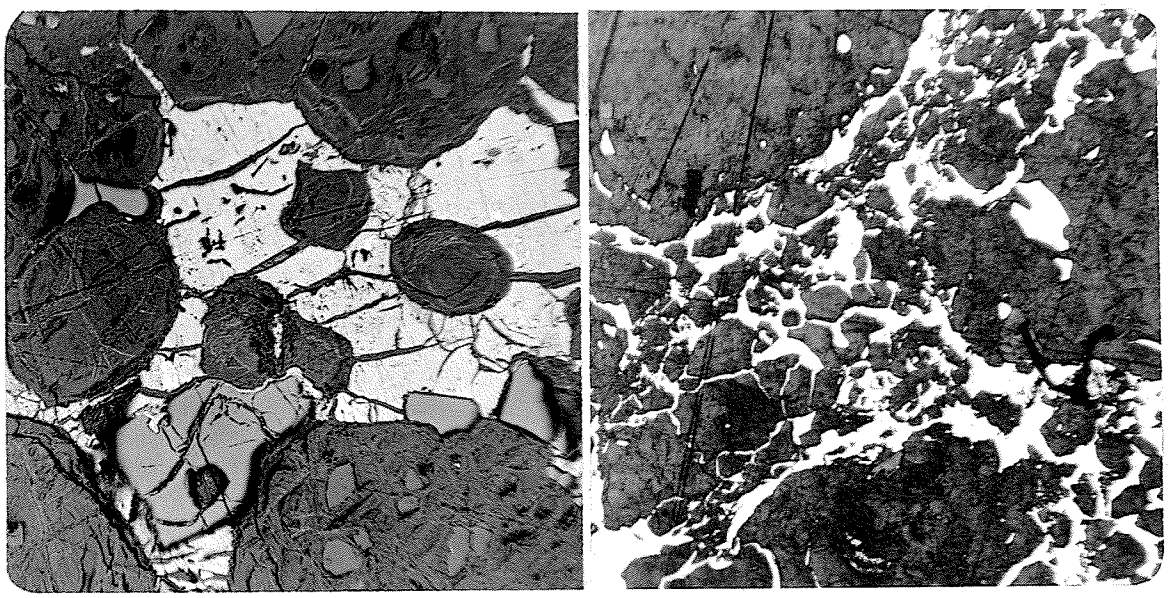

PLATE 44: A: Pyrrhotite interstitial to and surrounding rounded serpentine pseudomorphs after olivine. #125. (x22) Mystery Lake.

B: Net-texture pyrrhotite in serpentinite. Abundant inclusions in sulphide show partial replacement. #94. (x22). Moak Lake.

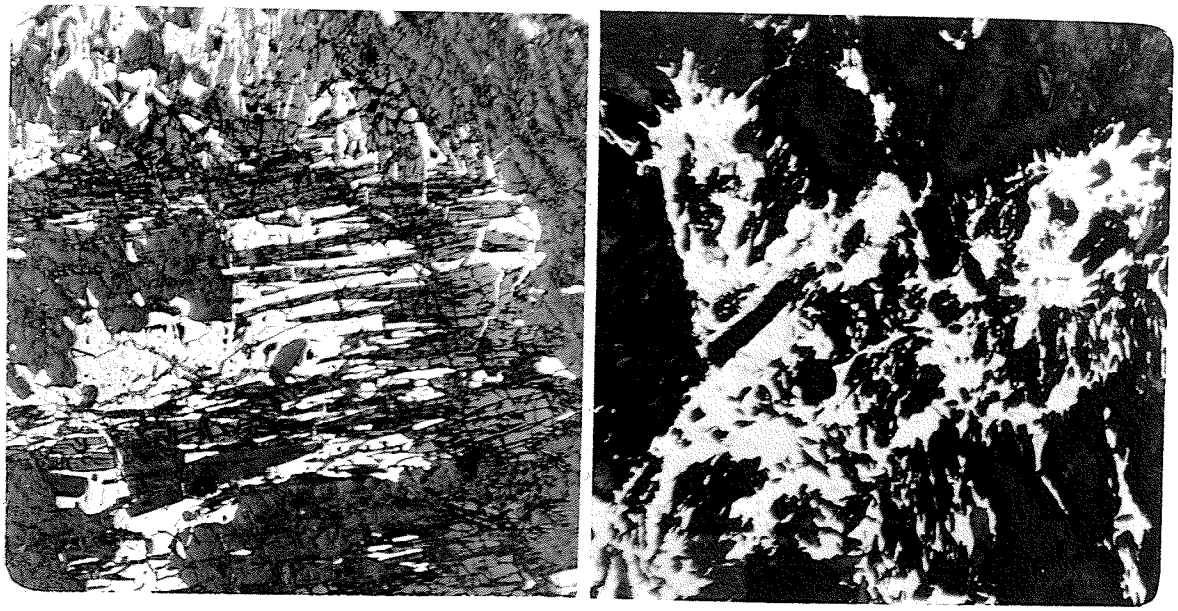

PLATE 45: A: Pyrrhotite occupying interstitial areas between tremolite laths which replace serpentine. #78. (x25), Mystery Lake.
B: Pyrrhotite net-texture. #99. (x25) Pipe Lake.

PHOTOMICROGRAPHS * PENTLANDITE

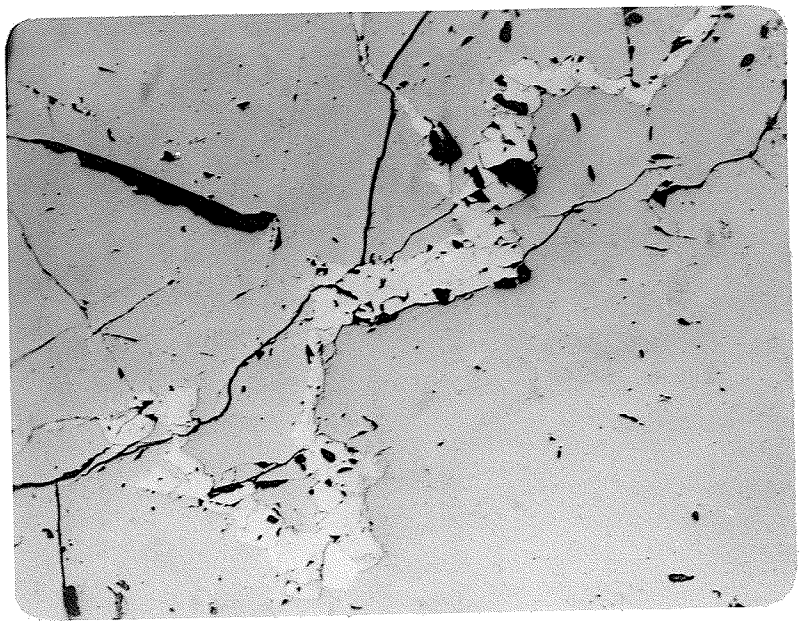

PLATE 46: Cell-texture pentlandite separating grains of pyrrhotite. Small white grain in pentlandite (top centre) is possibly a cobalt-bearing mineral. #121. (x22). Wabowden.

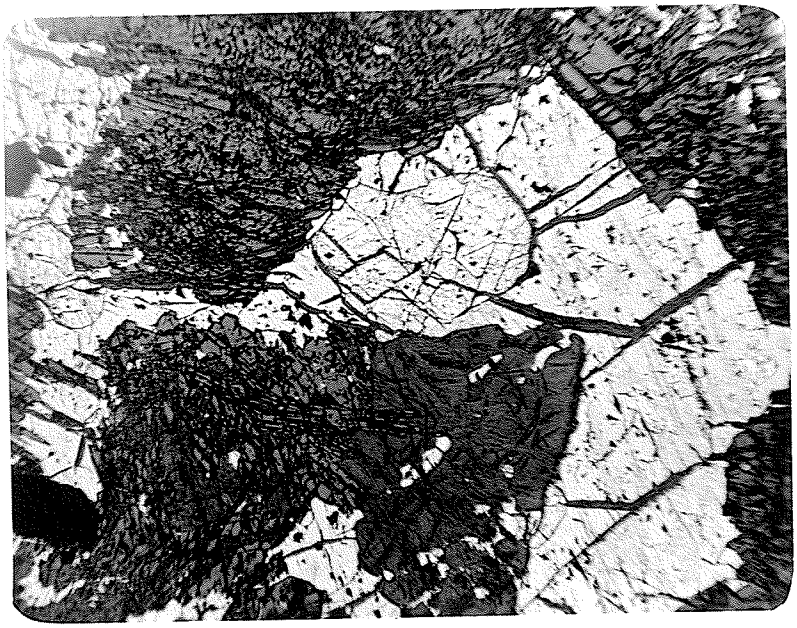

PLATE 47: Subhedral grain of pentlandite (octahedral cleavage) enclosed in pyrrhotite. #78. (x22). Mystery Lake.

crystal boundaries.

Of rarer occurrence are coarser grained veinlike masses of pentlandite, which exhibit smooth to highly ragged contacts with adjacent pyrrhotite. Locally, such masses may equal or even exceed the amount of pyrrhotite present. They give no suggestion of being an exsolved product.

Commonly, pentlandite occurs as discrete crystals in pyrrhotite (Plates 47, 48, 49). These generally have squarish outlines and often a well developed octahedral cleavage. Some marginal alteration to violarite has been noted in some specimens. This mode of occurrence of pentlandite is most predominent in the disseminated sulphides present in the ultramafic rocks of the nickel belt. At least 90 percent of the pentlandite takes this form.

Chalcopyrite

Chalcopyrite is not a common mineral in the disseminated sulphides found in the ultramafic rocks. Where present, it occurs as fine veins cutting pyrrhotite and occupying interstitial areas among the gangue minerals. It occasionally forms granular aggregates of small irregularly rounded grains with mutual to slightly interlocking boundaries. These may include optically continuous fragments of pyrrhotite (Plate 48). Chalcopyrite has also been noted occupying the cleavages of violarite after pentlandite, and the boundary line between pyrrhotite and pentlandite grains. Silicate fragments, where present within chalcopyrite, generally have highly ragged and

PHOTOMICROGRAPHS * PENTLANDITE, CHALCOPYRITE

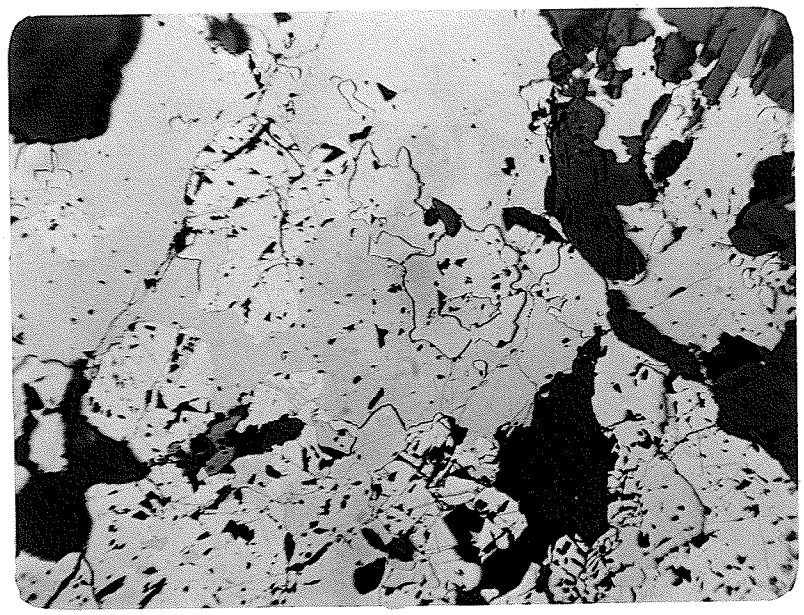

PLATE 48: Subhedral pentlandite (white, with cleavage) surrounded by pyrrhotite (grey). Irregular chalcopyrite grains replace pyrrhotite. #121. (x22). Wabowden.

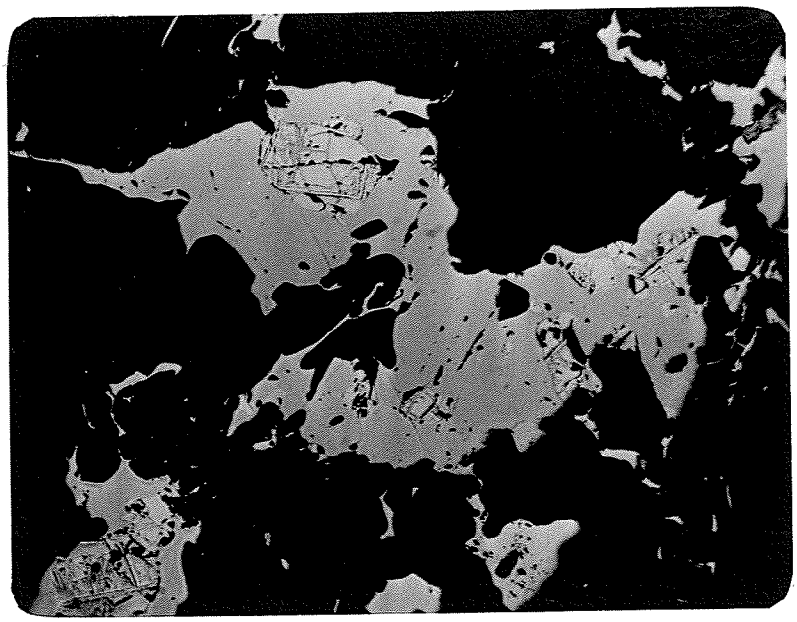

PLATE 49: Subhedral pentlandite grains (white) in pyrrhotite (grey). #94. (x20) Moak Lake.

corroded terminations.

In general, it may be said, that although chalcopyrite is a relatively rare sulphide in these rocks, it does occur occasionally and exhibits the normal paragenetic relationship to pyrrhotite and pentlandite.

Marcasite

Rare marcasite occurs as an alteration product of pyrrhotite in some of the mineralized ultramafic rocks from Pipe Lake. It is white in colour, shows typical anisotropism and is commonly associated with violarite and limonite. This mode of occurrence suggests that the marcasite is a supergene mineral formed by weathering at the expense of pyrrhotite.

Pyrite

Large vuggy grains of pyrite are occasionally found within the ultramafic rocks, generally to the accompaniment of fractured and faulted zones. In polished section, occasional pyrite grains with a general rounded but highly serrated outline are present within pyrrhotite, from which they appear to have developed by supergene alteration.

Violarite

The alteration of pentlandite to violarite takes place along cleavages and crystal boundaries. It is relatively rare and has developed by supergene alteration.

ORIGIN OF THE DISSEMINATED SULPHIDES

Due to widely scattered locations and variable composition of available sulphide bearing serpentinite material and the lack of systematic sampling of any particular mineralized body, no serious attempt has been made in the present work, to reach conclusions regarding the genesis of the disseminated sulphides. For the sake of completeness however, it is necessary to consider briefly the possible modes of origin in the light of prevailing hypotheses.

Three possible modes of origin for the disseminated sulphides can be entertained. First an igneous origin, whereby the sulphides crystallized from an ultrabasic intrusive magma containing an original high sulphur content. Secondly a metamorphic origin can be seriously considered, where a metasomatic introduction of sulphur during conditions of metamorphism results in the transfer of metallic elements, in this case principally nickel, from the nickel-rich ultramafic rocks to a developing sulphide phase. Thirdly the sulphides may have been deposited from hydrothermal fluids derived from igneous sources at depth. The source of such fluids could be a more siliceous and volatile-rich magma than that from which the ultramafic rocks were derived. Of these three possibilities the hydrothermal origin is considered the least likely to have resulted in the formation of the disseminated nickel sulphides. Some chemical aspects of hydrothermal activity affecting the ultramafic rocks will be considered in Chapters V1 and V11. It will be shown that this effect has barely altered

the nickel content of the rocks or resulted in the deposition of sulphides. Conversely, the presence of disseminated sulphides is not accompanied by any noticeable hydrothermal alteration. The abundant source of water required for extensive serpentinization in the rocks cannot be considered as the hydrothermal fluid also responsible for the deposition of sulphides. Serpentinization and sulphide mineralization are not spacially related, although both of course, do occur together.

The magmatic theory of origin in which the sulphide and silicate phases have crystallized from the same source material, is an obvious possibility. Hawley (1962) has shown in a comprehensive study of the Sudbury district, that certain ore deposits are the result of settling of a sulphide liquid to form both disseminated and massive zones of mineralization. Wager, Vincent and Smales (1957) describe detailed investigations of the sulphide minerals in the Skaergaard Intrusion in East Greenland. Immiscible sulphide liquids of copper and iron formed late in the fractionation of the Skaergaard magma, when nickel had been largely removed from the magma and incorporated in the crystal structures of olivine, pyroxene and magnetite. The authors suggest that the original low sulphur concentration in the magma was one of the chief factors in causing the late separation of an immiscible sulphide liquid from the silicate magma.

A high sulphur content in the nickel belt peridotite intrusions could have resulted in the early formation of a nickel-rich sulphide phase. Injection of a liquid sulphide

phase after crystallization of the silicate magma might have produced the massive and late stringer ores of the Thompson mine and other areas. The formation of an immiscible sulphide liquid during fractionation however, presupposes a liquid state for the intruding body. As will be discussed in a later Chapter, it is extremely doubtful that firstly, ultrabasic material having the composition of the nickel belt intrusive bodies was derived by fractionation from a less basic magma and secondly, that it was intruded in anywhere closely resembling a liquid state.

In an area of high grade metamorphic gneissic rocks where the serpentinites have been subjected to metamorphism, an origin by some metamorphic process must be considered. From geological observations made on the Thompson area, Sullivan (1959) has suggested that post-peridotite granitization and metamorphism brought about an extraction of nickel from the peridotites and its subsequent concentration with iron sulphides present in the area. Wilson and Brisbin (1961) consider a similar possibility, noting evidence of considerable sulphur metasomatism in the area. Metamorphosed banded iron formations consisting of quartz, grunerite and magnetite, in many places and over considerable lengths show conversion of the iron oxide to pyrrhotite. The authors cite the evidence of laboratory experiments in which the presence of hydrogen sulphide will form nickeliferous pyrrhotite in peridotite and will convert magnetite to pyrrhotite in the temperature range 400-650°C. at standard pressures.

Recent experimental work by Kullerud and Yoder (1963) has demonstrated that sulphur readily reacts with many of the common rock-forming silicates over wide temperature-pressure ranges to produce sulphides and oxides. Phase relations in the system Fe-S-O-SiO_2 at 800°C. and 2000 bars were deduced by experiments with fayalite and varying amounts of sulphur. In one experiment with 33⅓ mole percent S, derived products were pyrrhotite, magnetite, quartz and pentlandite. Sulphur can thus react with and cause the breakdown of silicates such as olivine to produce pyrrhotite and pentlandite with textures similar to that commonly observed in ore deposits. Kullerud and Yoder believe that magnesium in silicates probably does not react with sulphur to form sulphides but that the process readily takes place with elements such as iron, manganese, nickel, cobalt and copper. Naldrett and Kullerud (1965) have since described two examples where evidence suggests a sulphurization process of this type may have taken place adjacent to ore deposits.

Mineralogical evidence from the nickel belt occurrences, described earlier in this chapter, is of little assistance in reaching conclusions concerning the genesis of the sulphides. The net-texture relationship between the disseminated sulphides and surrounding silicate minerals, in which the sulphides occupy interstices between original silicate grains or their serpentinized pseudomorphs is indicative of the late crystallization of a magmatic sulphide phase or the selective replacement of the interstitial material. If the interstitial material

contained a higher Fe content that the remaining silicate minerals, reaction with introduced sulphur could conceivably produce the texture. Evidence of silicate replacement by sulphides as noted from polished and polished thin sections suggests the movement of sulphide material was the latest feature involved in the history or the ultramafic rocks. Redistribution under conditions of metamorphism undoubtedly played a part in determining the final disposition of the sulphide material.

DISTRIBUTION OF NICKEL

The partition of nickel between silicate minerals of basic and ultrabasic rocks and a coexisting sulphide phase has received attention from a number of research workers in recent years. In a study of the distribution of nickel in some mineralized basic intrusions in Finland, Häkli (1963) observed that the nickel content of olivine increases with the increasing nickel content of the sulphide phase. This positive correlation becomes even more pronounced when the atomic ratio Ni/Mg is plotted against the nickel percentage of the sulphide phase, that is, when the magnesium percentage of olivine is taken into consideration. A similar relationship exists between the pyroxenes and amphiboles and the coexisting sulphide phase, although for the amphiboles the linearity is not good. It is evident that a chemical equilibrium prevails in the distribution of nickel between the silicate and sulphide phases.

Shteinberg and Malakhov (1963) have found that in the

ultramafic rocks of the Urals there is a considerable variation in the ratio of sulphide nickel to silicate nickel but a definite constancy to the total nickel content. They found that the sulphide nickel content is usually proportional to the sulphur content. The authors suggest that the sulphide nickel in peridotites forms in situ at the expense of silicate nickel as a result of the relative immobility of nickel and mobility of sulphur.

The distribution of nickel between the silicate and sulphide phases in some of the mineralized ultramafic rocks of the nickel belt was determined as part of the present study. It is proposed to continue this program at a later date, when more abundant drill hole samples of a mineralized serpentinite would allow positive conclusions to be made regarding the distribution of nickel and the genesis of the sulphide minerals. In the present work, specimens of mineralized serpentinite and partially serpentinized ultramafic rock from widely scattered localities were analysed for nickel and sulphur as part of the complete rock analysis. As the fine grain size of much of the disseminated sulphides in the rocks made mechanical separation of the silicate and sulphide fractions impractical, a process of sulphide solution was used to leach sulphides and their constituent metallic elements from the silicate and associated oxide fractions. The solution process is described in Appendix 11. Re-analysis of the treated material gave the nickel content of the combined silicate-oxide phases, free of that originally present in the sulphides.

From 8 specimens of group A serpentinites, the silicate nickel content was found to vary between .000-.077% NiO with

an average value of .027% NiO. In this group of specimens, combined nickel content varied between .04-1.92% NiO. The average value of .027% silicate nickel is close to the value of .03% determined by Naldrett (1964) from mineralized peridotite containing more than .5% S, at the Alexo mine. However, Naldrett found that the silicate nickel content did not fall below the value of .03% regardless of the amount of S present as sulphides in the rock. Lack of analyses for low concentrations of S in the Manitoba occurrences prevents a complete picture of the nickel distribution being attained. Treated specimens of ultramafic rock containing different proportions of various silicate minerals, gave as might be expected, highly variable values of silicate nickel content.

Although conclusions from this phase of the study must be regarded at present, as being highly tentative, it is evident that the silicate and oxide minerals of serpentinites containing a disseminated sulphide phase, contain a much lower nickel content than serpentinites with no associated sulphides. Average values for analyses of the latter are presented in a later section of this report. Nickel has been removed from the silicates and incorporated in the sulphides phase. Many of the ultramafic bodies along the belt are either free of sulphides or contain disseminated sulphides in some sections. Although it cannot be regarded as positive evidence, the lack of homogeneity in distribution of the sulphides possibly favours the origin of sulphur from some external source, rather than regarding it as a component of the original ultrabasic material.

As Häkli (1963) has pointed out, a state of equilibrium

in the distribution of nickel is easily attained providing the temperature remains sufficiently high for a suitable length of time. Sulphide-bearing iron formations represent an abundant source of sulphur in some areas of the nickel belt. Interaction of sulphur from some such source with ultrabasic material during or shortly after intrusion is considered the most probable mode of origin for the disseminated sulphides.

CHAPTER VI

COMPOSITIONAL VARIATION OF THE M14 SERPENTINITE, SETTING LAKE

INTRODUCTION

The paucity of exposures of the ultramafic rocks along the nickel belt has prevented their complete examination. However, many complete drill hole intersections have been studied, and compilations prepared of the structure and geological environment of individual intrusions. In this section, certain features of the M14 ultramafic body, which underlies the waters of Setting Lake, some six miles north of the town of Wabowden are examined.

The M14 ultramafic intrusion has been intersected by a number of drill holes, which indicate a minimum length of 2200 feet and maximum width of 400 feet. It is lens-like, sinuous and apparently conformable to the enclosing rocks. Strike direction is NE and dips vertical to steeply dipping to the SE. The geological setting of the body is illustrated in Fig. 14. Principle host rocks to the intrusion are a series of interbedded quartzose greywackes and fine grained schistose metavolcanics, which have similar lithology to the Assean Lake group of rocks, occurring further north. The sediments vary from dark grey biotite-garnet-quartz schists to fine bedded

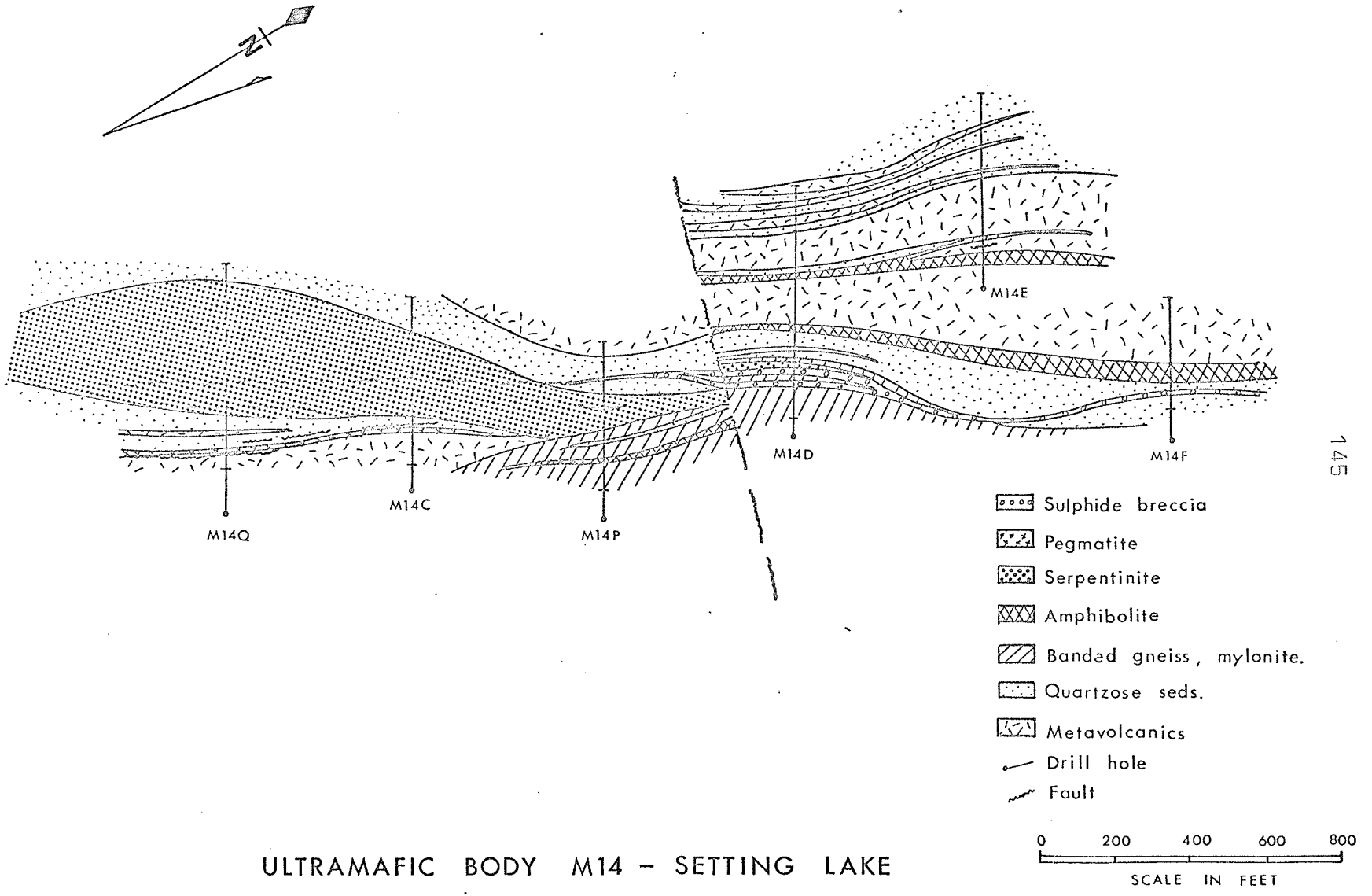

FIG. 14 : Sketchmap showing geology of the M14 serpentinite, Setting Lake. Compiled from drill hole information.

quartzites. Silimanite is occasionally present. A well developed gneissic banding, with biotite-rich seams alternating with granular quartz bands is often well developed. The metavolcanic series consist of dark green, fine grained amphibole schists. Considerable bronze biotite is present in some sections where fracturing is well developed, ramifying veinlets of pyrite, occasional quartz and carbonate are sometimes abundant.

The banded gneiss series, consisting of quartz-feldspar-hornblende banded gneisses occupies the area to the east of this sequence of less metamorphosed rocks. These rocks, especially in the region of their westerly contact are often highly mylonitized, indicating they have been faulted and intensely sheared. Evidence of faulting is common throughout the whole sequence of rocks, including the ultramafic intrusions. The latter show marginal shearing as well as internal zones of movement. Long narrow zones of sulphide breccia, preferentially found within the quartzose greywackes, but occasionally crossing unit boundaries into other formations, are composed of pyrrhotite and occasionally pyrite surrounding rounded fragments of quartz-biotite gneiss, quartz, amphibole schist, serpentinite and mylonite. It is evident that the formation of the sulphide breccia took place at a late stage in the deformational history of the region.

MINERALOGY AND COMPOSITION OF THE M14 SERPENTINITE

It is necessary to outline its present mineralogy to under-

stand fully the chemical variations which occur within this intrusive body. The chemistry and mineralogy of this ultramafic body has been studied from nineteen samples from section M14Q (Fig. 14), which crosses the intrusion at approximately its widest point. The specimens are closely spaced in the marginal areas but have been selected at wider intervals in the more central parts. Estimated modal analyses of all specimens are given in Appendix V111 and the chemical compositions in Appendix 1X.

The M14 ultramafic body is a massive olive green to dark green serpentinite in which diffuse lenses, or stringer-like segregations of magnetite are commonly dispersed. A 1 foot wide breccia zone, composed of irregular fragments of biotite gneiss and serpentinite surrounded by granular pyrite occurs along its east contact with a dark grey biotite-quartz schist. The west contact of the serpentinite and quartz-biotite gneiss does not show any evidence of faulting. Fractured and brecciated zones within the serpentinite are highly veined with late apple green picrolitic serpentine and white carbonate. Fracture surfaces are commonly stained with bright red hematite. Marginal alteration of the body against the enclosing country rocks is evident in the progressive changes of colour and texture, which first make their appearance some 20 feet from the contact. The rock becomes light grey to greenish-grey in colour and with the reduction in serpentine content, much harsher to the touch. An unusual band of biotite rock occurs in the east-central portion of the M14 body. The biotite rock is 10 feet wide and has sharp

contacts with the adjacent serpentinite. Fine red earthy spots of hematite and thread-like stringers of late serpentine are present throughout. Some tremolite accompanies the biotite in parts of the zone. For short distances on either side of the biotite, the serpentinite shows the pale grey to bluish-green alteration which is present along the outer margins of the intrusion.

Although the occurrence of monomineralic biotite zones are common along ultramafic-country rock boundaries (Phillips and Hess, 1936) and adjacent to pegmatite intrusions (see next section), they are seldom encountered entirely within the serpentinites. It is interesting to note that breccia fragments of quartz-biotite gneiss are enclosed within the serpentinite on the east side of the biotite rock, a few feet from its contact. It might seem therefore, that the biotite zone may represent an original inclusion of country rock, which by reaction with the serpentinite became desilicated. This would not explain however why adjacent inclusions remain relatively unaltered. The biotite on the other hand may represent the locus of shear zone up which hydrothermal solutions rich in potassium and aluminum, possibly derived from a pegmatite source, have invaded the serpentinite and brought about the alteration over a considerable width. Reference to this type of alteration will be made in the following section.

Mineralogically, the specimens which make up section M14Q are predominantly serpentinites which contain accessary amounts of spinel, carbonate minerals, magnetite, brucite, phlogopite, chlorite and sulphide minerals. X-ray diffraction pattern has

shown the serpentine to be orthochrysotile with a 3-layer structure (Fig. 8, #5). The diffraction pattern from specimen #12 is identical to #5 except in the presence of peaks attributed to chlorite. Minor amounts of "bastite" serpentine within the rocks indicate the former presence of some pyroxene. From fragmentary evidence of this type, the original nature of the serpentine is considered to have been an olivine-rich peridotite.

As in most bodies of this type, marginal alteration of the M14 serpentinite, produces profound changes in the mineralogy. This is especially prominant on the west side of M14, where the place of serpentine is taken by tremolite, anthophyllite and chlorite. The alteration is first observable in specimen #17, at 21 feet from the contact, where 35% tremolite and 10% carbonate accompany the serpentine. Anthophyllite appears in #18 at 11 feet from the contact, increases to a maximum of 60% in #19 and then quickly diminishes to 5% in #20 at a distance of 3 feet from the contact. Tremolite shows a steady increase to a maximum of 91% in #20. Chlorite first appears in specimen #21, taken at a distance of 1 foot from the contact, where it constitutes 20% of the rock, the remainder being tremolite. The chlorite content increases rapidly over a distance of a few inches until it forms a 6 inch wide monomineralic zone. It is considered that this zone represents completely altered country rock and that the contact between it and the serpentinite falls between the monomineralic chlorite zone and the chlorite-tremolite phase of specimen #21. The chlorite could not be examined in thin section but comparison with the marginal biotite zones, which form as the altered margin of pegmatites

cutting serpentinite, to be described in the next chapter, suggests that it constitutes an extreme alteration phase of the silicious country rock. This is in agreement with the views of Phillips and Hess (1936), Chidester (1962), Read (1934) and others who have described zoned contacts of this nature. Biotite takes the place of chlorite a few inches past the monomineralic zone and makes up 50% of the rock together with feldspar, minor quartz and tremolite at footage 890.5. There is a quick but even reduction in biotite to the general level prevalent in the country rock schists and gneisses, at a distance of 1.5 feet from the contact. Quartz content of the gneisses also quickly increases, once the limit of influence of the contact alteration is passed.

The chlorite of the monomineralic zone occurs as parallel brittle and non-elastic micaceous flakes. Its X-ray diffraction pattern was not sufficiently clear to be sure of its identification, but it compared fairly well with the pattern recorded for kotschubeite, a chromium bearing chlorite structurally similar to penninite. The analysis of sample #21 containing 20% of this mineral is rather low in chromium however. In thin section, it is seen to be replacing a highly birefringent biotite. It is pleochroic with X = pale yellow brown, Y = blue green and Z = deep blue green. Nearly isotropic basal sections give $(-)2V = 5^{\circ}$ approximately. Birefringence is anomalous blue to brownish-blue. The chlorite appears to be penninite, which has developed from biotite. It can thus be assumed that the monomineralic chlorite zone developed from an original

marginal zone of biotite, by retrograde metamorphism, probably induced by marginal shearing.

In addition to the marginal alteration of the serpentinite, related to the contact with country rocks, a narrow zone of fracturing at 37 feet from the west contact has brought about the development of 8 inches of anthophyllite rock (see Plate 15, # 15). The origin of anthophyllite is discussed below as a feature of pegmatite intrusion into serpentinite. Its presence in the M14 body as a monomineralic zone related to fracturing confirms the hydrothermal and metasomatic origin set forth for the latter type of occurrence. In the oxide variation diagrams and discussion on composition which follows, the anthophyllite zone (#15) has been omitted, in that it is not directly related to the marginal alteration and is separated from these changes by unaltered serpentinite (#16). The composition of the anthophyllite however is included in the analyses listed in Appendix 1X.

The chemical variation across the M14 serpentinite is represented by plotting oxide weight percentage against distance in feet for nineteen specimens selected from drill hole M14Q.(Figs. 15A and 15B). Distance in this case is core length and not true horizontal width. Successive specimens from left to right on the figures are thus at successively decreasing elevations within the serpentinite body. For practical purposes however, they may be regarded as successive specimens along a horizontal line.

The marginal alteration at the west contact of the M14 ultramafic body is represented in more detail in Fig. 16,

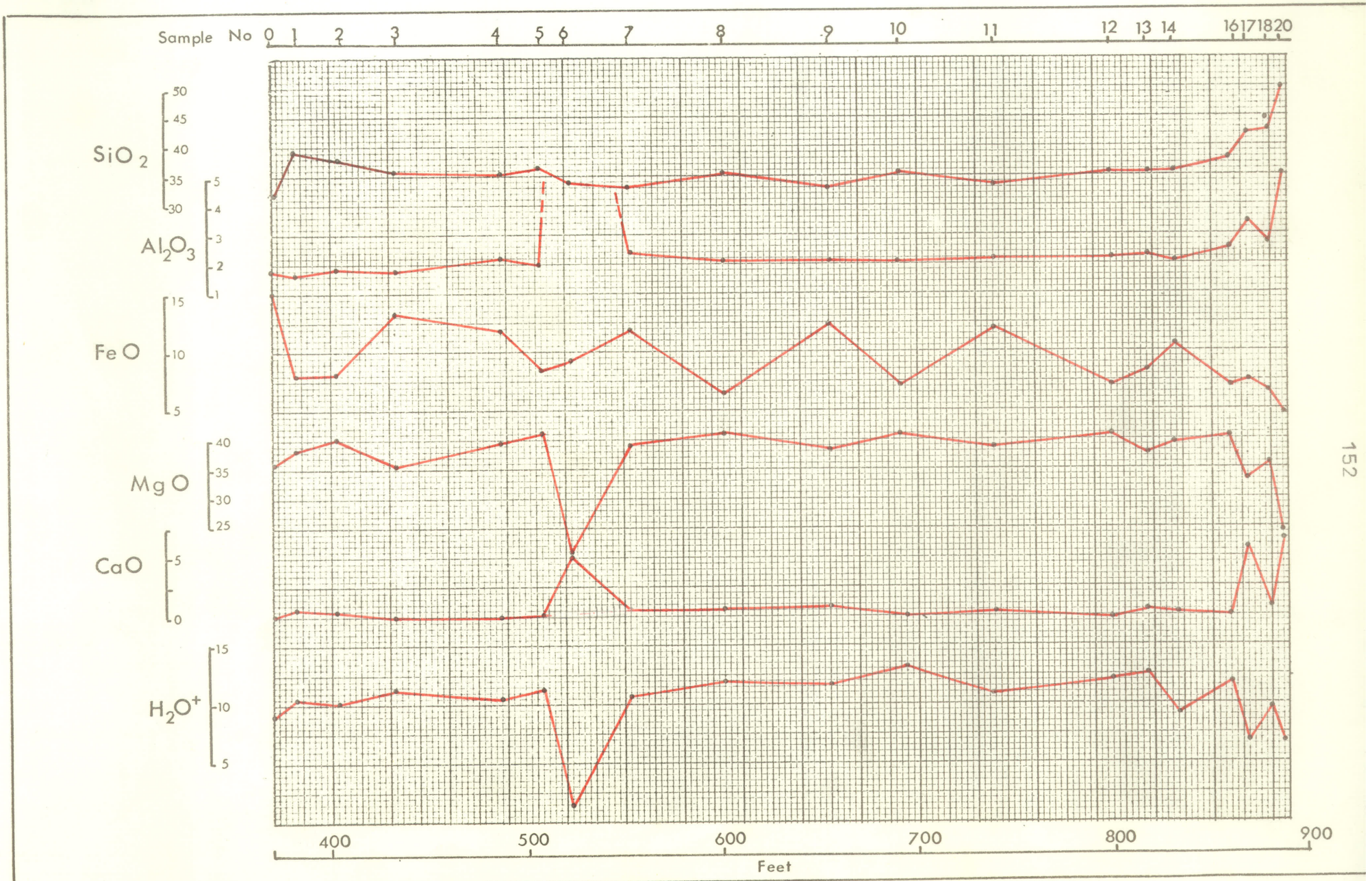

FIG. 15A : Variation diagram showing compositions (wt.%) of specimens across the M14 serpentinite.

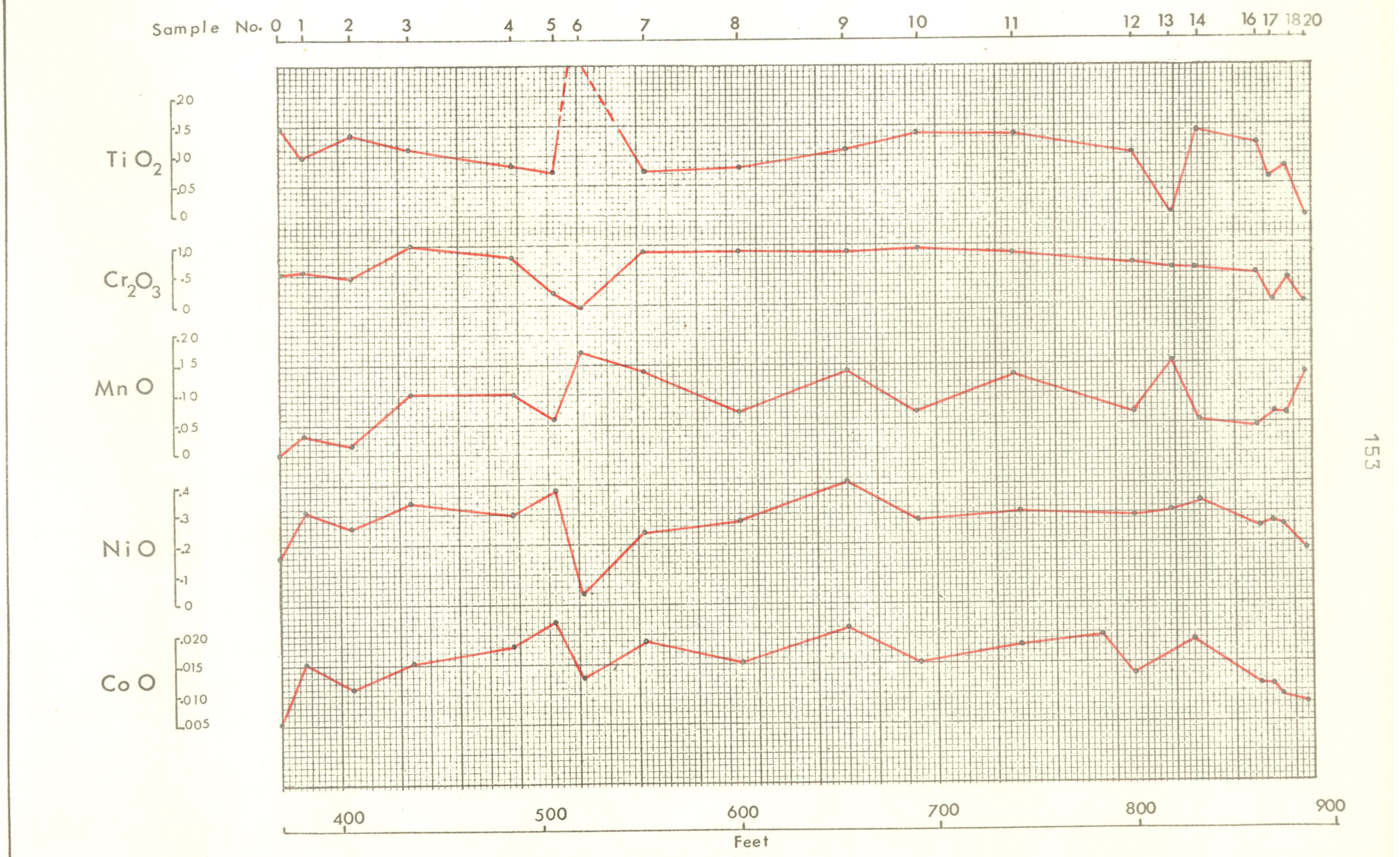

FIG. 15B : Variation diagram showing compositions (wt.%) of specimens across the M14 serpentinite.

showing the chemical composition of the modified standard cells (MSC). Calculation of the MSC has been made from the analyses of 6 marginal ultramafic samples and 1 of the adjacent quartz-biotite-garnet schist, following the method of Chidester (1962). Computation of the analyses on this basis allows direct comparison of the composition of specimens with variable degrees of alteration and widely differing densities. Contents of the MSC's for the 7 specimens across the contact are listed as MSC rock formulas in Table 8, following the method of Chidester (1962). Total cations and oxygen equivalents (Oeq) of each cell are also listed. The gains and losses of constituents are readily apparent from Fig. 16. Procedures used in determining the contents of the modified standard cells and the calculations from the analyses of the 7 specimens used in this study are included as Appendix X. Using the data compiled on Figs. 15A, 15B and 16, the geochemistry of each of the constituents on which information is available and the course of movement of the elements during marginal alteration will be discussed briefly.

Silica (SiO_2)

The silica content of the M14 serpentinite remains fairly uniform around 35% but rises rapidly along the margins. It has a maximum value of 51.8% in the contact anthophyllite-tremolite zone (#19). The drop off in silica on the left side of Fig. 15A for sample #0 (east margin of serpentinite) is due to the high sulphide content in this specimen. The left and right sides of the diagram are therefore not really comparable chemically, and

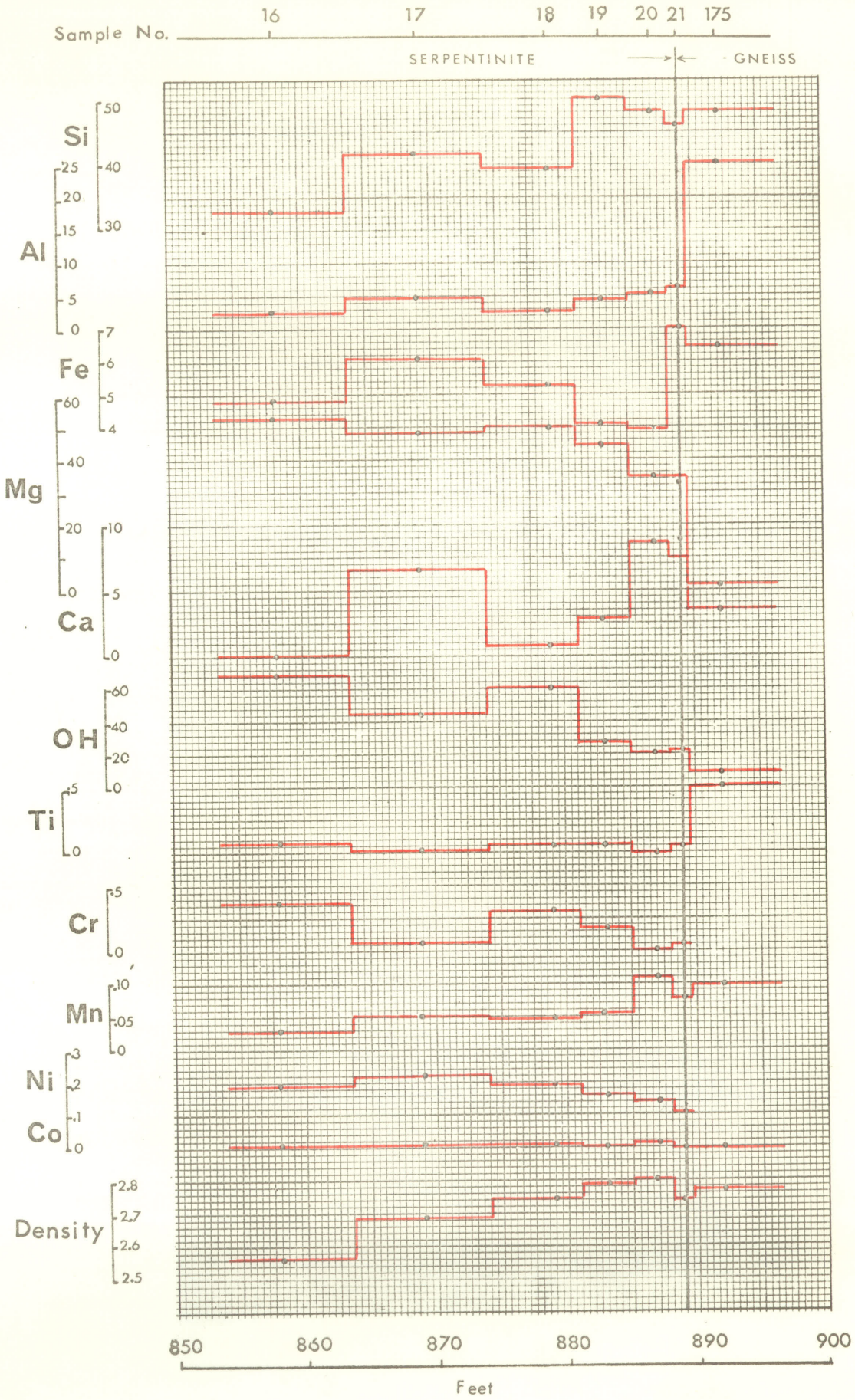

FIG. 16 : Variation diagram based on modified standard cells (MSC) for specimens across west contact of M14

in the following discussion the variations on the right side (west contact) will be regarded as the type example.

The alteration of serpentinite to tremolite, anthophyllite and chlorite bearing rocks requires a considerable addition of silica, some of which has been obtained from the chlorite zone and the remainder from the marginal country rocks. The silica contact of the latter is considerably reduced (#175-52.6%) adjacent to the contact, in contrast to the higher values further out (#176-66.0%).

Alumina Al_2O_3

Alumina is a minor constituent of the ultramafic rock being present with a more or less constant value of slightly greater than 2%, in contrast to the high aluminous, biotite-rich marginal zone of the country rock. Slight gains in Al_2O_3 are coincident with the development of tremolite, anthophyllite and chlorite in the marginal ultramafic rocks.

Ferrous iron (FeO)

The rapid undulations in the curve for Fe^{+2} (Fig. 15A) can be correlated with the modal content of magnetite in the serpentinite. This variation in magnetite content, masks any variation which may be present in the Fe^{+2} content of the serpentinite. It is clear however that Fe^{+2} is lost in the alteration process affecting the serpentinite and concentrated in the chlorite-rich zone (Fig. 16).

TABLE 8

MSC ROCK FORMULAS, WEST CONTACT, M14 ULTRAMAFIC BODY

Sample	
16	$[K_{.00}Ca_{.00}Mg_{53.14}Fe^{+2}{}_{4.90}Mn_{.03}Ni_{.19}Co_{.01}Al_{2.65}Cr_{.36}Ti_{.07}Si_{32.95}O_{94.43}(OH)_{68.8}]$
	Cations = 94.30 Oeq = 163.23
17	$[K_{.00}Ca_{6.28}Mg_{48.20}Fe^{+2}{}_{6.16}Mn_{.05}Ni_{.22}Co_{.01}Al_{4.22}Cr_{.04}Ti_{.04}Si_{41.85}O_{126.32}(OH)_{45.30}(CO_2)_{2.69}]$
	Cations = 109.77 Oeq = 178.43
18	$[K_{.00}Ca_{.93}Mg_{51.95}Fe^{+2}{}_{5.26}Mn_{.05}Ni_{.20}Co_{.01}Al_{2.99}Cr_{.31}Ti_{.06}Si_{39.66}O_{112.62}(OH)_{60.41}]$
	Cations = 101.43 Oeq = 173.03
19	$[K_{.00}Ca_{2.63}Mg_{45.45}Fe^{+2}{}_{4.11}Mn_{.05}Ni_{.15}Al_{4.0}Cr_{.17}Ti_{.06}Si_{50.02}O_{146.14}(OH)_{25.36}(CO_2)_{.70}]$
	Cations = 107.34 Oeq = 172.91
20	$[K_{.00}Ca_{9.16}Mg_{34.52}Fe^{+2}{}_{3.94}Mn_{.11}Ni_{.14}Co_{.01}Al_{5.66}Cr_{.00}Ti_{.00}Si_{48.01}S_{.54}O_{129.87}(OH)_{21.71}]$
	Cations = 101.55 Oeq = 173.83
21	$[K_{.00}Na_{.55}Ca_{7.98}Mg_{34.54}Fe^{+2}{}_{7.08}Mn_{.08}Ni_{.10}Al_{6.25}Cr_{.06}Ti_{.05}Si_{46.01}O_{140.01}(OH)_{23.27}]$
	Cations = 102.72 Oeq = 163.28
22	$[K_{3.49}Na_{9.53}Ca_{3.47}Mg_{1.54}Fe^{+2}{}_{6.37}Mn_{.10}Co_{.00}Al_{25.88}Ti_{.52}Si_{47.89}O_{148.95}(OH)_{9.41}]$
	Cations = 98.81 Oeq = 158.35

Magnesia MgO

Magnesia is a major constituent of the serpentinite, ranging between 35-40% with an average value near 40%. A steady increasing loss of MgO is evident in the alteration zone (Fig. 16), with the greatest change starting at a maximum of 6 feet from the contact. The MgO migrated outwards, and although no analysis is available, a considerable part is undoubtedly incorporated in the monomineralic chlorite zone. Some MgO has migrated past this zone into the adjacent schists, where fine thread-like veinlets of serpentine are occasionally present. It appears that MgO was fairly mobile during the alteration process and where it could not be contained in chlorite or biotite developing in the contact zone, was deposited as hydrated magnesium silicate in the surrounding rocks. Evidence to this effect will be expanded in the following chapter, where the deposition in brecciated pegmatites is more clearly developed.

Lime CaO

The curve for calcium oxide duplicates that for magnesia but in the reverse sense. The peak representing the tremolite content of the biotite zone (#6) is accompanied by a reduction in magnesia. Similarly the contact zone shows corresponding increases of calcium in tremolite-rich samples (#17, 20) but decreases where anthophyllite is the dominant phase (#18). Average CaO content of unaltered serpentinite is less than 0.5% and most of this amount is present as dolomite. There has thus

been a considerable gain in CaO in the ultramafic marginal zone. Some of this has migrated from the adjacent schists. The origin of late tremolite in a large number of the nickel belt serpentinites, requires an external source of Ca, the source of which must be adjacent country rocks or solutions of a hydrothermal nature finding access along the contact.

Water H_2O

Water content of the serpentinite shows small variation between 10-12%. It is directly equatable with the serpentine content and decreases sharply with the appearance of other less hydrous silicate minerals in the contact zone. Part of this displaced water is taken up by the chlorite and biotite rich marginal zone of the country rocks and the remainder completely expelled from the system.

Titania TiO_2

Titania content of the serpentinite ranges between .05-.15%, whereas the biotite schists generally contain greater than .5% TiO_2. Movement of titania during marginal alteration of the serpentinite is not evident.

Chromium Oxide Cr_2O_3

Chromium content of the M14 serpentinite is constant at 0.9 weight percent in the central section, but declines gradu-

ally towards the margins. It is absent in the biotite rock (#6) and some of the highly altered marginal phases. Chromium occurs in the serpentinite chiefly in chromium spinels, which in this ultramafic body have a deep reddish-brown colour and narrow opaque borders.

Manganese Oxide MnO

Manganese is a minor but persistent constituent in the serpentinite. It occurs in slightly greater amounts in the siliceous country rocks. Mn is similar geochemically to Fe^{+2} and its content in the serpentine (Fig. 15B) shows a close relationship to that of Fe^{+2} (Fig. 15A). A slight gain is registered in Mn for the tremolite-rich rocks close to the contact (#20, 21, Fig. 16).

Nickel Oxide NiO

Nickel content of the serpentinite varies between .25-.40 weight percent. Some of the higher values may be attributed to the presence of nickel-bearing pyrrhotite, but most occurs in silicates in substitution for Mg^{+2} and Fe^{+2}. Accompanying the reduction of the elements in rocks of the marginally altered zone, there is a gradual but steady loss in nickel (Fig. 16). The NiO content of the adjacent siliceous rocks and of the chlorite zone has not been determined, so that the final disposition of this element could not be ascertained.

Cobalt Oxide CoO

Cobalt is present in trace amounts in both the serpentinite and siliceous country rock. It probably is contained in silicate minerals in substitution for Mg in the same manner as Fe^{+2}, Mn^{+2} and Ni^{+2}. No appreciable change in Co content occurs during the alteration of serpentinite.

Density

Densities are plotted for all specimens in which the contents of the modified standard cell have been determined. The serpentinite (#16) has density of 2.556, which increases steadily in the rocks towards the contact, reaching a maximum of 2.799 for the tremolite rich marginal sample #20. Density of the country rock adjacent to the contact (#175) is 2.774.

Absolute gains and losses per modified standard cell, for the alteration of serpentinite to the various tremolite, anthophyllite and tremolite-chlorite rocks of the marginal zone are listed in Table 9. The lack of an analysis for the monomineralic chlorite zone and adjacent biotite-rich gneissic country rock prevents a similar listing of gains and losses resulting from alteration on that side of the contact. Table 9 shows that major changes in the alteration of serpentinite include considerable loss of MgO and H_2O and substantial gains in SiO_2, Al_2O_3 and CaO.

TABLE 9

GAINS AND LOSSES (PER MSC) DURING ALTERATION

	SERPENTINITE (#16) ALTERING TO				
	#17 Tremolite Serpentinite	#18 Anthophyllite Serpentinite	#19 Antho.-trem. Serpentinite	#20 Tremolite	#21 Tremolite-chlorite
Si	+8.90	+6.71	+17.07	+15.06	+13.06
Al	+1.57	+0.34	+1.35	+3.01	+3.60
Fe^{+2}	+1.26	+0.36	-0.79	-0.96	+2.18
Mg	-4.94	-1.19	-7.69	-18.62	-18.60
Ca	+6.28	+0.93	+2.63	+9.16	+7.98
Na	nd	nd	nd	nd	+0.55
K	.00	.00	.00	.00	.00
OH	-23.5	-8.39	-43.44	-47.44	-45.53
CO_2	+2.69	nd	+0.70	nd	.00
Ti	-0.03	-0.01	-0.01	-0.07	-0.02
Cr	-0.32	-0.05	-0.19	-0.36	-0.30
Mn	+0.02	+0.02	+0.02	+0.08	+0.05
Ni	+0.03	+0.01	-0.04	-0.05	-0.09
Co	.00	.00	nd	00	nd
S	+1.42	nd	nd	+0.54	nd
O	+31.89	+18.19	+51.71	+35.44	+45.58
Oeq	+15.20	+9.80	+9.68	+10.60	+0.05

(+) indicates gain with respect to serpentinite #16

(-) indicates loss with respect to serpentinite #16

nd - not determined.

SUMMARY AND CONCLUSIONS

The foregoing chemical investigation of the composition of the M14 serpentinite has shown that, for the most part, there is considerable uniformity in the content of major elements. Oxide weight percent curves indicate we are dealing with a single homogeneous intrusive body. Among the major elements, the greatest variations occur in the content of ferrous iron. It has been shown above, that the release of iron during serpentinization of primary silicate minerals, does not generally result in an even distribution of magnetite. A form of metamorphic differentiation takes place in which iron aggregates at separate centres of crystallization. This in turn leads to a widely variable magnetite content between single specimens. Of the minor elements, Mn, Ni and Co show the largest variations.

Marginal alteration of the serpentinite along its contact with siliceous country rocks, is significant for a maximum width of about 20 feet. The most profound changes however, take place within 5 feet of the contact. Tremolite, anthophyllite and chlorite are developed in an overlapping zonal arrangement, from the contact inward towards the serpentinite. A 6-inch monomineralic zone of chorite constitutes the most altered part of the country rock adjacent to the serpentinite. The chorite has developed by replacement from a marginal zone of biotite. The chlorite quickly passes into unaltered biotite in the country rock a few inches beyond the chlorite zone. In the descriptions given by Phillips and Hess (1936), the arrangement of minerals at M14 would correspond to their higher temp-

erature type of alteration affected by a later, lower temperature stage, during which the biotite alters to chlorite.

The chemical changes taking place in the serpentinite alteration are graphically represented in Fig. 16 and summarized in Table 9. Gains are registered for Si, Al, Ca and Mn while Mg, Fe, OH, Cr and Ni show losses. It is uncertain whether losses and gains from the serpentinite are counterbalanced by corresponding gains and losses from the marginal country rocks. Quantitative estimates would require more detailed sampling, analyses and calculations of modified standard cells for specimens of adjacent country rock. Certainly, if the origin of the biotite and tremolite rock (#6) located within the serpentinite, far from the contact, is considered to have resulted from hydrothermal solutions, these must have been transporting large amounts of alkalies, alumina, iron and calcium.

One of the most prevalent minerals replacing the serpentinite, both at the M14 location under discussion, and many other ultramafic bodies along the nickel belt, is tremolite. The formation of tremolite in serpentinite could result in a number of ways. It could be formed isochemically during regional metamorphism, from Ca originally contained in clinopyroxene. Ca could be obtained from the country rocks during the interchange of materials previously described or it could be obtained from introduced hydrothermal solutions. Remnant clinopyroxene is extremely rare in the serpentinites in comparison to orthopyroxene. The former is generally more difficult to serpentinize and if present in any abundance originally, more evidence of its presence would be expected. The serpentinites themselves

are extremely low in Ca. The country rocks are a possible source for some Ca, but specimen #175 close to the serpentinite contact, contains more Ca than is generally present in these rocks. This is caused in some respect by the greater proportion of plagioclase and much reduced quartz content of this rock compared to the less altered specimens. It might seem therefore, that considerable Ca has been introduced into the marginal zones of serpentinites by the solutions which brought about and caused the migration of the other elements described above.

CHAPTER V11

ALTERATION OF SERPENTINITE AS A RESULT OF PEGMATITE INTRUSION

INTRODUCTION

Alteration of the serpentinized ultramafic rocks due to metamorphism and metasomatism has been described petrologically in chapter 111. It is often difficult to account for certain features of the alteration because the overall mineralogy of an ultramafic body cannot be determined from a small number of specimens available in drill core. One of the more highly altered intrusions, which has been explored by drilling in considerable detail, provides information which can be extrapolated to single specimens from other localities. The ultramafic intrusion in question is M11A, located a few miles south of Wabowden, towards the southwest end of the nickel belt.

Fig. 17 is a surface plan of the body prepared from drill hole information, combined with a map of local outcrop. It can be seen that the areas of outcrop form ridges of high ground, which border areas of low swampy ground. The ultramafic rock underlies the low swampy areas and has no surface outcrop.

Outcrops consist of pink quartz-feldspathic gneisses, fine banded hornblende gneiss and coarse grained pink and white pegmatite material. These units are inextricably mixed, with pink gneisses rapidly taking the place of hornblende gneiss over short distances on any single outcrop. Coarse quartz-

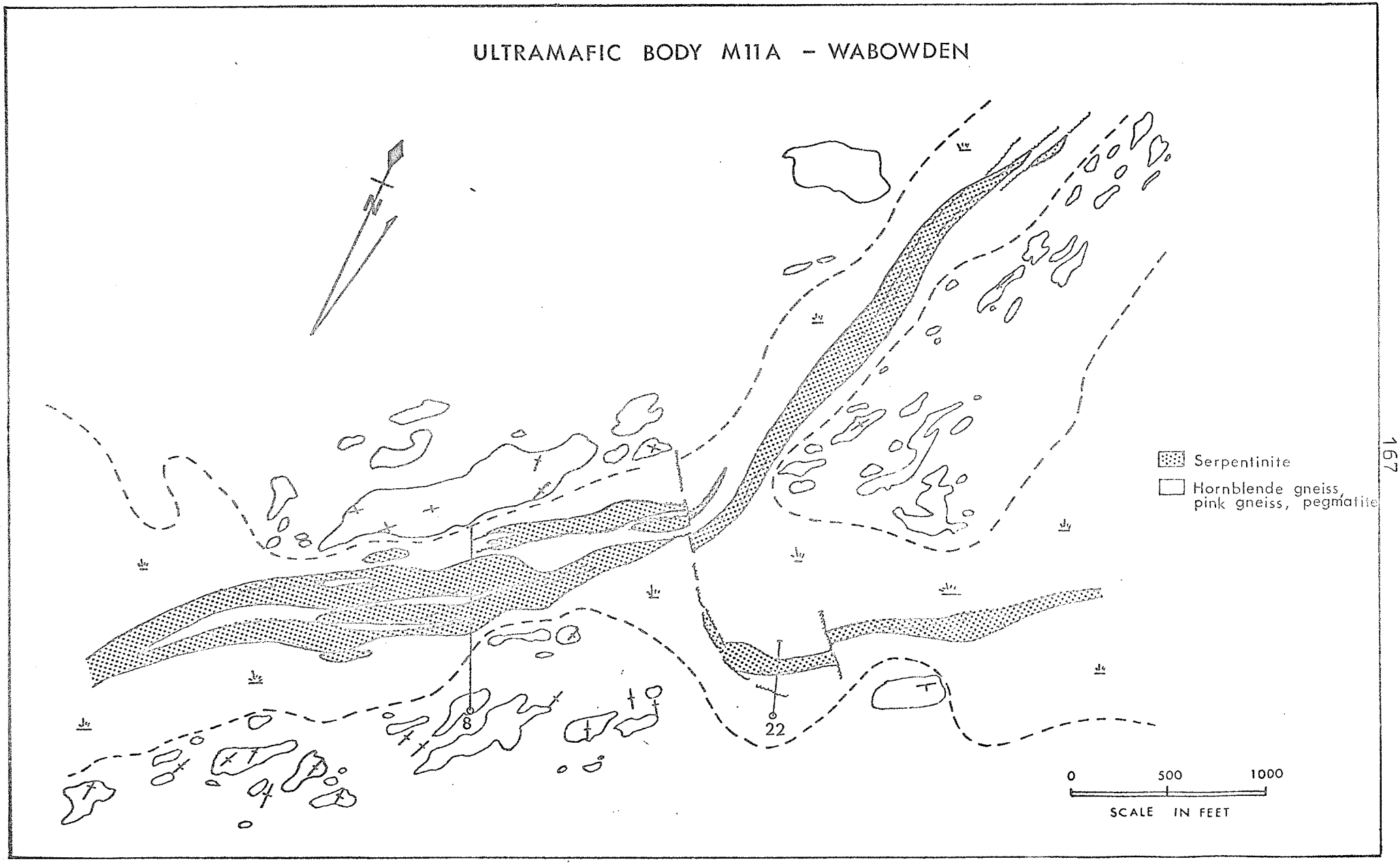

FIG. 17 : Sketchmap showing geology of the M11A serpentinite, Wabowden. Compiled from surface and drill hole information.

feldspar pegmatite cuts the gneisses as narrow dykes or forms large irregular masses in the host rocks. Estimated pegmatite percentage of outcrops ranges generally between 10-15 percent. Gneissic trends are variable. At the south end of the ultramafic body, the trends of the bordering gneiss are NNE to NE, intersecting the line of the ultramafic rock at a small angle. To the northeast, gneissosity generally parallels the axis of the ultramafic body.

In a number of aspects, the M11A ultramafic intrusion differs from most others, which are equally well delineated and about which an equal amount of information is available. It is elongated, lensoidal and sinuous, but is apparently made up of a number of separate sections which form a Y shaped body striking approximately northeast-southwest. Total length of the intrusion is approximately 6000 feet. The main stem of the Y has a complex structure with long narrow inclusion-like blocks of country rock subdividing it into interconnecting sections. Four satellite bodies are closely associated along its outer margins. The limbs of the Y are narrower and less complex than the main stem.

Evidence of considerable faulting is a notable feature of this body. Faults and shears are present both within and along the margins of the ultramafic complex (Fig. 17). A prominent cross fault bisects the body. The southeast limb has "smeared" out along this fault, suggesting the movement had a large horizontal component, with the east side moving south. The strike faults within the ultramafic rock are most easily recognized at the contact of pegmatite dykes which intersect

the serpentinite with considerable frequency. The precise attitude of pegmatites within the body is not known but the majority appear to strike parallel to the long axis. Where movement has taken place along pegmatite-ultramafic rock contacts, the pegmatite is brecciated and the fragments surrounded by a sheared matrix of chlorite, amphibole and biotite, intricately veined by green waxy serpentinous material. In many places the matrix to the pegmatite breccia consists entirely of this material which is apple green, soft, homogeneous and closely resembles some picrolites. A specimen of this, (11A6-"picrolite", Wabowden) has been described in the previous section. Faulting of the ultramafic material, where no pegmatite is present and along contacts with the gneissic country rocks, results in highly sheared and altered chloritic zones. These may contain breccia fragments of less altered ultramafic rock. Rarely, faults can be recognized by the presence of a typical muddy fault gouge material containing granulated fragments of pegmatite and ultramafic material. Although not well preserved in drill core, evidence indicates such zones can be 2-3 feet in width.

Certain points of regional significance can be made from examining the general structure of the Wabowden ultramafic intrusion.

1) The location of the body is controlled by a major through-going fault system, two branches of which appear to meet at the centre of the Y shaped body.

2) The ultramafic mass was emplaced prior to the end of the

granite and pegmatite intrusion processes, which affected the rocks of the area. As these rocks are known to have a retrograde amphibolite facies of metamorphism caused by the Hudsonian orogeny (Rance, 1964)*, it is reasonable to assume that the introduction of late pegmatites took place during this period. 3) Fault movements continued subsequent to this, brecciating the pegmatites, shearing and altering the ultramafic rocks.

At present, no other ultramafic body of the nickel belt is known to have been invaded by such an abundance of pegmatite. In general, the pegmatite dykes are less than 10 feet in width. Some however, are thought to be much wider, up to 25 feet across, but with the uncertain knowledge of dyke attitudes, true width determinations must be considered as only approximate. Pegmatite samples from the ultramafic body are seen in thin section to consist of plagioclase (An_{28}) with minor quantities of brown biotite. The feldspar is considerably altered to a dusty brown clay material. Staining of two sections failed to indicate the presence of any potassium feldspar. An unusual feature is the complete absence of any quartz, although this mineral is easily recognizable in pegmatites intruding the exposed gneissic country rocks. It is evident that the pegmatites intersecting the ultramafic rocks are essentially feldspar dykes.

In order to study the mineralogical and chemical changes brought about in the ultramafic rock by the intrusion of pegmatite, care had to be taken to avoid material affected by faulting and shearing. The selected samples are from drill holes M11A-8 and M11A-22, the sites of which are located on Fig. 17.

*Rance (1964) - Personal communication.

MINERALOGICAL CHANGES IN SERPENTINITE

Pronounced physical changes take place in the ultramafic rock adjacent to feldspar pegmatite dykes. Of these, colour and texture are the most noticeable. The massive, greenish-black fine grained serpentinized rock in which occasional shiny cleavage surfaces of pyroxene may be discernable, changes gradually to a much paler, greyish-green or bluish-green colour with a more schistose texture. The appearance of new minerals in marginal alteration of this type takes place gradually, but over varying widths, which do not appear to be directly related to the thickness of the pegmatite. An illustration of this feature can be observed in Fig. 18, which is a diagrammatic presentation of estimated modal compositions of specimens close to pegmatite dykes. The ultramafic rock in section M11A-22 (Fig. 18A) is 27 feet wide and bounded on either side by pegmatites. The left side pegmatite is 10 feet wide and that on the right 3.3 feet wide. Fig. 18B illustrates the M11A8 section in which only one pegmatite dyke, with a width of 11.7 feet, is involved.

Fig. 18A shows that the greatest mineralogical changes in the M11A-22 section occur adjacent to the right hand or smaller pegmatite, with less pronounced changes taking place in the ultramafic rock against the 10' foot pegmatite on the left side. At approximately the central point between the pegmatites (#52) the ultramafic rock is composed of 16% olivine (Fo_{84}), 10% orthopyroxene, 30% tremolite, 39% serpentine and minor accessories. Both olivine and orthopyroxene diminish in

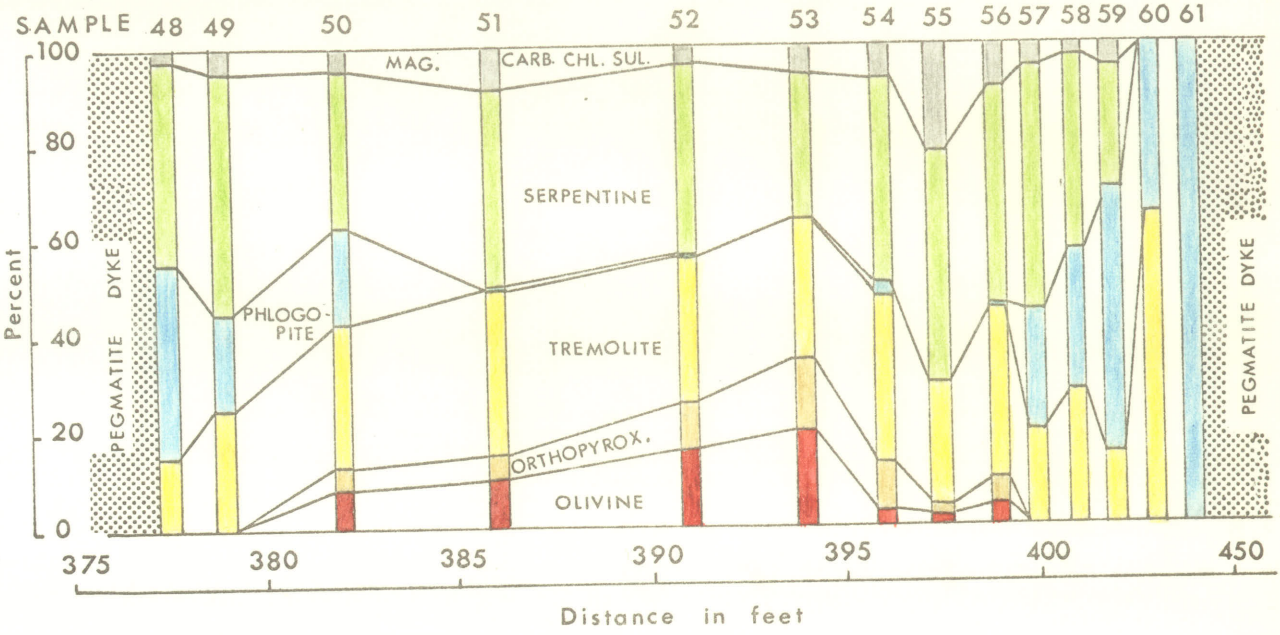

A. SECTION MIIA-22

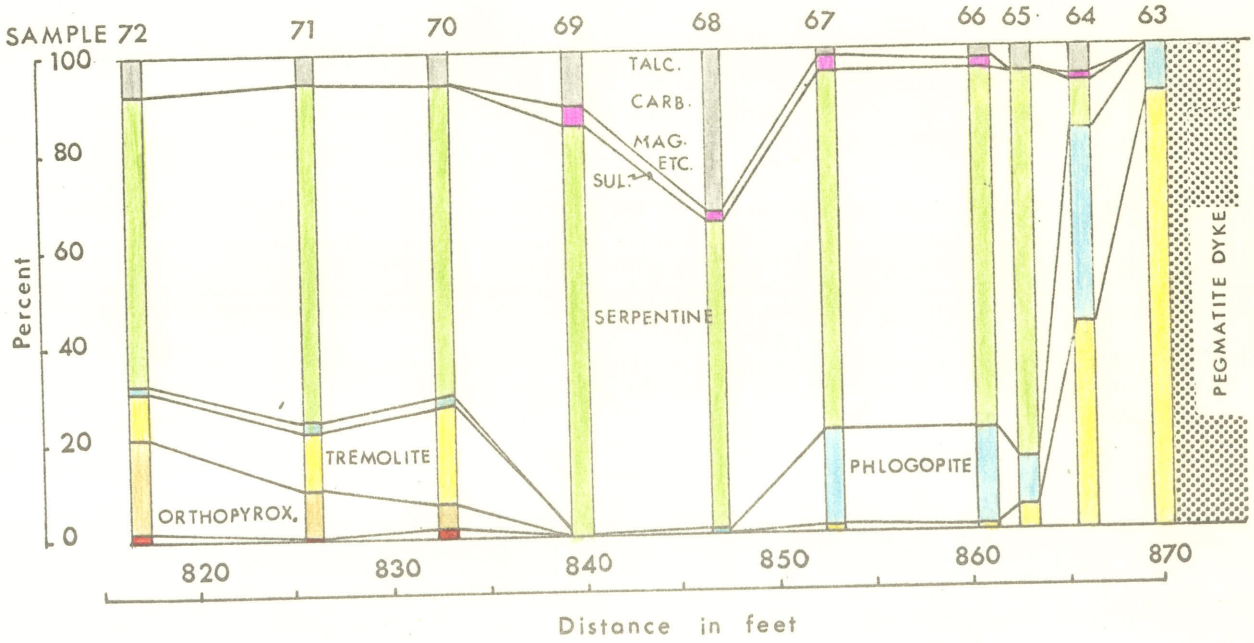

B. SECTION MIIA-8

FIG. 18 : Diagram showing estimated modal compositions of sections in ultramafic body M11A, Wabowden.

quantity moving laterally from this point and disappear from the rock at about 4 feet from the contact with pegmatite. Tremolite content remains fairly constant throughout the central area but gradually decreases close to the margins. At the right contact, within 1 foot of the pegmatite, the tremolite content jumps to 65%. It is combined with 35% phlogopite to form a tremolite-phlogopite rock (#60). A sudden change of this nature does not take place adjacent to the left hand pegmatite.

Phlogopite shows a remarkable spacial control related to the pegmatite contacts. It is present in minor quantities or absent all together in the least altered rocks of the central area, but rapidly increases towards the contacts from a point about 5-7 feet out. The first appearance of considerable phlogopite in the rocks correlates with the disappearance of the primary silicates, olivine and pyroxene. Phlogopite development reaches a maximum at the right hand pegmatite contact, where it forms a 6 inch wide monomineralic zone (#61). This extreme concentration is not present at the left contact, where the border zone rock contains a maximum of 40% phlogopite (#48). The monomineralic phlogopite contains scattered fragments of feldspar indicating its derivation by extreme marginal alteration of the pegmatite. The ultramafic-pegmatite contact is therefore placed on the ultramafic side of the narrow sheath of massive phlogopite.

Chlorite is only present in the rocks in a narrow zone between 5-9 feet from the right pegmatite. It reaches a maximum development in #55, where it forms 16% of the rock, but

diminishes rapidly on each side. Serpentine content of the rock ranges between 25-50% with the lower value occurring in the phlogopite-rich sample (#59), 2 feet from the pegmatite on the right. It is completely absent in the narrow border zone along this contact. Accentuating the less intense alteration, caused by the left pegmatite dyke, serpentine is present in considerable quantities up to the actual contact.

A distinct zoning of significant minerals is evident in the serpentinite. Passing outward from the pegmatites the sequence is phlogopite, chlorite and tremolite. Tremolite however is present as a constituent in all samples except for the narrow monomineralic phlogopite zone adjacent to the right hand pegmatite. In addition, chlorite has not been recognized in the rather widely spaced samples close to the left pegmatite.

A second example of pegmatite alteration of ultramafic rock is shown in Fig. 18B and illustrates the variable mineralogy which can be produced by similar pegmatites. In this case, which constitutes part of section M11A-8, the serpentinized ultramafic rock has been sampled at more or less regular intervals for 53 feet adjacent to an 11.7 foot wide pegmatite dyke. The latter is shown at the right hand side of the diagram. An additional narrow pegmatite intrudes the ultramafic body at the 800 foot mark. On the diagram, this would be placed 17 feet to the left of specimen #72.

The ultramafic rock in this section contains between 60-85% serpentine. Primary silicates, orthopyroxene and minor olivine are present in those specimens furthest removed from the dyke (#70, 71, 72). Tremolite and minor phlogopite are also

present in each of these samples suggesting they may be within the range of influence of the narrow pegmatite mentioned above. Between 20-30 feet from the main pegmatite, the ultramafic rock is a serpentinite containing talc, carbonate, magnetite, and minor sulphide minerals (#68, 69). Phlogopite first appears in #68 at a distance of 23 feet from the pegmatite, but only becomes abundant at 17-20 feet from the contact. Accompanied by minor tremolite, the phlogopite content remains nearly uniform to approximately 5 feet from the contact. It then increases rapidly in specimen #64 at a distance of 4 feet from the dyke. Adjacent to the pegmatite, fibrous anthophyllite together with approximately 10% phlogopite constitute the marginal zone of the ultramafic body.

In this case the mineralogical zoning outwards from the pegmatite is anthophyllite, phlogopite, talc-carbonate and tremolite. The latter mineral is also present in variable quantities in the phlogopite zone. The zoning thus differs from the case previously described in the absence of a chlorite zone and in the occurrence of anthophyllite rather than phlogopite adjacent to the pegmatite intrusion. There is also a notable difference in the lateral extent of the alteration in two examples studied.

CHEMICAL CHANGES IN SERPENTINITE

Chemical changes in the ultramafic rocks of the M11A-22 and M114-8 sections are graphically represented in Fig. 19 and 20. Rock compositions have been determined according to the

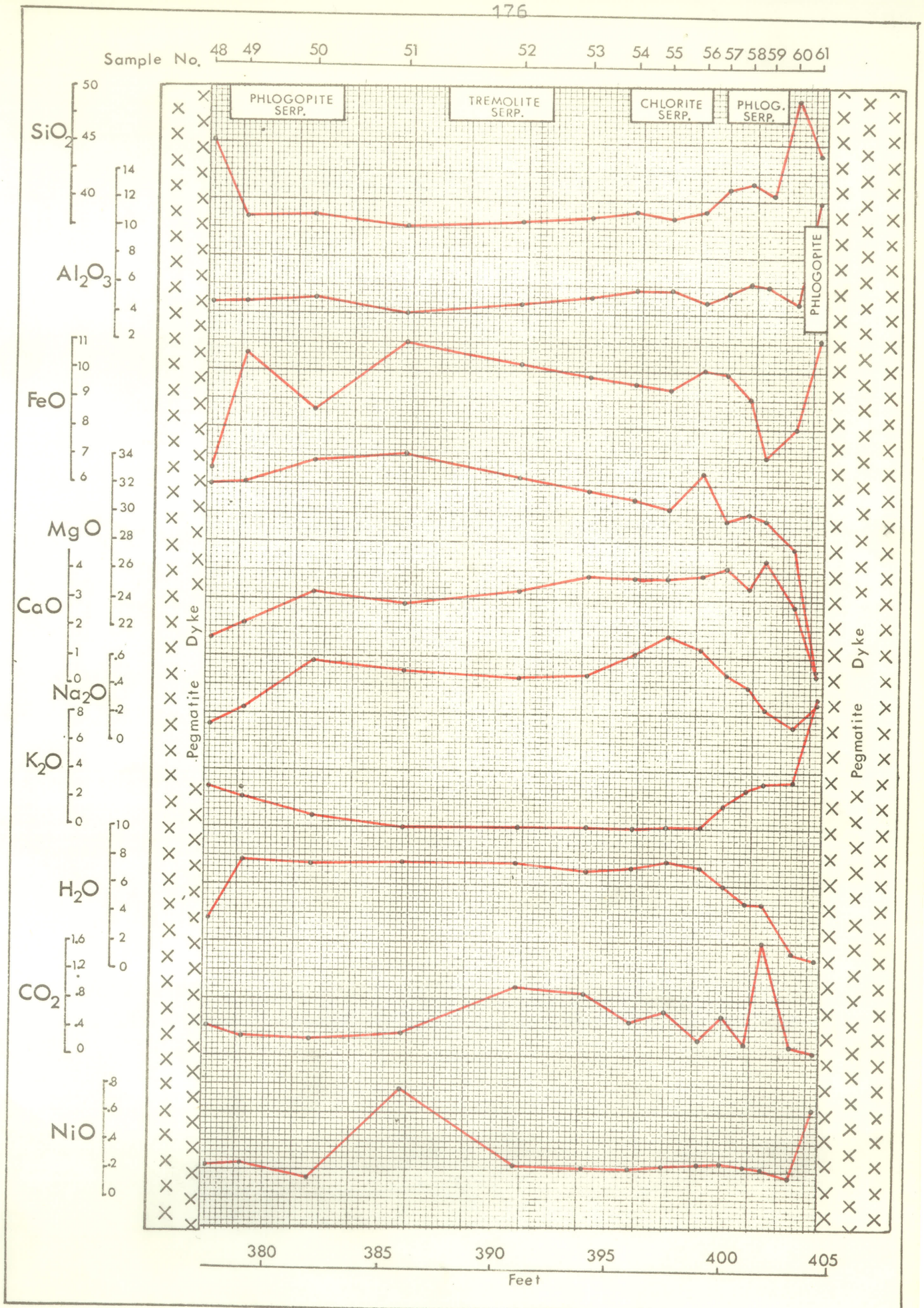

FIG. 19 : Variation diagram of oxide weight percents across part of section M11A-22, ultramafic body M11A, Wabowden

methods outlined in Appendix 1 and the complete analyses for all specimens are listed by number in Appendix 1X.

Considering first the chemistry of the ultramafic rock types between two intrusive pegmatite dykes in section M11A-22, Fig. 19 shows that pronounced changes take place in the marginal zones as would be expected from the mineralogy described above. Also, in accord with the less severe alteration produced by the left hand pegmatite, the symmetry of the curves of oxide percentages are not uniform at both contacts. A study of Fig. 19 shows some well defined features. Within the ultramafic rock adjacent to the pegmatites, there has been an addition of SiO_2, Al_2O_3 and K_2O and a reduction in MgO, CaO, Na_2O and H_2O. The concentration of FeO is also reduced in the marginal zones but increases in the massive phlogopite zone. A generally uniform NiO content of .25% in the rocks of the section is disturbed by a higher value in #51 which contains 4% sulphide and an abrupt increase to .65% NiO in the phlogopite zone. There is however a slight drop in the NiO content of the rocks, beginning at approximately 4 feet from the contacts.

The compositions of rocks in the M11A-8 section are represented in Fig. 20. Once again it is evident there is a general increase in the SiO_2, Al_2O_3 and K_2O contents of the ultramafic body on approaching the pegmatite and a reduction in FeO, MgO, CaO and H_2O. Sulphur content again appears to be the reason for the fluctuating NiO content. Where sulphides are absent, as in specimens #70, 71 and 72 which lie furthest from the pegmatite, NiO values remain steady in the .28-.30%

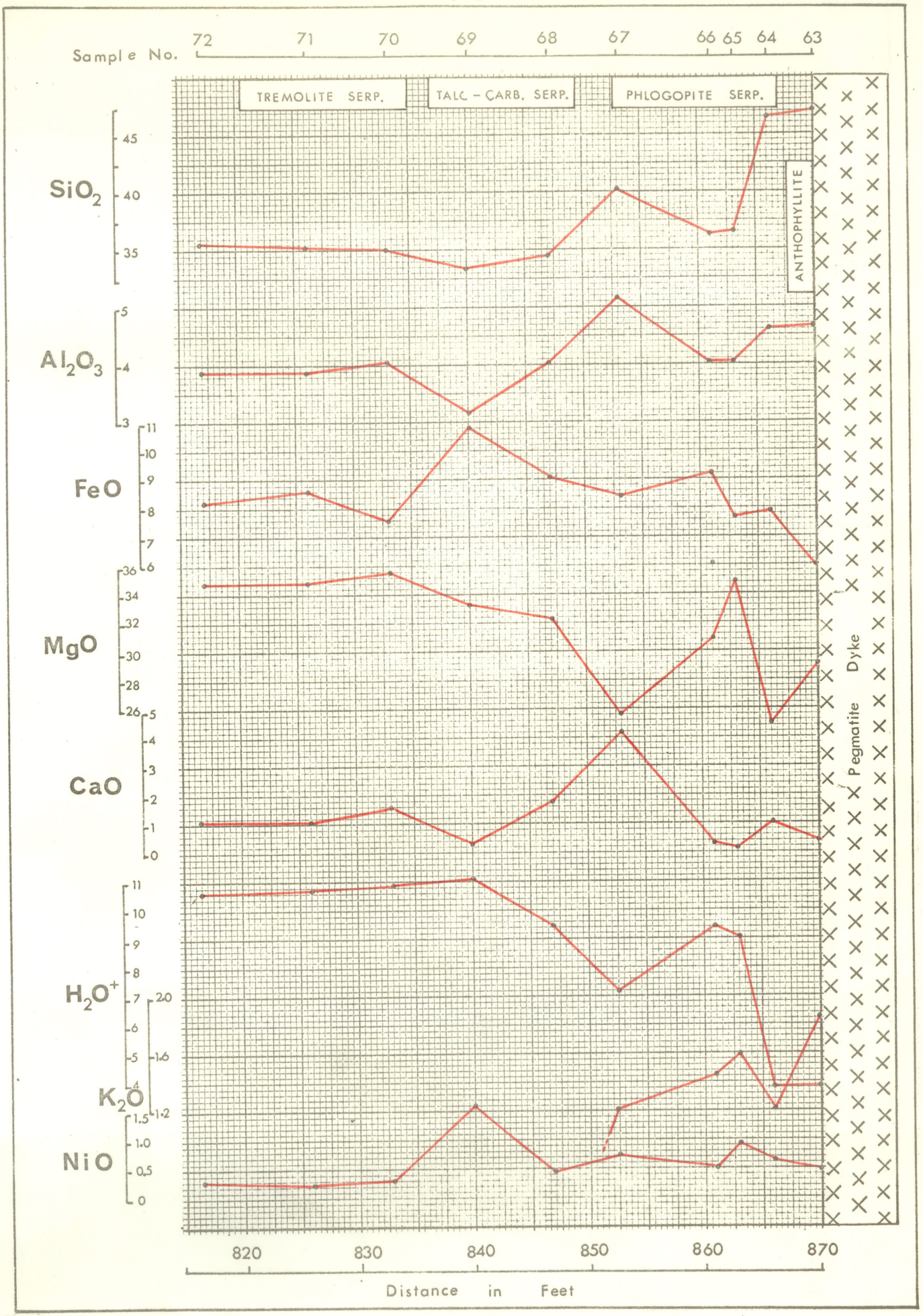

FIG. 20 : Variation diagram of oxide weight percents across part of section M11A-8, ultramafic body M11A,

range. Small amounts of TiO_2, Cr_2O_3, MnO and CoO are also present in the specimens examined. Their distribution is erratic and not considered significant in the present study.

The extreme limits of composition in the alteration area are shown by selected analyses in Table 10. Specimens #52 and 71 are tremolite-bearing serpentinites from the two sections. Except for a higher content of CaO in #52 due to a much greater percentage of tremolite, the compositions of the two rocks are extremely close. Analyses 60 and 63 show the compositions of the ultramafic contact zones adjacent to the pegmatites. The phlogopite rock (#61) forming the narrow zone of extreme pegmatite alteration is apparently nearly pure phlogopite in composition. This material however, was not examined in thin section. The marginal anthophyllite zone of section M11A-8 (#63) contains a minumum of 10% phlogopite and probably even more. This is reflected in the analysis, which shows a higher FeO and K_2O content and a lower SiO_2 content than would be expected for pure anthophyllite. The diffractogram (#63) of this rock showed the presence of only the two minerals anthophyllite and phlogopite, but no estimate could be made of their relative percentages.

ORIGIN OF THE MARGINAL RIMS AND ZONING

It is obvious that considerable movement of material has been involved in the serpentinite alteration and there is little doubt that the intrusive pegmatites have been both the source of the material and the cause of the movement. It can be assumed

TABLE 10

COMPOSITIONS OF SELECTED SERPENTINITES AND MARGINAL MONOMINERALIC ZONES

Sample	52	71	60	63	61
SiO_2	38.35	35.40	49.20	47.10	43.90
Al_2O_3	4.78	3.92	5.06	4.68	14.26
FeO	10.24	9.62	8.04	7.00	11.05
MgO	32.45	36.84	27.76	31.40	18.85
CaO	3.36	1.12	2.82	0.40	0.24
Na_2O	0.45	-	0.11	0.07	0.31
K_2O	0.00	0.00	3.11	1.83	9.34
H_2O^+	7.68	10.78	1.51	4.82	1.29
CO_2	1.00	0.78	0.19	0.13	0.08
TiO_2	0.22	0.21	0.16	0.23	0.16
Cr_2O_3	0.37	0.34	0.03	0.28	0.00
MnO	0.12	0.09	0.16	0.08	0.12
NiO	0.24	0.28	0.18	0.55	0.65
CoO	0.012	0.012	0.011	0.014	0.02
	99.27	99.39	98.34	98.58	100.27

52: Tremolite serpentinite. Central point of section M11A-22

71: Tremolite serpentinite. Section M11A8

60: Tremolite-phlogopite rock. Section M11A-22 contact zone

63: Anthophyllite rock with 10% phlogopite. Section M11A8 contact zone.

61: Phlogopite rock. Marginal pegmatite phase. Section M11A-22 Analyst. C. Coats 1964.

- indicates not determined.

although it is by no means certain, that the original ultramafic intrusive body of M11A had reached an advanced stage of serpentinization prior to the intrusion of the pegmatites, and that the primary silicates, olivine and orthopyroxene which are still present in small quantities in some specimens are remnant crystals having escaped complete serpentinization. The position of tremolite in the rock history is somewhat more difficult to explain. It has been shown previously that tremolite is a late silicate which replaces both original silicates and serpentine. It in turn is commonly altered by additional serpentine. Tremolite does not appear to have resulted directly from the thermal and metasomatic effects of the pegmatites alone, although this has probably enhanced its development in marginal areas. Its presence is probably due to a much wider hydrothermal effect from larger granitic intrusions, which are known to occur within the complex geological setting of the belt.

The zonation of minerals in altered ultramafic rocks and the development of monomineralic contact zones against siliceous country rock is a well known phenomena and has been described from a number of localities. The generation of phlogopite and anthophyllite zones in serpentinite by intruding feldspar dykes has been described in detail by Amin and Afia (1954) from Hafafit, Egypt. At this locality, the zoning from the feldspar dykes into the serpentine is phlogopite, anthophyllite, serpentine. Their origin is attributed to hydrothermal fluids accompanying the injection of the feldspar dykes, with the subsequent weathering of phlogopite to vermiculite. The authors note that tremolite and actinolite are associated with vermicu-

lite only where the feldspar dykes inject the contact of the serpentinite and the surrounding gneisses, and are absent where the dykes are confined within the serpentinite mass. As is the case in the present study, the origin of tremolite in serpentinite is not directly the result of pegmatite intrusion.

Compared to the Hafafit zoning, the sections M11A-22 and M11A-8 show considerable differences. In the former, phlogopite constitutes the outermost zone against the pegmatite, but there is no succeeding anthophyllite zone. In the latter case the zones are reversed compared to the Hafafit occurrence, with anthophyllite occurring next to the pegmatite succeeded inwards by phlogopite. In a study of the stability of anthophyllite, Greenwood (1963) has shown that the formation of a monomineralic zone of anthophyllite in serpentine by desilication of a younger acid intrusive, depends more on the gradients in the activity of H_2O than gradients in the chemical potential of SiO_2. If a steep gradient in the activity of H_2O across the zone at uniform temperature less than 500° C. is considered unlikely, an appeal must be made to an equally steep gradient in temperature. It would seem unlikely that different temperature gradients would result from varying sized pegmatite dykes, all of which were intruded at approximately the same time. One cannot therefore consider the variation in dyke widths in the two sections as bringing about the different mineralogy. The answer appears to rest in the composition and amount of material transferred across the boundary line between the pegmatite and serpentinite. The association of talc in the innermost zone and anthophyllite

as the marginal zone in section M11A-8, indicates a greater availability of SiO_2 and a more deeply penetrating alteration than occurred in the rocks of section M11A-22. The chemistry of the mineral changes would be as follows in a system open to SiO_2 and H_2O:

$$7(3MgO.2SiO_2.2H_2O) + 10SiO_2 \text{----} 3(7MgO.8\ SiO_2.H_2O) + 11H_2O$$

Serpentine — Anthophyllite

$$(3MgO.2SiO_2.2H_2O) + 2(SiO_2) \text{----} (3MgO.4SiO_2.H_2O) + H_2O$$

Serpentine — Talc

A reduced supply of SiO_2 accompanied by higher concentration of K_2O and Al_2O_3 might account for the mineralogy of the M11A-22 zonation. The mineralogy of the feldspar pegmatites within the ultramafic body, indicates that they have a much reduced SiO_2 content compared to those bounded by the acid gneissic country rocks. The source for SiO_2 in the serpentinite alteration zone has therefore been the pegmatite dykes. The K_2O content of pegmatites in the two environments has not been determined analytically, but the mineralogy suggests it is extremely low in the dykes which penetrate the serpentinite. K_2O is not detectable in the serpentinites beyond the range of influence of the pegmatites dykes.

Until the present, only addition of material to the serpentinite has been considered. The extraction of considerable MgO, together with lesser amounts of FeO, H_2O and Na_2O has been noted from the oxide variation diagrams. FeO lost from the serpentinite marginal zone has concentrated in the biotite alteration zone of the pegmatite. The same is possibly true

for Na_2O, but in addition, there is a concentration in the serpentinite accompanying the development of chlorite. The occurrence of a rather peculiar serpentinous mineral as matrix material in many brecciated pegmatites, supplies the answer to the whereabouts of the extracted MgO. Because of its physical similarity, this mineral is described as a "picrolite" (#11A6) in Chapter IV and has been shown to have an extremely poor crystallinity and an unusual DTA curve. Its composition is listed in Table 11 together with analyses of 4 picrolites from different localities for comparison. The Wabowden material is a hydrated magnesium silicate with much lower MgO and higher Al_2O_3 and FeO contents than the other picrolites. Contamination by feldspar particles may account for some of this difference, but nevertheless, it has a rather unusual composition. Within the pegmatites intruding the Wabowden ultramafic body, it only occurs where brecciation has produced a suitable locus of deposition. In a few places narrow stringers occur within the highly altered marginal zones of serpentinite.

SUMMARY AND CONCLUSIONS

The alteration of serpentinite caused by intrusive pegmatite dykes is similar chemically and mineralogically to that normally present along serpentinite-siliceous country rock contact areas. Width of alteration zones adjacent to pegmatites is not directly proportional to widths of the pegmatites. During intrusion into serpentinites, the pegmatites became desilicated

TABLE 11

SELECTED ANALYSES OF PICROLITES

	B109 (Grubb, 1962)	3 (Selfridge,	4 1936)	321 Pipe Lake	11A6 Wabowden
SiO_2	39.54	42.94	43.79	39.90	42.35
Al_2O_3	0.44	-	-	0.88	8.14
Fe_2O_3	2.52	3.33	-	-	-
FeO	0.14	1.88	2.05	2.27	5.78
MgO	42.47	36.53	41.03	45.04	31.58
CaO	0.00	-	-	0.10	.70
Na_2O	0.03	-	-	-	-
K_2O	0.00	-		0.00	0.00
H_2O^+	14.16	13.21	12.47	11.94	10.12
TiO_2	-	-	-	.278	.064
NiO	-	1.61	-	0.00	-
Cr_2O_3	-	-	-	.072	-
MnO	-	-	-	-	.192
	99.30	100.22	99.34	100.48	98.92

B109 - Light green slip-picrolite vein in Munro serpentine. Anal. W. Herdsman.
3 - Picrolite, Buck Creek, Clay County, N. C. (Ref. Selfridge, 1936).
4 - Picrolite, Texas, Penn. (Ref. Selfridge, 1936).
321 - Dark green picrolite, Pipe Lake, Manitoba. Anal. C. Coats.
11A6 - Light green "picrolite", M11A ultramafic body, Wabowden, Manitoba. Anal. C. Coats.
- - Dash indicates not determined.

to the extent that they are now composed principally of feldspar. A narrow zone of biotite forms a sheath along the outer edge of many, but not all pegmatites within the serpentine. Fragments of remnant feldspar within this biotite zone indicate it constitutes a highly altered, marginal rim to the pegmatites.

The zonation of minerals developed in the serpentinite at two locations studied, are phlogopite-chlorite-tremolite and anthophyllite-phlogopite-talc carbonate, from the pegmatite contact passing into the serpentinite. The differences between them are considered principally due to availability and abundance of introduced materials.

Within the alteration zone of the serpentinite, the rock has gained SiO_2, Al_2O_3, K_2O and CO_2 and lost MgO, FeO and H_2O. Most of this movement of ions appears to have been an isochemical readjustment of elements between the two rock types. The final disposition of large amounts of MgO lost from the serpentinite is a waxy "picrolitic" material which forms the matrix in many brecciated pegmatites. Where such sites of deposition are not available, as when the pegmatites are massive and unfractured, veinlets of "expelled picrolite" are retained within the serpentinite alteration zone.

There is an indication, on somewhat scanty evidence, that nickel is removed in small quantities from serpentinites close to pegmatites. In section M11A-22, described above, the nickel removed has only migrated a short distance and is concentrated in the monomineralic phlogopite zone. In contrast to Mg and Fe however, Ni appears to be rather immobile.

CHAPTER V111

GEOCHEMISTRY AND GENESIS OF THE ULTRAMAFIC ROCKS

INTRODUCTION

In this chapter, the results of additional analytical work on the ultramafic rocks of the Manitoba nickel belt are presented and comparisons made with analyses from occurrences in other areas of the world. Analyses have been made using the procedures outlined in Appendix 1 and all results are listed by number in Appendix 1X. The compositional grouping of the ultramafic rocks follows that used in Chapter 111, based on mineralogical composition. A summary of the mineralogy of the groups is contained in Table 1.

COMPOSITION OF THE ULTRAMAFIC ROCKS

Average compositions of the ultramafic rock groups have been calculated from complete rock analyses of the specimens listed in Table 12. The serpentinites of group A constitute the most abundant type analysed. Relatively pure serpentinite material containing little or no additional silicate minerals, forms the most abundant ultramafic rock type occurring along the nickel belt but the number of analysis in the other groups of Table 12, is not indicative of the frequency of occurrences

TABLE 12

ANALYSED SPECIMENS USED IN THE CALCULATION OF AVERAGE COMPOSITIONS OF THE ULTRAMAFIC GROUPS.

ROUPS

A	B	C	D	E	F	G	M14Q
82	74	80	111	109	104	105	1
88	78	114	132	117	112	120	2
90	79	116		118	127	152	3
91	83	133		125	130	172	4
92	86	136		153	148		5
96	131	137		158	151		7
98	138	141		164	159		8
101	146	144			165		9
102	154	145			166		10
107		169			168		11
108							12
110							13
122							14
126							
128							
139							
140							
142							
149							
150							
155							
157							
160							
163							

Group A: Serpentinites
B: Tremolite serpentinites
C: Tremolite phlogopite serpentinites
D: Phlogopite serpentinites
E: Serpentinized peridotites
F: Tremolite olivine orthopyroxenites
G: Amphibole orthopyroxenites
M14Q: Serpentinite, M14Q body, Setting Lake. Marginal altered zones omitted.

High sulphide-bearing samples included within these groups in Appendix V111 are omitted from the above table. Additional specimens are omitted for which no analyses are available.

of rocks with a mineralogical content denoted by the group. Any attempt at estimating relative abundance or percentages of mineralogical types which the groups represent, would be unsatisfactory. Such an attempt would require a much broader and more uniform sampling of the presently known ultramafic bodies along the nickel belt. However, the groups, whose mineralogical composition has been defined within arbitrary limits, make repeated appearances in thin sections and although the origin of some phases is still in doubt, averaging the compositions of groups is believed to be justified. Without even a rough estimate of group volume percentages, it is not possible to calculate an average composition for the ultramafic rocks of the nickel belt as a whole. At the present time only group compositions can be given and the assumption made that as the serpentinites of group A are the most prevalent, the composition of group A most closely suggests the bulk composition of the ultramafic rocks.

The average compositions are listed by group in Table 13. For each group the number of analyses used and the Mg/Fe molecular ratio are given. The M14Q group represents the average of 13 analyses of serpentinite from the central portion of the M14Q body in Setting Lake. The marginal zones of alteration with highly variable compositions, as discussed in the previous chapter, have been omitted from the calculation. The analysis is therefore not an indication of the bulk composition of the M14Q ultramafic body, but solely represents an average of the serpentinite. This average is nearly identical to that of group

TABLE 13

AVERAGE COMPOSITIONS OF THE ULTRAMAFIC ROCKS OF THE MANITOBA NICKEL BELT

Group	A	B	C	D	E	F	G	M14Q
SiO_2	35.73	39.53	41.37	38.65	35.46	42.01	47.38	35.56
Al_2O_3	1.95	5.39	5.13	2.27	3.67	5.19	4.85	2.10
FeO*	8.48	10.62	9.05	7.46	11.88	10.27	9.07	9.79
MgO	39.10	29.83	30.39	37.80	33.74	29.85	27.93	39.40
CaO	.29	4.16	4.50	.00	1.34	4.63	3.61	.28
Na_2O	-	-	.36	-	.05	.19	.46	-
K_2O	.00	.00	.72	.58	.00	.10	.74	.00
H_2O+	12.11	7.18	5.87	12.39	10.02	4.74	1.65	11.25
CO_2	.60	.87	.73	.05	.57	1.00	.88	-
TiO_2	.10	.27	.30	.09	.19	.29	.21	.10
S	.63	-	-	-	1.27	.41	1.08	-
Cr_2O_3	.54	.30	.31	.79	.69	.32	.24	.74
MnO	.05	.11	.12	.03	.12	.12	.12	.09
NiO	.34	.28	.21	.20	.36	.17	.19	.31
CoO	.02	.01	.01	.01	.02	.01	.01	.02
Total	99.94	98.55	99.07	100.32	99.38	99.30	98.42	99.64
Mg/Fe ratio	8.2	5.0	5.9	9.0	5.1	5.2	5.5	7.2
No. of analyses	24	9	10	2	7	10	4	13

*Total Fe as FeO

- Dash indicates not determined for most specimens.

A, which represents analyses of serpentinite from many scattered locations along a 100 mile length of the belt.

Average compositions of the groups are graphically represented in Fig. 21, where they are arranged in order of decreasing MgO content. The serpentinites of groups A and M14Q have the highest MgO content at just over 39%, but this decreases steadily in the other groups, reaching a low of 28% in the amphibole orthopyroxenites of group G. With decreasing MgO there is a corresponding increase in SiO_2 content of the rocks, the two curves crossing at a value of 38%, close to the phlogopite serpentinites of group D.

The serpentinites contain about 2% Al_2O_3 but this increases rapidly to around 5% for those rocks containing high modal contents of tremolite, phlogopite and orthopyroxene. Total Fe as FeO is lowest in the serpentinites but increases to an average value of 10% in the other groups. The high average FeO content of 11.88% in group E can be attributed to generally high sulphide content which the specimens of analysed serpentinized peridotite contained. The serpentinites have an extremely low to negligable CaO content but this increases to around 4% accompanying the presence of considerable tremolite in the other groups. The CaO content appears to bear an inverse relationship to the MgO content.

As would be expected, the content of combined H_2O is highest in the serpentinites but decreases with increasing SiO_2 content in the groups containing less hydrous and anhydrous silicate minerals. The higher value of group B is in

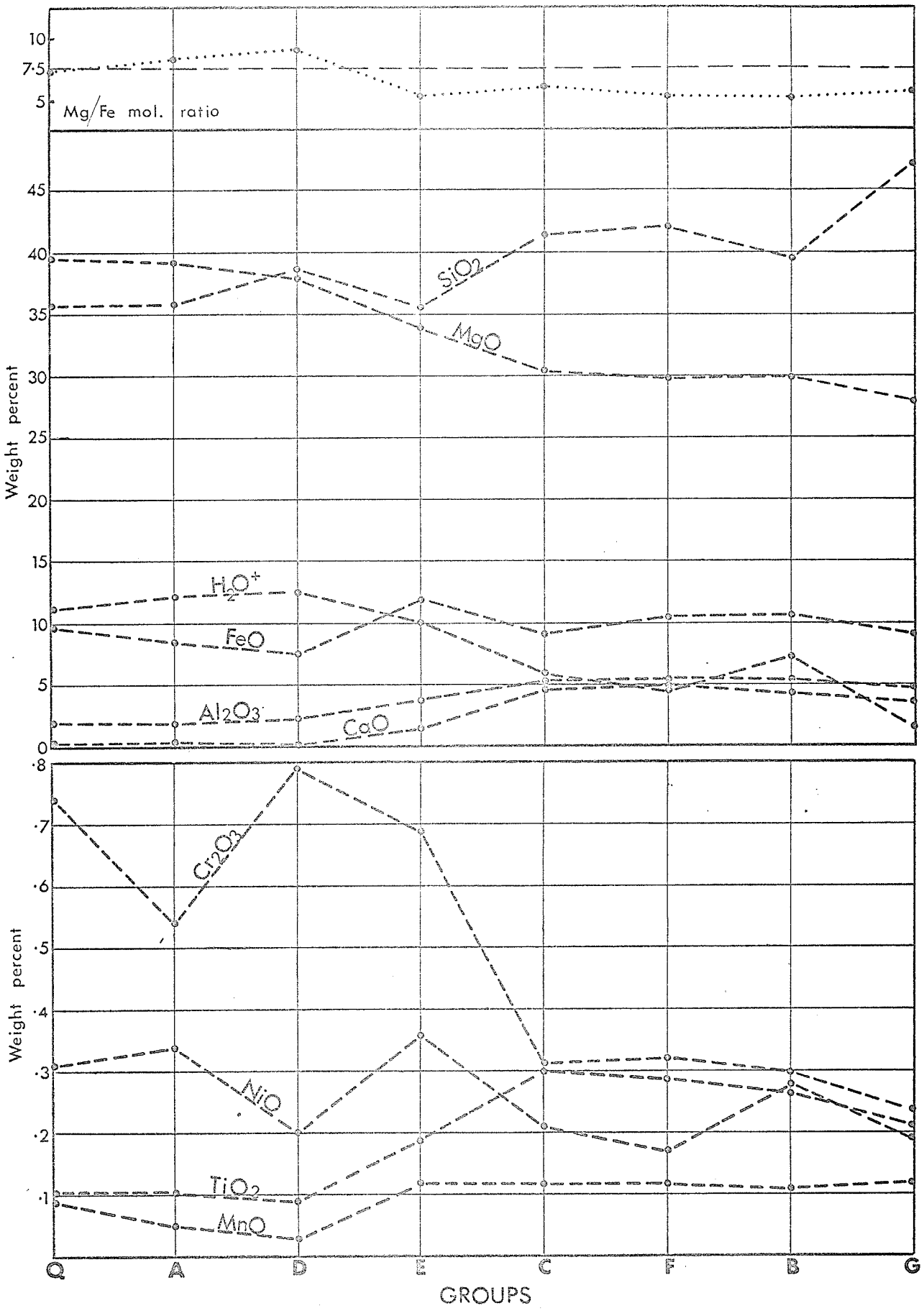

FIG. 21 : Distribution of major and minor constituents in the ultramafic rock groups of the Manitoba nickel belt.

accord with its modal composition and name of tremolite serpentinite.

The alkali content of the ultramafic rocks is extremely low. Many specimens were not analysed for Na_2O so that average values for some groups could not be obtained. From the available specimens for which Na_2O was determined, the average content is less than 0.5%. K_2O is absent in the analyses of serpentinites from groups A, B and M14Q and from the serpentinized peridotites of group E. With the presence of modal phlogopite and biotite in groups C, D, F and G, K_2O becomes a significant component. The introduction of K_2O into ultramafic rocks from adjacent pegmatite intrusions has been discussed previously.

Of the minor elements occurring in the ultramafic rocks, chromium and nickel are the most abundant. Cr_2O_3 reaches its greatest abundance in the serpentinites and serpentinitized peridotites thus corresponding with those groups containing the highest MgO content. From a value of between 0.5-0.8%, it decreases to a range of close to 0.3% in the more siliceous ultramafic phases. NiO shows less of a variation between groups than does Cr_2O_3, and appears to vary sympathetically with the FeO content. The serpentinites contain an average of .32 NiO with a range in value for the 37 analysed specimens of between .04-.59% NiO. The higher values were obtained from those serpentinites containing some nickel-bearing sulphides. Average nickel content for the remaining groups is in the order of .2%, except for group E, for which a value of .36% has been obtained. Many specimens analysed in this group contain sulphur and it

is not surprising that it also has the highest average FeO content. The higher NiO value is thus attributed to the presence of sulphides. The CoO content of the nickel belt ultramafic rocks is very low, amounting to 5-10% of the NiO content.

The oxides MnO and TiO_2 increases in the groups possessing a lower MgO content. Fig. 21 shows that the MnO and TiO_2 curves have an inverse relationship to the Mg/Fe molecular ratio. Hess (1938) has used the Mg/Fe ratio of 7.5 to distinguish between the serpentinites, dunites and peridotites of the ultramafic magma series, which have a ratio greater than 7.5 and the ultramafic differentiates of a mafic magma, where the ratio ranges between 3.5 and 7.5. Pyroxenites of the ultramafic magma series generally have ratios between 6 and 7. In an effort to verify whether the relationship between the MnO and TiO_2 contents to the Mg/Fe ratio, noted in the nickel belt rocks, is a consistent feature in the chemistry of all ultramafic rocks, the compilation of data in Table 14 has been plotted in diagrammatic form in Fig. 22.

There is a pronounced difference in the average MnO and TiO_2 contents of ultramafic rocks having a Mg/Fe molecular ratio above and below the value of 7.5. Rocks above 7.5, being those derived from the ultramafic magma series as defined by Hess (1938), have a mean MnO content of .096% and a mean TiO_2 content of .036%. In contrast, those ultramafic rocks which have a Mg/Fe molecular ratio below 7.5 have a mean MnO content of .147% and a mean TiO_2 content of .204%. The latter group include those derived by crystallization differentiation from

TABLE 14

CONTENT OF MnO AND TiO_2 AND Mo/Fe MOLECULAR RATIOS OF SELECTED ULTRAMAFIC ROCKS

No.	Mo/Fe	TiO_2	MnO %	Reference
A	8.2	.10	.05	Manitoba nickel belt ultramafic rocks.
B	5.0	.27	.11	"
C	5.9	.30	.12	"
D	9.1	.09	.03	"
E	5.1	.19	.12	"
F	5.2	.29	.12	"
G	5.5	.21	.12	"
14Q	7.2	.10	.09	"
1	5.7	.15	.17	Peridotite, Layered Series, Rhum. Brown (1956).
2	10.8	.10	.10	Serp.Perid.SDM 150.Mt.Albert.MacGregor (1962).
4	5.2	.30	.16	Peridotite M-667-58.Cuthbert L.McDonald (1960).
5	4.9	.34	.16	Ultrabasic Sill.Labrador.Fahrig(1962)
6	6.9	.18	.15	Ultrabasic pillow lava.Cyprus.Gass (1958).
7	4.9	.06	.19	Peridotite MB.20 Stillwater.Hess(1938)
8	8.6	.04	.09	Serpentinite.Type C.Mayaquez.Hess, Otalora (1964)
10	8.6	.00	.09	Peridotite. Cuba 33.Hess (1938)
11	8.6	.00	.11	Peridotite.Cuba 34. Hess (1938)
12	7.8	Tr.	.07	Peridotite. Cuba 39. Hess (1938)
13	9.5	.04	.10	Peridotite.Newfoundland 9.Hess(1938)
14	8.8	.04	.21	Peridotite.Newfoundland 21.Hess(1938)
16	3.8	-	.11	Serpentinite EB.92.Stillwater.Hess (1938).
17	6.7	.15	.09	Serpentinite.Moak Lake.McDonald(1960)
18	3.7	.42	.21	Serpentinite aver.Ungava.Shepherd (1960)
19	8.9	.00	.10	Dunite.SDM 6.Mt.Albert.MacGregor(1962)
20	9.2	.01	.09	Serpentinite, aver.of 3.Vermont. Chidester (1962).
21	4.1	.18	.20	Serpentinite,W60-533.Watkinson,Irvine (1964).
22	3.9	.25	.17	Serpentinite W60-514.Watkinson,Irvine (1964)
23	3.7	.18	.18	Peridotite I60-94.Watkinson,Irvine (1964).
24	5.2	.11	.14	Peridotite,Gordon Lake.Anal.C.Coats.
25	4.8	.19	.19	Peridotite Sill,aver. of 6.Timmins Naldrett (1964)
26	11.7	.01	.11	Serpentinite SA.443.Timmins. Naldrett (1964).

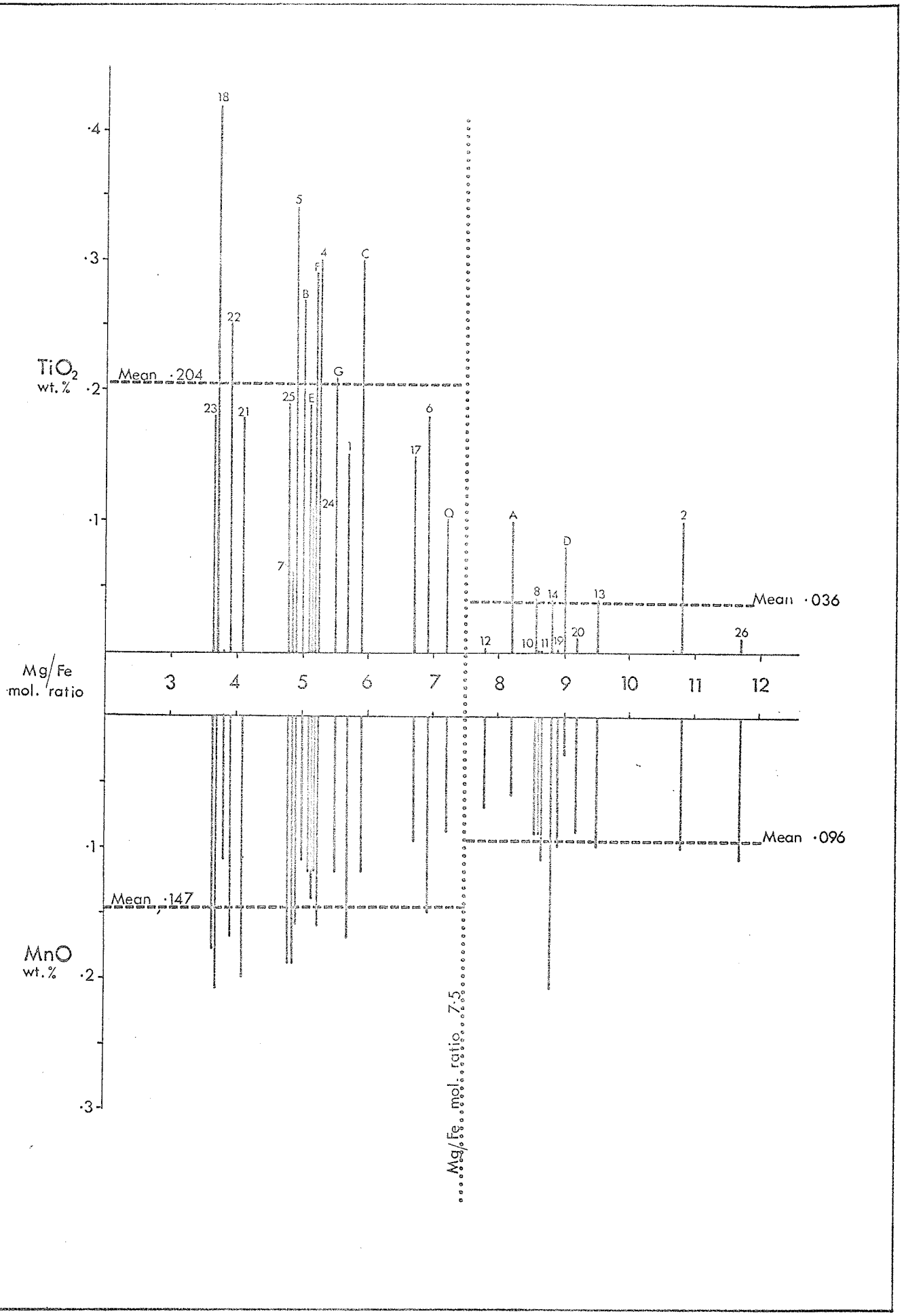

FIG. 22 : Diagram showing the relationship of TiO_2 and MnO contents to the Mg/Fe molecular ratio in ultramafic rocks. Compiled from data in Table 14.

a mafic magma, as cited by Hess (1938) and also some of the more altered ultramafic groups from the Manitoba nickel belt, which have lower Mg/Fe ratios than those for the purer serpentinite groups.

Additional analyses would undoubtedly change the mean TiO_2 and MnO values slightly in Fig. 22, but the basic difference between rocks with Mg/Fe ratios above and below 7.5, would probably remain apparent. In a study of the minor element content of serpentine minerals, Faust, Murata and Fahey (1956) concluded that Ti and Mn concentrations are non-diagnostic for determining the genetic class to which a serpentine belongs. The serpentines were divided into Class A, derived from ultrabasic rocks and Class B which included those derived from metamorphosed linestones, dolomites, contact metamorphic deposits and hydrothermal veins. Their research did not attempt to subdivide the serpentines of Class A into groups derived from ultrabasic rocks of varying composition and origin.

AVERAGE COMPOSITION OF MANITOBA NICKEL BELT SERPENTINITES AND COMPARATIVE ANALYSES OF ULTRAMAFIC ROCKS

It has been indicated previously that the most abundant ultramafic rock type occurring along the nickel belt is the serpentinites of group A. This group has an average Mg/Fe molecular ratio of 8.2. Closely allied to group A in composition and mineralogy are the serpentinites of M14Q and the phlogopite serpentinites of group D, having Mg/Fe ratios of 7.2 and 9.0

TABLE 15

AVERAGE COMPOSITIONS OF MANITOBA NICKEL BELT SERPENTINITES

(All are water-free and recalculated to 100%)

OXIDE	A.[1] SERPENTINITES	M14Q.[2] SERPENTINITE	D.[3] PHLOG. SERPENTINITES
SiO_2	40.68	40.23	43.96
Al_2O_3	2.22	2.38	2.58
FeO*	9.66	11.08	8.48
MgO	44.52	44.57	42.99
CaO	.33	.32	.00
Na_2O	-	-	-
K_2O	.00	.00	.66
CO_2	.68	-	.06
TiO_2	.11	.11	.10
S	.72	-	-
Cr_2O_3	.61	.84	.90
MnO	.06	.10	.03
NiO	.39	.35	.23
CoO	.02	.02	.01
Total	100.00%	100.00%	100.00%

1. Average of 24 analyses, listed by number in Table 12 and individually recorded in Appendix 1X.
2. Average of 13 analyses of the M14Q serpentinite body, Setting Lake, Manitoba.
3. Average of 2 analyses as listed by number in Table 12 and individually recorded in Appendix 1X.

* Total Fe as FeO.

\- Dash indicates not determined.

respectively. The M14Q serpentinite analysis represents the average of 13 specimens from a single intrusive body and as such, has been considered separately from the group A serpentinites. Average compositions of the A, M14Q and D group serpentinites have been recalculated to 100% assuming 0% H_2O and are listed in Table 15.

Significant features of these average analyses are the low Al_2O_3 and extremely low CaO contents. CaO is absent in the two analyses averaged for group D. K_2O is absent or below the limit of detection by the method of analysis, in groups A and M14Q, but is present as a minor constituent in the phlogopite serpentinites. The three groups contain an average of .78% Cr_2O_3 and .32% NiO whereas the values for TiO_2, MnO and CoO are extremely low.

Hess (1964) has listed analyses of rocks thought to be representative of material from the upper mantle. The list has been reproduced in Table 16. These include olivine nodules found in basalts, described in detail by Ross, Foster and Myers (1954), and ultramafic intrusions such as the Lizard of Cornwall, Tinaquillo in Venezuela and St. Paul's Rocks on the Mid-Atlantic Ridge. The serpentinized peridotite (Type C) from Mayaquez, Puerto Rico is similar chemically and has been included in the above list by Hess (1964). All the analyses of Table 16 have been recalculated on a water-free basis. The mineralogy described for these rocks and for the olivine nodules in basalts, indicate they all contain the four phases, magnesium olivine, enstatite, diopside and a spinel group mineral.

TABLE 16

CHEMICAL ANALYSES OF ROCKS THOUGHT TO BE REPRESENTATIVE OF THE UPPER MANTLE

(All are water-free and recalculated to 100%) - From Hess (1964).

OXIDE	MAYAGUEZ (AVERAGE TYPE C)	TINAQUILLO, VENEZUELA (v.336)	OLIVINE NODULE (N.S.WALES)	ST.PAUL'S ROCKS	OLIVINE NODULE (LUDLOW)	OLIVINE NODULE (JAPAN)	TINAQUILLO VENEZUELA (V.1460)	ST.PAUL'S ROCKS (WD55)	LIZARD (AVERAGE)
SiO_2	43.56	43.91	44.14	44.24	44.27	44.50	44.93	44.57	44.77
Al_2O_3	2.36	2.65	2.78	2.91	2.97	3.24	3.21	4.10	4.16
Fe_2O_3	1.00	1.44	1.02	1.04	.67	1.68	.09	1.17	-
FeO	7.77	7.23	7.33	7.00	7.59	6.83	7.58	6.85	8.21
MgO	41.53	42.01	41.65	41.36	40.73	41.02	40.03	39.07	39.22
CaO	2.51	2.02	2.15	2.37	2.55	2.22	2.99	2.87	2.42
Na_2O	.32	.13	.19	.07	.20	.22	.18	.32	.22
K_2O	.005	.00	.01	.00	.01	.05	.02	.07	.05
TiO_2	.04	.06	.12	.17	.14	.06	.08	.12	.19
Cr_2O_3	.40	.41	.25	.50	.41	-	.45	.46	.40
MnO	.10	.15	.12	.13	.13	.17	.14	.13	.11
P_2O_5	.07	.00	-	-	.02	.01	.04	.02	.01
NiO	.34	-	.23	.21	.31	-	.26	.25	.24
Total	100.00	100.00	100.00	100.00	100.00	100.00	100.00	100.00	100.00

For detailed references to sample source, location and authors, see Hess (1964).

Comparison of the analyses of the rocks thought to be representative of the upper mantle with the serpentinites of the Manitoba nickel belt in Table 15, shows certain minor differences. A higher MgO and distinctly lower CaO content are evident in the Manitoba rocks. SiO_2 is also slightly less but the Al_2O_3 content is essentially the same. It seems likely from the chemistry therefore, that the Manitoba serpentinites were originally dunites and peridotites with a high olivine-pyroxene ratio and a low to negligible CaO content in the orthopyroxene. The latter point is confirmed by the rarity of exsolved diopsidic lamellae in orthopyroxenes of the nickel belt rocks.

The average composition of upper mantle material (Hess 1964) is listed with an additional eight comparative analyses of ultramafic rocks in Table 17. The latter are peridotites or serpentinized peridotites except for the vitrophyric pillow lava with an ultrabasic composition described by Gass (1958) from an occurrence in Cyprus. These analyses of ultramafic rocks have been selected to give representative compositions of material which crystallized under a wide range of geological environments and with distinctly different modes of origin. Compositional differences and similarities between them and the ultramafic rock groups of the nickel belt are seen to advantage when the analyses are plotted as phases in triangular diagrams representing the chemical systems $MgO-FeO-SiO_2$ (Bowen and Schairer, 1935) and $CaO-MgO-FeO-(SiO_2)$(Wyllie, 1960). Fig. 23 gives the triangular plots of the analyses in the two systems.

TABLE 17

SELECTED COMPARATIVE ANALYSES OF ULTRAMAFIC ROCKS

	1	2	3	4	5	6	7	8	9
SiO_2	41.06	43.0	43.54	42.21	38.65	43.00	40.06	44.32	39.48
Al_2O_3	4.82	3.4	3.99	5.92	6.59	4.64	1.67	3.15	1.44
Fe_2O_3	2.07	2.3	2.51	2.96	4.24	2.42	6.05	0.90	5.84
FeO	9.46	5.0	9.84	7.25	6.93	6.47	7.52	7.38	2.73
MgO	36.15	43.3	34.02	29.07	29.74	33.45	35.55	40.74	37.60
CaO	4.27	1.8	3.46	4.68	3.52	3.99	2.34	2.46	0.35
Na_2O	0.65	-	0.56	0.70	0.15	0.25	0.32	0.21	0.23
K_2O	0.02	-	0.25	0.21	0.10	0.05	0.12	0.02	0.11
H_2O+	0.97	-	0.76	5.06	8.35	3.83	6.01	-	11.48
H_2O-	0.06	-	-	0.20	0.24	1.22	0.28	-	0.67
CO_2	-	-	-	0.15	0.59	-	-	-	-
TiO_2	0.15	0.1	0.81	0.30	0.34	0.18	0.06	0.11	-
S	-	-	-	0.07	0.21	-	-	-	-
Cr_2O_3	0.51	0.4	-	0.36	0.08	0.51	0.21	0.36	0.38
MnO	0.17	0.1	0.21	0.16	0.16	0.15	0.19	0.13	-
NiO	-	0.3	-	0.48	0.14	-	-	0.20	0.17
CoO	-	0.004	-	-	-	-	-	-	-
P_2O_5	.00	-	0.05	0.03	0.06	-	0.00	0.02	-
Total	100.36	99.70	100.00	99.78	100.09	100.16	100.38	100.00	100.48
Mg/Fe ratio	5.7	10.8	5.0	5.2	4.9	6.9	4.9	8.9	8.3

1. Peridotite from Unit 10, Layered Series, Rhum. Average of 7 specimens. Brown (1956)
2. Serpentinized peridotite SDM 150. Recalc. to give 0% H_2O. Mt. Albert. MacGregor (1962)
3. Average peridotite, 23 analyses. Nockolds (1954)
4. Peridotite M-667-58, Cuthbert Lake, Man. McDonald (1960)
5. Ultrabasic sill, composite sample. Labrador. Fahrig (1962)
6. Ultrabasic pillow lava, vitrophyric type. Cyprus. Gass (1958)
7. Secondary peridotite, MB.20. Stillwater. Hess (1938)
8. Rocks thought representative of Upper Mantle. Average of 9 analyses (from Table 16). Hess (1964).
9. Average peridotite. Average of 24 analyses. Hess (1938).

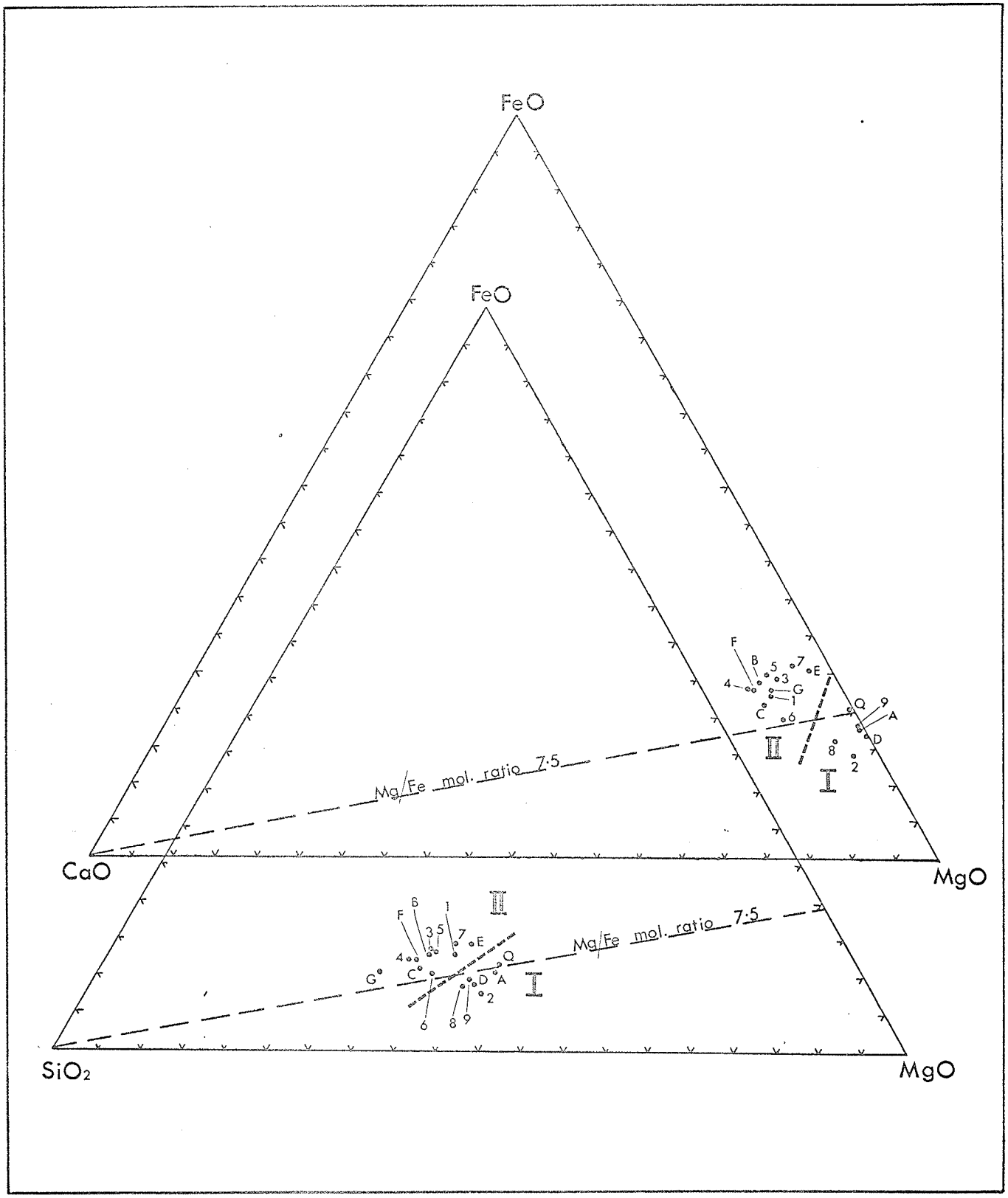

FIG. 23 : Triangular plots of the SiO₂-MgO-FeO and CaO-MgO-FeO components of Bentinck Island and other selected ultramafic rocks. Compiled from data in Tables 13 and 17.

Inspection of Fig. 23 shows that in both triangular diagrams, the plots are easily divided into two distinct groups. The first group has lower CaO and SiO_2 contents and are enriched in MgO with respect to the rocks of the second group. The first group consists of typical alpine-type peridotites (Hess 1938, Thayer 1960) and peridotites and serpentinites thought to be representative of upper mantle material (Hess, 1964). This group includes the Manitoba nickel belt serpentinites, groups A, D and M14Q as listed in Table 15. The second division of plots in Fig. 23 contain ultramafic rocks from layered and differentiated intrusive bodies and the glassy pillow lava from Cyprus (Gass, 1958). Into this group falls the ultramafic nickel belt rocks contained in groups B, C, E, F and G, listed in Table 13.

The line representing the Mg/Fe molecular ratio of 7.5 has been added to each of the triangular diagrams in Fig. 23. This line accentuates the chemical division of the ultramafic rocks into their two principal groups.

GENESIS OF THE NICKEL BELT ULTRAMAFIC ROCKS

GENERAL STATEMENT

In this section, evidence concerning structural aspects, petrological features and chemical characteristics of the nickel belt's ultramafic rocks is reviewed. A probable mode of origin is presented and briefly discussed in relation to current literature on the problems of serpentinites and related ultramafic rocks.

STRUCTURAL FEATURES

The ultramafic intrusive bodies are variable in size and irregular in shape. Smaller bodies have a tendency to be elongated lensoidal in shape. Their linear distribution along the nickel belt is fault controlled. Faults are steeply dipping and braided in surface expression suggesting the pattern resulted from major wrench faulting. In general the intrusions are essentially structureless and massive, but many of the ultramafic bodies for which sufficient information is available have sheared marginal zones with accompanying significant changes in mineralogy. So far as is known, gabbroic rocks are not associated with the ultramafic intrusions at any locality along the nickel belt. Finally, detailed examination by thin section and analyses of the adjacent rocks to a serpentinite body in Setting Lake area, failed to reveal any evidence of contact metamorphism.

PETROLOGIC FEATURES

Petrologically, the most significant similarity of the ultramafic intrusive bodies is their high degree of serpentinization. It is not intended here to discuss at great length the processes and theories of origin of serpentine. However the importance of the serpentine group minerals in the mineralogy of the rocks under consideration, requires that a brief examination of salient facts regarding their origin be given.

1) Serpentine minerals have developed by replacement of primary silicate minerals, principally olivine and orthopyroxene and in rare instances, clinopyroxene.

2) The stability field of serpentine in the system MgO-SiO_2-H_2O has an upper temperature limit of 500° C. (Bowen and Tuttle, 1949). These writers suggest that olivine and pyroxene are intruded in the crystalline state without water and are subsequently serpentinized below 500° C. by water vapour acquired through contact with wet wall rocks. Sosman (1938) has suggested some water may have been present as an intergranular lubricating fluid, assisting flow of the solid intrusion. Earlier, Hess (1938) had concluded from field evidence that the low temperature environment and lack of contact metamorphism surrounding alpine-type ultramafic bodies resulted from the addition of water to a primary peridotite magma to form a serpentine magma. The suggestion of a solid intrusion in the form of crystal mush has been supported by petrofabric work on some bodies (Turner, 1942, Fahrig, 1953). Serpentine textures have been described in the present work, which suggest a preferred orientation to olivine crystals prior to serpentinization. However, occurrences of this type are rare. Undoubtedly, serpentinization took place during the active emplacement of the ultramafic bodies. In accordance with the experimental work of Bowen and Tuttle (1949) and providing sufficient water was available, alteration of olivine and pyroxene to serpentine would occur as fast as reaction rates permitted, when the stability field for serpentine was encountered during conditions of falling

temperature.

3) Source of sufficient water to bring about serpentinization has generally been attributed to country rocks into which the intrusion of ultramafic bodies has taken place. Supporting this concept is evidence obtained from ultramafic bodies with host rocks of varying composition and showing varying degrees of serpentinization. (Fahrig 1962, Du Rietz 1935, Hess 1938). These writers suggest that the extent of serpentinization is controlled by the composition of the country rocks and have shown that bodies in gneissic terrain have a lower degree of serpentinization. Cooke (1937) considers size of body a factor in determining the degree of serpentinization. In the Thetford area of Quebec, smaller bodies of peridotite are more highly serpentinized than larger masses. Neither size of body nor type of country rock have had any measurable control on the extensive serpentinization of the nickel belt ultramafic rocks. All are enclosed in gneissic rocks, whose high grade metamorphism precludes the possible presence of any substantial amounts of water. It has been shown previously however that the ultramafic bodies were emplaced at an early stage in the metamorphic history of the region, when the sedimentary rocks could conceivably have contained an adequate content of water to bring about serpentinization.

4) Equations illustrating the replacement of olivine by serpentine show that a considerable increase in volume might be expected. In general, field evidence does not support the concept of a large increase in volume during serpentinization

(Turner and Verhoogen 1960). Fracturing and faulting have been put forward as evidence of expansion during serpentinization but most writers agree from microscopic evidence that little if any volume increase has occurred. Olsen (1959) on the other hand cites evidence that a volume increase took place during the serpentinzation of a saxonite in Quebec. Olivine fragments have been rotated and fractured and fractures in pyroxene contain chrysotile, which requires a tensional environment for growth. Microscopic study of the nickel belt rocks indicates some expansion has taken place. Radiating expansion cracks around partially serpentinized olivine grains enclosed in pyroxene (Plate 4) testifies to a volume increase. Serpentinite textures themselves would not be expected to reveal evidence of expansion.

5) No attempt has been made in the present work to determine the amount and composition of material gained or lost from the original intrusions during serpentinization. Obvious additions are H_2O and CO_2, the latter combining with Ca and excess Mg to form dolomite. X-ray diffraction patterns of the serpentines commonly showed peaks caused by the presence of small amounts of dolomite and by magnesite in one sample.

In addition to serpentine minerals, the serpentinization process has resulted in most places, in the formation of minor quantities of talc and brucite.

Additional minerals developed in the ultramafic rocks of the nickel belt are tremolite, anthophyllite, phlogopite, vermiculite and chlorite. Their distribution has been discussed

in Chapter 111. Thin section study shows that they are younger in age than the principal period of serpentinization. It is not uncommon however, to find tremolite partially serpentinized by a yellowish-brown pleochroic variety of late origin. The secondary development of tremolite in serpentinized ultramafic rocks has been recorded by a number of writers included Wilkinson (1953), F. C. Phillips (1927), Durrell (1940) and Chatterjee (1955). Tremolite may also be an original constituent in peridotites (Flett and Hill, 1946). Where developed in the Manitoba rocks, tremolite may occasionally be observed replacing primary pyroxene. The common association of tremolite and phlogopite in some ultramafic bodies (e. g. M11A. Wabowden) testifies to considerable metamorphic and metasomatic effects from intrusive granitic rocks. Tremolite and phlogopite require considerable CaO and K_2O, which occur in rather low concentrations in the serpentinites. It is considered probable that these were introduced during a late period of granite and pegmatite intrusion.

The development of zones of anthophyllite and chlorite in Manitoba rocks has been discussed earlier. Monomineralic zones containing anthophyllite at the margin of serpentine nodules in schist has been described by Pabst (1942). Deposits of economic interest occur with vermiculite in serpentine adjacent to feldspar veins at Hafafit, Eygpt (Amin and Afia, 1954) and also in bodies of dunite, hydrothermally altered by the Idaho batholith near Kamiah (Anderson, 1931). A similar association of pegmatite in dunite has produced reaction rims with the

mineral sequence of phlogopite, anthophyllite and talc zones outward from the pegmatites at the Day Book dunite deposit in North Carolina (Kulp and Brobst, 1954). At this locality, alteration of phlogopite by weathering has produced vermiculite. As with the Manitoba occurrences, these minerals have developed by the reaction of ultrabasic rock and hydrothermal solutions associated with acid intrusive bodies.

CHEMICAL FEATURES

Earlier in this chapter, it has been shown that the ultramafic rocks can be divided chemically into two groups (Fig. 23). Group 1 includes the Manitoba serpentinites of groups A, Q and D, which are chemically comparable to alpine-type peridotites and ultramafic rocks thought to be representative of the upper mantle. They contain higher MgO, lower FeO, CaO and generally lower SiO_2 contents compared to the rocks which are included in group 11. The latter includes layered ultrabasic bodies, and the Manitoba rocks contained in groups B, C, E, F and G. From geological association and mineralogical evidence, it is now known that groups B, C and E are highly altered phases of an original ultramafic rock with a composition approaching that determined for group A, and that groups F and G are pyroxenitic phases of the same rock, derived from the same source. It is clear that in a chemical study of rocks of this type, a single, or a small number of specimens would not necessarily indicate the chemical makeup of the original source

material. With the study of a much larger number of specimens, it is now reasonable to suggest that the serpentinzed ultramafic bodies from the nickel belt have chemical compositions closely approximately those of the group A and Q serpentinites. It remains to consider the source of this ultrabasic material, and its manner of introduction into the highly deformed linear zone of Precambrian rocks in Central Manitoba.

ORIGIN AND MODE OF INTRUSION

The literature contains many references to ultramafic bodies and complexes with considerable discussion of petrogenesis and environment of emplacement. Ultramafic intrusions have been classed into two major genetic types, the stratiform-type of which the Bushveld complex and the Stillwater complex are prime examples, and the alpine-type, which are characterized by irregularity of form and structure and occur along highly folded geosynclinal belts. Notable proponents of this classification have been Hess (1938, 1955) and Thayer (1960). Ultramafic complexes which do not fit this restricted classification have been discussed in detail by Smith (1958) and Noble and Taylor (1960).

Although the association of gabbro with peridotite is an obvious relationship in the stratiform-type, it remained for the detailed listing of definitive features by Thayer (1960) to show that associated gabbroic rocks are a common feature of alpine-type occurrences as well. Smith (1958) has described

the Bay of Islands complex in Newfoundland, where gabbroic rocks form 10-12 percent of the exposures in the ultramafic plutons with characteristics of the alpine-type and suggests the existence of a pluton series ranging from the true stratiform-type to the alpine-type serpentinite bodies. The Bay of Islands complex thus conforms to an intermediate type and is described by Thayer (1960) as a pseudostratiform alpine-type complex. Smith suggests that the variable abundances of gabbro associated with peridotite intrusions are a result of differences in cooling, emplacement history and post-emplacement deformation. The close association of gabbro and peridotite at the Bay of Islands indicates a genetic relationship between them.

The origin of the alpine-type peridotite-gabbro complexes is explained by Thayer (1960) as resulting from the intrusion of crystal mushes with peridotitic and gabbroic compositions, which must have been emplaced together under the same environmental conditions. The two fractions were obtained from different layers in differentiated zones of the deep crustal or upper mantle regions. Mixing of the semi-solid gabbro and peridotite during upward flowage would result in the intermediate banded zones common to many complexes. Gravitative differentiation of a magma at depth into a largely fluid gabbro fraction and an ultrabasic mush is considered by Smith (1958) to best explain the origin of the Bay of Islands complex. The more fluid gabbro fraction advanced into the upper crust ahead of the more solid ultrabasic portion during a period of active tectonic forces.

Bowen and Tuttle (1949) have shown the temperature of

intrusion of an olivine mush would have to be between 1100° and 1200° C. An essentially liquid magma at this temperature would leave a well defined contact metamorphic effect on the enclosing rock. However if the crystal mush had only minor associated quantities of liquid, margins of the body would be rapidly cooled. An influx of water from the wallrocks would inhibit contact metamorphism and the temperature would soon drop to within the stability field of serpentine. It is notable that contact metamorphic aureoles are pronounced around the Mt. Albert body (MacGregor 1962) and the Bay of Islands complex (Smith 1958). In both cases, serpentinization of the ultramafic rocks is incomplete suggesting a lack of water inflow from the host rocks.

From the Manitoba occurrences, little can be deduced regarding mode of intrusion. Serpentine textures at one locality, #190 (M14V-820 Setting Lake), indicates a preferred orientation of original olivine and hence an intrusion of a crystal mush. Where remnant olivine fragments are present in serpentine pseudomorphs, a definite change in optical orientation between the olivines of adjacent pseudomorphs indicates a lack of any orientation. From the preceeding discussion however, the intrusion of a partly solidified magma with quick marginal cooling and subsequent serpentinization from water in the enclosing rocks or from within the faults themselves, appears the most probable mode of intrusion. Although the serpentinites have been subjected to orogenic forces during the Hudsonian, no evidence is known at the present time to suggest that any of the serpentinite masses have been re-intruded as solid

serpentine bodies from their original locations into adjacent areas. That such a phenomena is possible is verified by the mapping of Neale (1957) and Smith (1958) in Newfoundland and Thomas (1951) in California. The shearing along the serpentinite margins in Manitoba is due to their position within zones of faulting, which undoubtedly remained active over a long period of time.

Whether genetically related gabbroic material had any place in the petrogenesis of the ultrabasic bodies remains to be determined. If one takes the viewpoint that peridotite and gabbro are genetic associates of alpine-type intrusions, the total absence of gabbro must be explained in terms of post intrusion deformation and present day erosion levels. Smith (1958) has observed in the Bay of Islands Complex that plutons with the most ultrabasic material are the most highly deformed. These represent blocks from lower levels in the original body, brought to their present structural position by thrust faulting and associated transverse faulting. Level of crustal erosion is considered more significant in the nickel belt. Preliminary geophysical work (Hall and Brisbin, 1965) indicates a probable reduction in depth to the Mohorovic discontinuity of 3 km. on crossing over the Bouguer gravity low anomaly from the Churchill block towards the Superior side. It is apparent therefore that the rocks to the southeast of the gravity anomaly, in which by far the greatest number of ultramafic bodies are contained, represent exposure of a deeper level in the crust. It may well be that gabbroic rocks were once associated with the ultrabasic

bodies at higher structural levels, but this is entirely speculative.

The close correlation of a regional gravity low anomaly and a major zone of faulting indicates the faulting resulted from or was the cause of the structural conditions in the crust producing the anomaly. Whichever is the case, the fault system is sufficiently deeply penetrating to have tapped a source of ultrabasic material in some region of the lower crust or upper mantle and facilitated its upward rise and emplacement near the surface.

CHAPTER 1X

CONCLUSIONS

The main conclusions reached as a result of this investigation are as follows:

1. Ultramafic intrusive bodies are found localized within a complex, northeast-trending zone of faulting in north-central Manitoba. Presently known bodies are distributed within this zone for a length of 125 miles and across a maximum width of 8 miles. The axis of a regional Bouguer gravity low anomaly closely follows the zone on its northwest or convex side. Meager field evidence and the braided surface expression suggests the fault system results from major wrench movements.

2. The age of the ultramafic bodies is considered to be Churchill, intruded at some stage in the early history of the Hudsonian orogeny, which terminated some 1640 million years ago.

3. Individual intrusions range in size from elongate lensoidal bodies less than 1000 feet in length and 150 feet in width, to larger masses with maximum dimensions of $5\frac{1}{2}$x1 miles. The larger bodies are more irregular in shape while retaining basic lensoid forms.

4. A classification of ultramafic rock types, based on modal compositions gives the following groups: A. Serpentinites, B. Tremolite serpentinites, C. Tremolite phlogopite serpentinites, D. Phlogopite serpentinites, E. Serpentinized peridotites,

F. Tremolite olivine orthopyroxenites, G. Amphibole orthopyroxenite, and H. Miscellaneous altered types. From petrographic and chemical data, the original ultramafic rocks are considered to have been dunites, peridotites and orthopyroxenites.

5. The forsterite content of eighteen olivines from a number of different intrusions, ranges from Fo_{74} to Fo_{99}. Fifteen of the specimens have compositions in the range Fo_{84} to Fo_{90} with a mean value of $Fo_{86.2}$.

6. Orthopyroxene ranges in composition from En_{77} to En_{85}. Clinopyroxene is an extremely rare mineral in the ultramafic rocks, being found in only three specimens from two separate intrusions.

7. Chrome spinels are common accessory minerals, being generally primary crystallates but some are of secondary origin. Colour variations of the spinels are reddish-brown, brown, yellow-brown, yellow, green, greenish-brown, black and red. Cell edge dimensions in the spinels range from 8.112Å for the pale green variety to 8.32Å for the black opaque varieties.

8. Amphiboles present in many of the ultramafic bodies include tremolite and anthophyllite. The occurrence of the latter is restricted to marginal zones of alteration.

9. Phlogopitic mica is commonly present in marginal zones and areas altered by late acid intrusive rocks.

10. Chlorite in the serpentinites and other ultramafic types is commonly a magnesium-rich clinochlore, near leuchtenbergite in composition. Cleavage in the chlorite often contain minute lenses of dolomite and plates of a dark brown to nearly opaque mineral of unknown composition.

11. Vermiculite, derived from phlogopite, brucite, talc, calcite and dolomite are found in many intrusions in minor quantities.

12. Magnetite occasionally is present as a primary crystallate but is ubiquitous as a secondary mineral, formed from iron released from primary silicates by serpentinization. A form of metamorphic differentiation is evident from the movement of iron during serpentinization, a process believed to occur with the iron in the form of a ferrous hydrosol.

13. Serpentinites, wholly composed of serpentine group minerals and accessary oxides, comprise the most abundant ultramafic rock type found in the nickel belt.

14. Optical studies on the serpentine minerals indicates the predominant type is a fibrous serpentine resembling chrysotile. Minor antigorite and lizardite are present in some areas. It is thought that antigorite develops by the replacement of chrysotile during thermal metamorphism.

15. X-ray powder diffraction patterns from the nickel belt fibrous serpentines, although similar in some ways to the published powder pattern of 6-layer orthochrysotile, could only be satisfactorily indexed on the basis of a 3-layer structure. The derived 3-layer ortho-hexagonal cell with a_o = 5.346Å, b_o = 9.205Å and c_o = 21.93Å gives good agreement between observed and calculated d values for a wide range of reflections.

16. The X-ray powder diffraction pattern of antigorite serpentine from Ospwagan Lake is compared with patterns derived from "williamsite", Lancaster Co., Pa. and serpentine from Island Lake, Manitoba and with the published data of the Caracas

antigorite. All possess essentially identical structures.

17. X-ray diffraction and optical studies indicate the presence of a mixture of clinochrysotile and lizardite in a specimen from the Pipe Lake occurrence (#122).

18. Differential thermal analysis in the temperature range 25° C.-1000° C. shows that distinctions can be made between the chrysotile and antigorite groups, but that the different polymorphs of chrysotile cannot be distinguished from one another, nor from lizardite.

19. Disseminated sulphide minerals contained within a variety of serpentinite bodies include pyrrhotite, pentlandite, chalcopyrite, pyrite and marcasite. Pentlandite most commonly occurs as discrete crystals in pyrrhotite. Theories of origin for the sulphides are discussed but the genesis of the Manitoba occurrences is still in doubt.

20. A detailed investigation of the M14 serpentinite body in Setting Lake, the original nature of which is considered to have been an olivine-rich peridotite, shows it to be essentially chemically homogeneous except adjacent to the margins of the body. Marginal alteration has resulted in the formation of tremolite, anthophyllite and chlorite zones. Calculation of the composition of the modified standard cells (MSC) of specimens across the 20 foot wide alteration zone of the west contact, show increases in Si, Al, Ca and Mn, while Mg, Fe, OH, Cr and Ni register losses. The increase in Ca is significant in its resultant formation of considerable tremolite.

21. Mineralogical and chemical changes induced in serpentinite

by younger acidic intrusives are displayed to advantage in the M11A body at Wabowden. Width of alteration zones adjacent to pegmatites is not directly proportional to widths of the pegmatites. Within the serpentinites, pegmatite intrusions become desilicated and are represented as feldspar dykes. At two locations studied, mineralogical changes in serpentinite adjacent to pegmatite have resulted in the development of zones of phlogopite, chlorite and tremolite in one occurrence and anthophyllite, phlogopite and talc-carbonate in the second occurrence, from the pegmatite contacts passing into the serpentinite. Chemical studies indicate the serpentinite has gained, within the zone of alteration, significant amounts of SiO_2, Al_2O_3, K_2O and CO_2 and lost MgO, FeO and H_2O. The final disposition of large amounts of MgO lost from the serpentinites is in waxy "picrolitic" serpentine material which forms the matrix to brecciated pegmatites. In contrast to Mg and Fe, Ni appears to be a more immobile element under the conditions of this type of alteration.

22. The chemical composition of the group A serpentinites most closely represents the average composition of the nickel belt ultramafic rocks.

23. The content of MnO and TiO_2 oxides shows an inverse relationship to the Mg/Fe molecular ratio in ultramafic rocks in general.

24. In comparison to the composition of rocks thought to be representative of the upper mantle, Manitoba serpentinites contain slightly higher MgO and lower SiO_2 and CaO contents. The content of Al_2O_3 is essentially the same. Chemically the

Manitoba serpentinites are typical of alpine-type peridotites. Altered and pyroxenite groups have compositions similar to layered and differentiated types of ultramafic intrusions.

25. Mode of intrusion of the Manitoba rocks is considered to have been in the form of a semi-solid crystal mush, with quick marginal cooling and subsequent serpentinization from water in the enclosing rocks or from within the faults up which the ultrabasic material emerged.

26. The system of faults and the regional gravity low anomaly are related to major crustal deformation. The faults are sufficiently deeply penetrating to have tapped a source of ultrabasic material in the upper mantle.

BIBLIOGRAPHY

AMIN, M. S. and AFIA, M. S., (1954):
Anthophyllite - vermiculite deposit of Hafafit, Eastern Desert, Egypt. Econ. Geol. vol. 49, pp. 317-327.

ANDERSON, A. L., (1931):
Genesis of the anthophyllite deposits near Kamiah, Idaho. Jour. Geol., vol. 39, pp. 68-81.

ANDERSON, D. T., (1963):
The distribution of nickel, copper and cobalt in igneous rocks and in synthetic sulphide-silicate melts. Unpub. PhD. Thesis, Univ. of Manitoba. 1963.

ARUJA, E., (1945):
An X-ray study of the crystal structure of antigorite. Min. Mag. vol. 27, pp. 65-74.

BATES, T. F. SAND, L. B. and MINK, J. F., (1950):
Tubular crystals of chrysotile asbestos. Science, 111, pp. 512-513.

BELL, C. K., (1966):
Churchill-Superior Province Boundary in Northeastern Manitoba. In Jenness, S. E., Geol. Surv. Can., Paper 66-1. pp. 133-136.

BENSON, W. N., (1926):
The tectonic conditions accompanying the intrusion of basic and ultrabasic igneous rocks. Mem.Nat.Acad.Sci. vol. 19, No. 1, pp. 1-90. Washington.

BOWEN, N. L. and SCHAIRER, J. F., (1935):
The system MgO-FeO-SiO_2. Amer.Jour.Sci., 29, pp. 151-217.

BOWEN, N. L. and TUTTLE, O. F., (1949):
The system MgO-SiO_2-H_2O. Geol. Soc. Amer. Bull., vol. 60, pp. 439-460.

BROWN, G. M., (1956):
The layered ultrabasic rocks of Rhum, Inner Hebrides. Roy. Soc. Lond., Phil. Trans. vol. 240, pp. 1-53.

CAILLÈRE, S., and HÉNIN, S., (1957):
The chlorite and Serpentine minerals. The Differential Thermal Investigation of Clays. Chap. V111. Ed. by R. C. Mackenzie. Min. Soc. Lond.

CHATTERJEE, S. C., (1955):
Peridotites of Manput, Singhbhum District of Bihar, India and the origin of associated asbestos deposits. Geol. Soc. Amer. Bull., v. 66, pp. 91-104.

CHIDESTER, A. H., (1962):
Petrology and geochemistry of selected talc-bearing ultramafic rocks and adjacent country rocks in north-central Vermont. U. S. Geol. Sur.Professional Paper 345.

COOKE, H. C., (1937):
Thetford, Disraeli and eastern half of Warwick map areas, Quebec. Can. Geol. Sur. Mem. 211.

DAVIES, J. F., (1960):
Geology of the Thompson-Moak Lake District, Manitoba. Can. Mining Jour. vol. 81, no. 4, pp. 101-104.

DAVIES, J. F., et al, (1962):
Geology and Mineral Resources of Manitoba. Dept. of Mines and Natural Resources, Manitoba.

DAVIES, J. F., (1964):
Mineral Deposits related to major structures in the Precambrian of Manitoba. C.I.M.M. Bull. v. 57, June 1964. pp. 661-665.

DAWSON, A. S. (1941):
Assean-Split Lakes Area. Manitoba Mines Br., Rept. 39-1.

DEER, W. A., HOWIE, R. A., and ZUSSMAN, J., (1962):
Serpentines. Rock Forming Minerals, vol. 4-Sheet Silicates. Longmans.

DURIETZ, T., (1935):
Peridotites, serpentines and soapstones of Northern Sweden. Geol. Foren. Förhan., v. 57, 2, pp. 133-260. Sweden, 1935.

DURRELL, Cordell, (1940):
Metamorphism in the southern Sierra Nevada northeast of Visalia, California. Dept. Geol. Sci., Bull. v. 25, p. 1-117. Univ. of California.

FAHRIG, W. F., (1962):
Petrology and geochemistry of the Griffis Lake Ultrabasic Sill of the Central Labrador Trough, Quebec. Geol. Sur. Can. Bull., 77 pp. 1-39.

FAUST, G. T., and FAHEY, J. J. (1962):
The serpentine group minerals. USGS. Prof. Paper 384-A, pp. 1-87.

FAUST, G. T. MURATA, J. J., and FAHEY, J. J., (1956):
Relation of minor element content of serpentines to their geological origin. Geochem. et Cosmochim Acta. vol. 10, pp. 316-321.

FLETT, J. S., and HILL, J. B., (1946):
Geology of the Lizard and Meneage. Geol. Sur. Great Britain, England and Wales. Mem. 2nd Ed. by Sir John Smith Flett. 208 pp.

FRANCIS, G. H.,(1956):
The serpentinite mass in Glen Urquhart, Inverness-shire, Scotland. Amer. Jour. Sci., 254, pp. 201-226.

GASS, I. G., (1958):
Ultrabasic pillow lavas from Cyprus. Geol. Mag. v. 95, pp. 241-251.

GILL, J. C., (1951):
Geology of the Mystery Lake Area. Manitoba Mines Branch. Publ. 50-5.

GILL, J. E., (1952):
Early History of the Canadian Precambrian Shield. Geol. Assoc. of Canada. vol. 5, pp. 57-68.

GILLERY, F. H., (1959):
X-ray study of synthetic serpentines and chlorites. Amer. Min., vol. 44, pp. 143-152.

GREENWOOD, H. J., (1963):
The synthesis and stability of anthophyllite. Jour. Petrol., vol. 4, pt. 3, pp. 317-351.

GRUBB, P. L. C., (1962):
Serpentinization and chrysotile formation in the Matheson ultrabasic belt, Nothern Ontario. Econ. Geol. vol. 57, pp. 1228-1246.

GRUNER, John W., (1937):
Notes on the structure of serpentines. Amer. Min. vol. 22, pp. 97-103.

HÄKLI, A., (1963):
Distribution of nickel between the silicate and sulphide phases in some basic intrusions in Finland. Bull. de la Commission Geologique de Finlande. No. 209, 1963. pp. 1-54.

HALL, D. H., and BRISBIN, W. C., (1965):
Crustal Structure from Converted Head waves in central western Manitoba. Geophysics. (In press).

HAWLEY, J. E., (1962):
The Sudbury Ores: Their Mineralogy and Origin. Can. Min. vol. 7 part 1, pp. 1-207.

HESS, H. H. (1937):
Island Arcs, Gravity Anomalies and Serpentinite Intrusions - A Contribution to the Ophiolite Problem. Rep. 17th Int. Geol. Cong., Moscow, ii, pp. 263-283.

HESS, H. H., (1938):
A Primary Peridotite Magma. Amer. Jour. Sci., vol. 35, pp. 321-344.

HESS, H. H., (1955):
Serpentinites, Orogeny and Epeirogeny. Geol. Soc. Amer. Spec. Paper 62, pp. 391-408.

HESS, H. H., (1960):
Stillwater Igneous Complex, Montana. Geol. Soc. Amer. Memoir 80.

HESS, H. H., (1964):
The Oceanic Crust, the Upper Mantle and the Mayaguez Serpentinized Peridotite. A Study of Serpentine. NAS-NRC, Pub. 1188, pp. 169-175.

HESS, H. H., DENGO, G., and SMITH, R. J. (1952):
Antigorite from the vicinity of Caracas, Venezuela. Amer. Min. vol. 37, pp. 68-75.

HESS, H. H., and OTALORA, G., (1964):
Mineralogical and chemical composition of the Mayaguez serpentinite cores. NAS-NRC Pub. 1188. A Study of Serpentine pp. 152-168.

INNES, M. J. S., (1960):
Gravity and Isostasy in Manitoba and Northern Ontario. Publ. Dom. Obs., vol. xx1, No. 6.

JAMBOR, J. L. and SMITH, C. H., (1964):
Olivine composition determination with small-diameter X-Ray powder cameras. Mineralogical Mag. Vol. 33, no. 264. pp. 730-741.

KALOUSEK, G. L. and MUTTART, L. E., (1957):
Studies on the chrysotile and antigorite components of serpentine. Amer. Min. v. 42. pp. 1-21.

KRSTANOVIĆ, I., and PAVLOVIĆ, S., (1964):
X-Ray study of chrysotile. Amer. Min. vol. 49, pp. 1769-1771.

KULLERUD, G., and YODER, H. S., Jr. (1963):
Sulphide-Silicate relations: Ann. Rept. Director Geophysical Lab. Carnegie Inst., Washington. Year Book 1962, pp. 215-218.

KULP, J. L., and BROBST, D. A., (1954):
Notes on the dunite and the geochemistry of vermiculite at the Day Book dunite deposit, Yancy County, North Carolina. Econ. Geol., v. 49, pp. 211-220.

KUNZE, G., (1956):
The wave structure of antigorite. Z. Kristallog, 108, pp. 82-107.

LOWDON, J. A., (1961):
Age Determinations by the Geological Survey of Canada, Rept. 2-Isotopic Ages: Geol. Sur., Canada, Paper 61-17.

MACGREGOR, I. D., (1962):
Geology, petrology and geochemistry of the Mount Albert and associated ultramafic bodies of Central Gaspe, Quebec. Unpub. MSc. Thesis. Queen's University, 1962.

MACGREGOR, I. D., and SMITH, C. H., (1963):
The use of chrome spinels in petrographic studies of ultramafic intrusions. Can. Min. vol. 7, pt. 3. pp. 403-412.

MCDONALD, J. A., (1960):
A petrological study of the Cuthbert Lake ultrabasic and basic dyke swarm: A comparison of the Cuthbert Lake ultrabasic rocks to the Moak Lake type serpentinite. Unpub. MSc. Thesis, Univ. of Manitoba.

MIDGLEY, R. G., (1951):
A serpentine from Kennock Cove, Lizard, Cornwall. Min. Mag. vol. 29, pp. 526-530.

MILLER, 111, R., (1953):
The Webster-Addie ultramafic ring, Jackson Co., North Carolina, and secondary alteration of its chromite. Amer. Min. v. 38, pp. 1134-1147.

NAGY, B. (1953):
The textural pattern of the serpentines. Econ. Geol. vol. 48, pp. 591-597.

NAGY, B. and FAUST, G. J., (1956):
Serpentines: natural mixtures of chrysotile and antigorite. Amer. Min., 41, pp. 817-838.

NALDRETT, A. J., (1964):
Ultrabasic rocks of the Porcupine and related nickel deposits. Unpub. PhD. Thesis. Queen's Univ. 1964.

NALDRETT, A. J. and KULLERUD, G., (1965):
Two examples of sulphurization in nature. Abstract. Econ. Geol. vol. 60, p. 1563.

NEALE, E. R. W., (1957):
Ambiguous intrusive relationship of Betts Cove-Tilt Cove serpentinite belt, Newfoundland. Proc. Geol. Assoc. Can. vol. 9, pp. 95-107.

NOBLE, J. A. and TAYLOR, H. P., (1960):
Correlation of the ultramafic complexes of SE. Alaska with those of other parts of N. America and the world. Inter. Geol. Cong. (1960) - Copenhagen, pp. 188-197.

NOCKOLDS, S. R., (1954):
Average chemical compositions of some igneous rocks. Geol. Soc. Amer. Bull. v. 65, pp. 1007-1032.

OLSEN, E., (1959):
Metamorphic differentiation during serpentinization. Unpub. PhD. thesis, Univ. of Chicago, 1959.

PABST, A., (1942):
The mineralogy of metamorphosed serpentine at Humphreys, Fresno County, California. Amer. Min. v. 27, pp. 570-585.

PARRISH, W., and MACK, M., (1963):
Charts for the Solution of Bragg's Equation. Data for X-Ray Analysis. 2nd Ed. vol. 1. Philips Technical Library.

PATTERSON, J. M., (1963):
Geology of the Thompson-Moak Lake area. Man. Mines Branch Pub. 60-4, 1963.

PHILLIPS, F. C., (1927):
The serpentines and associated rocks and minerals of the Shetland Islands. Geol. Soc. London, Quart. Jour. vol. 83, pp. 622-652.

PHILLIPS, A. H. and HESS, H. H., (1936):
Metamorphic differentiation of contacts between serpentinite and siliceous country rocks. Amer. Min. vol. 21, pp. 333-362.

POLDERVAART, A. E., (1950):
Correlation of physical properties and chemical composition in the plagioclase, olivine and orthopyroxene series. Amer. Min. v. 35, pp. 1067-1079.

QUINN, H. A., (1954):
Nelson House, Manitoba. Geol. Sur., Canada, Paper 54-13.

READ, H. H., (1934):
On the zoned associations of antigorite, talc, actinolite, chlorite and biotite in Unst, Shetland Islands. Min. Mag. vol. 33, pp. 519-540, 1934.

RIORDAN, P. H., (1955):
The genesis of asbestos in ultrabasic rocks. Econ. Geol. vol. 50, no. 1, pp. 67-81.

ROGERS, A. F., and KERR, P. F. (1942):
Optical Mineralogy, McGraw-Hill, Publ.

ROSS, C. S., FOSTER, M. D., and MYERS, A. T., (1954):
Origin of dunites and olivine-rich inclusions in basaltic rocks. Amer. Min. vol. 39, pp. 693-738.

SCHWARTZ, G. M., (1958):
Alteration of biotite under mesothermal conditions. Econ. Geol. vol. 53, pp. 164-177.

SELFRIDGE, G. C., (1936):
An X-ray and optical examination of the serpentine minerals. Amer. Min. v. 21, pp. 463-503.

SHAND, S. J., (1947):
The genesis of intrusive magnetite and related ores. Econ. Geol. vol. 42, no. 7, pp. 634-636.

SHAPIRO, L. and BRANNOCK, W. W., (1956):
Rapid analysis of silicate rocks. U. S. Geol. Sur. Bull. 1036-C.1956.

SHEPHERD, Norman, (1960):
The petrography and mineralogy of the Cross Lake area, Ungava, New Quebec. Unpub. PhD. Thesis, Univ. of Toronto, 1960.

SHTEINBERG, D. S., and MALAKHOV, I. A., (1963):
Distribution of nickel in ultramafic rocks of the Urals. Geochemistry, No. 11, pp. 1020-1033, 1963.

SMITH, C. H., (1958):
Bay of Islands Igneous Complex, Western Newfoundland. Geol. Sur. Can. Mem. 290. pp. 1-132.

SMITH, C. H. (1961):
Ultramafic intrusions in Canada and their significance to Upper mantle studies. Can. Geophys. Bull. v. 14 pp. 157-169.

SOSMAN, R. B., (1938):
Evidence on the intrusion temperature of peridotites. Amer. Jour. Sci., vol. 35A, pp. 353-359.

STOCKWELL, C. H. (1964):
Age determinations and geological studies. Part 11.- Geological studies. Geol. Sur. Can. Paper 64-17.

SULLIVAN, C. J. (1959):
The origin of massive sulphide ores. C.I.M.M. Bull. vol. 52, pp. 4-10.

THAYER, T. P., (1946):
Preliminary chemical correlation of chromite with the containing rocks. Econ. Geol. v. 41, pp. 202-217.

THAYER, T. P., (1960):
Some critical differences between Alpine-type and Stratiform peridotite-gabbro complexes. Inter. Geol. Cong. - Copenhagen. 1960. pp. 247-259.

THOMAS, R. G., (1951):
An example of re-intrusion of serpentine. Trans. Amer. Geophys. Union, vol. 32, pp. 462-465.

TURNER, F. J., (1942):
Preferred orientation of olivine crystals in peridotites with special reference to New Zealand examples. Trans. Roy. Soc. New Zealand, v. 72, pt. 3, pp. 280-300.

TURNER, F. J. and VERHOOGEN, J., (1960):
Igneous and Metamorphic Petrology. Ed. 2. McGraw-Hill, New York.

WAGER, L. R., VINCENT, E. A., and SMALES, A. A., (1957):
Sulphides in the Skaergaard Intrusion, East Greenland. Econ. Geol. vol. 52, pp. 855-903.

WATKINSON, D. H., and IRVINE, T. N., (1964):
Peridotite intrusions near Quetico and Shebandowan, Northwestern Ontario: A contribution to the petrology and geochemistry of ultramafic rocks. Can. Jour. of Earth Sciences, vol. 1, pp. 63-98, 1964.

WHITTAKER, E. J. W. and ZUSSMAN, J., (1956):
The characterization of serpentine minerals by X-ray diffraction. Min. Mag., vol. 31, pp. 107-126.

WILKINSON, J. F. G., (1953):
Some aspects of alpine-type serpentinites of Queensland. Geol. Mag. v. 90, pp. 305 321.

WILSON, H. D. B., and BRISBIN, W. C., (1961):
Regional structure of the Thompson-Moak Lake Nickel Belt. Can. Inst. Min. Met. Bull. Nov. 1961, pp. 470-477.

WILSON, H. D. B., and BRISBIN, W. C., (1962):
Tectonics of the Canadian Shield in Northern Manitoba. Royal Soc. of Canada. Spec. Pub. 4, pp. 60-75.

WINCHELL, A. N., (1951):
Elements of optical mineralogy, pt. 2, 4th ed: John Wiley and Sons, Inc., New York.

WYLLIE, P. J., (1960):
The system $CaO-MgO-FeO-SiO_2$ and its bearing on the origin of ultrabasic and basic rocks. Min. Mag. vol. 32, pp. 459-470.

VENING MEINESZ, F. A., (1954):
Indonesian Archipelago: A Geophysical Study: Bull. Geol. Soc. Amer. vol. 65, pp. 143-167.

ZURBRIGG, H. F., (1963):
Thompson Mine Geology. C.I.M.M. Bull. vol. LXV1, 1963. pp. 227-236.

ZUSSMAN, J., and BRINDLEY, G. W., (1957):
Serpentines with 6-layer ortho-hexagonal cells. Amer. Min. vol. 42, pp. 666-670.

ZUSSMAN, J., BRINDLEY, G. W., and COMER, J. J., (1957):
Electron diffraction studies of serpentine minerals. Amer. Min. v. 42, pp. 133-153.

APPENDIX 1

X-RAY FLUORESCENT ANALYSIS

The following oxides were determined with the X-ray fluorescence spectrometer; SiO_2, Al_2O_3, total Fe (calibrated as Fe_2O_3 and recalculated to FeO), MgO, CaO, K_2O, MnO, TiO_2, NiO, Cr_2O_3 and CoO. The analyses were made in the Department of Geology, University of Manitoba, by Mr. C. Coats, under the direction of Mr. K. Ramal.

Equipment

Applied Research Laboratories multi-channel Vacuum X-Ray Quantometer with two Scanners and fitted with a tungsten target X-ray tube.

Sample Preparation

A mixture of 500 mg. sample, 500 mg. of La_2O_3 and 1000 mg. of $Li_2B_4O_7$ were fused in a graphite crucible at 1000°C. for 20 minutes. To compensate for loss on ignition, granular boric acid was added to the resultant bead to bring the weight up to 2100 mg. The bead and boric acid were reground in a Bleuler automatic mixer-grinder for 30 seconds and then compressed into a pellet with a boric acid backing for strength, at a pressure of 50,000 psi.

Operating conditions

Table A-1 below, lists the operating conditions and range for each of the oxides determined.

TABLE A-1

X-RAY FLUORESCENCE SPECTROMETER OPERATING DATA

OXIDE	WAVELENGTH Å	SCANNER TIME SETTINGS		POWER		ZERO DEPRESS	RANGE
		CHANNEL SETTING	STD.	MA	KV		
SiO_2	7.126	25	11	30	40	62.0	30-80%
Al_2O_3	8.339	29	11	30	40	9.0	0-20%
Fe_2O_3	1.937	8	11	30	40	13.0	0.20%
MgO	9.889	10	11	30	40	42.7	0-40%
CaO	3.360	19	11	30	40	1.0	0-20%
K_2O	3.744	13	11	30	40	3.0	0-10%
TiO_2	5.5065	24	11	30	40	76.1	0-2%
MnO	2.1085	20	11	30	40	23.1	0-1%
NiO	1.6692	14	18	30	40	7.0	0-2%
NiO	1.6692	18	18	30	40	87.0	0-0.2%
Cr_2O_3	4.5828	14	18	30	40	132.0	0-4%
Cr_2O_3	2.2909	24	13	30	40	180	0-2000 ppm.
CoO	1.7960	27	18	30	40	140	0-1000 ppm.
Cu	1.5529	20	18	30	40	180	0-1000 ppm.

Standards

Working curves were prepared from the following primary standards; G1, W1, NBS. 88, NBS. 97, NBS. 99, CAAS. sulphide ore and CAAS. syenite rock. In addition, two sets of standards, the PO. and PM. series, approximating the composition of peridotites and containing varying quantities of Cr, Ni, Co and Cu were prepared in the Dept. of Geology, and used in the analytical

work on the Manitoba serpentinites.

Precision

As a general rule all samples were run three times and the results averaged. To illustrate machine reproducibility and precision, a single sample preparation of serpentinite (#167) was run six times at different periods during the analytical work. Listed below in Table A-2 are the results, the means and standard deviations. It can be seen that the reproducibility is good with the greatest standard deviation being .41, obtained for magnesia at the concentration listed.

TABLE A-2

	SiO_2	Al_2O_3	FeO	MgO	CaO	K_2O	MnO	TiO_2
Run 1	38.6	4.72	10.58	34.00	2.26	.17	.075	.276
Run 2	39.0	4.86	10.58	33.76	2.22	.16	.076	.266
Run 3	38.8	4.86	10.55	34.40	2.20	.17	.072	.300
Run 4	38.7	4.80	10.69	33.60	2.30	.18	.068	.296
Run 5	38.6	4.78	10.64	34.64	2.24	.18	.072	.240
Run 6	38.7	4.86	10.69	33.76	2.36	.17	.074	.300
Mean	38.7	4.81	10.62	34.03	2.26	.17	.073	.280
Std. Dev.	.15	.058	.06	.41	.059	.008	.003	.081

Accuracy

To determine the accuracy of X-ray fluorescent analysis of ultrabasic rocks, six separate sample preparations of serpentine #167 were analysed consecutively. By this means a test of the accuracy of sample mixing, weighing and pellet prep-

aration is made. The test results from the six samples are listed in Table A-3. As in previous cases each analysis represents the average of three separate runs.

TABLE A-3

	SiO_2	Al_2O_3	FeO	MgO	CaO	K_2O	MnO	TiO_2
167-A	39.0	5.04	10.54	34.36	2.66	.21	.080	.342
167-B	38.8	4.98	10.42	34.32	2.62	.20	.084	.338
167-C	39.25	5.28	10.42	33.96	2.56	.20	.080	.324
167-D	38.65	5.04	10.47	34.04	2.32	.19	.080	.312
167-E	38.8	5.10	10.56	33.60	2.36	.18	.081	.306
167-F	38.2	4.92	10.43	33.72	2.26	.17	.074	.258
Mean	38.95	5.06	10.47	34.00	2.46	.19	.079	.313
Std. Dev.	.398	.124	.063	.308	.171	.015	.003	.018

The accuracy is reasonably good. The greatest standard deviations are obtained for silica (.398) and magnesia (.308).

Determination of Iron (FeO)

The quantometer determines iron as total Fe, but is calibrated to give the percentage as Fe_2O_3. This is converted entirely to FeO in all the analyses made of the nickel belt ultramafic rocks. The error involved in converting some iron present in the ferric state to the ferrous state is considered to be small.

Determination of Nickel (NiO)

The standard curve for nickel determinations was prepared from the PO. (peridotite ore) artificial standard series containing 14.8% Fe_2O_3 and nickel content varying between 0-2% NiO. For reference the curve is reproduced in Fig. A-1.

The observed intensity of the nickel analytical line is effected by the amount of iron present in the sample. This effect is due to the excitation of the Fek_α line (1.937Å) by NiK_α (1.659Å) resulting in an absorption effect on the nickel. The enhancement effect of iron by nickel was small, due to the minor quantity of nickel present in most samples. The effect on the observed intensity of the nickel line was determined by varying the iron content of standards containing known amounts of nickel. Table A-4 lists the standards used in deriving the nickel correction curve as a function of iron content (2-33.5% Fe_2O_3), which is reproduced in Fig. A-2.

TABLE A-4

DERIVATION OF X-FACTOR FOR Ni CORRECTION CURVE

Std.	%Fe_2O_3	%NiO (True)	%NiO (observed)	X-Factor T/O
1	2.0	.127	.162	.784
2	10.75	.192	.206	.932
3	13.3	.384	.392	.980
4	14.8	2.00	2.00	1.00
5	15.7	.576	.564	1.022
6	18.3	.768	.724	1.060
7	23.4	1.152	1.020	1.109
8	28.5	1.536	1.292	1.188
9	33.5	1.92	1.56	1.231

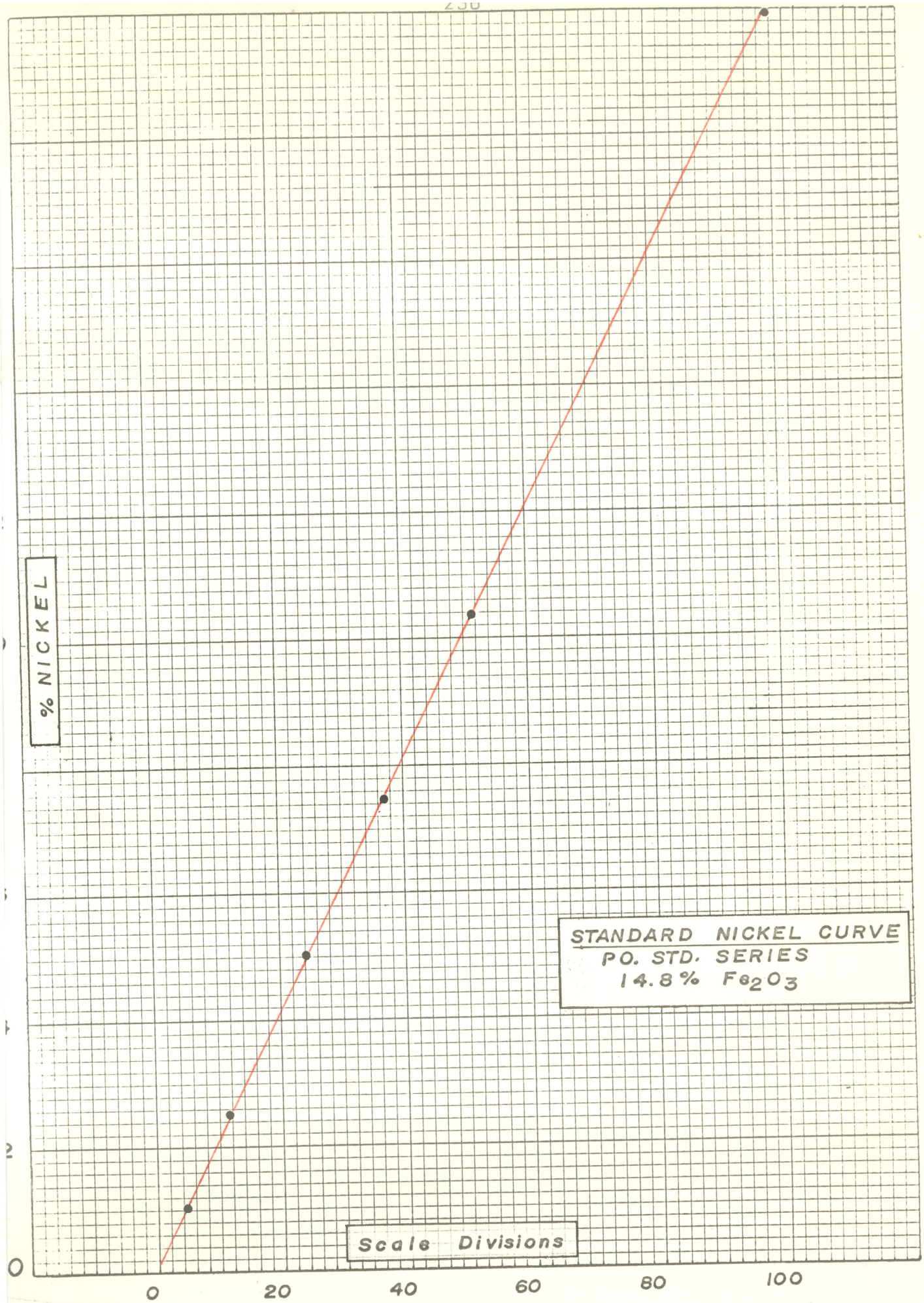
% NICKEL
STANDARD NICKEL CURVE
P.O. STD. SERIES
14.8% Fe_2O_3
Scale Divisions
0
20
40
60
80
100

Fig. A-1

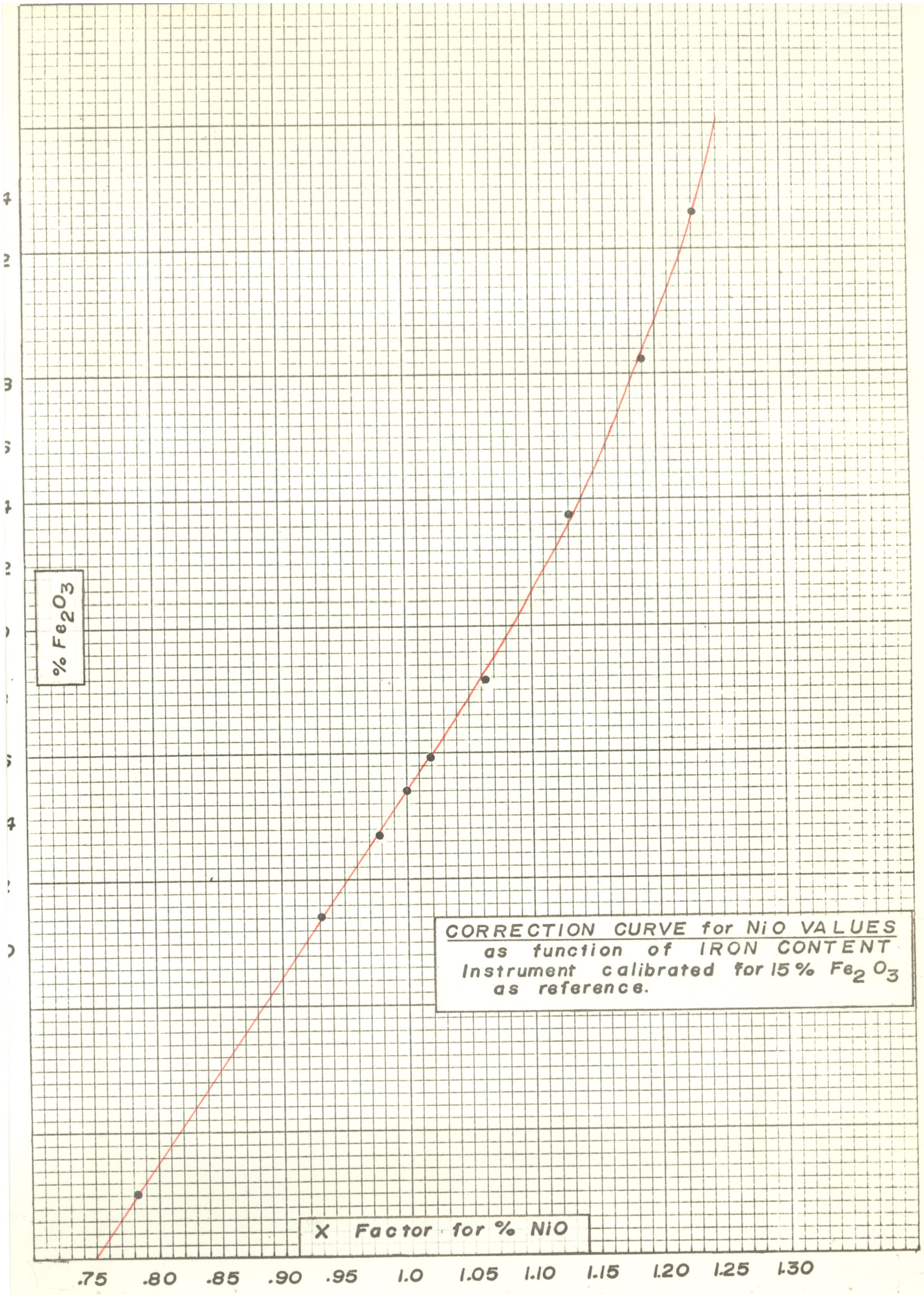
% Fe_2O_3
CORRECTION CURVE for NiO VALUES
as function of IRON CONTENT
Instrument calibrated for 15% Fe_2O_3
as reference.
X Factor for % NiO
.75
.80
.85
.90
.95
1.0
1.05
1.10
1.15
1.20
1.25
1.30

Fig. A–2

Determination of Cobalt (CoO)

The low content of cobalt compared to iron in all samples, made necessary the derivation of a cobalt correction curve. The effect of iron on cobalt is an additive one due to the proximity of FeK_β (1.757Å) to CoK_α (1.791Å).

The change in the observed values for cobalt were plotted against iron content and gave as expected, a straight line. Corrections were applied to CoO determinations by subtracting the scale divisions as determined by the iron content of the sample, to the observed reading. Table A-5 lists the relevant data of the standards used and the curve is reproduced in Fig. A-3 for reference.

TABLE A-5

DATA FOR DERIVATION OF CoO CORRECTION CURVE

Std.	%Fe_2O_3	Reading (Scale Div.)		Correction
		True	Observed	
GM-500	2.0	47.0	46.8	0
DM-500	10.0	50.0	61.0	+11.0
S3.6	15.8	19.0	36.8	+17.8
S4.8	18.35	23.4	45.3	+21.9
S7.3	23.4	32.6	62.0	+29.4
S9.6	28.5	41.9	78.0	+36.1
Sul. Ore	33.5	51.0	92.4	+41.4

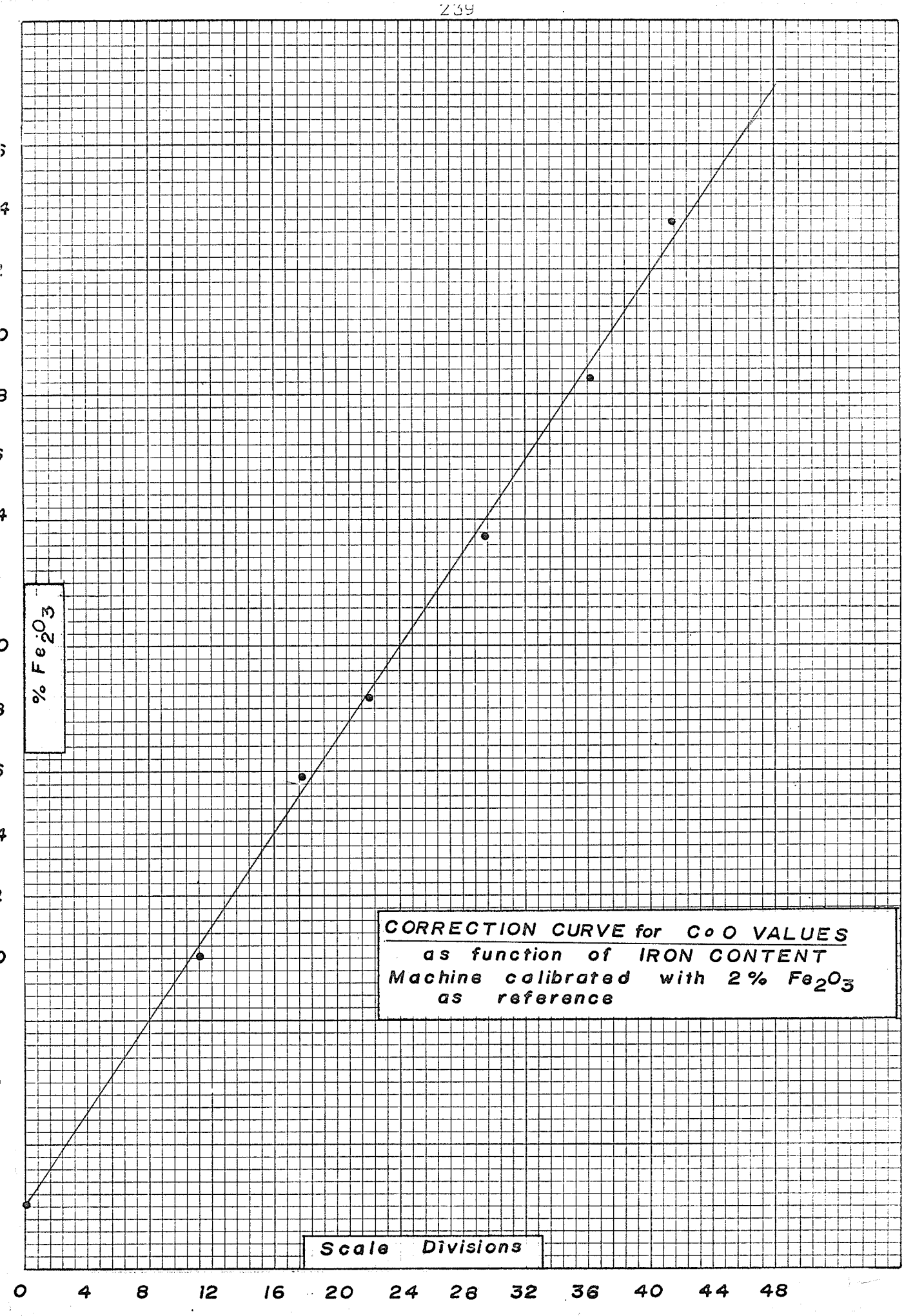
% Fe_2O_3
CORRECTION CURVE for CoO VALUES
as function of IRON CONTENT
Machine calibrated with 2% Fe_2O_3
as reference
Scale Divisions
0 4 8 12 16 20 24 28 32 36 40 44 48

Fig. A-3

Determination of Soda (Na_2O)

Sodium values were determined in the chemical laboratory of the Department of Geology by Mr. K. Ramlal using a Coleman Flame Photometer. Samples were brought to solution in the manner described by Shapiro and Brannock (1956). Standard solutions used contained 0-50 ppm. Na_2O.

Determination of Water (H_2O)

Water was determined by a modification of the Penfield method as outlined by Shapiro and Brannock (1956). All samples were oven-dried at 105°C. for 2 days prior to determining water content.

Determination of Carbon Dioxide (CO_2)

Carbon dioxide content of samples was determined by treatment with 1:1 HCl and absorbion of CO_2 on Caroxite. Samples were periodically duplicated to ensure the attainment of reproducible results.

Determination of Sulphur (S)

Sulphur determinations were made by Mr. John Campbell in the Metallurgical Laboratories of Falconbridge Nickel Mines using a modified Leco Combustion Method with acid-base titration. For the latter step, the Fisher automatic potentiometric titrimeter was employed.

APPENDIX 11

SULPHIDE SOLUTION PROCESS

Samples containing disseminated sulphides were finely pulverized in a Bleuler grinder for three minutes. Depending on the original concentration of sulphide material, anywhere from 1-3 gm. samples were weighed and placed in a 250 ml. tall form beaker to which was added approximately 200 ml. absolute methyl alcohol. A teflon-coated stirring magnet was put in the beaker, which was then placed on a magnetic stirrer. Chlorine gas from a portable cylinder was bubbled through the slurry at a steady rate for 25-30 minutes and a slow current of air allowed to pass over the beaker to prevent auto-ignition. In general, it was found the reaction was speeded up by placing the 250 ml. beaker in a 400 ml. beaker containing warm water.

Once the reaction was complete, the suspension was filtered in a Buchner vacuum funnel, washed repeatedly with alcohol, then with distilled water to remove all cations in solution, dried and retained for analysis.

The chemical reaction involved in the process was the attack of chlorine on the sulphide phase to form sulphuryl chloride ($SOCl_2$), which liberated the cations in the sulphides (Ni, Fe, Co, etc.) and caused them to remain in solution.

The above process is essentially that described by Anderson (1963).

APPENDIX 111

CELL EDGE DETERMINATIONS OF SPINEL GROUP MINERALS

Concentration

Selected serpentinites containing >1% spinel group minerals were crushed and two fractions, -150 + 200 mesh and -200 + 270 mesh, collected separately. Each fraction was placed on a Haultain Superpanner until a heavy mineral concentrate had been obtained. Separation of magnetite by hand magnet and additional concentration using a Franz Isodynamic Separator enabled final hand picking to give a clean concentrate of spinels.

Cell Edge Determinations

X-ray diffraction powder photographs were made of spinel concentrates, using fine collimators in cameras of diameter 114.592 mm., iron radiation and manganese filters. Each sample was prepared as a fine collodion rolling. Exposure times varied between 23 and 38 hours. Cell edge calculations represent an average value from three careful measurements of back reflections indexed as 642, 731 and 800. For each film a correction factor was applied, calculated from the ideal diameter of the camera divided by a calculated "effective diameter" for the particular film. The correction values multiplied to 28 varied between 1.00437 and 1.00047. An estimation of the accuracy of each cell edge determination was calculated and found to be generally in the order of .002Å.

APPENDIX 1V

X-RAY DIFFRACTION OF THE SERPENTINE MINERALS

X-ray diffraction data was obtained on powdered serpentine material using a Phillips X-ray diffractometer equipped with a pulse height analyser. Samples were X-rayed in spinning shallow cell sample holders. Radiation was from a copper tube operating at 50Kv and 20Ma., with a nickel filter. Scan speed was 1° of 2θ per minute and a time constant of 2 seconds. Scale setting for most runs was 4×10^2, a full chart width thus corresponding to 400 counts/second. A scale setting of 1×10^3 was occasionally found useful.

In the conversion of 2θ to d spacings the Charts for solution of Bragg's Equation by Parrish and Mack (1963), were used. In these Cuk$_\alpha$ is 1.5418Å.

Diffraction patterns for all samples were made in the range 10°-75° 2θ. Diffractograms reproduced in the body of this report have been reduced from their original size by approximately one-half.

APPENDIX V

FORTRAN PROGRAM FOR INDEXING REFLECTIONS IN ORTHORHOMBIC SYSTEM

```
C       R IS D(OBSERVED)
C       N IS NUMBER OF D(OBS),LIMITED TO 100
C       M,K,L ARE MAX.VALUES OF H,K,L TO BE COMPUTED
C       A,B,C ARE CELL DIMENSIONS
        DIMENSION R(100)
  202 FORMAT(4I2)
  200 FORMAT (3F8.3)
  201 FORMAT (F8.3)
  203 FORMAT (2F8.3,3F6.0)
   51 READ 200,A,B,C
      READ 202,N,M,K,L
      READ 201,(R(I),I=1,N)
      HH=0.
      XKK=0.
      XLL=0.
      H=HH
      DO 9 IH=1,M
      XK=XKK
      DO 8 IXK=1,K
      XL=XLL
      DO 5 IXL=1,L
    7 D=A*B*C/SQRTF(H*H*B*B*C*C+XK*XK*A*A*C*C+XL*XL*A*A*B*B)
      IF(D-2.0) 16,16,60
   60 IF(D-3.0) 61,61,70
   16 DO 11 I=1,N
      T=R(I)-D
      IF(T-.02)13,15,12
   12 IF(.02-T)11,15,15
   13 IF(-.02-T)15,15,11
   15 PUNCH 203,D,R(I),H,XK,XL
   11 CONTINUE
      GO TO 5
   61 DO 69 I=1,N
      T=R(I)-D
      IF(T-.05) 62,63,64
   64 IF(.05-T) 69,63,63
   62 IF(-.05-T) 63,63,69
   63 PUNCH 203,D,R(I),H,XK,XL
   69 CONTINUE
      GO TO 5
   70 DO 79 I=1,N
      T=R(I)-D
      IF(T-.15) 72,73,74
   74 IF(.15-T) 79,73,73
   72 IF(-.15-T) 73,73,79
   73 PUNCH 203,D,R(I),H,XK,XL
   79 CONTINUE
    5 XL=XL+1.
    8 XK=XK+1.
    9 H=H+1.
      GO TO 51
      END
```

APPENDIX V1

X-RAY DIFFRACTION DATA FOR 6-LAYER AND 3-LAYER ORTHOCHRYSOTILES

6-LAYER ORTHO-TYPE (Zussman, Brindley, 1957).			3-LAYER ORTHO-TYPE (Manitoba serpentinites)**				
dÅ	I	hkl	dÅ(obs)	No*	Ic/s+	dÅ(calc)	hkl
			7.44	1	400		
			7.43	1	400		
7.33	100	006	7.40	6	400	7.310	003
			7.37	5	346		
			7.36	2	340		
			4.62	2	82		
			4.61	2	62		
4.60	60	020	4.60	9	76	4.602	020
			4.59	1	80		
			4.57	1	40		
4.40	10	023					
4.25	10	024	4.28	1	20	4.243	022
			4.23	1	20	4.259	112
4.09	10	025					
			3.93	1	28		
3.90	5	026	3.91	1	30	3.907	113
			3.90	2	36	3.894	023
			3.68	4	275		
3.66	100	0.0.12	3.67	4	319	3.655	006
			3.66	7	225		
			3.56	1	28	3.543	114
3.53	5	028	3.52	1	16	3.525	024
3.35	5	029					
3.17	5	0.2.10					
3.02	5	0.2.11					
2.865	5	0.2.12	2.894	1	5	2.862	026
			2.867	2	9	2.867	116
2.720	5	0.2.13					
			2.663	2	25	2.641	131

Appendix V1 continued.

APPENDIX V1 (cont'd)

dÅ	I	hkl	dÅ(obs)	No*	Ic/s*	dÅ(calc)	hkl
2.623	30	203	2.652	9	20	2.653	201
			2.622	4	19	2.627	018
			2.508	2	172	2.510	203
2.502	100	206	2.502	9	141	2.500	133
			2.495	4	131	2.499	212
			2.455	4	56		
			2.449	2	48		
2.450	10	0.2.15	2.442	4	47	2.439	108
			2.440	3	44	2.436	009
			2.436	1	48		
			2.433	1	36		
2.335	70	209	2.334?	2	18		
2.149	60	2.0.12	2.151	12	45	2.151	136
			2.146	3	49	2.153	029
1.963	70	2.015				1.831	235
			1.831	4	14	1.830	1.1.11
1.815	5	0.0.24	1.824	5	12	1.829	146, 0.2.11
			1.817	1	12	1.827	0.0.12
						1.815	052
1.791	10	2.0.18	1.797	8	29	1.797	139
			1.791	7	22	1.792	0.1.12
			1.749	2	11	1.749	310
			1.742	1	12	1.743	240, 311
1.739	108	310	1.740	4	16	1.740	150
			1.737	3	15	1.738	241
			1.717	1	8	1.735	151
						1.719	152
1.636	40	2.0.21	1.636?	2	12	1.643	322
			1.542	1	44		
			1.539	1	56	1.544	0.1.14
1.535	80	060	1.538	3	61	1.540	330
			1.537	7	73	1.537	331
			1.535	3	82	1.534	060
			1.509	1	28	1.509	2.2.11
			1.508	2	38	1.508	2.0.12
			1.507	1	32	1.507	333
1.501	70	2.0.24	1.505	8	46	1.506	1.3.12, 0.4.11
			1.504	1	32	1.503	1.0.14
			1.503	2	38	1.501	252, 063
			1.467	2	8	1.468	059, 327
			1.465	1	16	1.461	0.0.15
1.452	2	0.0.30	1.463	7	10	1.461	254
			1.459	1	12	1.461	162
			1.457	1	6	1.453	335
			1.421	1	8		
			1.419	2	8	1.418	249
			1.416	1	6	1.417	2.3.11

Appendix V1 continued.

APPENDIX V1 (cont'd)

dÅ	I	hkl	dÅ(obs)	No*	Ic/s+	dÅ(calc)	hkl
1.415	20	0.6.12	1.415	6	9	1.416	159
			1.414	1	6	1.414	066
			1.411	3	10	1.410	0.5.10,1.0.15
			1.398	1	12		
1.379	20	2.0.27					
1.329	10	403	1.327	2	10	1.327	1.0.16
			1.325	1	16	1.326	258, 402
			1.311	3	17	1.312	2.4.11
			1.310	4	24	1.311	1.5.11
1.309	50	406	1.309	3	28	1.309	263
			1.308	4	28		
			1.307	1	24		
1.296	2	0.6.18					
1.283	5	409	1.283	1	20	1.283	420
			1.281	6	12	1.282	2.0.15
						1.281	421, 1.3.15
1.276	5	2.0.30	1.278	1	12	1.278	351, 405
						1.277	0.1.17
						1.276	3.2.11
1.210	10	0.0.36					
1.182	2	2.0.33					
1.168	5	4.0.18					
1.121	5	4.0.21					

**Combined reflections from the following 15 samples: (5, 39, 88, 91, 96, 107, 110, 128, 140, 155, 157, 160, 189, 190, 206)

*Represents number of reflections recorded from 15 samples.

+Intensities relative, measured as peak height/background in counts/seconds (c/s).

APPENDIX V11

DIFFERENTIAL THERMAL ANALYSIS OF THE SERPENTINE MINERALS

The apparatus for differential thermal analysis (DTA) as used in this study is a R. L. Stone Co. model DTA-13M with controlled atmosphere equipment. Curves for the serpentine minerals were all made over the temperature range 25° C to 1000° C. at a heating rate of 10° C. per minute. Thermograms were recorded on Leeds and Northrup Speedomax H strip charts with a width of 7 inches. Sensitivity of the thermogram recorder was 150 microvolts for the full chart width. All samples were heated in air with a furnace starting voltage of 44 volts using powdered alumina (-150+200 mesh) in the standard cell.

The curves were calibrated using quartz as a standard and recorded temperature measurements are estimated to be within ±5° C. of their true values.

The thermograms reproduced in the text have been reduced from their original size by approximately one third. For easy comparison of the various thermograms, the temperature points of 600°, 700° and 800° C. are shown. All curves have been adjusted laterally so that the 700° C. marks lie on a straight line. In conformity with international custom, the curves are shown with endothermic peaks pointing downward and exothermic peaks pointing upward, towards the top of the page.

APPENDIX V111

ESTIMATED MODAL COMPOSITIONS OF THE ULTRAMAFIC ROCKS OF THE MANITOBA NICKEL BELT

A. SERPENTINITES

Sample	Field No.	SERPENTINE	TREMOLITE	BRUCITE	PHLOGOPITE	MAGNETITE	SPINEL	CARBONATE	CHLORITE	SULPHIDE	TALC
76	Mys.-1	73				5	2	Tr		20*	
82	Osp.5-5	85				5	5	4		1	
88	Pip 8-2	89				10	1				
90	Pip 8-6	90				10	<1				
91	Pip 8-8	84				15	1				
92	Pip 8-9	92				8		Tr			
94	Moak-1	64		Tr		10		1		25	
96	Moak-58	92				8		Tr			
98	Pip.8-15	90				5				5	
101	M14R-673	90		1		7				2	
102	M14R-975	90		Tr		8				2	
107	M76B-544	85				8		Tr	<1	5	2
108	M76B-752	85			Tr	4		5		6	
110	W19G-839	95		1		4					
122	Pip 8-5	96				1				3	
126	4-445	63			3	19	1	7			7
128	W62A-389	90				5	1	4			
139	M12N-455	83		1		5				1	10
140	M12N-484	95				1	Tr		2	1	<1
142	M70A-128	90	<1		1		<1	1	1	3	4
149	W19C-290	89				9*	<1		1		
150A	W19C-419	97			Tr	1	1		<1		
155	Hambone-1	96			<1	1	1			<1	
157	S.Marshall	90			<1	5	<1	3			Tr
160	Muskeg C.	93				5	Tr			2	
163	Manason N.	85				5	5		5		
189	M14W-772	95				3	1		1		
190	M14W-820	97				3					
201	M14V-860	98						1	1		
205	W93A-287	75				25					
206	M76B-650	90				8	Tr			2	
207	M76B-663	85				5				10	

*Mainly hematite.

B. TREMOLITE SERPENTINITES

Sample	Field No	SERPENTINE	OLIVINE	TREMOLITE	ORTHO-PYROXENE	BRUCITE	PHLOGOPITE	MAGNETITE SPINEL	CARBONATE	TALC	SULPHIDE	CHLORITE
74	NS-5	10		85				1	2	2		
77	Mys. 2	59	Tr	20				5 1			15	
78	Mys.3	50	10	30				6			2	2
79	Th.-1	70		19				2 Tr	1		3	5
83	Osp.7-1	10		89		Tr		1				
86	Jo-5	60		30			1	5 1	3			
119	W62J-480	70		10		<1	<1	5 <1	3		9	
124	M11A7-422	53	1	25	2			5 1			8	5
131	W62D-379	50		18	2			1 3	5	15	3	3
138	M12A-420	30	10	36				9	2		1	12
146	W21K-593	20	Tr	60				9 <1	<1		1	10
154	Top-15	85		6			<1	5 <1	1			<1

C. TREMOLITE-PHLOGOPITE SERPENTINITES

80	Th-2	25	1	50			9	2		2	1	10
114	W62K-540	40	5	33	2		5	5	2			8
116	W62N-526	30	10	10	15		15	5	5	10		
133	W5A-400	16	66				6*	1	8	3		
136	W5B-296	20	70				4*	3				3
137	W5B-353	20	55				5	1	<1	8		10
141	W54A-622	54	5	32		Tr	5	3	1		Tr	
144	W38C-158	50		10			30	4	2			4
145	W21K-279	20	1	45	2		25	3			3	1
169	M19D-314	35		25	3		35	<1	Tr Tr		1	1

*Vermiculite.

D. PHLOGOPITE SERPENTINITES

Sample	Field No.	SERPENTINE	PHLOGOPITE	MAGNETITE	SPINEL	CARBONATE	HEMATITE	TALC	CHLORITE
111	W19G-1456	88	10		1			<1	
132	W54B-615	65	15	15		1	4		
188	M14W-731	80	16	2	1				<1
192	M14W-888	80	10	5					5

E. SERPENTINIZED PERIDOTITES

Sample	Field No.	SERPENTINE	OLIVINE	ORTHO-PYROXENE	TREMOLITE	BRUCITE	PHLOGOPITE	MAGNETITE	SPINEL	CARBONATE	CHLORITE	SULPHIDE
109	A-453	35	22	Tr	18			10			15	
117	W62L-734	28	40	25			1	3	1	2		
118	W62L-885	30	20	25		1		4	2	3		15
125	Mys.-Isl	35	10	10	25			10	5			5
153	Tr-1	40	10	35	5		1	5	Tr	<1	3	
158	Paint-S	47	5	10	36			1		1		
164	M11A7-377	50		10	36		Tr	3	1			
185	W62D-475	45	20	5	20			1	4	Tr	5	

F. TREMOLITE-OLIVINE ORTHOPYROXENITES

Sample	Field No.	SERPENTINE	OLIVINE	ORTHO-PYROXENE	TREMOLITE	PHLOGOPITE	MAGNETITE	SPINEL	CARBONATE	TALC	CHLORITE	SULPHIDE
104	M12T-251	35	5	40	5		2			<1	4	8
112	M20A-463	25	15	20	35		4	1				
127	21B-550	25	5	20*	39		5	1	3		2	Tr
130	W62B-595	5	10	45	37		1	<1				1
147A	M15B-208		17	60		20	Tr	<1				2
148	M17A-426		15	35	44		1	Tr	3	2		
151	H140B-390		10	40	45	<1	3	1				
159	Walters L.	45		40	14		<1					<1
165	Jo-3	43	1	20	20	10	5	1	<1			
166	W62xB-62	5	20	58		15			1	1		
168	M19D-208	18	10	38	16	1	5	<1	9		2	1
186	M11A39-252	25	15	50	5		5	Tr				

*Clinopyroxene

G. AMPHIBOLE ORTHOPYROXENITES

Sample	Field No	SERPENTINE	OLIVINE	ORTHO-PYROXENE	TREMOLITE	ANTHO-PHYLLITE	PHLOGOPITE	MAGNETITE	SPINEL	CARBONATE	TALC	SULPHIDE
105	M8AE-253	5	2	60		20	5	3	Tr		2	3
120	W62J-618			22	70		3*		<1	<1	2	1
152	H140B-430			40	50		9	1			Tr	Tr
172	M17F-215			45	20		35*	Tr		Tr	Tr	

*Biotite

H. MISCELLANEOUS ULTRAMAFIC ROCK TYPES

Sample	Field No.	SERPENTINE	TREMOLITE	ANTHO-PHYLLITE	BRUCITE	PHLOGOPITE	VERMICULITE	MAGNETITE	TALC	CARBONATE	CHLORITE	SULPHIDE	SPINEL
75	Ass. 1-4	45*		30	1			3	1	20			5
84	Osp.6-1	60						10			25		5
99	Pip 6	53						2			35	10	
100	Moak-DH	75						2			23		
101-1	M14R-746	55		25		Tr		10				10	
128A	W62A-342		30	30+		20		4				1	15
128B	W62A-378			10		25	3		48		8	1	5
129	W62A-456	20			Tr		40	4		35		1	
134	W5A-447	8	48			1	40	2		<1			
161	Manasan 7a	8		20				2	40	30	Tr		
162	Manasan 7b			25				2	35	10	25	3	
170	M8AA-244	68						5		15	2	10	

*20% Olivine

+ brown opaque alteration, probably after orthopyroxene.

ESTIMATED MODAL COMPOSITIONS

SECTION M14Q-SETTING LAKE

No.	Field No.	SERPENTINE	ORTHO-PYROXENE	TREMOLITE	ANTHOPHYLLITE	BRUCITE	PHLOGOPITE	MAGNETITE	SPINEL	CARBONATE	CHLORITE	SULPHIDE
0	370	85				Tr			<1		4	10
1	384	94				Tr		4	1			
2	405	93				<1	Tr	5				1
3	435	90				Tr	Tr	10	Tr			
4	487	92					Tr	8				
5	508	80						20				
6	521			35			55			10		
8	600	97						3				
9	654	90						10				
10	691	94						4	1	1		
11	739	80						18	1	1		Tr
12	798	93						3	1		3	
13	818	91				1		5	1	2		Tr
14	830	87						5	1	2	5	
15	853				95			5				
16	858	94				<1		5				Tr
17	869	45	4*	35				5		10	1	Tr
18	879	50	10*		30			10				
19	883	3		35	60			1			1	
20	887			91	5			1			3	
21	889			79							20	1
	889.5										100	

* Brown opaque alteration after pyroxene.

SECTION M11A-22, WABOWDEN

No	Field No	SERPENTINE	OLIVINE	ORTHO-PYROXENE	TREMOLITE	PHLOGOPITE	MAGNETITE	SPINEL	CARBONATE	TALC	SULPHIDE	CHLORITE
48	377.5	43			15	40	1		<1			
49	379	50			25	20	5					
50	382	32	8	5	30	20	5					
51	386	40	10	5	35	1	5				4	
52	391	39	16	10	30	<1	2	<1				1
53	394	30	20	15	30	Tr	5					Tr
54	396	42	3	10	35	3	5					2
55	397.5	48	2	2*	26		5		1			16
56	399	45	5	5*	35	1	4					5
57	400	50			20	25	3		1		2	
58	401	40			28	30	2					
59	402	25			15	55	<1		5			
60	403				65	35	<1					
61	404					100						

SECTION M11A-8, WABOWDEN

63	868					10						90+
64	866	10		43*		40	1			5		
65	863	80			5	10	5					
66	861	75			Tr	20	3		<1		2	
67	853	75			1	19	1		<1		4	
68	847	65				<1	5		15	13	2	

SECTION M11A-8, WABOWDEN cont'd

No	Field No	SERPENTINE	OLIVINE	ORTHO-PYROXENE	TREMOLITE	PHLOGOPITE	MAGNETITE	SPINEL	CARBONATE	TALC	SULPHIDE	CHLORITE
69	840	85					4		1	5	5	
70	833	65	2	5	20	2	4	1	1			
71	826	70		10	12	2	3	1		1		1
72	817	60	<1	20	10	<1	5	1	<1	1		

*Brown opaque alteration of pyroxene

+Anthophyllite.

APPENDIX 1X

COMPOSITION OF THE ULTRAMAFIC ROCKS

Oxide	0 M14Q-371	1 M14Q-384	2 M14Q-405	3 M14Q-435	4 M14Q-487	5 M14Q-508	6 M14Q-521	7 M14Q-554	8 M14Q-600
SiO_2	32.25	39.30	37.80	35.85	34.90	36.30	34.05	33.35	35.65
Al_2O_3	1.84	1.78	1.88	1.82	2.22	2.00	15.72	2.40	2.12
FeO	15.32	8.13	8.42	13.30	11.80	8.47	9.29	12.38	6.71
MgO	35.64	38.48	40.06	35.40	39.68	41.08	21.28	38.96	41.36
CaO	0.00	0.42	0.50	0.06	0.00	0.00	5.72	0.48	0.32
Na_2O	-	-	-	-	-	-	0.67	-	-
K_2O	0.00	0.00	0.00	0.00	0.00	0.00	7.00	0.00	0.00
H_2O^+	9.00	10.69	10.22	11.56	10.52	11.28	1.49	10.30	12.08
CO_2	-	-	-	-	-	-	3.73	-	-
TiO_2	0.148	0.104	0.140	0.114	0.09	0.076	0.748	0.078	0.080
S	10.00	-	0.74	-	0.67	-	-	-	-
Cr_2O_3	0.49	0.53	0.49	1.02	0.86	0.25	0.00	0.91	.90
MnO	0.00	0.032	0.011	0.102	0.100	0.060	0.170	0.142	0.075
NiO	0.16	0.31	0.26	0.35	0.30	0.38	0.05	0.25	0.28
CoO	0.005	0.015	0.011	0.015	0.018	0.022	0.013	0.019	0.015
Less O≡S	5.00	-	0.37	-	0.34	-	-	-	-
Total	99.85	99.79	100.16	99.59	100.82	99.91	100.93	99.27	99.60

Dash indicates not determined.

COMPOSITION OF THE ULTRAMAFIC ROCKS-cont'd.

Oxide	9 M14Q-654	10 M14Q-691	11 M14Q-739	12 M14Q-798	13 M14Q-818	14 M14Q-830	15 M14Q-853	16 M14Q-858	17 M14Q-869
SiO_2	32.73	35.55	33.80	36.08	35.60	35.45	52.80	37.80	41.40
Al_2O_3	2.12	2.16	2.20	2.18	2.26	2.12	2.42	2.58	3.54
FeO	12.40	7.11	12.02	7.12	8.65	10.81	6.88	6.73	7.28
MgO	38.16	41.20	38.68	41.00	38.30	39.84	32.78	40.92	32.00
CaO	0.50	0.04	0.40	0.00	0.62	0.26	2.24	0.00	5.80
Na_2O	-	-	-	-	-	-	-	-	-
K_2O	0.00	0.00	0.00	0.00	0.00	0.00	0.00	0.00	0.00
H_2O^+	11.84	12.90	10.94	11.82	12.52	9.60	1.41	11.84	6.72
CO_2	-	-	-	-	0.96	-	-	-	1.95
TiO_2	0.112	0.144	0.136	0.104	0.00	0.142	0.066	0.124	0.060
S	-	-	0.95	-	-	-	-	-	0.75
Cr_2O_3	0.91	0.97	0.89	0.63	0.61	0.61	0.37	0.52	0.05
MnO	0.140	0.072	0.136	0.072	0.154	0.054	0.060	0.044	0.069
NiO	0.40	0.29	0.31	0.29	0.32	0.34	0.24	0.27	0.27
CoO	0.021	0.015	0.018	0.013	0.013	0.019	0.015	0.012	0.012
Less O≡S	-	-	0.47	-	-	-	-	-	0.37
Total	99.33	100.45	100.02	99.30	100.00	99.24	99.29	100.83	99.53

COMPOSITION OF THE ULTRAMAFIC ROCKS-cont'd.

Oxide	18 M14Q-879	19 M14Q-883	20 M14Q-887	21 M14Q-889	48 M11A22-377	49 M11A22-379	50 M11A22-382	51 M11A22-386	52 M11A22-391
SiO_2	41.85	51.80	50.05	48.25	45.65	38.75	38.80	37.50	38.35
Al_2O_3	2.68	3.52	5.00	5.56	4.76	4.92	5.12	4.06	4.78
FeO	6.64	5.09	4.92	8.88	6.62	10.52	8.65	10.96	10.24
MgO	36.80	31.60	24.16	24.32	32.00	32.20	33.72	34.12	32.45
CaO	0.92	2.54	8.92	7.82	1.58	2.14	3.22	2.92	3.36
Na_2O	-	-	-	0.30	0.15	0.27	0.59	0.50	0.45
K_2O	0.00	0.00	0.00	0.00	2.85	2.12	0.83	0.00	0.00
H_2O^+	9.56	3.94	6.79	3.66	3.54	7.62	7.54	7.72	7.68
CO_2	-	0.53	-	0.00	0.40	0.28	0.26	0.30	1.00
TiO_2	0.084	0.086	0.00	0.066	0.240	0.212	0.196	0.210	0.216
S	-	-	0.30	-	-	-	-	-	-
Cr_2O_3	0.42	0.22	0.00	0.08	0.25	0.32	0.26	0.28	0.37
MnO	0.061	0.062	0.138	0.100	0.158	0.086	0.089	0.111	0.116
NiO	0.26	0.20	0.18	0.14	0.22	0.25	0.15	0.79	0.24
CoO	0.009	-	0.008	-	0.012	0.018	0.016	0.018	0.012
Less O≡S	-	-	0.15	-	-	-	-	-	-
Total	99.28	99.59	100.32	99.18	98.43	99.71	99.44	99.49	99.27

COMPOSITION OF THE ULTRAMAFIC ROCKS-cont'd.

Oxide	53 M11A22-394	54 M11A22-396	55 M11A22-397.5	56 M11A22-399	57 M11A22-400	58 M11A22-401	59 M11A22-402	60 M11A22-403	61 M11A22-404
SiO_2	39.00	39.00	38.50	39.05	41.20	41.50	40.70	49.20	43.90
Al_2O_3	5.22	5.92	5.88	4.90	5.48	6.20	5.92	5.06	14.26
FeO	9.84	9.60	9.52	10.06	9.90	9.04	7.08	8.04	11.05
MgO	31.52	31.20	30.40	32.88	29.52	29.80	29.40	27.76	18.85
CaO	3.90	3.80	3.80	3.76	4.12	3.40	4.54	2.82	0.24
Na_2O	0.49	0.65	0.77	0.68	0.49	0.40	0.26	0.11	0.31
K_2O	0.00	0.00	0.00	0.00	1.69	2.81	3.07	3.11	9.34
H_2O^+	7.02	7.42	7.80	7.40	5.98	4.80	5.04	1.51	1.29
CO_2	0.93	0.47	0.62	0.21	0.62	0.32	1.64	0.19	0.08
TiO_2	0.162	0.196	0.188	0.282	0.292	0.180	0.162	0.160	0.158
S	-	-	-	-	-	-	-	-	-
Cr_2O_3	0.21	0.30	0.26	0.25	0.14	0.20	0.07	0.03	0.00
MnO	0.021	0.102	0.085	0.072	0.070	0.094	0.090	0.163	0.116
NiO	0.22	0.23	0.23	0.24	0.25	0.24	0.22	0.18	0.65
CoO	0.013	0.012	0.014	0.014	0.012	0.012	0.012	0.011	0.015
Less O≡S	-	-	-	-	-	-	-	-	
Total	98.64	98.44	98.07	99.79	99.76	98.99	98.20	98.34	100.27

COMPOSITION OF THE ULTRAMAFIC ROCKS -cont'd.

Oxide	63 M11A8-868	64 M11A8-866	65 M11A8-863	66 M11A8-861	67 M11A8-853	68 M11A8-847	69 M11A8-840	70 M11A8-833	71 M11A8-826
SiO_2	47.10	46.50	36.80	36.75	40.45	34.75	33.40	35.35	35.40
Al_2O_3	4.68	4.66	4.06	4.00	5.22	4.02	3.16	4.08	3.92
FeO	7.00	8.90	8.64	10.20	9.40	10.04	11.82	8.76	9.62
MgO	31.40	29.12	36.80	34.80	27.72	34.20	35.56	37.68	36.84
CaO	0.40	1.00	0.20	0.24	4.10	1.80	0.24	1.60	1.12
Na_2O	0.07	0.11	0.10	0.11	0.40	0.05	-	-	-
K_2O	1.83	1.20	1.60	1.45	1.20	0.00	0.00	0.00	0.00
H_2O^+	4.82	4.82	8.98	9.58	7.16	9.46	11.18	10.88	10.78
CO_2	0.13	0.12	0.29	0.80	0.74	3.07	0.66	0.63	0.78
TiO_2	0.228	0.280	0.244	0.232	0.462	0.256	0.282	0.160	0.206
S	-	-	-	0.55	0.77	0.43	1.90	-	-
Cr_2O_3	0.28	0.28	0.32	0.29	0.05	0.32	0.44	0.33	0.34
MnO	0.082	0.115	0.062	0.098	0.087	0.086	0.076	0.102	0.091
NiO	0.55	0.66	0.97	0.50	0.76	0.48	1.62	0.28	0.28
CoO	0.014	0.016	0.023	0.015	0.016	0.016	0.026	0.014	0.012
Less O≡S	-	-	-	0.27	0.38	0.21	0.95	-	-
Total	98.58	97.79	99.08	99.34	98.16	98.78	99.42	99.86	99.39

COMPOSITION OF THE ULTRAMAFIC ROCKS-cont'd.

Oxide	72 M11A8-817	74 NS-5	75 ASS 1-4	76 Mys.-1	77 Mys.-2	78 Mys.-3	79 TH.-1	80 Th.-2	82 OSP. 5-5
SiO_2	35.70	43.10	37.50	25.26	30.15	36.05	37.20	41.25	37.05
Al_2O_3	3.96	8.88	2.90	2.82	3.00	4.08	3.52	5.10	3.72
FeO	9.02	10.48	8.57	27.58	26.84	14.20	8.25	7.09	9.62
MgO	36.80	20.68	35.68	27.36	24.24	30.44	35.24	33.08	35.20
CaO	1.12	9.84	0.04	0.00	1.20	2.30	1.72	3.64	0.60
Na_2O	-	0.58	-	-	-	-	0.10	-	-
K_2O	0.00	0.00	0.00	0.00	0.00	0.00	0.00	0.00	0.00
H_2O^+	10.72	2.84	8.14	8.90	5.84	8.30	9.94	8.80	10.10
CO_2	0.86	1.04	5.55	0.61	-	-	1.05	-	1.00
TiO_2	0.204	0.486	0.118	0.188	0.204	0.142	0.182	0.228	0.184
S	-	-	-	8.40	9.80	-	1.70	-	-
Cr_2O_3	0.40	0.00	0.86	1.00	0.69	0.31	0.40	0.10	1.24
MnO	0.08	0.138	0.152	0.099	0.126	0.107	0.083	0.160	0.113
NiO	0.30	0.08	0.25	1.38	1.77	0.70	0.54	0.28	0.26
CoO	0.013	0.012	0.014	0.041	0.050	0.016	0.009	0.011	0.011
Less O≡S	-	-	-	4.20	4.90	-	0.85	-	-
Total	99.22	98.16	99.77	99.40	99.01	96.33	99.09	99.74	99.09

COMPOSITION OF THE ULTRAMAFIC ROCKS-cont'd.

Oxide	83 OSP.7-1	84 OSP.6-1	86 JO-5	87 PIP.8-1	88 PIP.8-2	89 PIP.8-4	90 PIP. 8-6	91 PIP. 8-8	92 PIP. 8-9
SiO_2	43.00	35.35	38.70	35.20	36.30	35.20	38.45	34.65	36.50
Al_2O_3	8.80	4.22	4.94	1.24	1.60	2.34	2.00	1.68	1.76
FeO	10.70	8.62	10.30	7.72	8.32	10.42	3.66	8.64	7.94
MgO	21.60	39.56	33.00	40.96	41.44	38.88	42.32	40.88	40.76
CaO	9.00	0.04	3.00	0.00	0.00	0.00	0.00	0.00	0.00
Na_2O	-	-	0.11	-	-	-	-	-	-
K_2O	0.00	0.00	0.11	0.00	0.00	0.00	0.00	0.00	0.00
H_2O^+	5.14	10.68	7.40	14.40	11.36	11.62	12.12	12.78	11.84
CO_2	-	-	0.68	-	-	-	-	0.37	-
TiO_2	0.536	0.198	0.270	0.260	0.022	0.126	0.116	0.158	0.124
S	-	-	-	-	-	0.80	-	-	-
Cr_2O_3	0.04	0.67	0.36	0.57	0.34	0.87	0.57	0.54	0.54
MnO	0.168	0.027	0.115	0.03	0.026	0.051	0.091	0.035	0.051
NiO	0.10	0.21	0.23	0.31	0.31	0.36	0.21	0.28	0.25
CoO	0.010	0.011	0.013	0.016	0.012	0.016	0.010	0.018	0.014
Less O≡S	-	-	-	-	-	0.40	-	-	-
Total	99.10	99.58	99.23	100.71	99.73	99.91	99.55	100.04	99.77

COMPOSITION OF THE ULTRAMAFIC ROCKS-cont'd.

Oxide	93 PIP.8-12	94 Moak-1	95 Moak-2	96 Moak-58	97 PIP 8-14	98 PIP8-15	99 PIP-6	101 M14R-673	101-1 M14R-746
SiO_2	36.40	28.70	38.40	34.45	35.75	35.10	32.60	34.35	35.95
Al_2O_3	2.06	2.38	5.66	1.88	1.72	1.68	3.92	1.92	2.46
FeO	7.82	22.36	23.40	9.32	7.94	10.67	13.36	10.78	14.47
MgO	40.76	31.44	15.00	40.48	39.92	38.00	35.00	38.72	34.32
CoO	0.00	0.04	8.00	0.00	0.00	0.00	0.00	0.00	0.20
Na_2O	-	-	-	-	-	-	-	-	-
K_2O	0.00	0.00	0.00	0.00	0.00	0.00	0.00	0.00	0.00
H_2O^+	11.46	9.04	2.06	12.23	12.24	11.12	10.56	12.14	8.56
CO_2	-	0.46	0.32	-	0.16	0.13	-	-	0.60
TiO_2	0.208	0.188	0.316	0.090	0.088	0.084	0.206	0.078	0.148
S	-	7.70	7.1	-	1.80	2.20	4.80	1.30	3.30
Cr_2O_3	0.53	0.21	0.31	0.43	0.40	0.31	0.49	0.41	0.71
MnO	0.099	0.007	0.242	0.043	0.073	0.018	0.067	0.032	0.078
NiO	0.26	1.77	1.93	0.40	0.45	0.57	0.48	0.27	0.25
CoO	0.015	0.022	0.039	0.014	0.009	0.021	0.019	0.010	0.016
Less O≡S	-	3.85	3.53	-	0.90	1.10	2.40	0.65	1.65
Total	99.62	100.47	99.23	99.33	99.65	98.80	99.11	99.36	99.42

COMPOSITION OF THE ULTRAMAFIC ROCKS-cont'd.

Oxide	102 M14R-975	104 M12T-251	105 M8AE-253	107 M76B-544	108 M76B-752	109 A-453	110 W19G-839	111 W19G-1456	112 M20A-463
SiO_2	32.70	38.25	44.85	37.20	35.75	35.00	34.35	39.20	38.75
Al_2O_3	1.78	4.38	4.12	1.48	1.58	3.34	2.44	2.92	5.08
FeO	10.67	11.76	8.46	9.76	9.74	14.50	7.63	4.92	9.62
MgO	38.48	34.32	30.98	35.92	35.60	33.24	41.92	38.28	33.60
CaO	0.00	0.48	2.52	0.08	0.62	0.32	0.00	0.00	3.36
Na_2O	-	-	0.22	0.003	0.00	-	-	-	-
K_2O	0.00	0.00	0.24	0.00	0.00	0.00	0.00	0.50	0.00
H_2O^+	14.66	6.92	3.90	11.60	9.66	12.62	13.07	13.44	7.50
CO_2	-	0.15	1.13	0.51	1.63	-	-	-	0.32
TiO_2	0.100	0.162	0.158	0.00	0.00	0.222	0.128	0.108	0.236
S	-	2.60	4.00	1.00	2.40	-	-	-	-
Cr_2O_3	0.69	0.51	0.27	0.32	0.34	0.74	0.59	0.80	0.38
MnO	0.062	0.133	0.070	0.057	0.030	0.090	0.070	0.050	0.112
NiO	0.40	0.17	0.21	1.76	1.92	0.20	0.40	0.20	0.20
CoO	0.019	0.005	0.006	0.020	0.024	0.015	0.022	0.008	0.013
Less O≡S	-	1.30	2.00	0.50	1.20	-	-	-	-
Total	99.56	98.54	98.92	99.21	98.09	100.29	100.62	100.43	99.17

COMPOSITION OF THE ULTRAMAFIC ROCKS-cont'd.

Oxide	114 W62K-540	116 W62N-526	117 W62L-734	118 W62L-885	119 W62J-480	120 W62J-618	122 PIP.8-5	123 PIP. 8-13	124 M11A7-422
SiO_2	38.15	35.10	36.20	33.25	32.50	50.50	39.00	38.05	36.10
Al_2O_3	4.54	2.80	2.98	3.42	2.96	3.34	1.58	2.32	3.68
FeO	9.56	8.10	7.93	15.13	13.51	8.55	3.18	4.24	9.00
MgO	35.72	38.76	38.28	34.32	34.56	31.04	42.84	41.04	37.92
CaO	1.78	1.58	1.82	1.14	1.20	3.76	0.26	0.00	1.64
Na_2O	-	0.08	-	-	-	-	-	-	-
K_2O	0.00	0.74	0.00	0.00	0.00	0.20	0.00	0.00	0.00
H_2O^+	7.10	8.66	10.60	7.28	9.86	0.46	12.10	12.22	10.60
CO_2	1.01	1.88	1.13	1.59	1.27	0.99	-	-	-
TiO_2	0.270	0.156	0.080	0.162	0.144	0.112	0.062	0.092	0.262
S	-	-	-	4.30	3.10	-	1.40	0.79	0.64
Cr_2O_3	0.58	0.73	0.30	0.22	0.42	0.22	0.17	0.64	0.44
MnO	0.081	0.150	0.139	0.202	0.090	0.083	0.035	0.115	0.079
NiO	0.26	0.34	0.25	0.59	1.12	0.22	0.24	0.23	0.57
CoO	0.018	0.016	0.014	0.013	0.023	0.015	0.011	0.009	0.011
Less O≡S	-	-	-	2.15	1.55	-	0.70	0.39	0.32
Total	99.07	99.10	99.72	99.06	99.20	99.49	100.18	99.36	100.62

COMPOSITION OF THE ULTRAMAFIC ROCKS-cont'd.

Oxide	125 Mys.-Isl.	126 4-445	127 218-550	128 W62A-389	129 W62A-456	130 W62B-595	131 W62D-379	132 W54B-615	133 W5A-400
SiO_2	32.75	32.70	39.95	36.30	39.00	45.25	39.30	38.10	43.65
Al_2O_3	4.92	2.74	6.70	1.26	3.20	6.84	3.72	1.62	8.26
FeO	16.96	15.83	10.14	8.60	7.50	10.64	9.01	10.00	11.26
MgO	28.68	33.52	25.60	36.48	31.28	25.32	30.68	37.32	23.20
CaO	2.54	1.52	9.46	1.66	3.84	7.72	3.92	0.00	7.98
Na_2O	-	-	0.42	-	-	-	-	-	1.09
K_2O	0.00	0.08	0.00	0.00	0.62	0.00	0.00	0.65	0.00
H_2O^+	8.08	9.10	4.16	11.10	8.04	1.38	7.90	11.34	2.32
CO_2	0.00	1.97	1.43	2.60	4.27	1.29	3.52	0.11	0.31
TiO_2	0.202	0.308	0.458	0.080	0.136	0.328	0.148	0.078	0.466
S	4.60	-	-	-	-	0.90	1.32	-	-
Cr_2O_3	1.53	1.93	0.10	0.68	0.75	0.14	0.39	0.77	0.22
MnO	0.107	0.059	0.170	0.093	0.072	0.136	0.066	0.00	0.141
NiO	0.77	0.35	0.16	0.32	0.30	0.12	0.32	0.21	0.12
CoO	0.026	0.010	0.009	0.013	0.010	0.008	0.012	0.007	0.008
Less O≡S	2.30	-	-	-	-	0.45	0.66	-	-
Total	98.87	100.12	98.76	99.18	99.02	99.63	99.66	100.21	99.03

COMPOSITION OF THE ULTRAMAFIC ROCKS-cont'd.

Oxide	134 W5A-447	136 W5B-296	137 W5B-353	138 M12A-420	139 M12N-455	140 M12N-484	141 W54A-622	142 M70A-128	144 W38C-158
SiO_2	43.15	43.00	44.60	39.95	32.85	34.35	42.30	40.50	41.80
Al_2O_3	7.76	5.90	4.86	4.24	2.00	1.26	2.90	1.84	6.22
FeO	9.82	9.06	8.84	12.75	9.75	7.42	10.16	12.12	8.40
MgO	24.64	26.84	27.68	32.40	40.52	40.48	33.84	31.16	28.40
CaO	7.44	6.86	5.00	1.14	0.00	0.00	2.42	1.18	5.70
Na_2O	1.01	0.65	0.60	-	-	-	-	-	0.63
K_2O	0.05	0.56	0.28	0.00	0.00	0.00	0.14	0.00	1.60
H_2O^+	3.58	4.40	4.56	6.44	12.84	15.00	7.22	8.54	5.90
CO_2	0.07	-	1.27	0.51	0.20	0.90	0.41	1.24	0.31
TiO_2	0.500	0.484	0.302	0.198	0.092	0.120	0.20	0.170	0.416
S	-	-	-	0.81	1.80	-	-	4.10	-
Cr_2O_3	0.09	0.29	0.24	0.74	0.68	0.26	0.40	0.10	0.19
MnO	0.106	0.108	0.122	0.152	0.00	0.036	0.190	0.063	0.075
NiO	0.14	0.16	0.17	0.08	0.59	0.28	0.23	0.04	0.16
CoO	0.006	0.010	0.006	0.011	0.015	0.014	0.014	0.010	0.006
Less O≡S	-	-	-	0.40	0.90	-	-	2.05	-
Total	98.37	98.32	98.53	99.01	100.44	100.29	100.41	99.01	99.82

COMPOSITION OF THE ULTRAMAFIC ROCKS-cont'd.

Oxide	145 W21K-279	146 W21K-593	148 M17A-426	149 W19C-290	150 W19C-522	151 H140B-390	152 H140B-430	153 TR-1	154 TOP-15
SiO_2	42.55	42.20	46.00	35.25	34.10	44.60	45.90	37.55	36.30
Al_2O_3	4.94	7.42	7.10	2.72	2.86	7.74	7.68	4.66	2.94
FeO	10.32	11.68	9.76	9.85	7.18	10.72	10.34	12.80	8.18
MgO	27.60	25.76	21.64	38.52	40.52	24.56	21.08	33.16	38.68
CaO	5.78	6.48	9.82	0.00	0.00	6.90	7.68	0.38	0.08
Na_2O	0.38	-	0.51	-	-	0.71	1.50	0.004	-
K_2O	1.23	0.00	0.00	0.00	0.00	0.00	0.30	0.00	0.00
H_2O^+	4.48	4.52	1.12	12.60	14.04	1.24	1.21	9.02	12.12
CO_2	0.26	0.49	2.05	-	0.45	0.53	0.60	0.98	0.52
TiO_2	0.242	0.412	0.382	0.134	0.114	0.414	0.368	0.202	0.078
S	0.44	-	-	-	-	-	0.32	-	-
Cr_2O_3	0.06	0.16	0.00	0.72	0.60	0.11	0.00	0.67	0.31
MnO	0.116	0.150	0.129	0.037	0.020	0.123	0.162	0.068	0.051
NiO	0.19	0.16	0.13	0.33	0.30	0.14	0.12	0.28	0.35
CoO	0.010	0.007	0.009	0.011	0.004	0.006	0.004	0.017	0.015
Less O≡S	0.22	-	-	-	-	-	0.16	-	-
Total	98.38	99.44	98.65	100.17	100.18	97.79	97.10	99.79	99.63

COMPOSITION OF THE ULTRAMAFIC ROCKS-cont'd.

Oxide	155 HAMBONE	156 SOAB	157 S.MARSHALL	158 PAINT S.	159 WALTERS	160 MUSKEG C.	162 MANASAN	163 MANASAN N.	164 M11A7-377
SiO_2	40.30	32.67	36.45	37.30	46.05	34.10	42.75	34.75	36.20
Al_2O_3	1.84	1.66	1.52	4.20	2.32	1.48	5.28	2.20	4.02
FeO	2.87	7.42	6.75	10.40	10.22	6.13	9.90	7.10	10.22
MgO	41.80	41.68	41.30	32.52	28.96	41.12	28.52	40.40	36.00
CaO	0.00	0.00	0.40	1.88	2.56	0.00	2.48	0.56	1.32
Na_2O	-	0.00	0.00	0.32	0.008	-	0.14	0.00	-
K_2O	0.00	0.00	0.00	0.00	0.00	0.00	0.00	0.00	0.00
H_2O^+	12.63	15.17	12.02	11.16	7.84	14.96	5.60	12.92	11.40
CO_2	-	0.61	1.24	0.32	0.00	0.93	3.98	1.26	-
TiO_2	0.012	0.046	0.020	0.178	0.212	0.084	0.224	0.112	0.256
S	0.42	-	-	-	-	0.65	-	-	-
Cr_2O_3	0.35	0.77	0.34	0.86	0.64	0.36	0.38	0.57	0.49
MnO	0.00	0.085	0.005	0.131	0.085	0.00	0.076	0.052	0.083
NiO	0.51	0.37	0.37	0.21	0.16	0.50	0.16	0.39	0.25
CoO	0.020	0.010	0.010	0.013	0.013	0.021	0.013	0.023	0.007
Less O≡S	0.21	-	-	-	-	0.32	-	-	-
Total	100.19	100.48	100.42	99.17	99.06	100.01	99.50	100.33	100.24

COMPOSITION OF THE ULTRAMAFIC ROCKS-cont'd.

Oxide	165 JO-3	166 W62XB-62	168 M19D-208	169 M19D-314	170 M8AA-244	172 M17F-215	175 M14C-527	11A6 M11A6	321 PIP6-Vein
SiO_2	37.50	42.05	41.70	41.10	32.40	48.25	52.60	42.35	39.90
Al_2O_3	4.74	3.16	3.80	5.74	2.82	4.24	24.12	8.14	.88
FeO	9.84	9.06	10.92	7.68	13.80	8.92	8.38	5.78	2.27
MgO	34.80	36.48	33.20	28.80	35.36	28.60	1.14	31.58	45.04
CaO	2.72	1.40	1.84	4.28	0.14	0.46	3.56	.70	.10
Na_2O	0.10	0.10	-	0.21	0.00	0.11	5.40	-	-
K_2O	0.16	0.83	0.00	2.69	0.00	2.45	3.00	.00	.00
H_2O^+	8.36	4.96	3.90	5.24	10.70	1.05	1.55	10 12	11.94
CO_2	0.56	1.13	2.50	1.85	0.89	0.78	-	-	-
TiO_2	0.296	0.212	0.184	0.272	0.152	0.182	0.774	.064	.278
S	-	-	0.57	-	6.70	-	-	-	-
CrO_3	0.44	0.29	0.58	0.32	0.43	0.26	-	-	.072
MnO	0.065	0.076	0.165	0.048	0.001	0.113	0.134	.192	.00
NiO	0.23	0.26	0.14	0.16	0.31	0.21	-	-	.00
CoO	0.011	0.010	0.008	0.007	0.015	0.012	0.004	-	.00
Less O≡S	-	-	0.28	-	3.35	-	-	-	-
Total	99.89	100.02	99.23	98.40	99.20	95.63	100.65	98.92	100.48

APPENDIX X

CALCULATION OF THE MODIFIED STANDARD CELL (MSC).

The modified standard cell, as described by Chidester (1962), allows the determination of chemical changes which have taken place between volumes of rock of equal and standard size. It is a standard volume of rock, that on an average contains about 100 electropositive ions. In precise terms the modified standard cell is the volume of rock that contains $2{,}064.8 \times N^{-1}$ cc, (where N is Avogadro's number 6.0247×10^{23}), which is represented by a cube 15.1 Å units on an edge. In practice it is convenient to leave the volumes in terms of N^{-1} cubic centimeters and regard them as proportions. The resultant formula numbers in the MSC are hence directly comparable between rocks of widely varying density. The calculations for the MSC of seven specimens used in the study of serpentinite alteration are included in this appendix. The method of calculation is as follows:

1) Weight percents are converted to equivalent molecular numbers by division with the appropriate equivalent weight (atomic weights of the oxide in terms of 1 cation eg $AlO_{3/2}$).

2) Equivalent molecular numbers are converted to equivalent molecular percents by division with the sum of the equivalent numbers less $HO_{\frac{1}{2}}$ + S.

3) Oxygen equivalents (Oeq), denotes an oxygen ion or an amount of another ion that occupies a volume approximately equivalent to that of an oxygen. The Oeq associated with 100 equivalent molecular percent is calculated by multiplying the equivalent percents by the number of oxygens (or their equivalent) in the symbol for the equivalent unit; eg. SiO_2 by x2, $AlO_{3/2}$ by $\frac{3}{2}$, S by 1

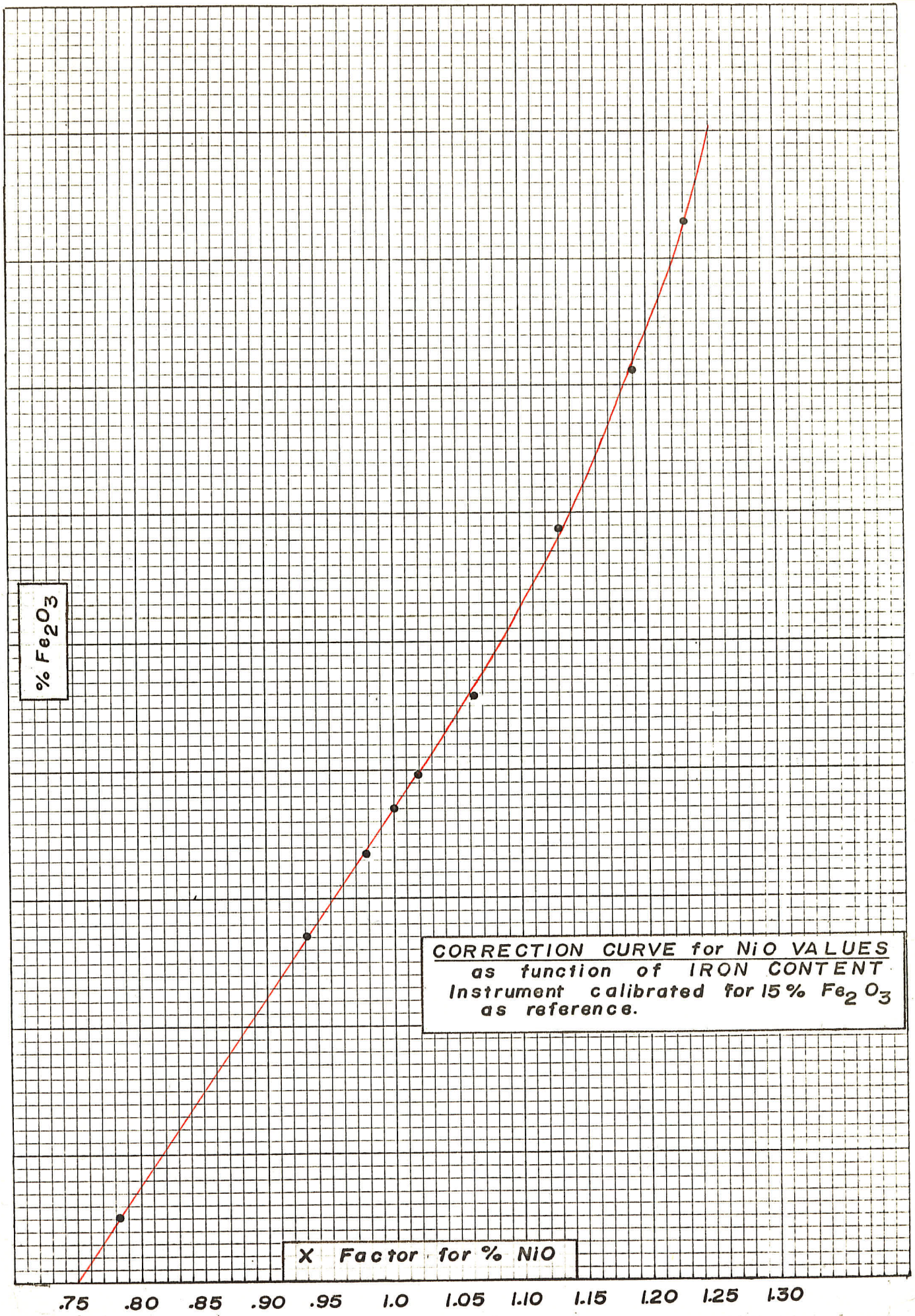
% Fe_2O_3
CORRECTION CURVE for NiO VALUES
as function of IRON CONTENT
Instrument calibrated for 15% Fe_2O_3
as reference.
X Factor for % NiO
.75
.80
.85
.90
.95
1.0
1.05
1.10
1.15
1.20
1.25
1.30

Fig. A–2

A. Calculation of modified standard all, sample #16

	Weight%	Equivalent Mol. Nos.	Equivalent Mol. %	Oeq.	Formula Nos in MSC
SiO_2	37.80	0.62937	34.94	69.88	32.95
$AlO_{3/2}$	2.58	.05062	2.81	4.22	2.65
FeO	6.73	.09367	5.20	5.20	4.90
MgO	40.92	1.01513	56.35	56.35	53.14
CaO	.00	.00000	.00	.00	.00
$NaO_{\frac{1}{2}}$	-	-	-		
$KO_{\frac{1}{2}}$	.00	.00000	.00	.00	.00
$HO_{\frac{1}{2}}$	11.84	1.31439	72.96	36.48	68.80
CO_2	-	-	-		
TiO_2	0.12	.00150	.08	.16	.07
$CrO_{3/2}$	0.52	.00684	.38	.57	.36
MnO	0.04	.00056	.03	.03	.03
NiO	0.27	.00361	.20	.20	.19
CoO	0.012	.00016	.01	.01	.01
S	-	-			
Total	100.83				
Less O for S	.00				
Total	100.83	3.11585	172.96	173.10	
Less $HO_{\frac{1}{2}}$+S		1.31439	72.96	36.48	
Total		1.80146	100.00	136.62	
Less $HO_{\frac{1}{2}}$+CO_2				36.48	
O				100.14	
Oeq				163.23	
Cations				94.30	
O				94.43	
W100				5597.1	
Density				2.556	
V100				2189.7	
Frk = Vmsc/V100 =				.9430	

B. Calculation of modified standard cell, sample #17

	Weight%	Equivalent Mol. Nos.	Equivalent Mol. %	Oeq.	Formula Nos. in MSC
SiO_2	41.40	0.68931	38.13	76.26	41.85
$AlO_{3/2}$	3.54	.06945	3.84	5.76	4.22
FeO	7.28	.10132	5.61	5.61	6.16
MgO	32.00	.79365	43.91	43.91	48.20
CaO	5.80	.10342	5.72	5.72	6.28
$NaO_{\frac{1}{2}}$	-	-			
$KO_{\frac{1}{2}}$	.00	.00000	.00	.00	.00
$HO_{\frac{1}{2}}$	6.72	.74600	41.27	20.64	45.30
CO_2	1.95	.04431	2.45	4.90	2.69
TiO_2	.06	.00075	.04	.08	.04
$CrO_{3/2}$	.05	.00066	.04	.06	.04
MnO	.07	.00099	.05	.05	.05
NiO	.27	.00361	.20	.20	.22
CoO	.01	.00013	.01	.01	.01
S	.75	.02339	1.29	1.29	1.42
Total	99.90			164.49	
Less O = S	.37			1.94	
Total	99.53	2.57699	142.56	162.55	
Less $HO_{\frac{1}{2}}$+S		.76939	42.56	21.93	
Total		1.80760	100.00	140.62	
Less $HO_{\frac{1}{2}}$+CO_2 O				25.54	
				115.08	

Oeq	178.43
Cations	109.77
O	126.32
W100	5061.9
Density	2.691
V100	1881.0
Frk = Vmsc/V100	1.0977

C. Calculation of modified standard cell, sample #18

	Weight%	Equivalent Mol. Nos.	Equivalent Mol. %	Oeq.	Formula Nos. in MSC
SiO_2	41.85	0.69680	39.10	78.20	39.66
$AlO_{3/2}$	2.68	.05258	2.95	4.43	2.99
FeO	6.64	.09241	5.19	5.19	5.26
MgO	36.80	.91270	51.22	51.22	51.95
CaO	0.92	.01641	.92	.92	.93
$NaO_{\frac{1}{2}}$	-	-			
$KO_{\frac{1}{2}}$	.00	.00000	.00	.00	.00
$HO_{\frac{1}{2}}$	9.56	1.06128	59.56	29.78	60.41
CO_2	-	-			
TiO_2	.08	.00100	.06	.12	.06
$CrO_{3/2}$	.42	.00553	.31	.47	.31
MnO	.06	.00085	.05	.05	.05
NiO	.26	.00348	.20	.20	.20
CoO	.01	.00013	.01	.01	.01
S	-	-			
Total	99.28				
Less O for S	.00				
Total	99.28	2.84317	159.57	170.59	
Less $HO_{\frac{1}{2}}$+S		1.06128	59.56	29.78	
Total		1.78189	100.01	140.81	
Less $HO_{\frac{1}{2}}$+CO_2 O				29.78 111.03	
Oeq.					173.03
Cations					101.43
O					112.62
W100					5571.6
Density					2.737
V100					2035.7
Frk = Vmsc/V100					1.0143

D. Calculation of modified standard cell, sample #19

	Weight	Equivalent Mol. Nos.	Equivalent Mol. %	Oeq.	Formmula Nos in MSC
SiO_2	51.80	0.86247	46.60	93.20	50.02
$AlO_{3/2}$	3.52	.06906	3.73	5.60	4.00
FeO	5.09	.07084	3.83	3.83	4.11
MgO	31.60	.78373	42.34	42.34	45.45
CaO	2.54	.04529	2.45	2.45	2.63
$NaO_{\frac{1}{2}}$	-	-			
$KO_{\frac{1}{2}}$	.00	.00000	.00	.00	.00
$HO_{\frac{1}{2}}$	3.94	.43739	23.63	11.82	25.36
CO_2	0.53	.01204	.65	1.30	.70
TiO_2	0.09	.00113	.06	.12	.06
$CrO_{3/2}$	0.22	.00289	.16	.24	.17
MnO	0.06	.00085	.05	.05	.05
NiO	0.20	.00268	.14	.14	.15
CoO	-	-	-		
S	-	-	-		
Total	99.59				
Less O = S	.00				
Total	99.59	2.28837	123.64	161.09	
Less $HO_{\frac{1}{2}}$+S		.43739	23.63	11.82	
Total		1.85098	100.01	149.27	
Less $HO_{\frac{1}{2}}$+CO_2 O				13.12	
				136.15	

Oeq	172.91
Cations	107.34
O	146.14
W100 (wt. of 100 equiv. molecules of rock)	5380.4
Density	2.797
V100	1923.6
Frk = Vmsc/V100 =	1.0734

E. Calculation of modified standard cell, sample #20

	Weight %	Equivalent Mol. Nos.	Equivalent Mol. %	Oeq.	Formula Nos. in MSC
SiO_2	50.05	0.83333	47.28	94.56	48.01
$AlO_{3/2}$	5.00	.09810	5.57	8.36	5.66
FeO	4.92	.06848	3.88	3.88	3.94
MgO	24.16	.59921	33.99	33.99	34.52
CaO	8.92	.15906	9.02	9.02	9.16
$NaO_{\frac{1}{2}}$	-	-			
$KO_{\frac{1}{2}}$	.00	.00000	.00	.00	.00
$HO_{\frac{1}{2}}$	6.79	.75377	42.76	21.38	21.71
CO_2	-	-			
TiO_2	.00	.00000	.00	.00	.00
$CrO_{3/2}$	.00	.00000	.00	.00	.00
MnO	.14	.00197	.11	.11	.11
NiO	.18	.00241	.14	.14	.14
CoO	.01	.00013	.01	.01	.01
S	.30	.00936	.53	.53	.54
Total	100.47			171.98	
Less O = S	.15			.80	
Total	100.32	2.52582	143.29	171.18	
Less $HO_{\frac{1}{2}}$+S		.76313	43.29	21.91	
Total		1.76269	100.00	149.27	
Less $HO_{\frac{1}{2}}$+CO_2				21.38	
O				127.89	

Oeq	173.83
Cations	101.55
O	129.87
W100	5691.3
Density	2.799
V100	2033.3
Frk = Vmsc/V100	1.0155

F. Calculation of modified standard cell, sample #21

	Weight	Equivalent Mol. Nos.	Equivalent Mol. %	Oeq.	Formula Nos in MSC
SiO_2	48.25	0.80336	44.79	89.58	46.01
$AlO_{3/2}$	5.56	.10908	6.08	9.12	6.25
FeO	8.88	.12359	6.89	6.89	7.08
MgO	24.32	.60317	33.63	33.63	34.54
CaO	7.82	.13944	7.77	7.77	7.98
$NaO_{\frac{1}{2}}$	0.30	.00968	.54	.27	.55
$KO_{\frac{1}{2}}$	.00	.00000	.00	.00	.00
$HO_{\frac{1}{2}}$	3.66	.40631	22.65	11.33	23.27
CO_2	.00	.00000	.00	.00	.00
TiO_2	.07	.00088	.05	.10	.05
$CrO_{3/2}$	.08	.00105	.06	.09	.06
MnO	.10	.00141	.08	.08	.08
NiO	.14	.00187	.10	.10	.10
CoO	-	-	-		
S	-	-	-		
Total	99.18				
Less O = S	.00				
Total	99.18	2.19984	122.65	158.96	
Less $HO_{\frac{1}{2}}$+S		40631	22.65	11.33	
Total		1.79353	100.00	147.63	
Less $HO_{\frac{1}{2}}+CO_2$				11.33	
O				136.30	
Oeq					163.28
Cations					102.72
O					140.01
W100					5529.9
Density					2.751
V100					2010.1
Frk = Vmsc/V100 =					1.0272

G. Calculation of modified standard cell, sample #175

	Weight %	Equivalent Mol. Nos.	Equivalent Mol. %	Oeq.	Formula Nos in MSC
SiO_2	52.60	0.87579	48.47	96.94	47.89
$AlO_{3/2}$	24.12	.47322	26.19	39.29	25.88
FeO	8.38	.11663	6.45	6.45	6.37
MgO	1.14	.02827	1.56	1.56	1.54
CaO	3.56	.06348	3.51	3.51	3.47
$NaO_{\frac{1}{2}}$	5.40	.17421	9.64	4.82	9.53
$KO_{\frac{1}{2}}$	3.00	.06370	3.53	1.77	3.49
$HO_{\frac{1}{2}}$	1.55	.17207	9.52	4.76	9.41
CO_2	-	-			
TiO_2	0.77	.00964	.53	1.06	.52
$CrO_{3/2}$	-	-			
MnO	.13	.00183	.10	.10	.10
NiO	-	-			
CoO	.004	.00005	.00	.00	.00
S	-	-			
Total	100.65				
Less O for S	.00				
Total	100.65	1.97889	109.52	160.26	
Less $HO_{\frac{1}{2}}$+S		.17207	9.52	4.76	
Total		1.80682	100.00	155.50	
Less $HO_{\frac{1}{2}}$+CO_2 O				4.76 150.74	

Oeq	158.35
Cations	98.81
O	148.95
W100	5570.6
Density	2.774
V100	2008.1
Frk = Vmsc/V100	0.9881